LOAD DISTRIBUTION FOR A DRILLED SHAFT IN CLAY SHALE

by

Vasant N. Vijayvergiya
W. Ronald Hudson
Lymon C. Reese

Research Report Number 89-5

Soil Properties as Related to Load-Transfer
Characteristics of Drilled Shafts

Research Project 3-5-65-89

conducted for

The Texas Highway Department

in cooperation with the
U. S. Department of Transportation
Federal Highway Administration
Bureau of Public Roads

by the

CENTER FOR HIGHWAY RESEARCH

THE UNIVERSITY OF TEXAS AT AUSTIN

MARCH 1969

The opinions, findings, and conclusions expressed in this publication are those of the authors and not necessarily those of the Bureau of Public Roads.

PREFACE

This report is the fifth in a series of reports from Research Project 3-5-65-89 of the Cooperative Highway Research Program. It describes the development of instrumentation capable of measuring axial load distribution along a drilled shaft and the development, with the aid of full-scale load testing, of a technique of analysis of observed data. The observed data have been correlated to the Texas Highway Department cone penetration test and a tentative design procedure for a drilled shaft is proposed.

This report is the product of the combined efforts of many people. Technical contributions were made by Harold H. Dalrymple, James N. Anagnos, Crozier Brown, Clarence Ehlers, Mike O'Neill, John W. Chuang, Walter R. Barker, and Frederick E. Koch. Preparation and editing of the manuscript were done by Art Frakes, Don Fenner, Joye Linkous, Marie Fisher, Eva Miller, and Jacquelyn West.

The Texas Highway Department Project contact representatives, Messrs Horace Hoy, H. D. Butler, and Malcolm L. Steinberg, along with the personnel from District No. 15 have been helpful and cooperative in the development of the work. Thanks are due them as well as the U. S. Bureau of Public Roads who jointly sponsored the work.

Vasant N. Vijayvergiya

W. Ronald Hudson

Lymon C. Reese

March 1969

LIST OF REPORTS

Report No. 89-1, "Field Testing of Drilled Shafts to Develop Design Methods," by Lymon C. Reese and W. Ronald Hudson, describes the overall approach to the design of drilled shafts based on a series of field and laboratory investigations.

Report No. 89-2, "Instrumentation for Measurements of Lateral Earth Pressure in Drilled Shafts," by Lymon C. Reese, J. Crozier Brown, and H. H. Dalrymple, describes the development and evaluation of pressure gages to measure lateral-earth pressures on the drilled shaft.

Report No. 89-3, "Studies of Shearing Resistance Between Cement Mortar and Soil," by John W. Chuang and Lymon C. Reese, describes the overall approach to the design of drilled shafts based on field and laboratory investigations.

Report No. 89-4, "The Nuclear Method of Soil-Moisture Determination at Depth," by Clarence J. Ehlers, Lymon C. Reese, and James N. Anagnos, describes the use of nuclear equipment for measuring the variations of moisture content at the drilled shaft test sites.

Report No. 89-5, "Load Distribution for a Drilled Shaft in Clay Shale," by Vasant N. Vijayvergiya, W. Ronald Hudson, and Lymon C. Reese, describes the development of instrumentation capable of measuring axial load distribution along a drilled shaft, the development, with the aid of full-scale load testing, of a technique of analysis of observed data, and the correlation of observed data with the Texas Highway Department cone penetration test.

ABSTRACT

Large diameter drilled shafts are used extensively in many areas of the world to support axial loads; however, the behavior of these shafts is not well understood. Frequently they are designed as point-bearing shafts only, with no account being taken of load distributed along the sides of the shaft. Questions arising with regard to the design of such shafts concern the interaction of wet concrete with soil, the possible shrinkage of concrete on drying, the eventual earth pressure at the interface of the shaft and the supporting soil, and the mechanics of the interaction of the shaft with the foundation. This report describes a comprehensive investigation aimed at gaining more information related to the above questions. A 30-inch by 28.5-foot drilled shaft was instrumented with electrical resistance strain gages, mechanical strain gages, earth pressure cells, and thermocouples and was subsequently tested under axial load. The instruments were read for a series of load increments. The shaft was tested five times with loads ranging up to almost 1,000 tons.

The test data were analyzed to obtain curves giving distribution of axial load along the shaft as a function of depth and curves showing load transfer at various depths as a function of downward movement of the shaft at that depth. Results of these analyses were correlated with soil properties obtained from Texas Highway Department cone penetrometer tests. A tentative design procedure is proposed and the load-settlement curves computed by this design procedure are compared with the observed curves.

TABLE OF CONTENTS

CHAPTER 1. INTRODUCTION

During the last decade an important development in foundation engineering has been the rise in popularity of the deep pier or shaft founded in clay. The term "shaft" here implies a drilled shaft, which may be defined as a cylindrical column of concrete cast in place and used to transfer load from the superstructure to the subsurface of the earth. Other terms sometimes used to designate a drilled shaft are bored pile, cast-in-place pile, caisson, and pier. Drilled shafts fall under the category of deep foundations. A drilled shaft is constructed by first drilling a hole of the required size to a desired depth and then placing a reinforcement cage in the hole (sometimes reinforcement is omitted) and filling it with concrete.

Foundations of this type carried to rock have been used for many years, for example, the hand-dug "Chicago wells and Gow caissons" (Ref 23); but the use of a drilled shaft, when the support is provided entirely by clay, represented a new departure.

The use of drilled shafts as structural foundations has expanded rapidly in the past two decades with the development of heavy-duty mobile equipment and the perfection of drilling and installation techniques for operating in a wide variety of soil conditions. As more and more information becomes available about the interaction between the shaft surface and surrounding soil, more drilled shafts are being designed on the basis of skin friction only. A recent example is that of the Canada Cement Company Limited plant at Brookfield, Nova Scotia, built in 1964 (Ref 11).

Mechanism of Load Transfer in a Drilled Shaft

The axial load applied on the top of a shaft is supported partly by the shearing resistance developed along the surface of the shaft and partly by the bearing support at the bottom of the shaft, as shown in Fig 1(a). The same can be stated mathematically as

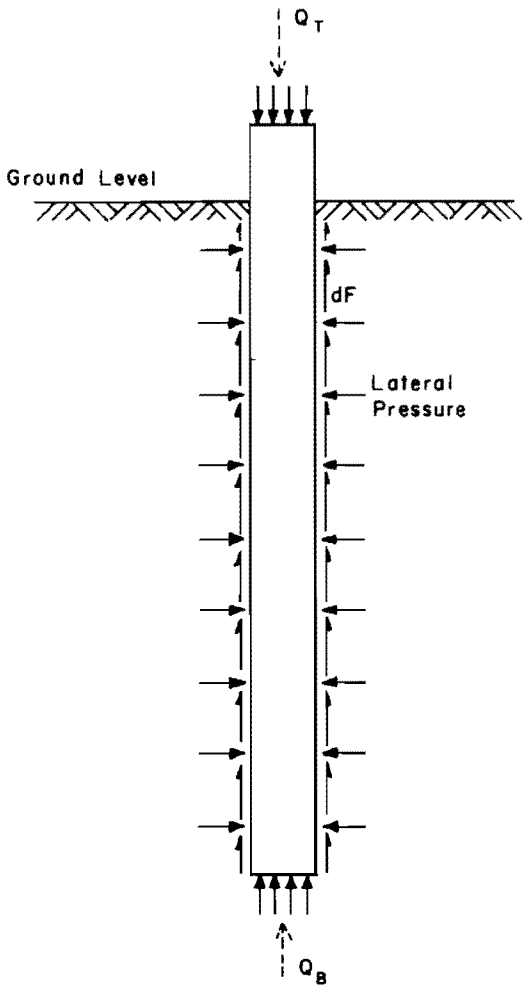

Fig 1(a). Forces acting on a drilled shaft.

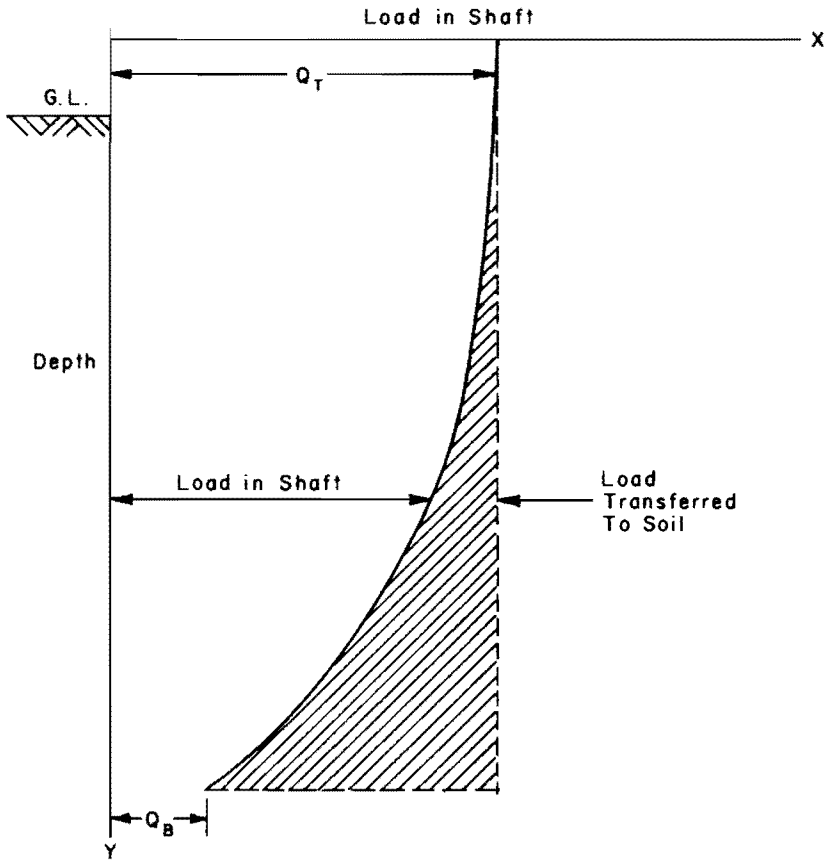

Fig 1(b). Typical curve for load distribution in a shaft.

$$Q_T = \Sigma(dF)(dA) + Q_B$$

where

Q_T = total load on top of the shaft,

dF = shearing stress developed on an elemental surface area dA of the shaft,

Q_B = bearing support at the tip of the shaft.

The source of shearing resistance depends on the type of soil. In the case of clay it is derived from c the cohesion of clay, and for sand it is derived entirely from ϕ the angle of shearing resistance of sand. However, for a mixed soil composed of sand and clay the shearing resistance will depend on both c and ϕ .

The amount of load transferred from the shaft to the soil increases gradually with depth, but the actual nature of the increase is not yet well understood. A typical load transfer or load distribution curve is shown in Fig 1(b). The amount of load transferred to the soil at any depth depends on several factors, such as properties of the soil and shaft, dimensions of the shaft, type of loading, and time effects. These factors are discussed in detail in the next chapter.

The development of shearing resistance along the surface of the shaft depends on the downward movement of the shaft. It may be pointed out that a slight downward movement of the shaft is essential to mobilize some shearing resistance. The relationship between downward movement of the shaft and the shearing resistance is not very well understood. A typical curve showing the relationship of load transfer and the downward movement of the shaft is shown in Fig 2. Similar curves were developed by Coyle and Reese (Ref 5) based on the laboratory studies on a miniature pile.

Project Objectives

The Texas Highway Department and other agencies have been using drilled shafts extensively for bridge foundations. Common practice has been to "bell" the bottom of the shaft to increase the bearing area in clays and to ignore the shearing resistance developed along the shaft surface. Since skin

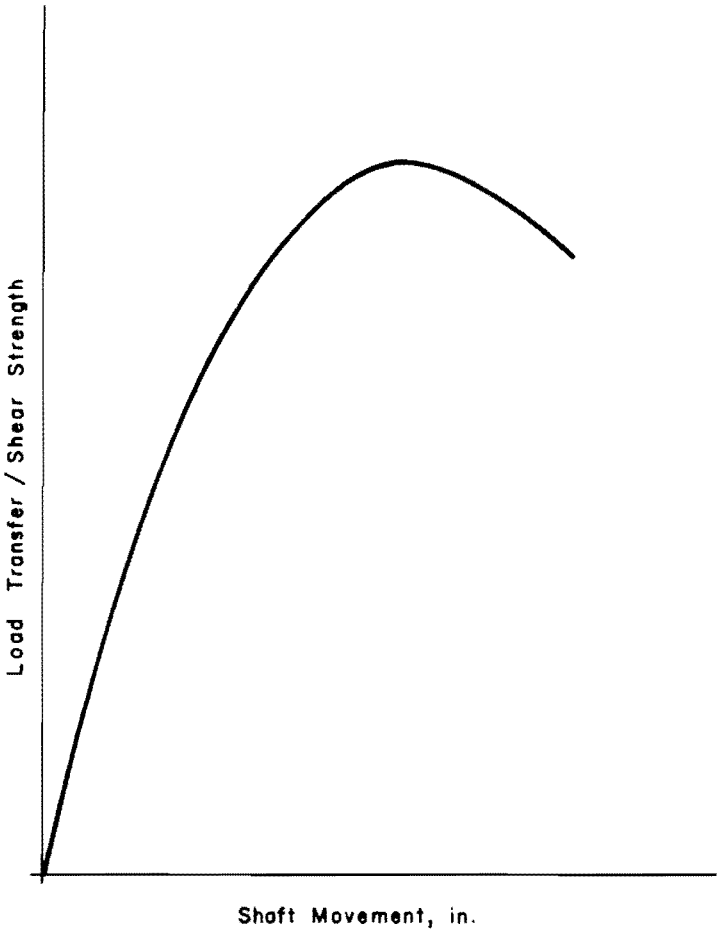

Fig 2. Ratio of load transfer to soil shear strength versus shaft movement.

friction is sizeable in some cases, this results in a conservative and uneconomical design. A research study has been undertaken to develop a rational procedure of design which would include the effects of shearing resistance or skin friction. The objectives of this research program are

(1) to design, construct, and test instrumentation capable of measuring load distribution and earth pressure distribution along a drilled shaft;

(2) on the basis of field measurements with this instrumentation and on the basis of certain laboratory tests, to develop methods by which the bearing capacity of a drilled shaft can be predicted from results of soil tests; and

(3) to develop the necessary design aids, charts, or computer programs to enable the prediction method to be used readily by practicing highway engineers.

Statement of Work for the Present Study

The objective of the research work described in this report is a part of the objectives described above and can be stated as follows:

To design, construct, and test instrumentation capable of measuring axial load distribution along a drilled shaft and to develop, with the aid of full scale load testing, a technique for analyzing the observed data and correlating them with the soil properties. Accordingly, a test site was selected near San Antonio. A 30-inch by 28.5-foot drilled shaft was instrumented with electrical resistance strain gages, mechanical strain gages, earth pressure cells, and thermocouples and was subsequently tested under axial load. The instruments were read for a series of load increments. The shaft was tested five times with loads ranging up to almost 1,000 tons. The test data were analyzed to obtain the relationship between axial load along the shaft and depth, load transfer at various depths and the downward movement at these depth. The test results were correlated with the Texas Highway Department cone penetrometer test. A procedure for the design of drilled shafts was developed.

CHAPTER 2. FACTORS AFFECTING THE LOAD DISTRIBUTION IN A DRILLED SHAFT IN CLAY

Understanding of the mechanism of deep foundations in cohesionless soils has improved considerably in recent years. However, the behavior of such foundations in clay is still not entirely clear. A soil engineer, even though knowing perfectly the drained as well as the undrained mechanical properties of a clay, is presently unable to forecast correctly the vertical point resistance as well as the skin friction of a pile driven or bored in a homogeneous saturated clay. The cause of uncertainty in predicting bearing capacity of deep foundations such as drilled shaft or piles in clay becomes more evident when the factors that affect it are studied. The various important factors that affect the load distribution in a drilled shaft are discussed here.

Soil Properties

The load transfer from the shaft to the surrounding clay depends mainly on the shear strength characteristics of the clay. The shear strength of clay is primarily affected by moisture variation, disturbance, and preconsolidation pressure.

Studies of Meyerhof and Murdock (Ref 13) indicate that water migrates from the green concrete into the soil surrounding the shaft, thereby increasing the moisture content and reducing the shear strength. Studies of shearing resistance between cement mortar and soil by Chuang and Reese (Ref 3) suggest that the amount of moisture migration is not only a function of grain size distribution, void ratio, and original moisture content of the soil, but is also a function of the water cement ratio of the cement mortar. They observed an increase of moisture content of as much as 10 percent in the soil close to the mortar surface. Their studies for a particular soil showed a decrease of 40 to 68 percent in shear strength of soil due to water migration from cement mortar to soil. However, the studies of DuBose (Ref 6) on laboratory samples show no significant moisture increase except for soil with very low initial moisture content. His results are also supported by full-scale test shafts

which were extracted from the ground. It appears from such divergent observations that the method of determining the change in moisture content of in situ soil needs further study. In this direction the nuclear method of measuring moisture content in the soil seems encouraging (Ref 4).

The disturbance of a natural clay causes a reduction in shear strength: the higher the sensitivity of clay, the larger the reduction. The extent of disturbance varies from almost complete in driven piles to partial in the case of drilled shafts. In a drilled shaft, the degree of disturbance also depends on the method used for drilling the bore hole. A further reduction in shear strength may result if the bore hole is left open for a long time. When the bore hole is left open for a long time, the clay along the inner surface of the bore hole dries out, and, when wet concrete is poured into the hole, the dry clay may start slaking, thus reducing the shear strength along the surface.

Studies of Coyle and Reese (Ref 5) on miniature sized piles in the laboratory indicate that load transfer, for any given movement of pile, increases with the confining pressure in the clay. It may then be expected that increasing overburden pressure would result in an increased load transfer to soil, but no conclusive evidence on this point is available. Further experiments in this direction seem desirable.

Shaft Dimensions

The ultimate bearing capacity Q_u of a drilled shaft in clay depends on its diameter and length in addition to soil properties. Neglecting the weight W of the shaft (Ref 20), Q_u can be computed from the formula

$$Q_u = Q_B + Q_f$$

$$= N_c A_c + A_p f_s \qquad (2.1)$$

where

Q_B = total tip resistance,

Q_f = total skin friction resistance,

N_c = bearing capacity factor,

L = length of the shaft in ground,

D = diameter of the shaft,

A = cross-sectional area of the shaft at base,

A_p = surface area of the shaft,

c = undrained shear strength of soil at base,

f_s = average skin friction over length L.

It may be seen from Eq 2.1 that the total tip resistance Q_B increases in proportion to D^2, while the total skin friction Q_f increases with the increase in L and D. Actual measurements of tip resistance by various investigators including Kerisel (Ref 9), and Koizumi and Ito (Ref 10) indicate that it seldom exceeds 20 to 30 percent of ultimate bearing capacity Q_u.

A comprehensive study of large bored piles in London clays by Whitaker and Cooke (Ref 23) indicated that for a given degree of mobilization of frictional resistance the settlement increased as the shaft diameter was increased and full mobilization occurred at a settlement which was between 0.5 percent and 1.0 percent of the shaft diameter. The mobilization of frictional resistance at any settlement appeared to be independent of shaft length and of whether or not the base was enlarged. They also observed that the degree of mobilization of the tip resistance increased as the settlement increased, reaching full mobilization at a settlement between 10 percent and 20 percent of the base diameter.

The value of N_c, the bearing capacity factor, depends on shaft dimensions. However, for ratio $L/D > 5$, N_c is considered to be constant. Skempton (Ref 19) has suggested a value of $N_c = 9$ for the ratio $L/D > 5$.

The base diameter of a shaft for given soil properties governs the ultimate settlement below the tip: the larger the diameter, the greater is the settlement under ultimate load. According to Skempton (Ref 19) the tip settlement s can be related to the base diameter D by

$$s = 2D\epsilon \qquad (2.2)$$

where

ϵ = the average axial strain corresponding to maximum deviator stress in undrained compression test run on soil samples taken from near the tip location.

Properties of Shaft Material

The roughness of the surface of the shaft depends on the state of the surface of the bore hole before concrete is poured. Generally speaking, the surface of the shaft is rough. When a casing is provided to prevent caving of the soil into the hole, the surface of the shaft in contact with the soil may be relatively smooth. The roughness appears to have some effect on the interaction of the shaft with the supporting soil. A rough surface provides a better interlocking with the surrounding soil and results in a higher load transfer to the soil. Quantitative information on such effects is not available for drilled shafts.

It is well recognized in the field of soil stabilization that the contact of cement particles with clay particles results in a physicochemical change. This phenomenon increases the shear strength of clay. In the case of drilled shafts without a casing such a change would occur at the interface of the soil and shaft. The zone of soil surrounding the shaft affected by such a physicochemical change is not known. The migration of moisture from the green concrete to soil also affects the shear strength as described earlier in this chapter.

Time Effects

The magnitude of total shaft settlement under a load test depends on the time duration of the load. The distribution of axial load along the depth of the shaft is also affected by time. Hanna (Ref 8) found that the load transferred to soil at various depths was greater after a 60-minute duration than after a two-minute duration. Whitaker and Cooke (Ref 23) observed an increase in skin friction with increasing time in their studies on large bored piles.

CHAPTER 3. INSTRUMENTATION

Introduction

Embedment strain gages and mechanical strain gages were used to measure axial strain in the shaft at various depths. Pressure cells were used to measure lateral pressures on the shaft at two depths. Thermocouples were used to measure the variation of temperature in the shaft.

Specifications of Embedment Strain Gages

Embedment strain gages of type PML-60, manufactured by Tokyo Sokki Kenkyujo Company of Japan, were used for instrumentation. Figure 3 shows the type of embedment strain gage used. It consists of a wire gage sandwiched between two pieces of resin plate and attached with 2-meter-long outgoing vinyl lead wire. The outer faces of the resin plates are coated with rough material for good bond with concrete. The specifications of the gages used are given below:

Nominal gage length	60 mm
Nominal gage width	1 mm
Nominal resistance	120 ohms
Gage factor	2.11
Base dimensions (mm)	125 × 13 × 5

The embedment type strain gage is found to be very suitable for strain measurement of the interior of concrete. It has very good electrical insulation. Ease of installation makes it particularly useful.

Laboratory Study of Embedment Strain Gages

Since little experience with these gages was available, an experiment was conducted to determine the accuracy of the strain measurements with the embedment strain gages in predicting load in the concrete. Three strain gages were embedded in a concrete cylinder 6 inches in diameter and 12 inches in length. At the time of casting these gages were equally spaced. After curing, the cylinder was loaded in increments of 2,000 to 3,000 pounds. The deformation

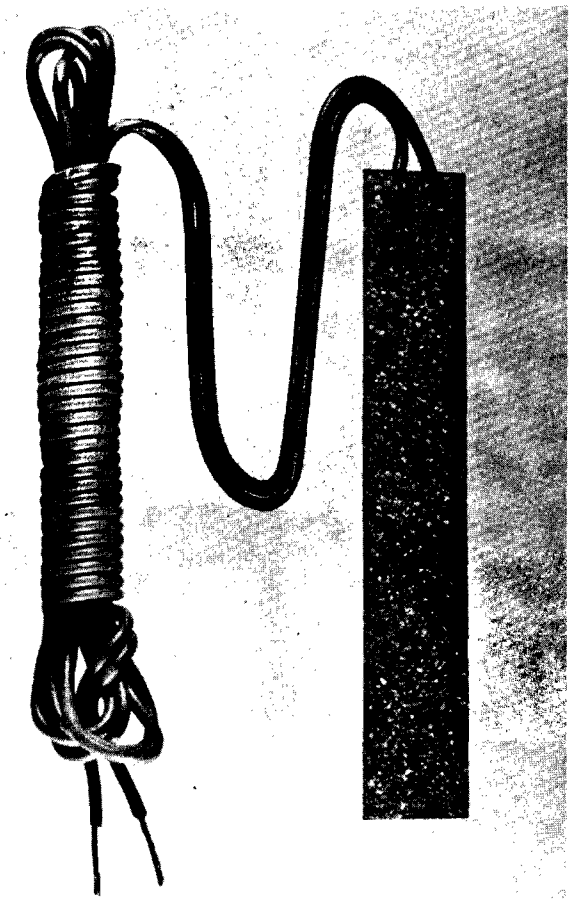

Fig 3. PML-6 type embedment strain gage.

was measured mechanically with the help of an extensometer and strain indicated by strain gages was measured directly with a Budd Strain Indicator. Based on the deformation, average strain was computed. The strain thus obtained mechanically and electrically for various loadings is shown in Fig 4. It may be seen from this figure that the strain measured by PML-60 gages is in close agreement with that measured mechanically.

Another test was set up to study the effect of placing the PML-60 gage in a cement mortar block 7 by 3 by 1 inch and then placing the block in a concrete cylinder for measurement of strain. This was thought necessary to protect the PML-60 gages from damage from impact due to pouring of concrete during shaft construction. The cement mortar consisted of cement and sand in the proportion of 1:2 by weight, respectively. Three blocks were cast, with one PML-60 gage in each, and cured for 7 days. These blocks along with bare PML-60 gages were placed in a concrete cylinder as shown in Fig 5. Two pairs, each consisting of one PML-60 gage in a block and one original PML-60 gage, were used to measure axial strain, and one pair was used to measure lateral strain. The gage leads were marked 1 through 6 as shown in Fig 5.

The test cylinder was placed on the Budd compression testing machine and load increased gradually. The strain experienced by each gage was measured with a strain indicator. The results of the test are shown in Fig 6. The pair of horizontal strain gages showed erratic variation. It was concluded from the test that the casting of the PML-60 gages in a cement mortar block does not appreciably affect the strain readings.

From these laboratory studies it was decided to use in future measurement in long shafts PML-60 gages precast in cement mortar blocks 7 by 3 by 1 inch. Precaution was taken to give a rough surface to the blocks.

Dummy Strain Gages

Dummy strain gages were used for compensation of temperature. The dummy gage consisted of a PML-60 strain gage placed inside a steel tube with an internal diameter of 1 inch and 6 inches in length with threaded ends. The gage was protected inside by sandwiching between two pieces of foam rubber. A cap was threaded on to each end. The lead wires of the strain gages were taken out through a 1/8-inch hole provided in one of the end caps. The space between threads and the cap was sealed with a Teflon thread seal compound.

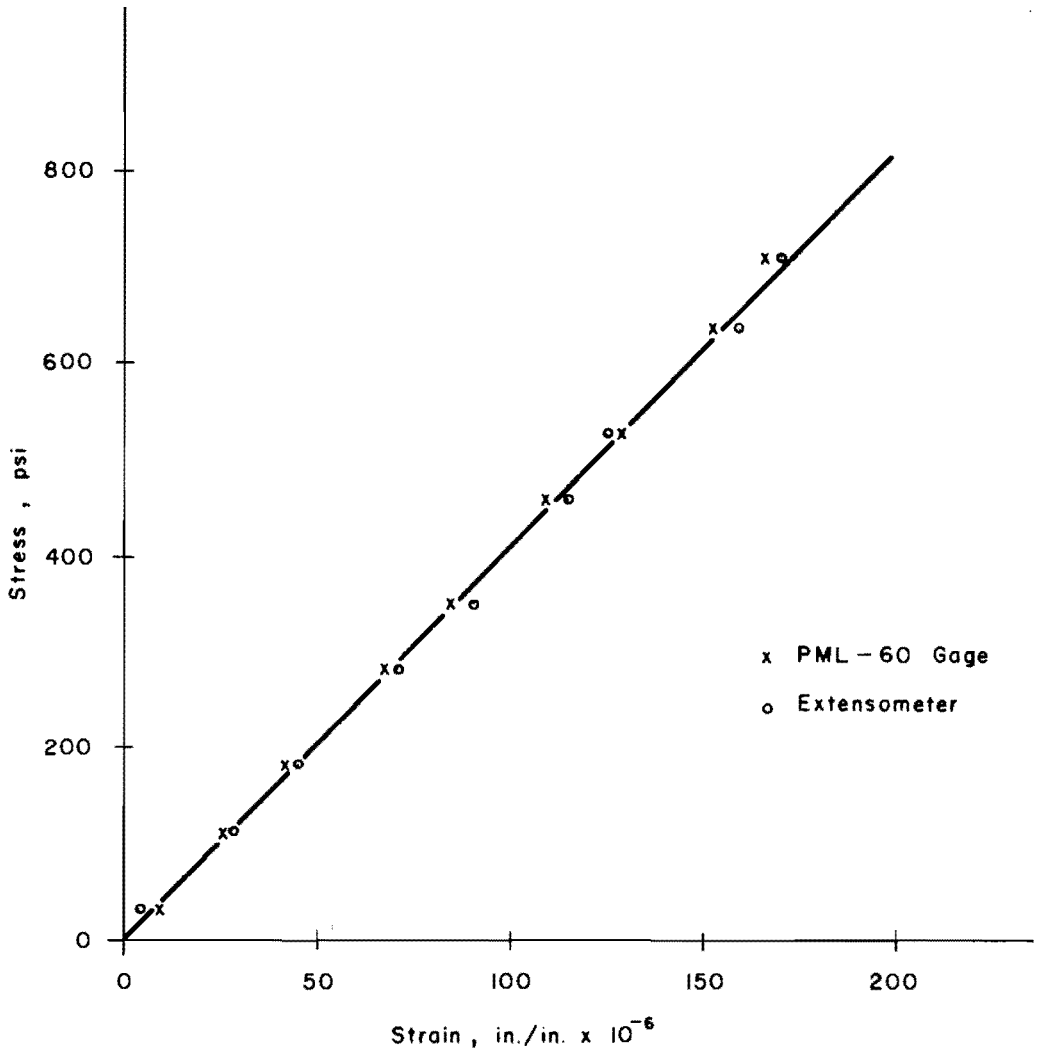

Fig 4. Comparison of strain measured by an extensometer and PML-60 gage.

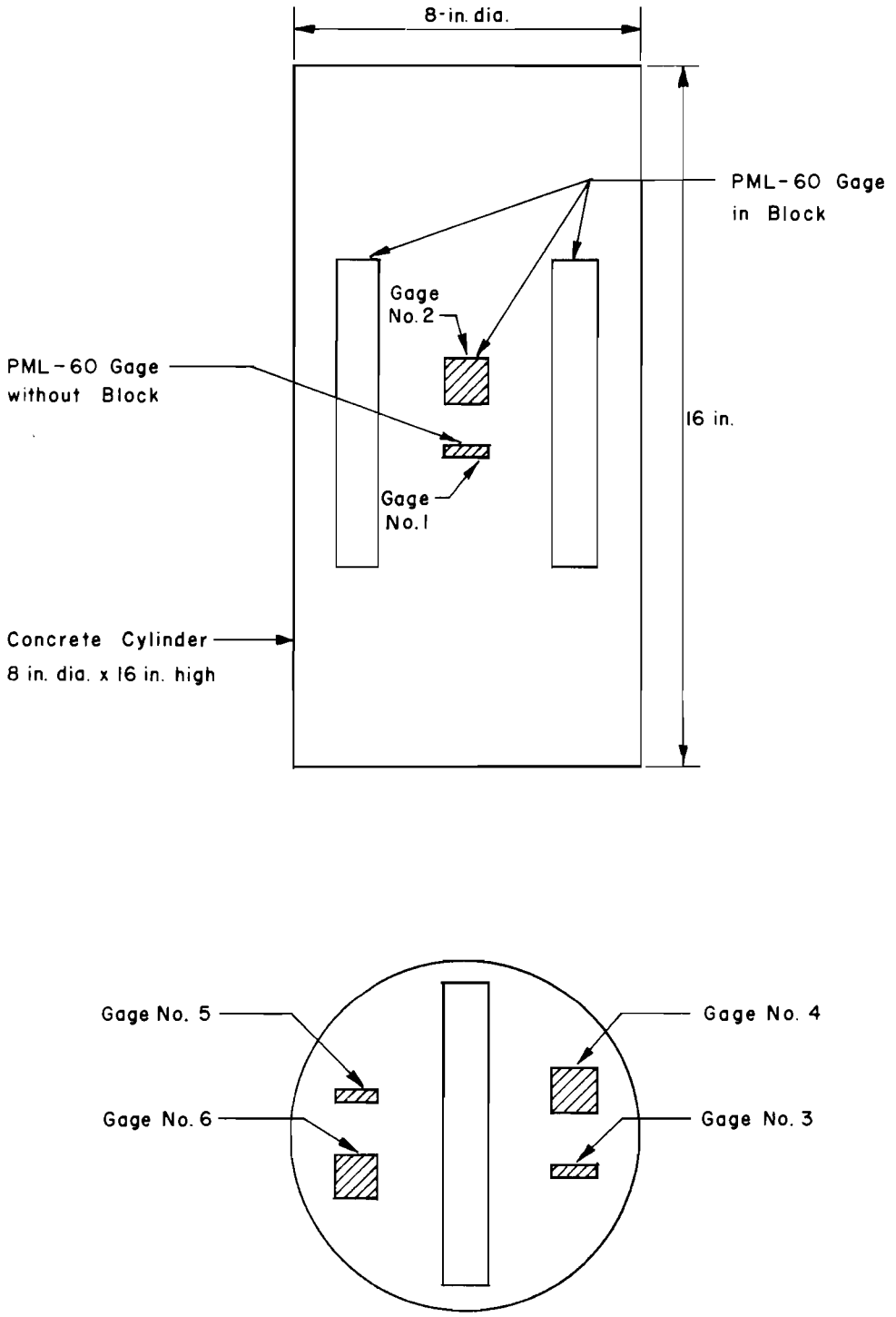

Fig 5. Details of strain gage placement in the concrete cylinder.

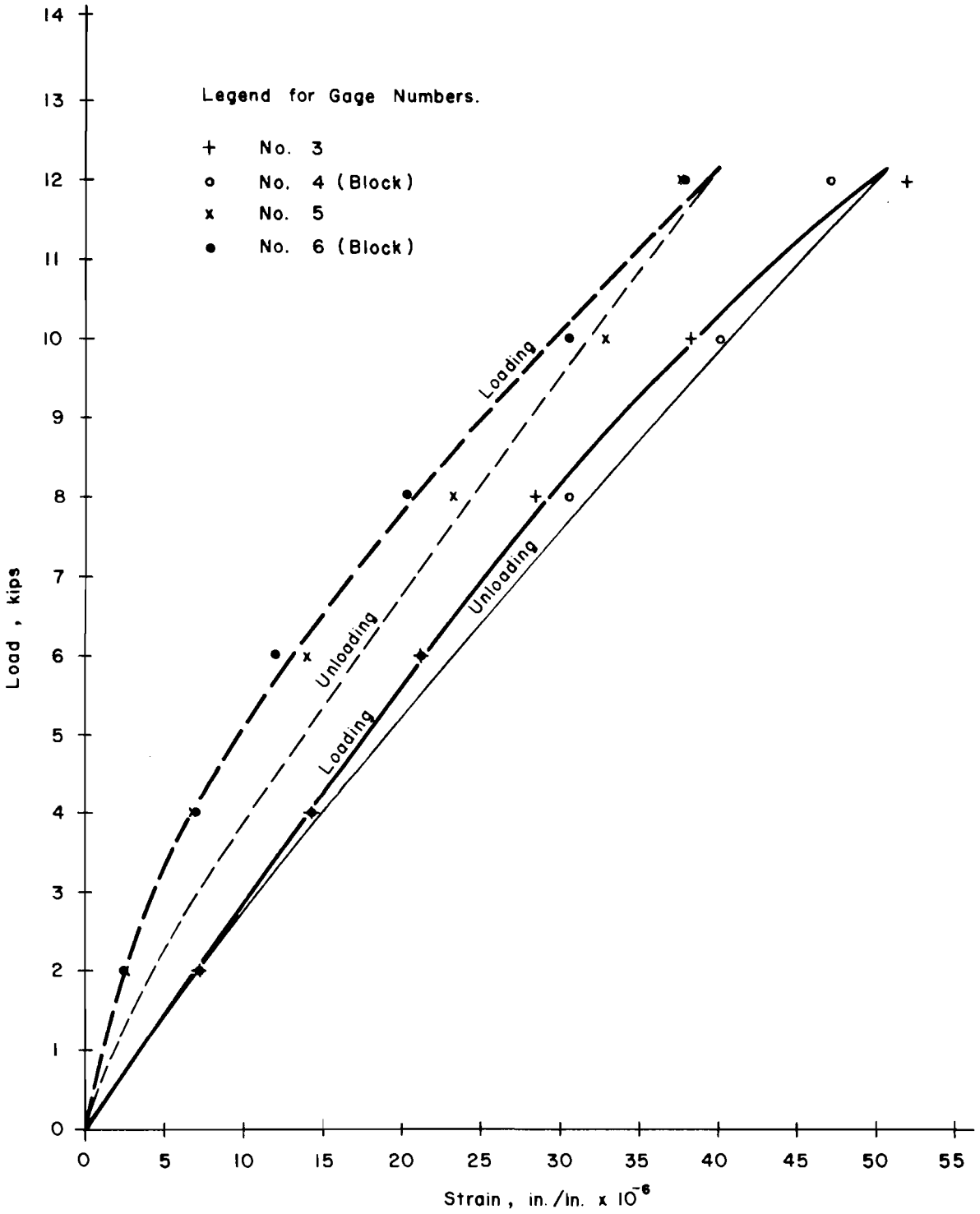

Fig 6. Comparison of strain measured by original PML-60 gages and gages placed in cement mortar blocks.

The hole through which the lead wires were taken out was sealed with "G. C. No. 35 Rubber-to-Metal Cement."

Tell-Tales

Mechanical devices that measure deformation of a shaft through unstrained rods have been used by some investigators (Refs 8 and 2). This method consists of measuring the elastic compression of the shaft through unstrained steel rods or tubes the bottom ends of which are anchored in the shaft. This method does not measure strain directly at a point in the shaft, but measures the total deformation (change in length) over some finite length (length of tell-tale).

Tell-tales, as used in this study, consisted of 1/2-inch-diameter steel tube screwed to a 3-inch-diameter steel plate 1/2 inch thick. An outer steel tube of 3/4-inch diameter was used around the 1/2-inch-diameter tube to protect it against contact with concrete and to ensure a free unrestrained movement of the inner tube. A sleeve 1 inch in diameter by 2 inches high was welded to the steel plate to receive the bottom end of the protective tube. An O-ring seal was provided between the sleeve and the protective tube to prevent the entry of concrete or cement slurry into the space between the inner tube and its protective tube. Before fixing the O-ring seal, the space between the sleeve and the protective tube was filled with grease as an extra precaution. The protective tube was kept 1/2 inch above the steel plate by inserting a pin across the inner and outer tubes near the top end. The length of the inner tube was made about 1 to 1-1/2 inches greater than the outer tube, so that it could have a clear projection of about 1/2 to 1 inch above the outer tube. A plug with smooth surface was inserted on the top end of the inner tube so as to provide an even surface for resting the stem of a dial indicator.

Tell-tales longer than 5 feet were made up of 5-foot sections plus shorter pieces needed to make up the total length. The ends of these small sections of inner tubes were connected to each other with plugs having male and female ends. The ends of outer tubes were connected together with conduit couplings. Figure 7 shows the basic components of the tell-tale setup.

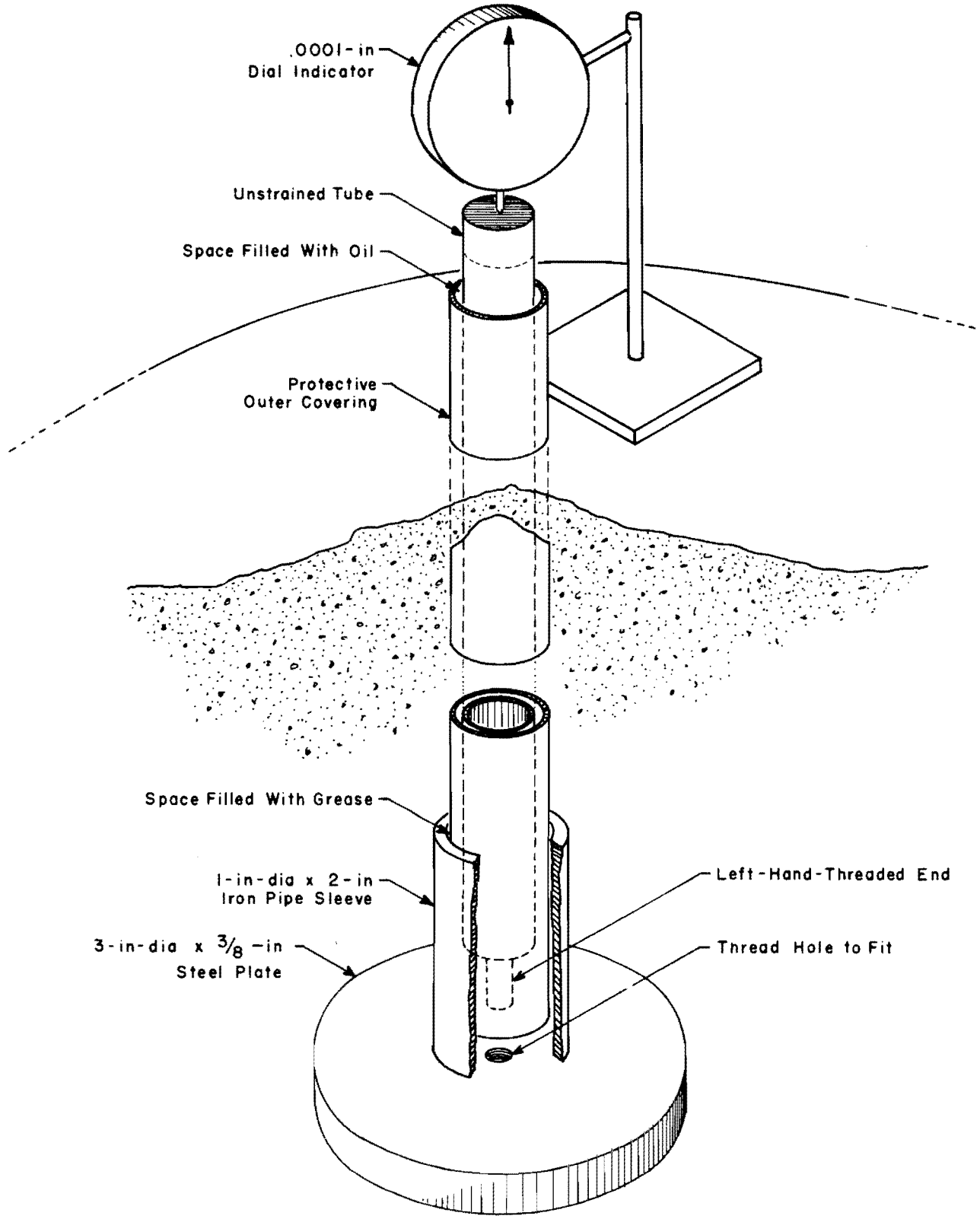

Fig 7. Details of the assembly of the tell-tale system.

Lateral Earth Pressure Cells

Lateral pressure cells (Ref 15) were used for the measurement of lateral earth pressure. These cells use a BLH full bridge diaphragm gage fixed to the diaphragm with epoxy (BLH Epy-150). For details, Center for Highway Research Report No. 89-3, entitled "Measurement of Lateral Earth Pressure Against a Drilled Shaft," may be consulted (Ref 15). Measurements from these gages were not used in this study since the results were very erratic.

Arrangement for Measurement of Settlement of the Shaft

The arrangement for the measurement of vertical movement of the shaft is shown in Fig 8. Reference beams of 4 by 4-inch by 20-foot-long timber were supported at each end by stakes driven about 18 inches into the ground. Supports for dial indicators were fixed on the reference beams. The stem of the dial indicators rested on the flat horizontal surface of the projecting aluminum angle that was cemented to the shaft.

A 2-foot 6-inch tube was fixed to the top steel plate with a 6-inch plastic engineer's scale cemented near the top of the tube. This scale with markings in millimeters was used as an independent device for measuring the settlement of the shaft periodically, with the aid of an engineer's transit. The dial indicator had a least count of .001 inch and a run of 1 or 2 inches.

Locations of Embedment Gages, Lateral Pressure Cells, and Tell-Tales

The locations of embedment gages, tell-tales, lateral pressure cells, and thermocouples in the shaft are shown in Figs 9 and 10.

The embedment gages at each level were placed so as to be located approximately midway between the two adjacent bottom plates of tell-tales. Three embedment gages were installed at each location, except for the bottom set, where four embedment gages were placed. All the gages were spaced approximately equally at each location. A dummy strain gage was placed at every measuring level. The embedment gages, contained in the cement mortar blocks, were tied to the inside of the reinforcement cage as shown in Fig 11. The tell-tales were also tied to the inside of the cage as shown in Fig 11. Lateral earth pressure cells were placed in the hole by hand. Details of installation of lateral pressure gages are given in Ref 15.

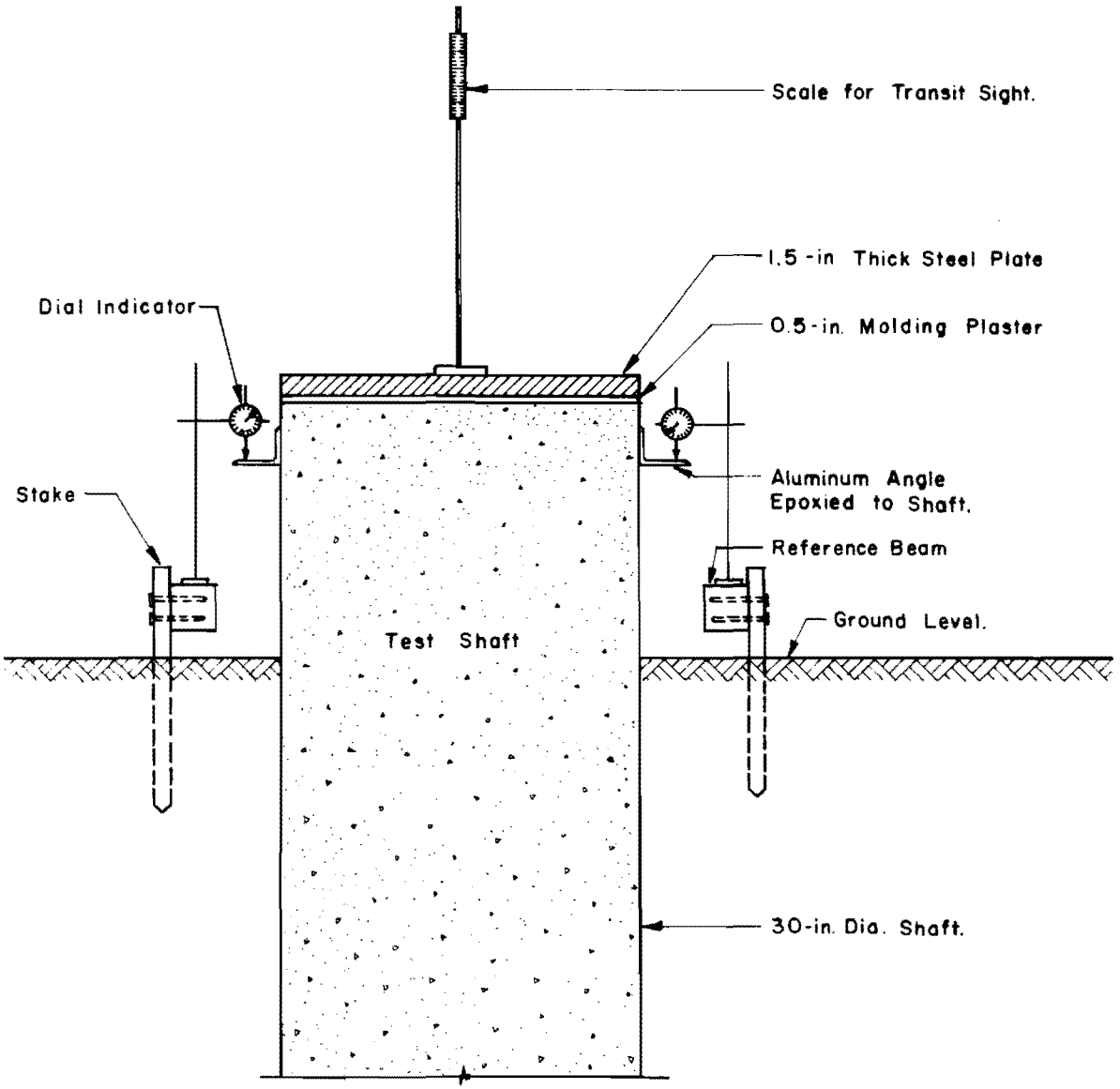

Fig 8. Setup for measurement of shaft movement.

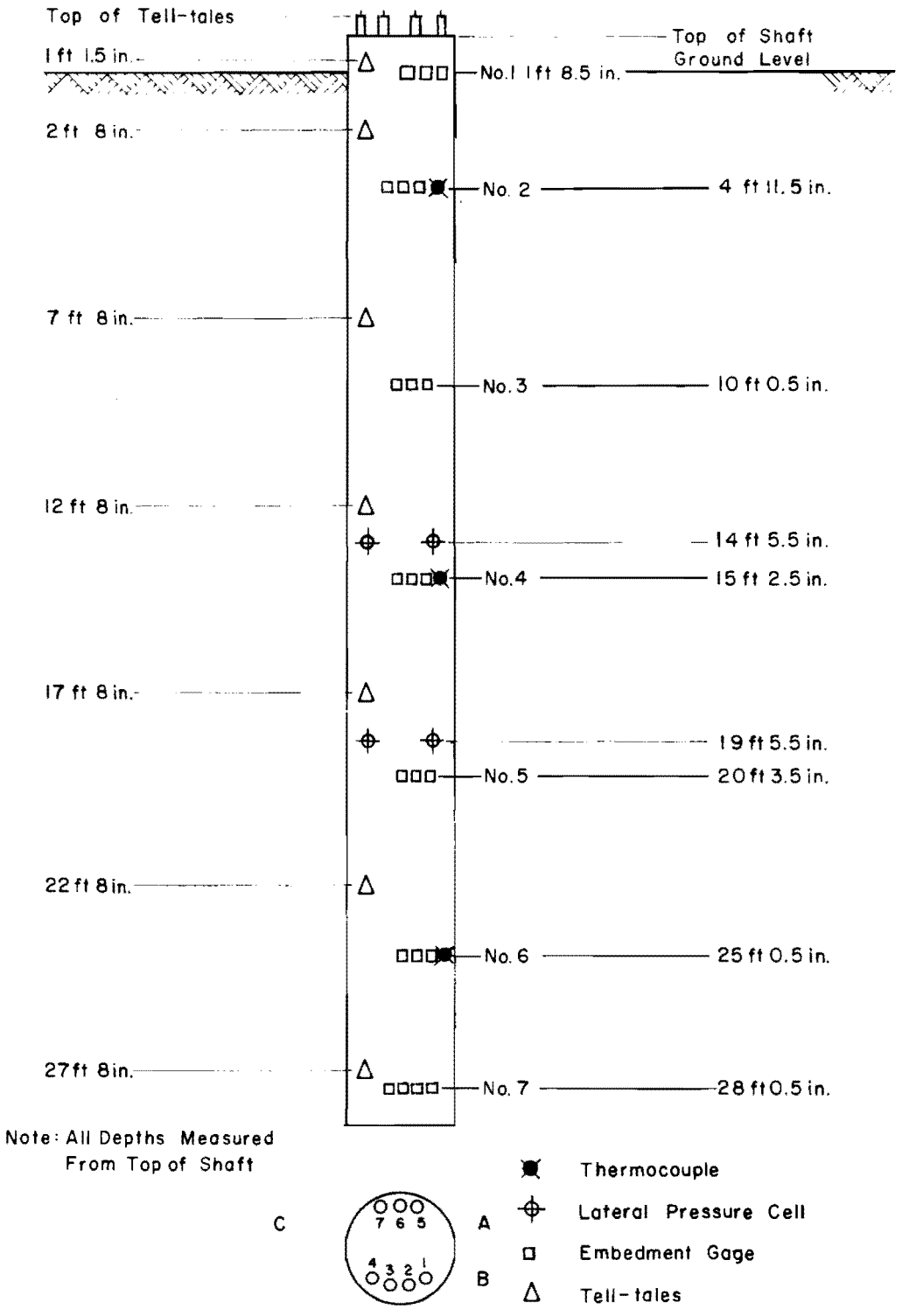

Fig 9. Location of embedment gages, lateral pressure cells, tell-tales, and thermocouples.

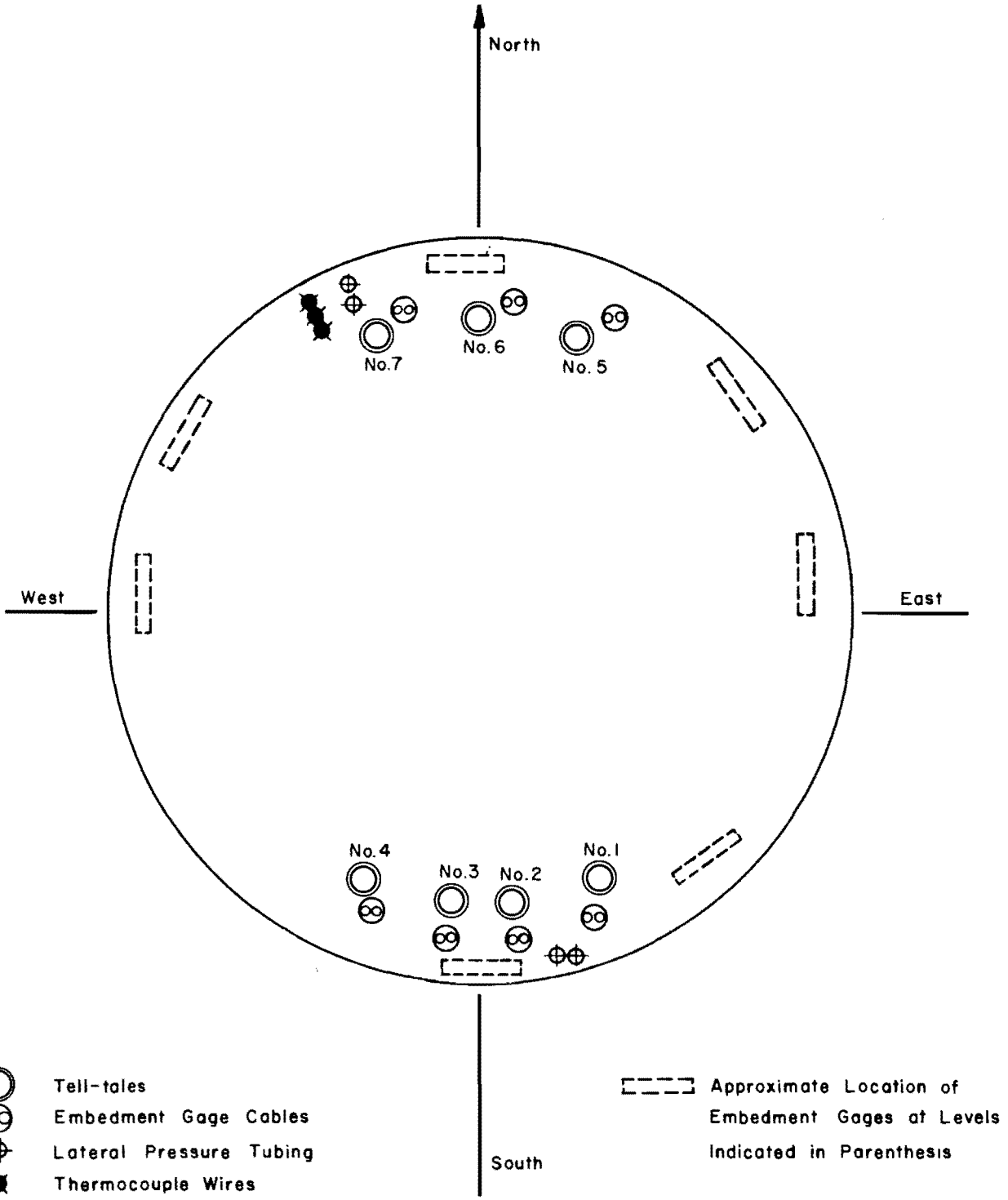

Fig 10. Plan of the shaft showing details of instrumentation.

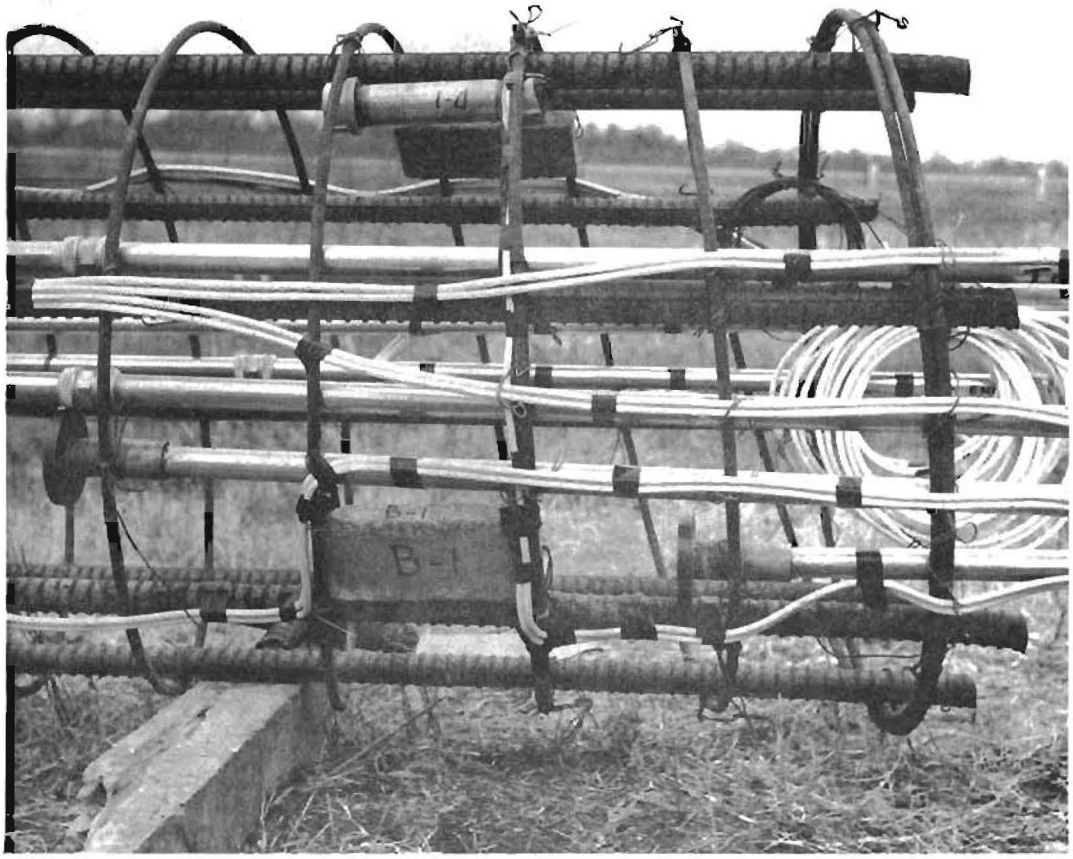

Fig 11. A close-up of the instrumented reinforcement cage.

After the installation of the instrumentation on the reinforcement cage, the cage was carefully lifted by crane and lowered into the bore hole. During the lowering the tell-tales were adjusted again to make them vertical, as shown in Fig 12.

Waterproofing of Strain Gages

Polyester mold gages are claimed to be waterproof by the manufacturer, and hence no extra coating of waterproofing material was applied to the embedment gages. However, since these gages are supplied with about 6-foot-long outgoing vinyl lead wires, splicing to cables was necessary. Splices were made by first baring and then soldering these wires. These splices had to be prevented from shorting to ground, either directly or through moisture which might migrate into the concrete shaft from the surrounding damp soil. This was accomplished by covering each connection with William Beam Gage Kote Nos. 2 and 5 and further by covering the entire splice zones with heat-shrinkable "spaghetti," and finally with "G. C. No. 35 Rubber-to-Metal Cement." Gage Kote No. 2 is a nitrate rubber which dries in 30 minutes when heated. It affords mechanical protection and withstands humid atmospheres, water, and other deleterious agents. Gage Kote No. 5 was used to encapsulate the splices coated with No. 2. It is a two-component rubber-like epoxy resin recommended for waterproofing for direct immersion in water.

Fig 12. Final adjustment of tell-tales and fixing of spacer blocks.

CHAPTER 4. SOIL CONDITIONS

Identification

The test site was located in San Antonio close to the intersection of S. W. Military Drive and U. S. Highway 90, in Bexar county. Three borings were drilled in July 1966 to outline subsurface conditions and to obtain soil samples for laboratory tests. Relatively undisturbed samples of soil 3 inches in diameter and disturbed samples of 5 inches in diameter were collected. Later in January 1968, three additional bore holes were made, essentially to conduct Texas Highway Department cone penetration tests. The locations of various bore holes in relation to the proposed test shaft are shown in Fig 13. Laboratory tests were run to determine natural moisture content, density, index properties, and shear strength. Drilling Reports are in Appendix 5.

Soil Profile

The general soil profile shown in Fig 14 may be summarized as follows. The upper layer is black or dark gray clay which gradually changes to light gray with increasing depth. This layer is about 10 feet thick and highly plastic. According to the unified classification system the soil may be classified as CH . The clay is highly slickensided and contains plant roots, gravel, and sea shells.

The second layer, 8 feet thick, consists of yellow to yellowish-brown clay of high plasticity. This layer contains very thin lenses of silt and falls in the CH group as per unified classification system. This layer also contains plant roots, sea shells, and is highly slickensided.

The layer from 18 feet to a depth of approximately 36 feet consists of brown clay shale with layers of sandstone and sea shells. The shale is of medium plasticity and is classified as CL . The stratum is erratic and some soft rock is encountered at places.

The stratum below the 36-foot depth is bluish-gray well-bonded clay shale and is very hard.

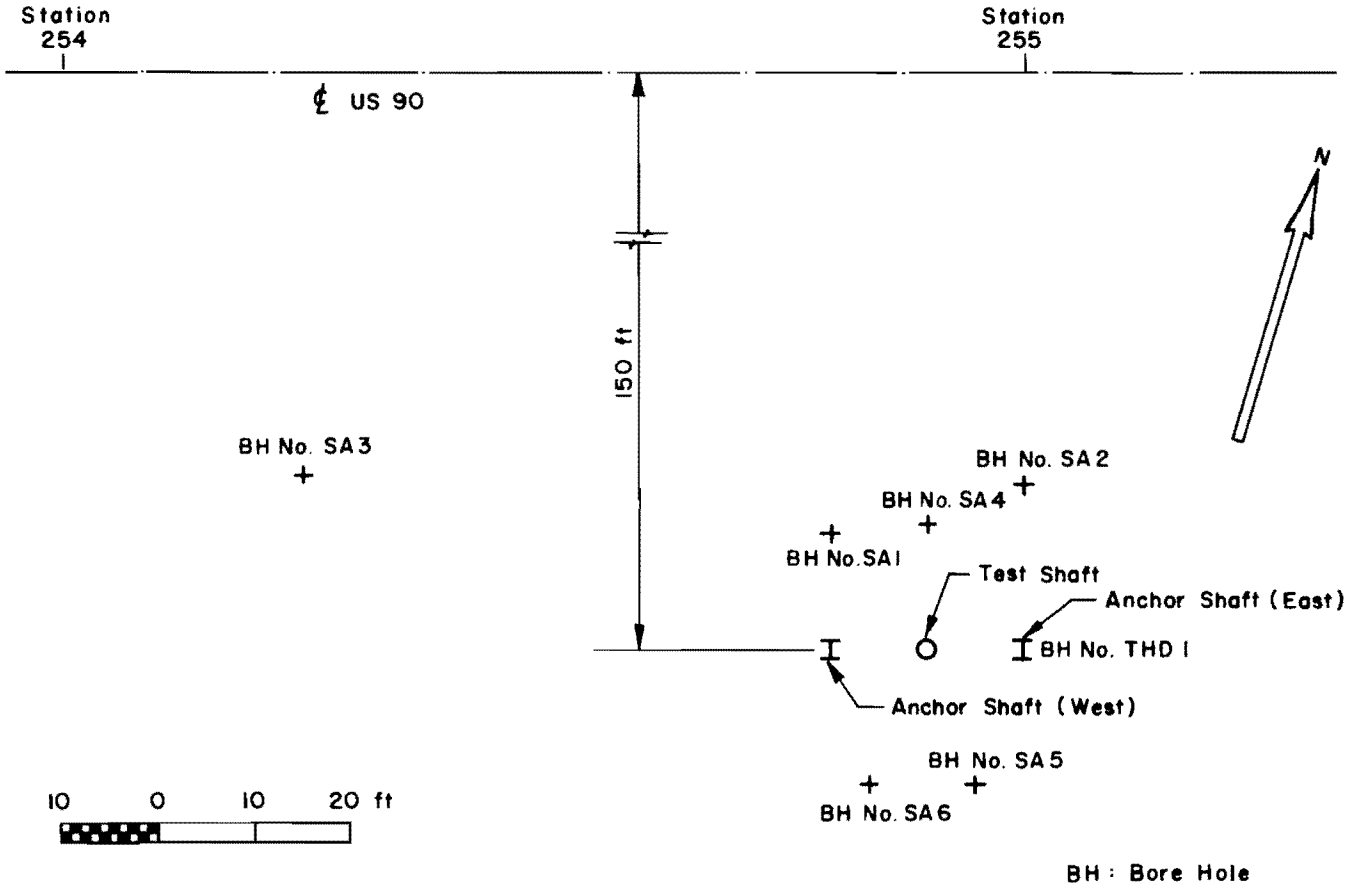

Fig 13. Location of test shaft and bore holes in San Antonio.

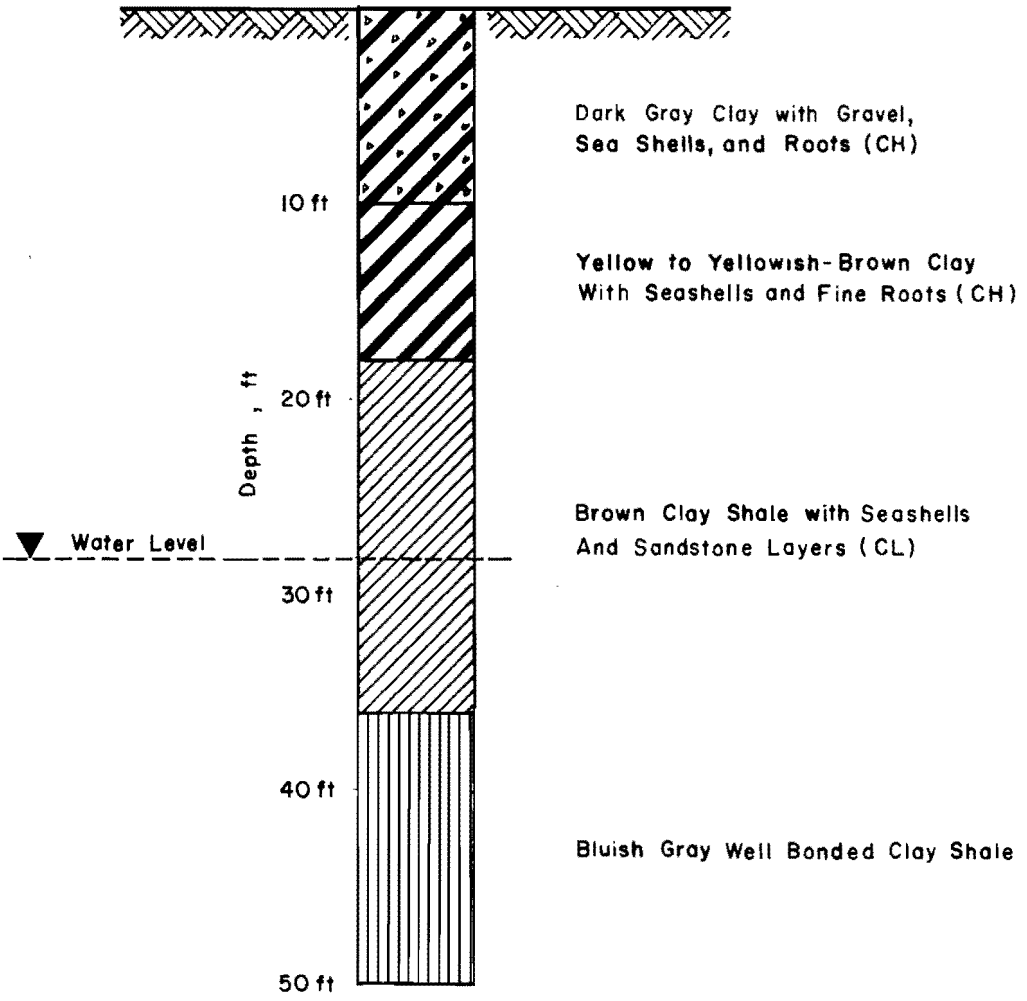

Fig 14. Representative soil profile at the test site.

Natural Moisture Content

Natural moisture content of soil samples was determined in the laboratory in the usual manner. The variation of moisture content versus depth is shown in Fig 15. It will be seen from this figure that the moisture content varied between 20 to 32 percent in clay in the upper 18 feet and 15 to 25 percent in the clay shale between 18 to 36 feet. A slight increase in moisture content is indicated below 36 feet. The water table was found to be about 25 feet below ground surface.

Since the fluctuation of moisture content is accompanied by change in shear strength of clay it was thought necessary to record periodically the changes in natural moisture content of the overburden clay. For this purpose a nuclear probe was used. The details of installation and method of measuring the moisture content with such a nuclear device are given in Center for Highway Research Report No. 89-4, entitled "The Nuclear Method of Soil Moisture Determination at Depth" (Ref 4). The extreme variations in water content with time are shown in Fig 16 for the period of 12 months during which various load tests were run. A record of variation for the same period is shown in Table 1.

Index Properties

The results of liquid limit and plastic limit tests are shown in Fig 17. For the upper 18 feet of clay, the plastic limit varies between 23 and 37 and the liquid limit ranges from 58 to about 76. For clay shale below 18 feet the plastic limit varies between 16 and 26 and the liquid limit between 28 and 62. Low plasticity of shale indicates its silty nature. The plastic limit of clay and clay shale are very close to their natural water content.

Soil Classification

Unified soil classification of both the upper layer of clay and clay shale is shown in Fig 18. Upper layer of clay is classified as CH and the clay shale as CL . Some samples of clay shale had large clay content and lie near the boundary between the CL and CH groups.

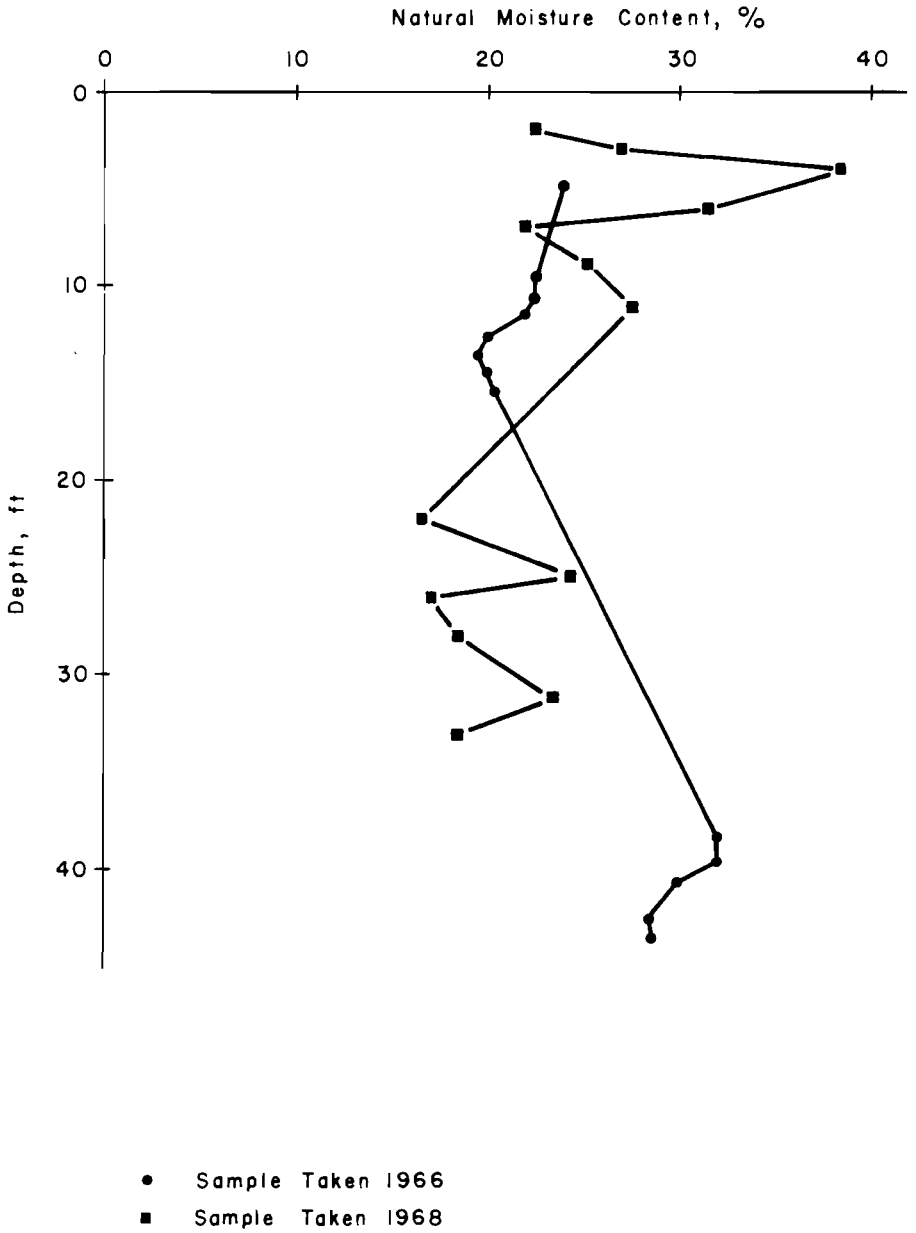

Fig 15. Natural moisture content versus depth.

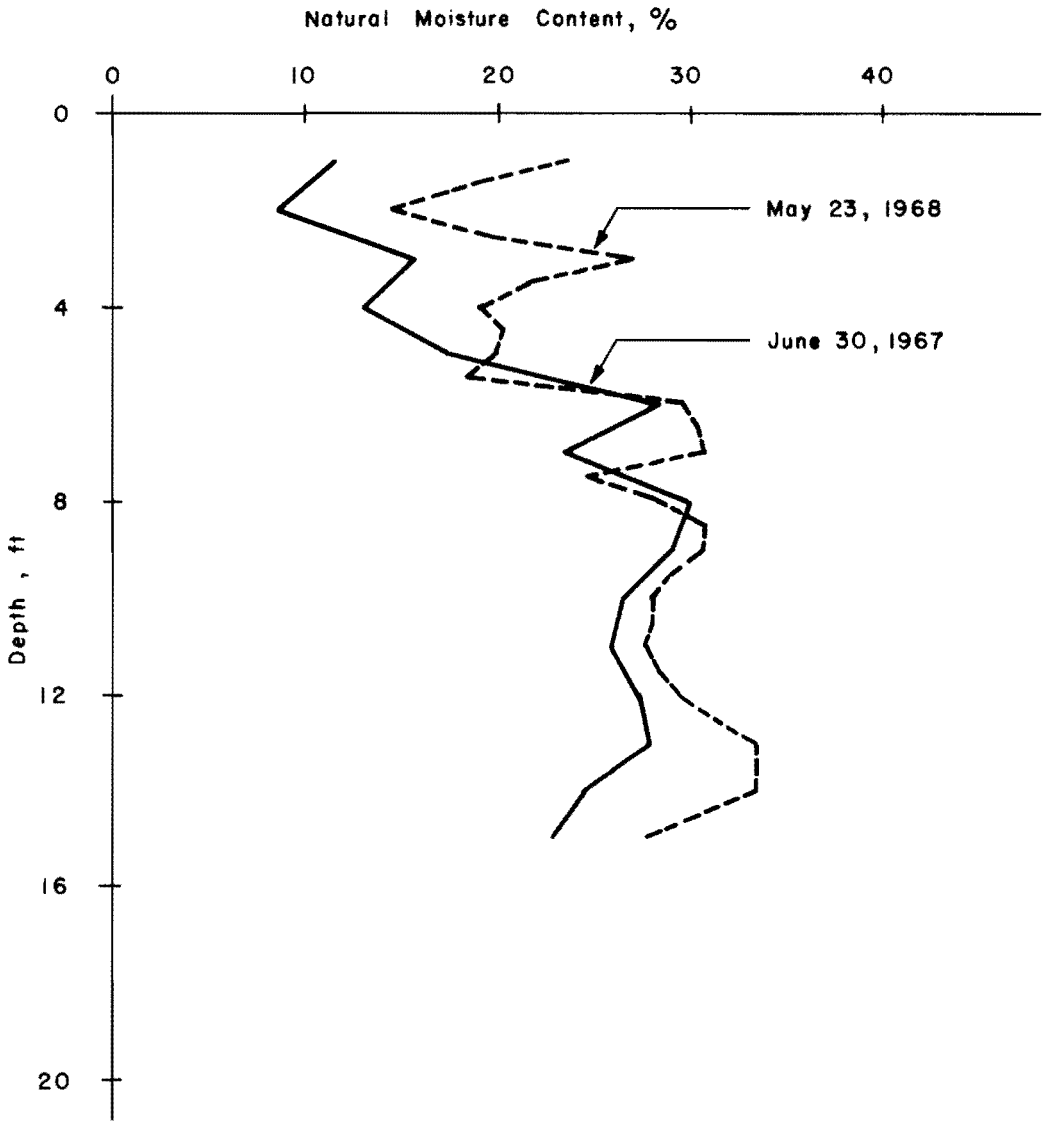

Fig 16. Variation of natural moisture content with depth during 12 months.

TABLE 1. RECORD OF MOISTURE VARIATION DURING 12-MONTH PERIOD OF TEST SERIES

DEPTH, FEET	MOISTURE CONTENT IN PERCENT						
	6-30-67	8-10-67	10-7-67	11-30-67	1-4-68	3-19-68	5-23-68
1.0	11.6	12.3		23.6	23.1	19.3	24.8
1.5				17.3	16.8	14.1	18.3
2.0	8.6	9.0	12.2	14.1	13.5	12.5	14.4
2.5				19.2	18.9	19.2	19.6
3.0	15.5	15.9		26.3	26.1	27.5	27.1
3.5				19.0	18.4	22.2	21.7
4.0	13.1	13.7	16.3	17.1	16.6	19.2	19.2
4.5				19.8	17.9	20.1	20.2
5.0	17.4	17.9		19.6	18.6	19.9	19.7
5.5				18.0	18.0	18.3	18.2
6.0	28.4	30.3	28.0	28.3	28.7	28.9	29.0
6.5				29.9	30.4	30.6	30.5
7.0	23.4	23.9		30.7	30.9	30.6	30.8
7.5				24.3	24.4	24.6	24.5
8.0	30.1	30.3	28.1	27.8	28.4	28.4	28.3
8.5				30.9	31.4	30.9	31.1
9.0	29.0	29.7		30.6	31.1	31.0	30.7
9.5				28.8	29.0	29.2	29.2
10.0	26.5	27.2	27.8	27.6	27.6	27.8	28.1
10.5				27.4	28.0	27.6	28.0
11.0	25.9	26.9		27.1	27.8	27.3	27.8
11.5				27.7	27.7	27.7	28.4
12.0	27.3	28.7	29.0	29.1	29.8	29.1	29.3
12.5				30.6	31.3	30.9	31.3
13.0	27.9	29.2		32.7	33.1	33.8	33.6
13.5				30.1	31.1	32.1	33.4
14.0	24.5	25.3	27.2	27.7	28.3	29.3	33.4
14.5				25.4	26.1	26.2	30.3
15.0	22.9	23.6		24.8	24.8	24.9	27.6

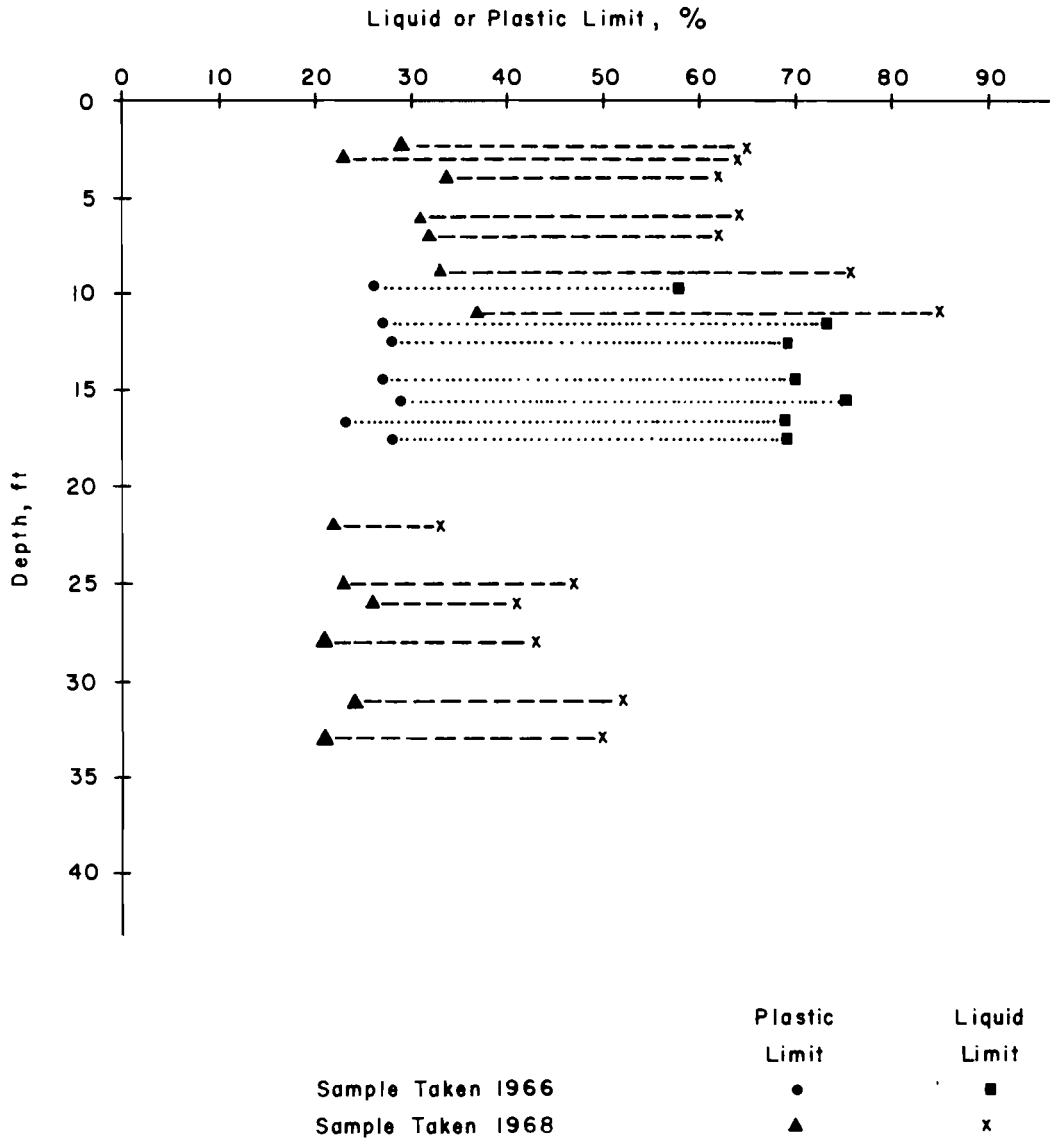

Fig 17. Liquid limit and plastic limit versus depth.

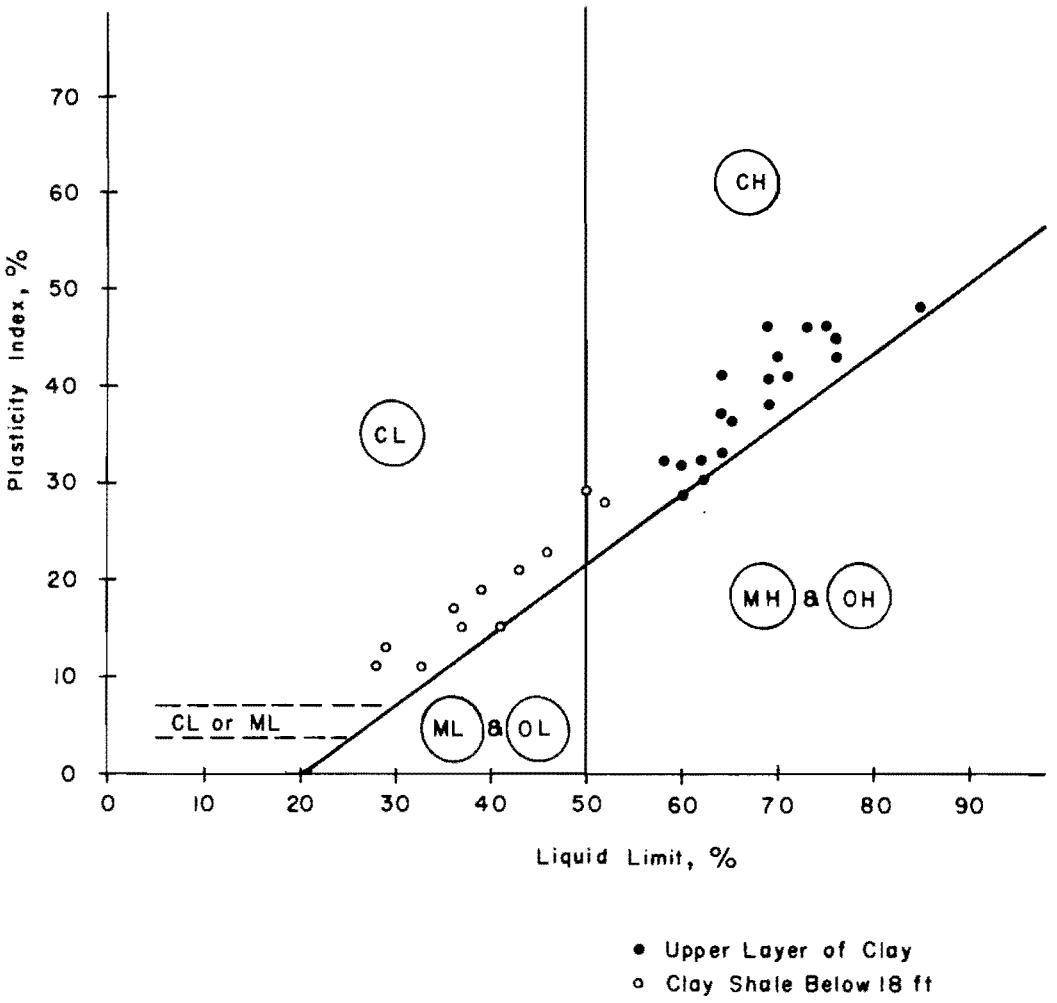

Fig 18. Unified soil classification.

Shear Strength from Laboratory Tests

Unconfined compression tests and triaxial tests of undrained and unconsolidated type were run on relatively undisturbed samples. However, a very limited number of tests could be run due to the difficulty in extracting fairly undisturbed test specimen. The soil is extremely slickensided and contains a large amount of fine plant roots, gravel, and sea shells. The presence of fissures and roots caused the undisturbed samples to break along weak planes. The nature of cracks in one of the undisturbed samples is shown in Fig 19.

Results of unconfined compression and triaxial tests are shown in Fig 20. A large variation in compressive strength of clay will be observed from this figure. This is chiefly due to the presence of roots, fissures, gravel, and sea shells. Some variation is attributed to the different moisture content of samples. Undisturbed samples could not be collected below the depth of 18 feet because a sampling tube could not be pushed into the clay shale.

Stress-strain curves for the various soil samples are shown in Fig 21. The value of confining pressure in tons/ft^2 is indicated on each curve along with the depth of sampling in parenthesis. Due to the presence of roots and fissures the failure stress varied considerably. In most of the samples, the failure was observed to be of brittle nature. The failure strain varied from 2.0 to 4.5 percent except in one case where it was as high as 13 percent, not shown in the figure. The deviator stress at failure varied from 1.52 to 8.57 tons/ft^2.

Shear Strength from Field Tests

Since undisturbed samples of shale could not be collected, other methods of evaluating shear strength were considered. As this report is intended to be of direct interest to Texas Highway Department, it was thought that a method of estimating shear strength in the field commonly used by Texas Highway Department would be most desirable. Thus, it was decided to conduct the standard THD cone penetration test. The details of the cone penetration test are as follows.

The cone penetration test was performed by attaching a 3-inch-diameter penetrometer cone, as shown in Fig 22, to the drill stem of 2-3/8-inch diameter and lowering it to the bottom of the hole. The anvil was attached to the top of the drill stem, and the automatic tripping mechanism with a 170-pound hammer

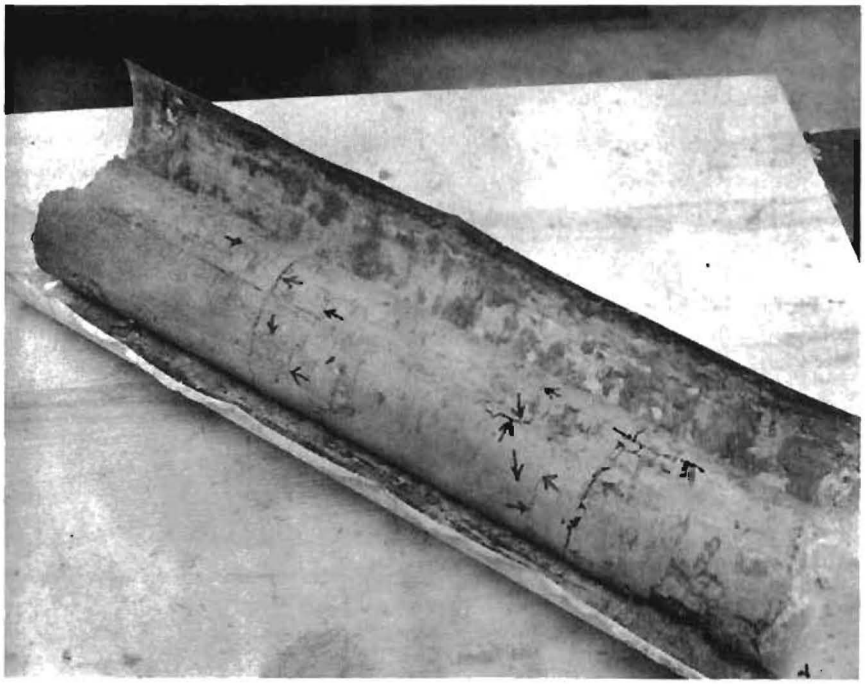

Fig 19. Cracking in undisturbed soil samples.

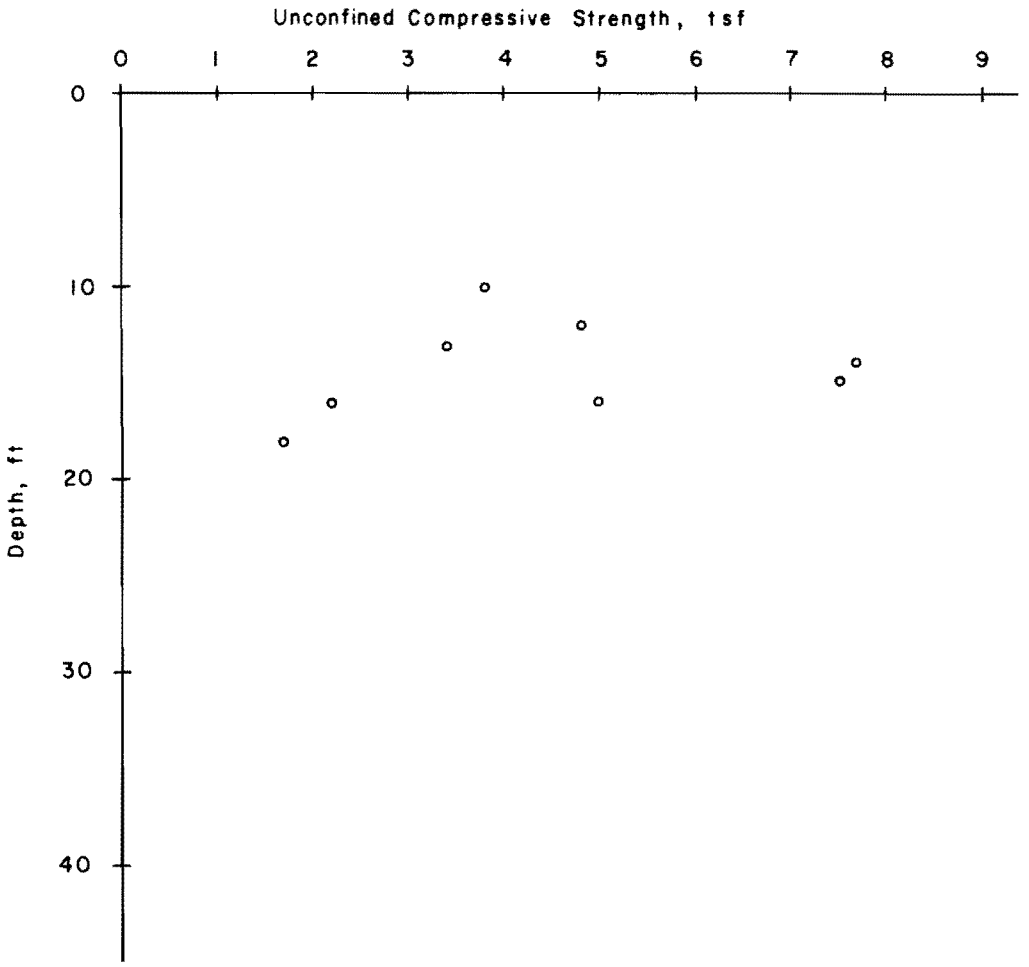

Fig 20. Compressive strength versus depth.

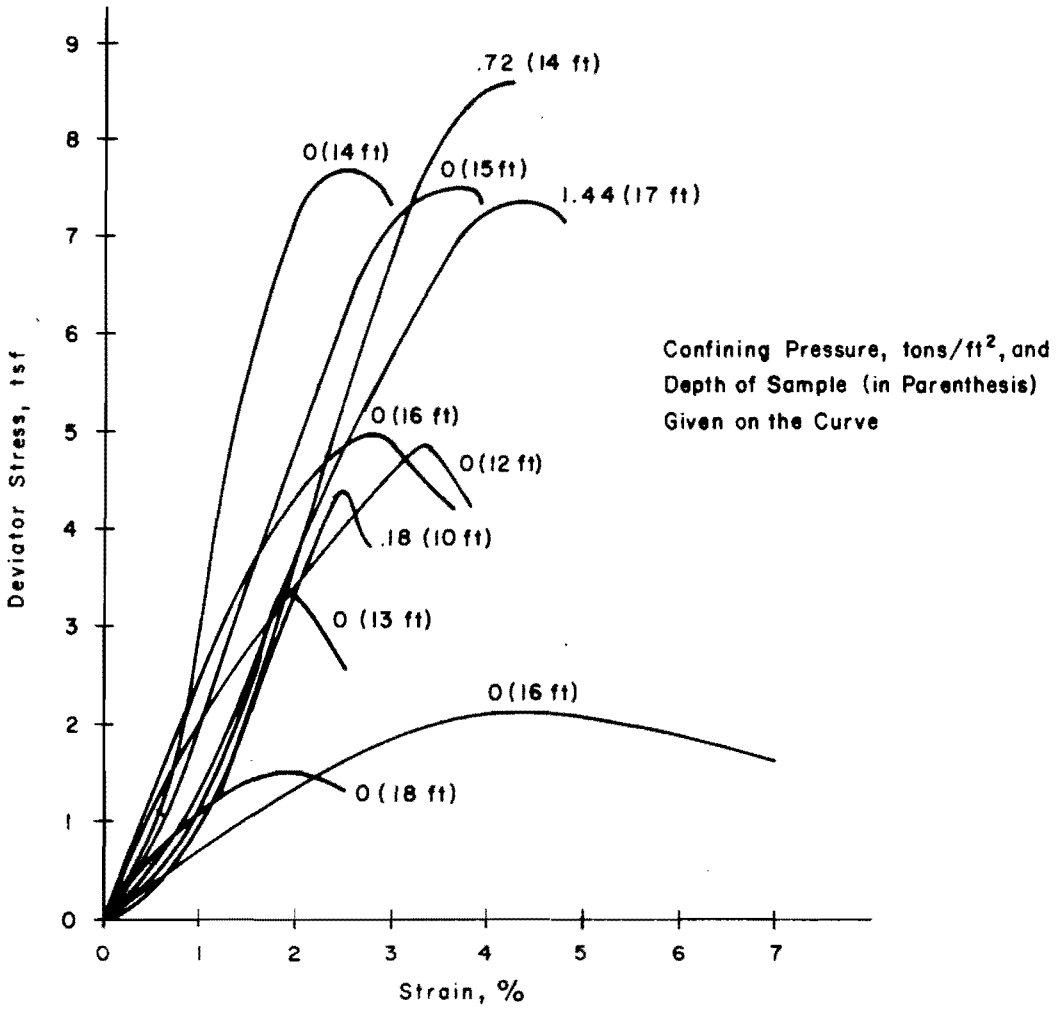

Fig 21. Stress-strain curves.

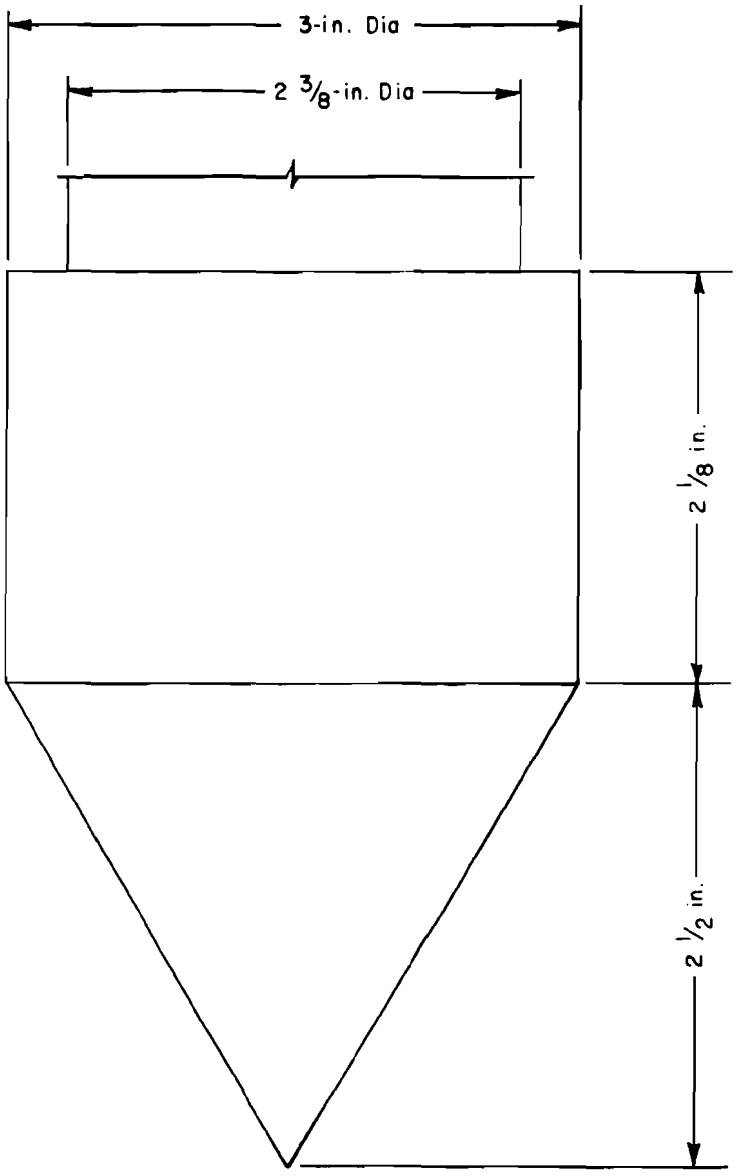

Fig 22. Details of THD cone penetrometer.

was placed in position on top of the anvil (Ref 21). The drop of the 170-pound hammer was regulated to be 2 feet. The cone was seated usually by 12 blows of the hammer. In relatively soft layers the penetrometer cone was driven one foot and the number of blows required for each 6-inch increment was recorded. In harder strata the penetrometer cone was driven with the resulting penetration in inches accurately recorded for the first and second 50 blows for a total of 100 blows. In either case, the penetrometer cone was driven into the stratum 6 inches or 50 blows for each increment, depending upon which occurred first.

The THD cone penetration test was conducted in 4 locations shown in Fig 13 by BH Nos. SA4, SA5, SA6, and THD1. Up to a depth of 18 feet the number of blows required to drive through 12 inches varied usually from about 10 to 40 and occasionally beyond 60. Below the 18-foot depth the cone could not be driven through 12 inches in less than 100 blows. Hence the penetration in inches for 100 blows was recorded. The results of these tests are therefore presented in two parts in Figs 23(a) and 23(b). It will be seen from these figures that resistance to cone penetration increases with increasing depth up to 18 feet. Scatter of points is due to presence of gravel and shell. However below 18 feet there seems to be a large scatter of points, showing erratic variation in resistance. Complete Drilling Reports are in Appendix 5.

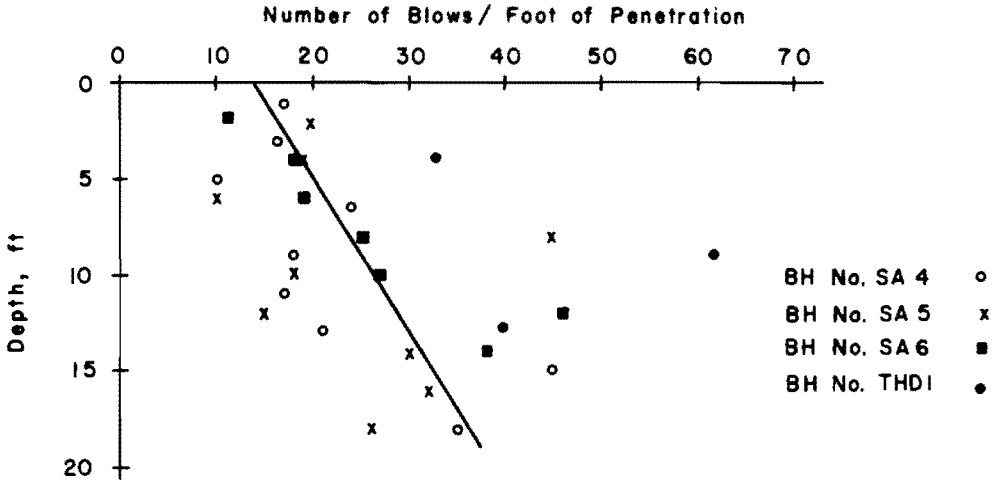

Fig 23(a). Variation of N , the number of blows down to a depth of 18 feet.

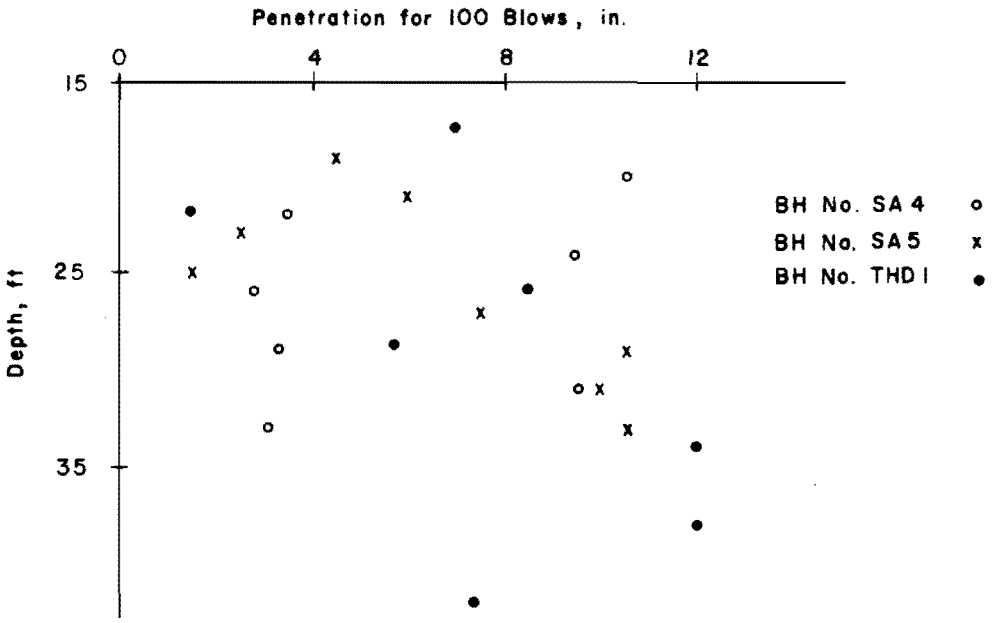

Fig 23(b). Variation of THD cone penetration in inches below 18 feet depth.

CHAPTER 5. DESIGN OF FIELD TEST SYSTEM

Design of Test Shaft

Drilled shafts with the diameter ranging between 24 inches and 36 inches and with an enlarged base are commonly used by the Texas Highway Department. Therefore, a 30-inch-diameter shaft with a length of 30 feet was proposed for the test. Since the present study was aimed at the analysis of load distribution in a shaft of uniform diameter, no enlarged base was provided.

The design load for the test shaft was computed on the basis of soil profile shown in Fig 26. The strength properties which were used for design are

Zone of Soil	Depth, feet	Unconfined Compressive Strength (q_u) Tons/ft^2	of Shear, $c = q_u/2$ Tons/ft^2
1	0 to 10	2	1
2	11 to 18	3 to 8	4
3	19 to 36	3 to 6	3
4	> 37	6	3

The ultimate bearing capacity Q_u of the test shaft was computed from the formula

$$Q_u = \sum_{i=1}^{3} c_i H_i C + c_3 N_c A \qquad (5.1)$$

where

c_i = shear strength of zone i ,

H_i = thickness of zone i ,

C = perimeter of shaft,

N_c = bearing capacity factor equals 9,

A = cross-sectional area of shaft at base.

Using the above formula Q_u for the test shaft was found to be 745 tons. In arriving at this value of Q_u, maximum values of C were used. This was necessary to obtain the upper limit of Q_u for the design of anchor shafts and reaction beams.

Design of Anchor Shaft

No rational approach is available for the design of an anchor shaft, hence the design was based on the approximate formula for pullout resistance, Q_{all} of an under-reamed shaft as given by;

$$Q_{all} = 7.4\, A_n c + W \tag{5.2}$$

where

A_n = cross-sectional area of under-reamed section less cross-sectional area of shaft,

c = average shear strength,

W = submerged weight of concrete shaft.

The above formula is based on the assumption that there is no bond developed between shaft surface and soil at the time of pullout. For an anchor shaft with dimensions shown in Fig 24, the Eq 5.2 can be written as

$$Q_{all} = 7.4\, c\, \frac{\pi}{4}(d_2^2 - d_1^2) + (h_1 + h_2)\, \frac{\pi}{4} d_1^2 (Y_c - Y_w) \tag{5.3}$$

where

Y_w = unit weight of water,

Y_c = unit weight of concrete.

For an anchor shaft of 3-foot diameter with a bell diameter of 9 feet and bell height of 5 feet, the total length h is found to be 50 feet for a

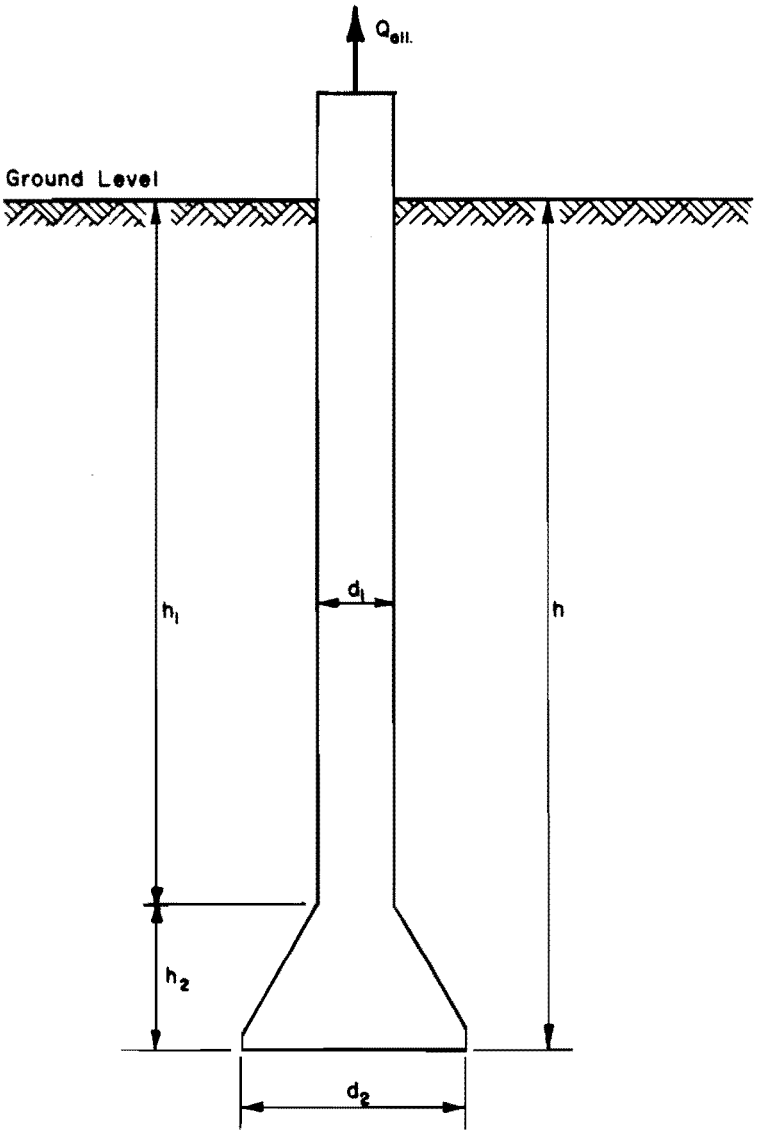

Fig 24. Dimensions of an anchor shaft as used in Eq 5.3.

pullout resistance of 745 tons. Two anchor shafts of the same dimensions were provided so as to give a factor of safety of two. Each anchor shaft was reinforced with a 14WF127 steel column, and with 10 NOS. of 1-1/4-inch diameter steel bars. The bell was reinforced with 10 inclined steel bars of 1-1/4-inch diameter as shown by dotted lines in Fig 25.

Figure 25 shows the general layout of the load testing setup. The reaction beams for transmitting the load from the test shaft to the anchor shaft are indicated in the same figure. Details of various connections are shown in Appendix 1. A view of the anchor shafts and reaction beams is shown in Fig 26.

Hydraulic Jacks and Pumping System

The two hydraulic rams, each of 400-ton capacity, which were used to apply the load, are shown in Fig 27. Each ram had a separate manually operated pump. The pumps were hooked so as to provide a common pressure line. Two pressure gages were attached to this common pressure line. One pressure gage had a resolution of 0.5 ton and was used for loads up to 125 tons. The other pressure gage had a resolution of 5 tons and was used for loads greater than 125 tons. During the earlier load tests it was found that these pumps could not be used for loads greater than 900 tons due to failure of O-ring seals. Therefore an air-operated hydraulic power unit was used for Tests No. 4 and 5.

Readout System

The measurement of strain with the help of electrical resistance strain gages requires balancing of the Wheatstone bridge. For each active strain gage in the shaft this procedure requires a separate balancing of the bridge. Since 22 active strain gages were installed in the shaft, it was felt necessary to design an effective switch system to minimize the time of reading each individual gage. For this purpose a 4-pole, 11-position switch with silver contacts was fabricated. The wire leads from various active strain gages and dummy gages, installed in the shaft, were brought out and hooked to this switchboard. The details of the switch and the scheme of connections to a Budd portable strain indicator for a typical level are shown in Fig 28. The scale on the strain indicator was calibrated to read the strain in 10^{-6} units. The switchboard along with the Budd strain indicator, as used in the field, is shown in Fig 29.

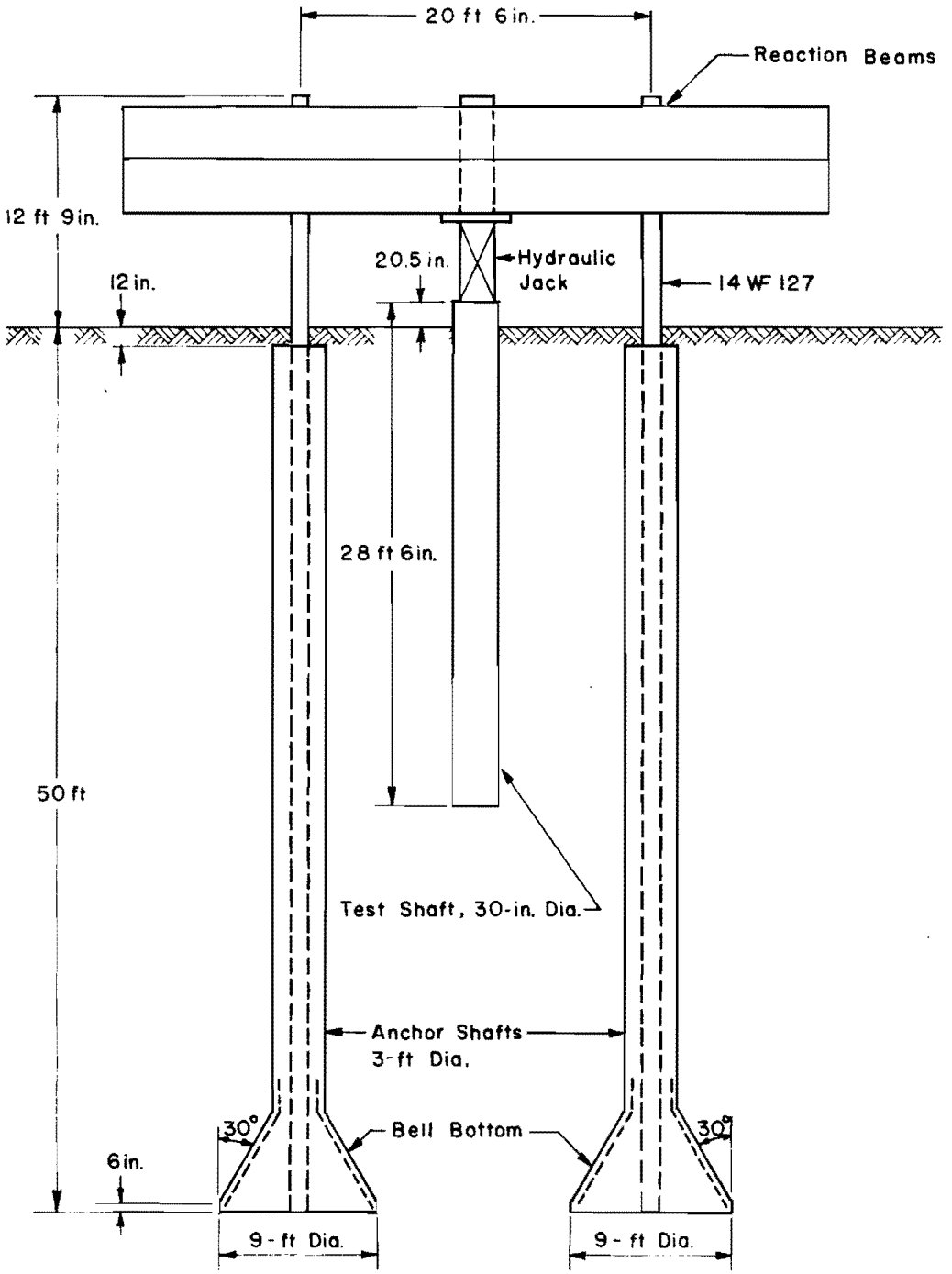

Fig 25. General layout of test shaft, anchor shafts, and reaction beams.

Fig 26. General view of reaction beams and other testing equipment ready for test.

Fig 27. Setup of hydraulic rams seated on a steel plate and reference beams for supporting dial indicators.

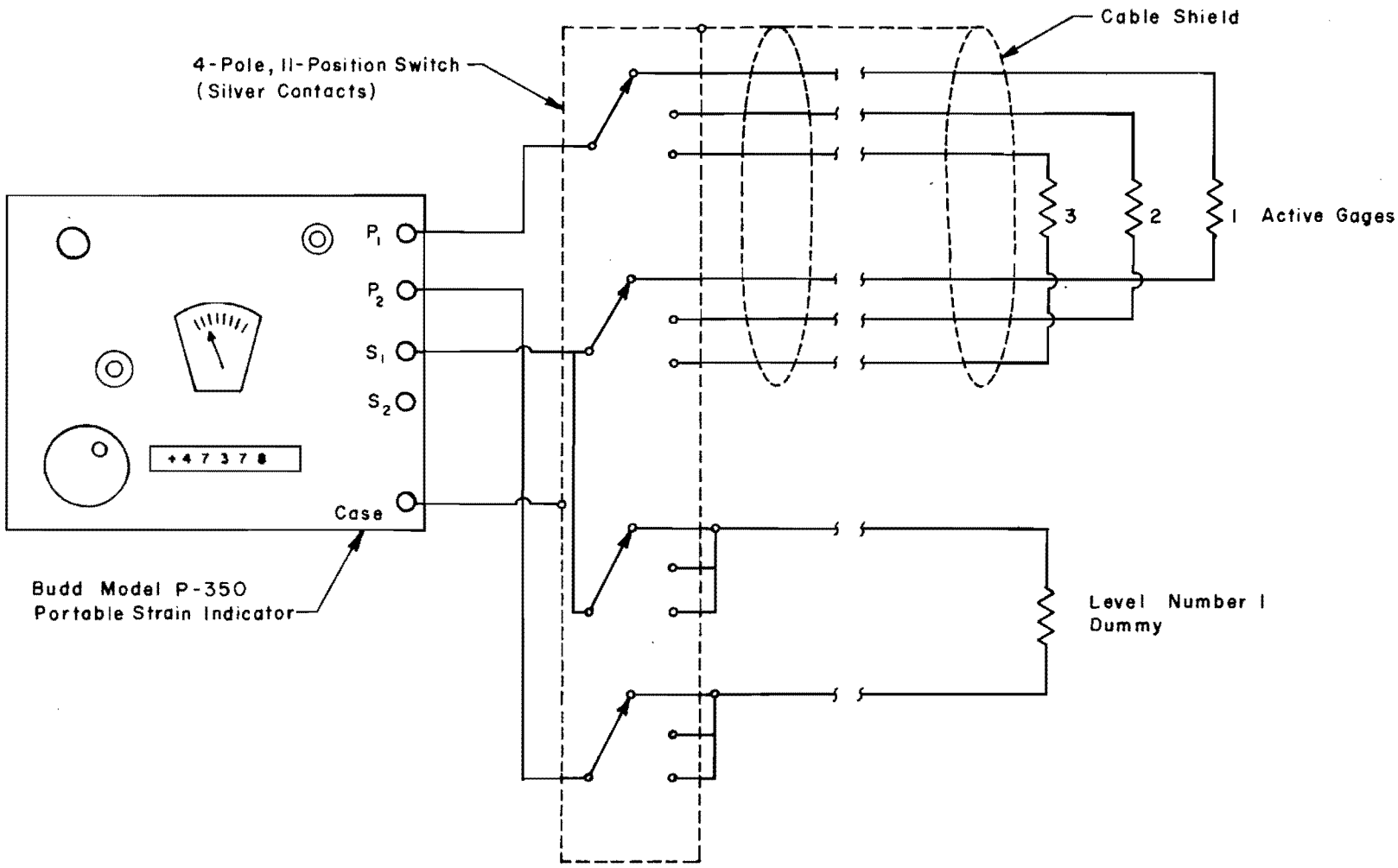

Fig 28. Embedment strain gage readout system (typical level).

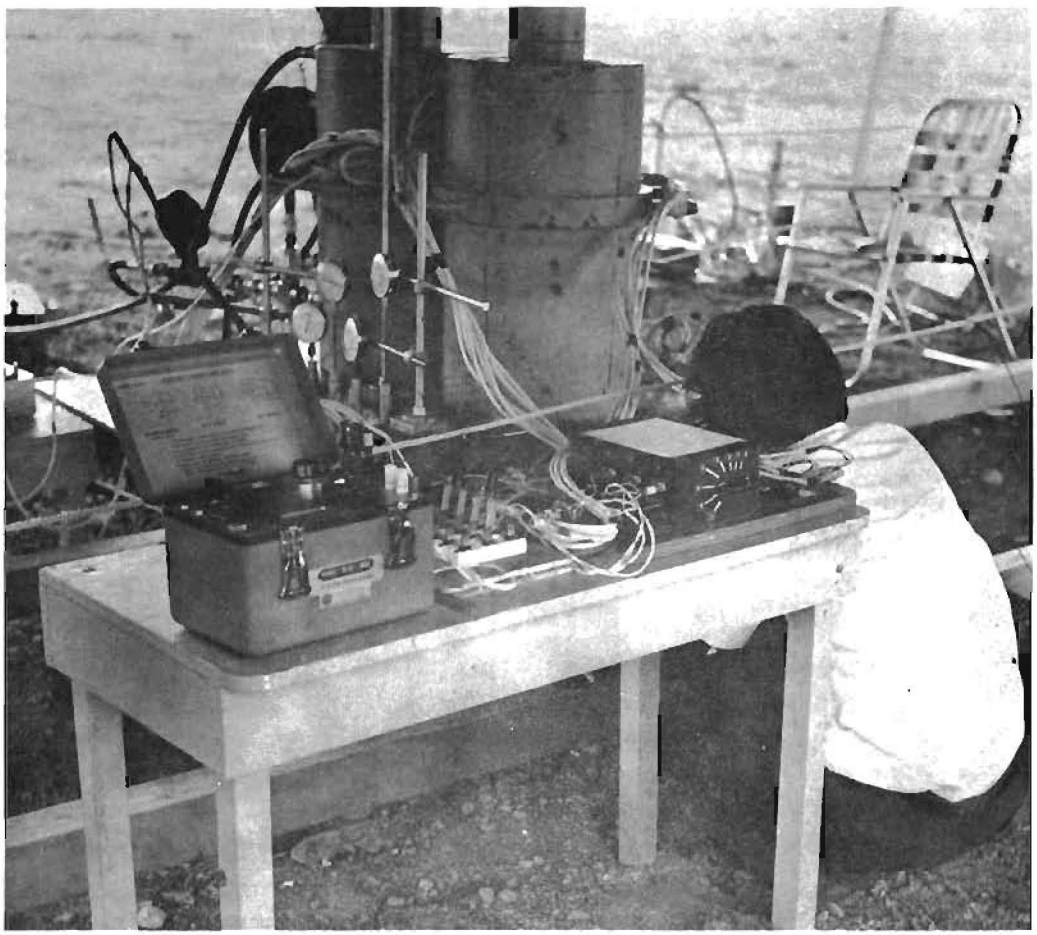

Fig 29. Readout system as used in the field.

The four arms of the Wheatstone bridge consisted of one active and one dummy gage from the shaft and two dummy gages from the strain indicator. Any drift in the system due to the differential temperature between the dummies built in the strain indicator was recorded periodically by zeroing the full bridge with two SR-4 strain gages installed close to each other on a separate steel plate.

CHAPTER 6. ANALYSIS OF TEST RESULTS

Load-Settlement Curves

In all, five load tests were run on this shaft. The dates on which these tests were run and the maximum load that was applied are summarized below.

Test No.	Date of Test	Rate of Loading	Load at Which Testing Was Ended Tons	Remarks
1	6/21/67	25T every 10 min	100	Preliminary test
2	6/30/67	50T every 12 min	715	Pumps failed
3	10/7/67	50T every 12 min	900	Pumps failed
4	5/14/68	50T every 12 min	990	Limit of loading system
5	5/14/68	50T every 2-1/2 min	905	Unable to hold load beyond 905T

Load Test No. 1 was a preliminary test and was run to evaluate a suitable test procedure. In this test the shaft was loaded to 100 tons in increments of 25 tons, at intervals of 10 minutes. The settlement gage readings were recorded at 0.5, 2, 4, 8, and 10-minute intervals, while tell-tale gages were read at 4 minutes after the load was applied. The strain gage readings were begun 4 minutes after load application. No lateral pressure gage readings were recorded. The total downward movement of shaft for 100 tons was observed to be 0.021 inch. The rebound seems to indicate that the shaft came out of the ground 0.013 inch, which may be possible if the disturbance of the load released prestress. The load-settlement curve for this test is shown in Fig 30. From this preliminary test it was concluded that a loading increment of 50 tons every 12 minutes would be most suitable for the full-scale load tests. This smaller time interval, as compared to the usual time interval recommended by ASTM (Ref 1), was considered desirable because of the very high failure load that was expected.

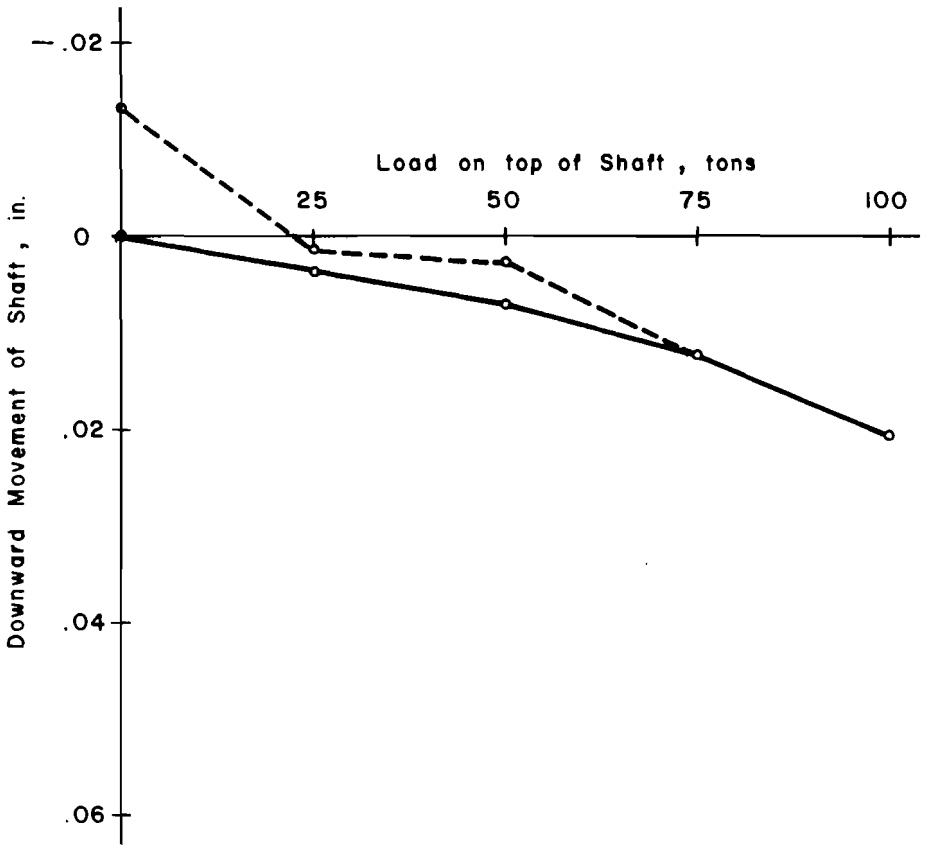

Fig 30. Load settlement curve for Test No. 1.

Test No. 2 was a full-scale load test which was conducted at night to minimize temperature variation. The minimization of temperature variation was considered essential to reduce the drift in embedment strain gages and to minimize the change in length of tell-tales due to temperature variations. To check the variation in zero readings of embedment strain gages, the observation of zero readings of all the strain gages began at 4:37 PM and continued until 8:50 PM, when the readings were found to be fairly stable. The actual test began at 8:50 PM. The load was increased in increments of 50 tons every 12 minutes. For each increment the settlement gages were read for elapsed times of 0.5, 2, 4, 8, and 11.5 minutes. The tell-tale dial gages were read at 4 and 8 minutes only. The embedment strain gage readings were begun after 4 minutes of load for each increment. Usually it took about 6 minutes to read the strain gages down and up the shaft. All went well up to 600 tons. When the load was being increased from 600 to 650 tons, the O-ring seal of one of the two pumps blew out. The other pump was used to raise the load. This worked well up to 700 tons; but when the load was being raised from 700 to 750 tons, the O-ring seal of the other pump blew out at about 730 tons and the load gradually dropped to 690 tons before unloading commenced. The maximum settlement of the top of the shaft was observed to be 0.570 inch. The load-settlement curve is shown in Fig 31. Net settlement was 0.267 inch.

Test No. 3 was run similarly to Test No. 2. This test had to be terminated at 900 tons due to failure of the pumping system. The maximum settlement of the top of the shaft for this test was observed to be 1.088 inches. The load-settlement curve is shown in Fig 31. The net settlement for this load cycle was 0.638 inch.

The procedure for Test No. 4 was the same as that of Tests No. 2 and 3. This test was run with an intention to reach a failure load, i.e., the load which results in continuous settlement. However, the test had to be terminated at 990 tons, the limiting capacity of the loading system. The gross settlement for this maximum load was found to be 1.997 inches and the net settlement of the cycle was 1.480 inches. The load-settlement curve is shown in Fig 31.

Test No. 5 was carried out on the same day as Test No. 4. The elapsed time between completion of Test No. 4 and start of Test No. 5 was one hour. This test was run according to the "Standard Quick Test" of the Texas Highway Department (Ref 22). During this test the load was increased every 2-1/2 minutes in increments of 50 tons. Because of the small interval of time the

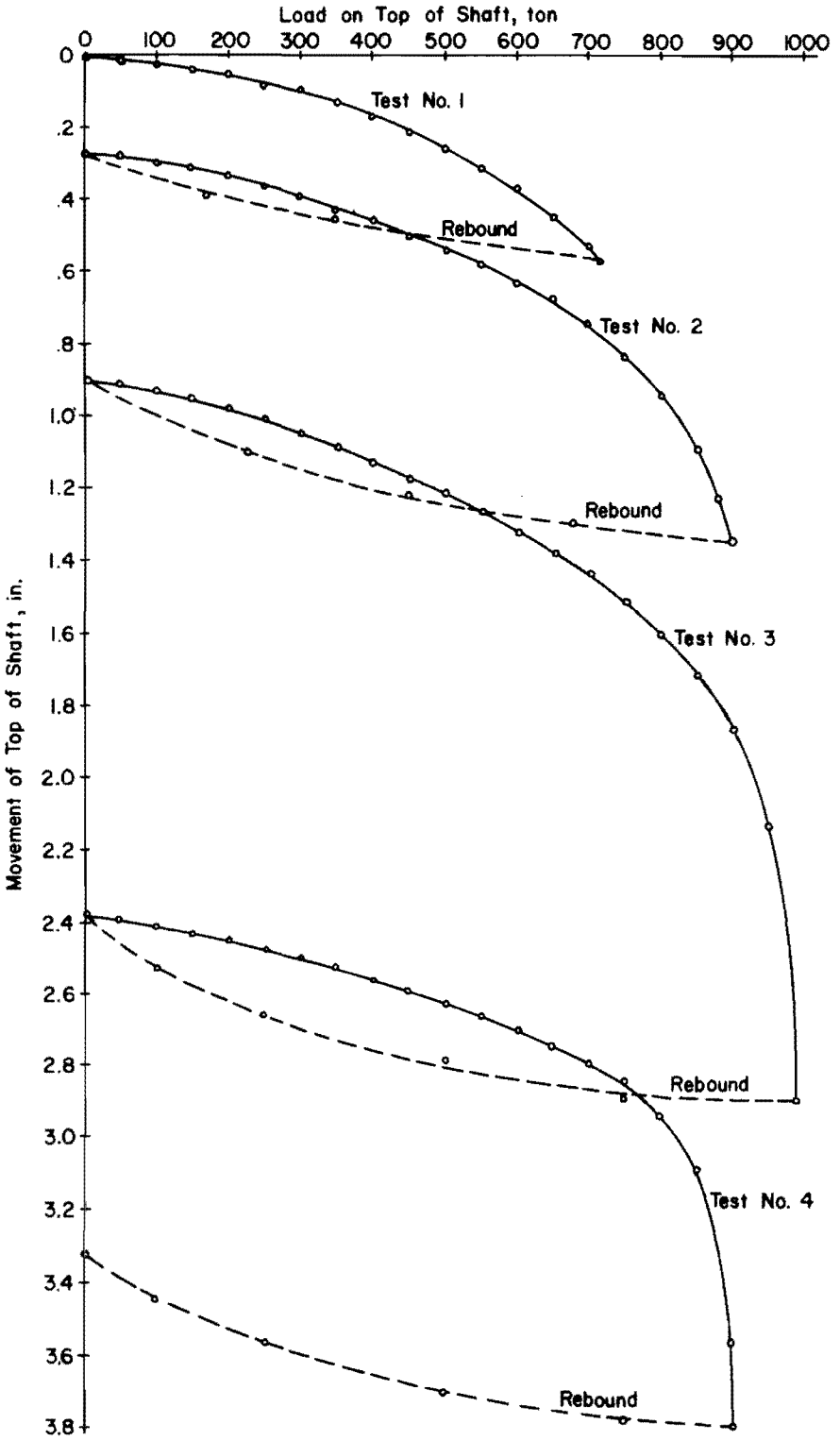

Fig 31. Load-settlement curves for various tests.

embedment strain gage readings and tell-tale readings were recorded only once for each loading after an elapse of 1/2 minute from the application of incremental load. However, settlement gage readings were recorded at 1/2-minute and 2-minute intervals. The failure load was found to be 905 tons and the corresponding gross settlement was observed to be 1.410 inches. The net settlement after rebound for the cycle was 0.977 inch. The load-settlement curve is shown in Fig 31.

The raw data obtained from the various load tests were used for analysis with minimum possible corrections or adjustments. Wherever any corrections were necessary, the reasons justifying the corrections have been given. Since the instrumentation in the shaft consisted of embedment strain gages and tell-tales, the method of analysis for each device is described separately. Embedment strain gages may also be referred to as strain gages in this study.

Computation of Strain from Embedment Strain Gages

When multiple gages are used to measure axial strain in the interior of concrete at any one level, the strain indicated by each gage for the same load can be slightly different. This may be due to several reasons: (1) the bond between the external surface of the strain gage and the concrete cannot be perfect, (2) the strain gages may not be placed truly vertical in the concrete, (3) an eccentricity in the loading system may result in the increased variation, and (4) heterogeneity in the concrete. To obtain the best estimate of strain in the shaft the following procedure was used.

The strain measured by various strain gages, at each depth, was plotted for different loads at the top of the shaft. Typical plots for Test No. 2 at various depths are shown in Figs 32 through 38. It will be seen from these plots that the trend in general appears to be linear. However, curve fit analysis, based on the method of least squares (Ref 13), was carried out to find the best estimate of strain at each depth corresponding to various loads at the top of the shaft. Curve fits for first order, second order, third order, and first order forced through origin were obtained for Test No. 2, and the results of such analysis are summarized in Table 2. Third-order curve fit gives the minimum standard error. However, the difference in standard error for first- and third-order curve fits is not appreciable. For the relationship between load and strain a curve through origin will be most desirable.

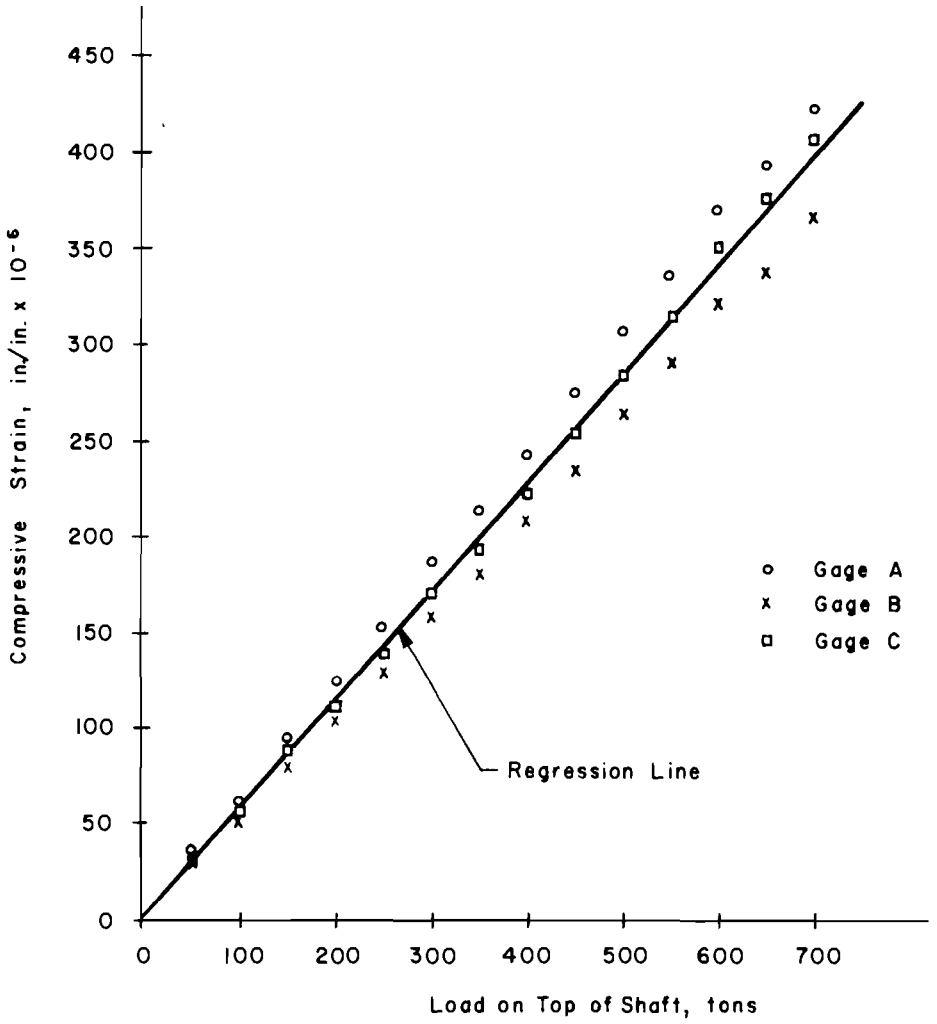

Fig 32. Observed strain at a depth of 1.71 feet below the top of the shaft (ground surface) Test No. 2.

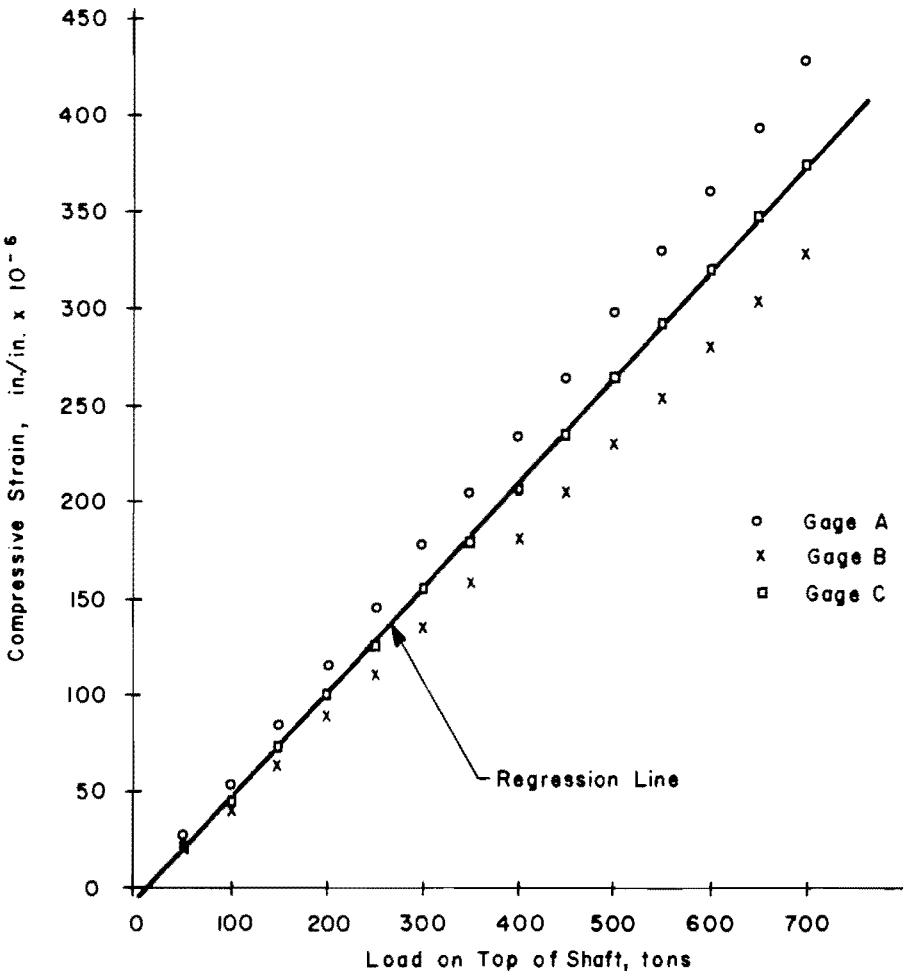

Fig 33. Observed strain at a depth of 4.96 feet below the top of the shaft Test No. 2.

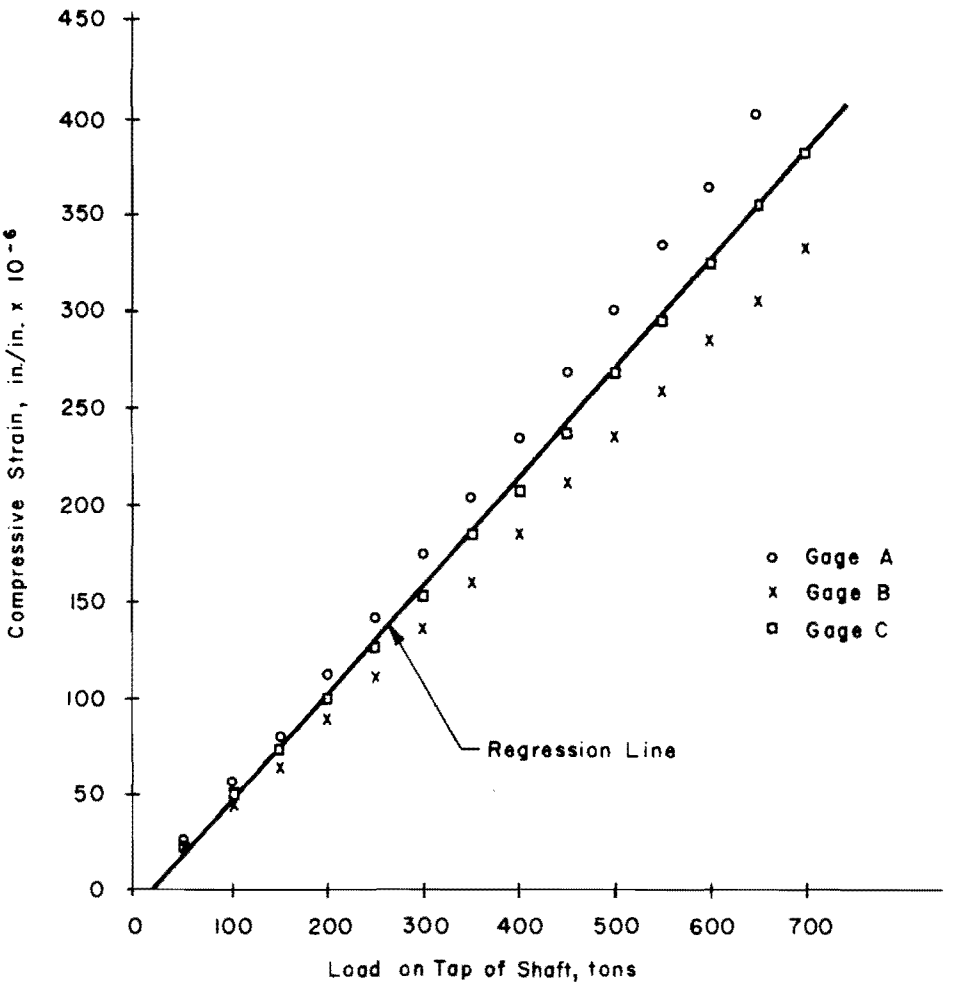

Fig 34. Observed strain at a depth of 10.05 feet below the top of the shaft Test No. 2.

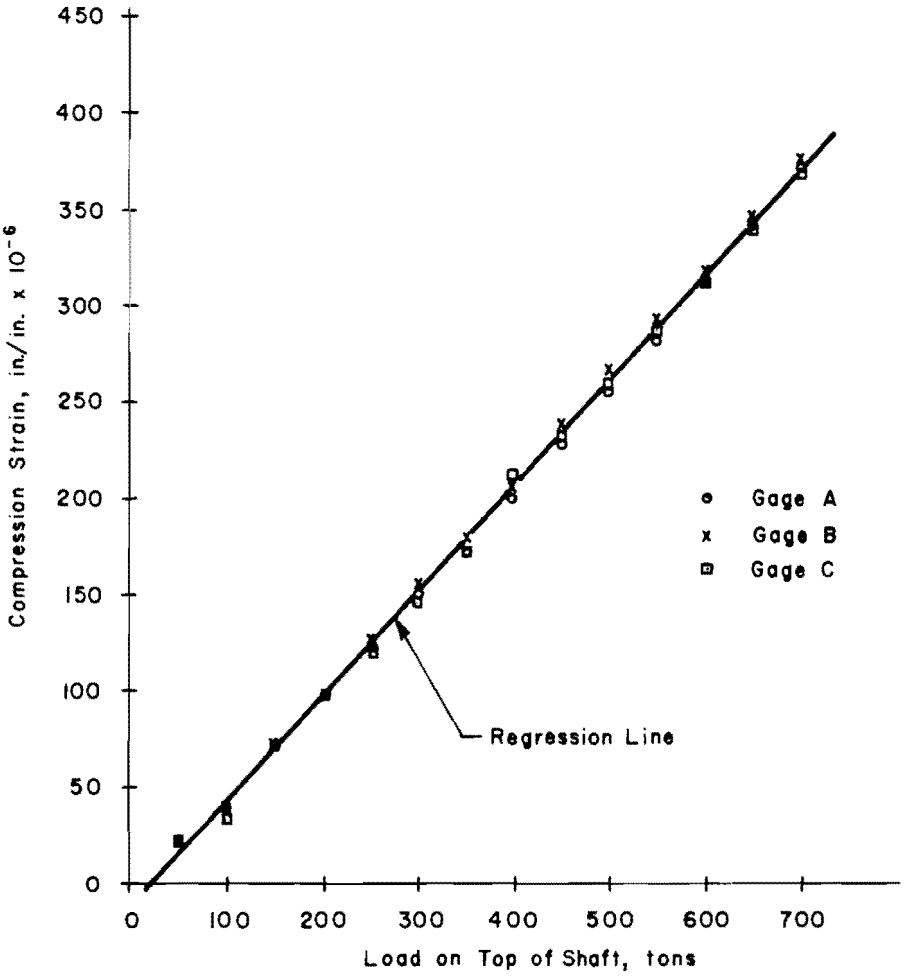

Fig 35. Observed strain at a depth of 15.20 feet below the top of the shaft Test No. 2.

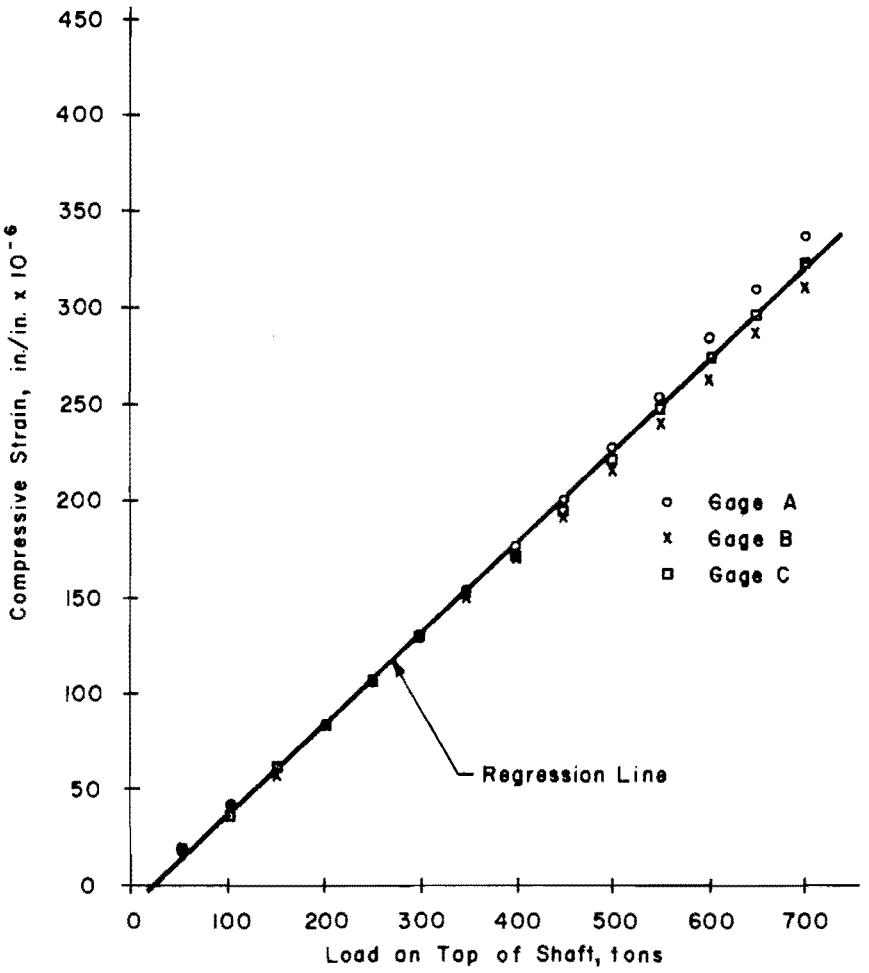

Fig 36. Observed strain at a depth of 20.30 feet below the top of the shaft Test No. 2.

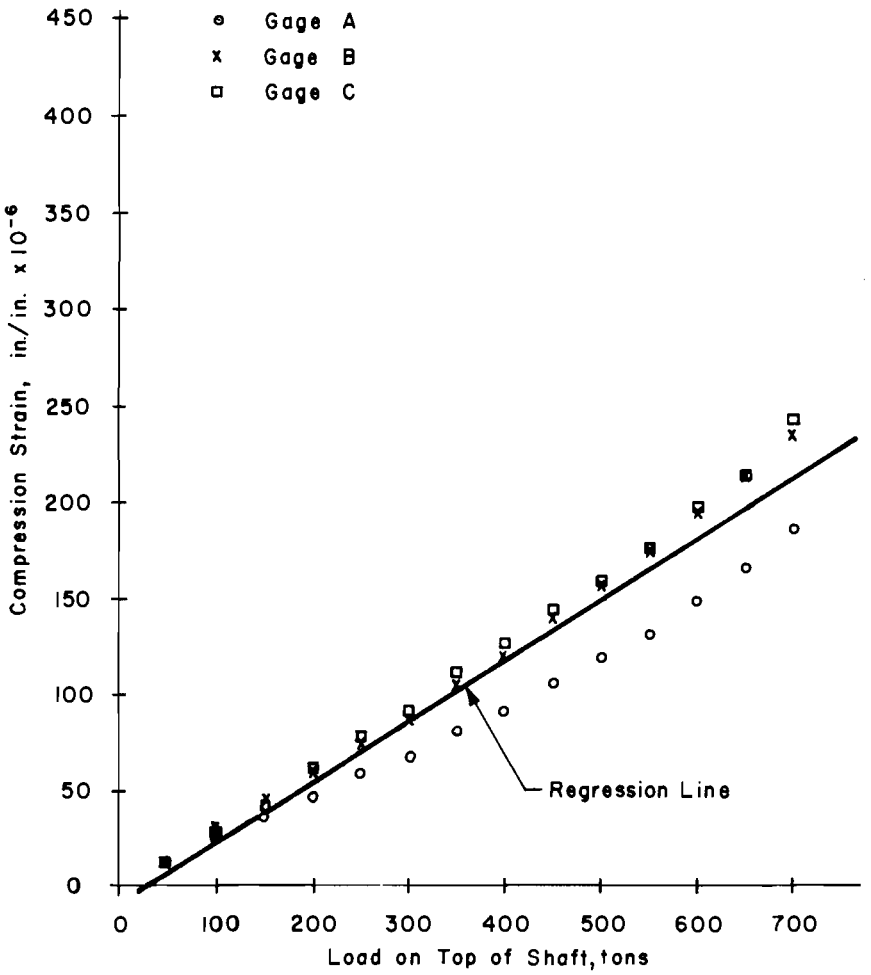

Fig 37. Observed strain a depth of 25.00 feet below the top of the shaft Test No. 2.

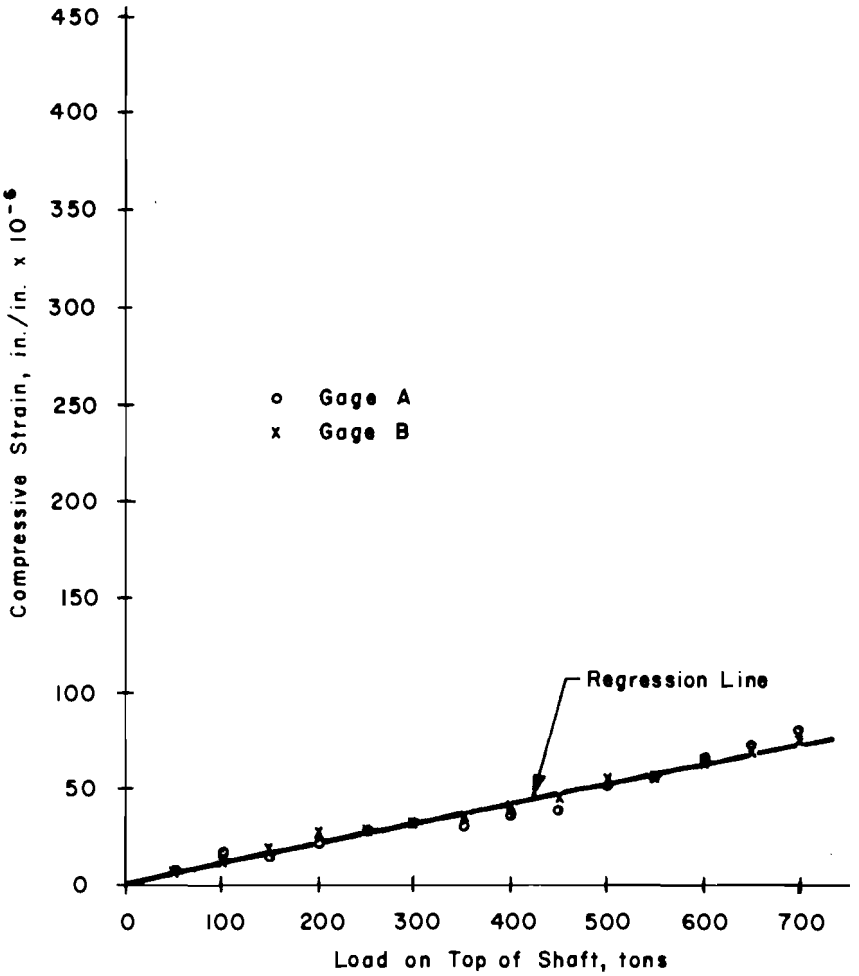

Fig 38. Observed strain at a depth of 28.05 feet below the top of the shaft Test No. 2.

TABLE 2. COMPARISON OF VARIOUS ORDERS OF CURVE FIT BY THE METHOD OF LEAST SQUARES

Depth, feet	Standard Error of Estimate			
	First Order Through Origin $Y = B_1X$	First Order $Y = A_1 + B_1X$	Second Order $Y = A_1 + B_1X + C_1X^2$	Third Order $Y = A_1 + B_1X + C_1X^2 + D_1X^3$
1.71	14.79	15.56	14.37	14.37
4.96	24.36	23.86	23.84	23.82
10.05	29.40	28.12	27.98	27.96
15.20	9.70	7.87	7.66	7.59
20.30	11.51	6.01	4.57	4.25
25.00	8.08	3.98	2.79	2.51
28.05	5.15	3.75	2.12	1.15

But the error introduced by forcing the curve through origin becomes considerably larger at some depths of the shaft. Hence, the first-order curve fit of the type given by Eq 6.1 was used to obtain strain at any depth for a given load at the top of the shaft. The first-order curve fit (regression line) is shown by solid lines in Figs 32 through 38.

$$Y = A_1 + B_1X \tag{6.1}$$

where

Y = strain at certain depth,

X = load on top of the shaft,

A_1 and B_1 = constants.

The plots for Tests No. 3, 4, and 5 are given in Appendix 2.

The strain distribution along the length of the shaft obtained from the best estimate of observed strains is shown in Figs 39 through 42 in solid lines corresponding to the load on top of the shaft shown on the curve in tons. It may be seen that for load Test No. 2 the strain observed at a depth of 4.96 feet is slightly smaller than the general trend of the curves. This would indicate an increased load in the shaft between 5 and 10 feet which hardly seems plausible. Test No. 3 indicates that the observed strain at depths of 1.71 feet and 4.96 feet below the top of the shaft are considerably affected by temperature variations. During Tests No. 4 and 5 the strain measured at a depth of 10.05 feet below the top of the shaft was considerably smaller than the general trend of the curves. Due to this erratic indication of strain near the top of the shaft some correction or adjustment seemed necessary. The corrections were made so as to be consistent with the general trend of strain distribution in the shaft. The adjusted curves after correction are shown in broken lines. Figure 41 indicates that the strain gages at depths of 20.3, 25.3, and 28.05 feet underwent some tension. This tensile strain at the bottom may have been due to the release of precompression in concrete that may have developed due to the swelling of surrounding clay. When the test was started and load on top gradually increased the bond between shaft surface and surrounding soil could have decreased, thus causing the shaft to expand or

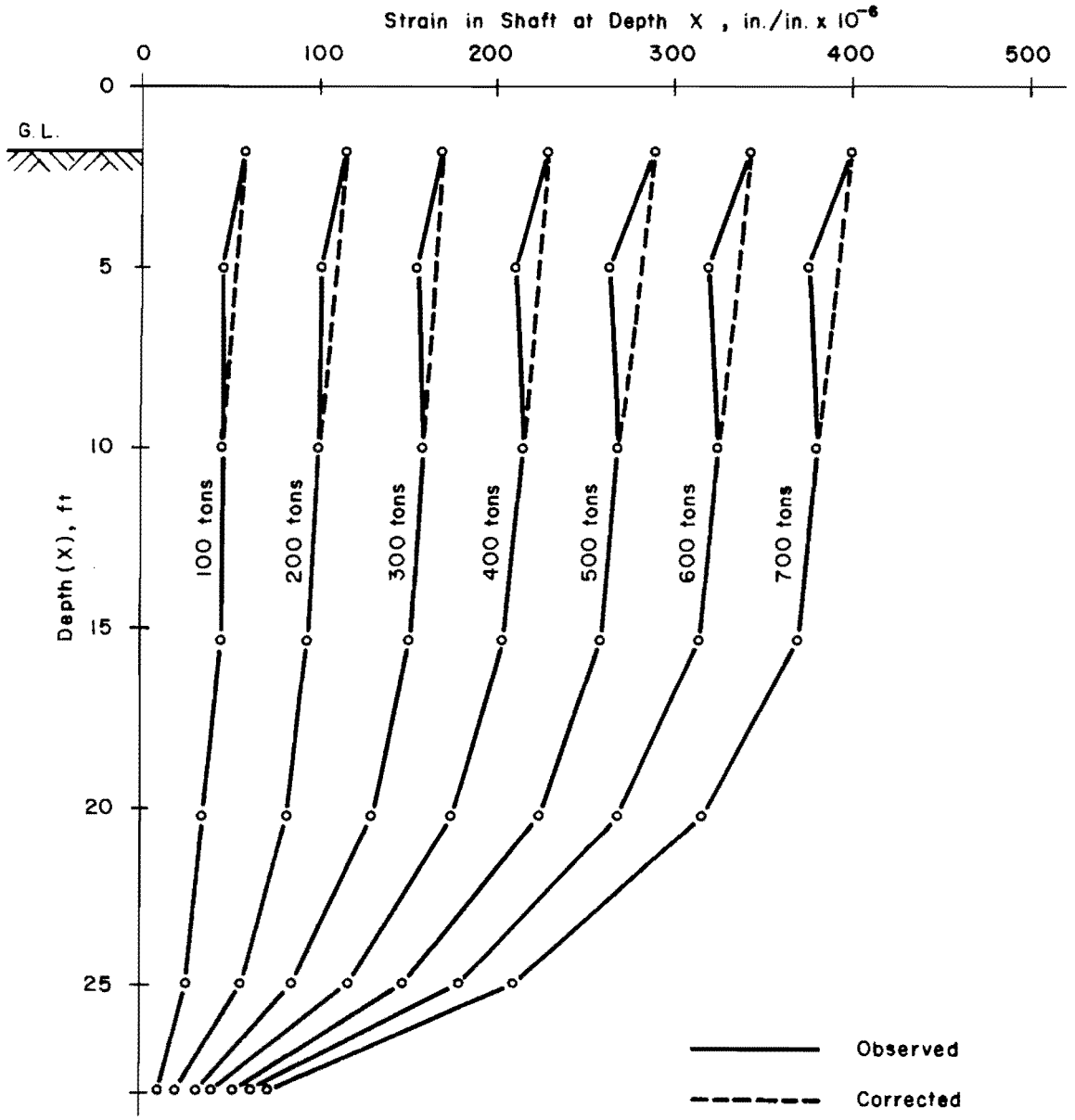

Fig 39. Strain variation along the shaft for various loadings during Test No. 2.

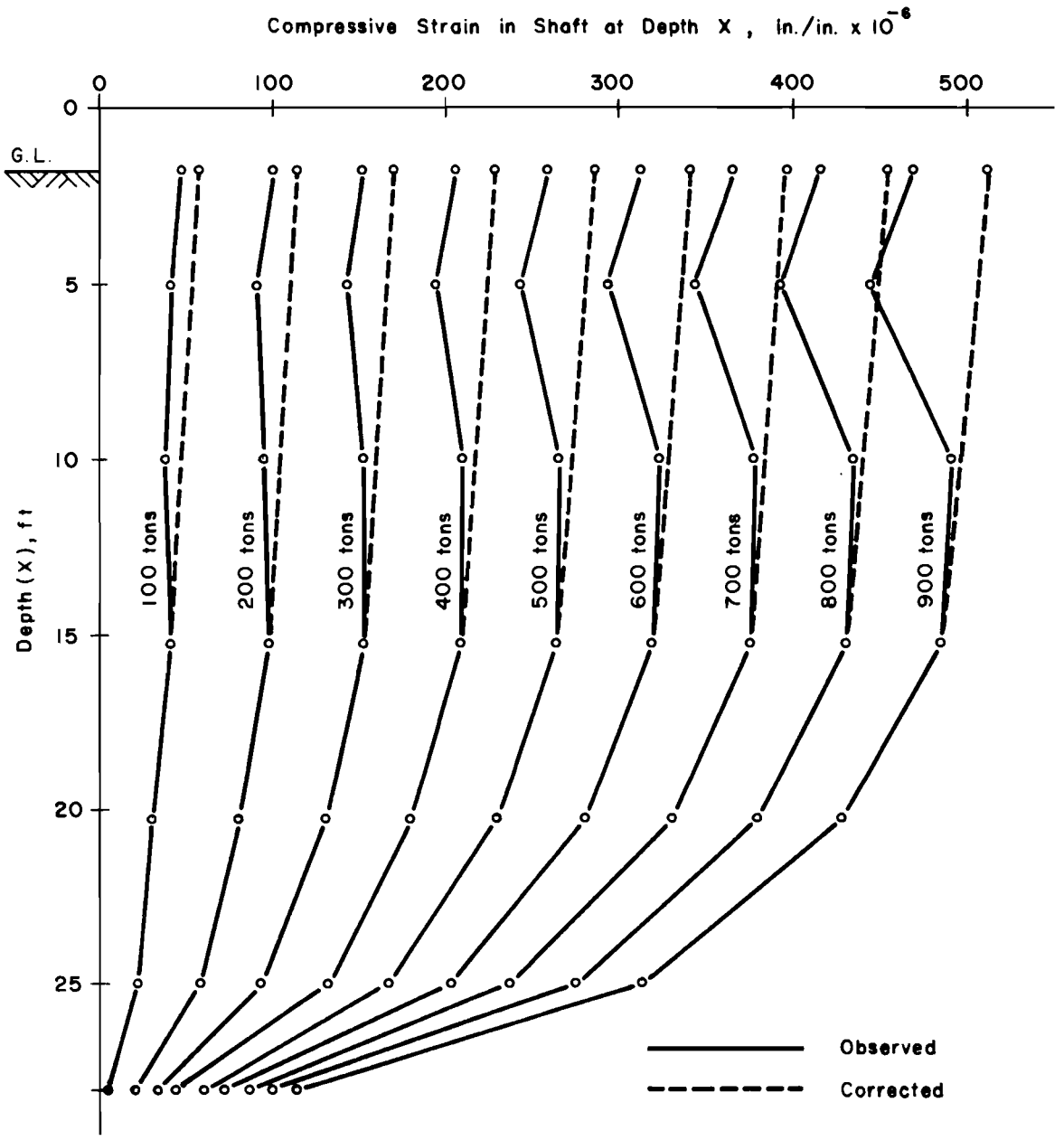

Fig 40. Strain variation along the shaft for various loadings during Test No. 3.

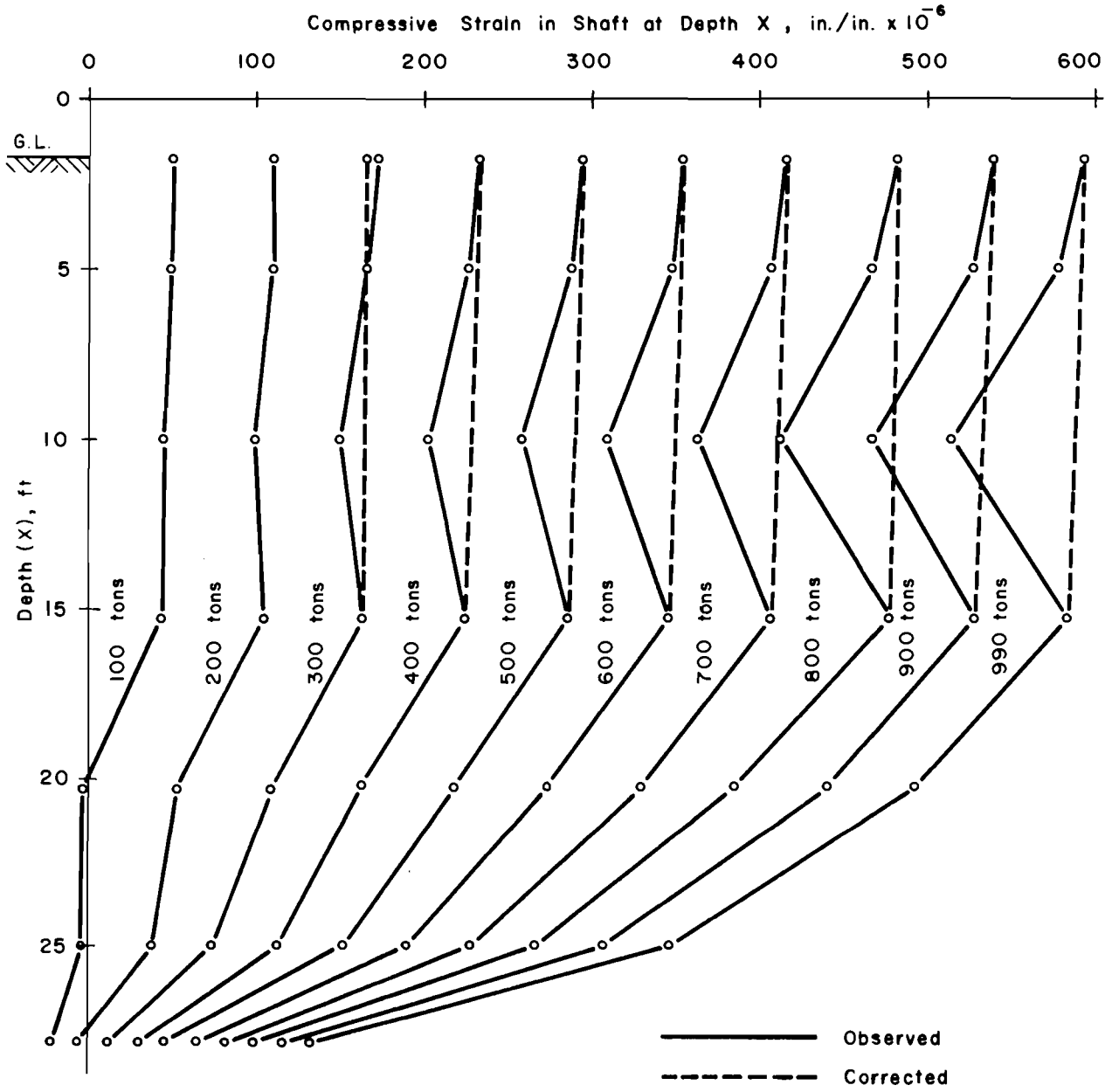

Fig 41. Strain variation along the shaft for various loadings during Test No. 4.

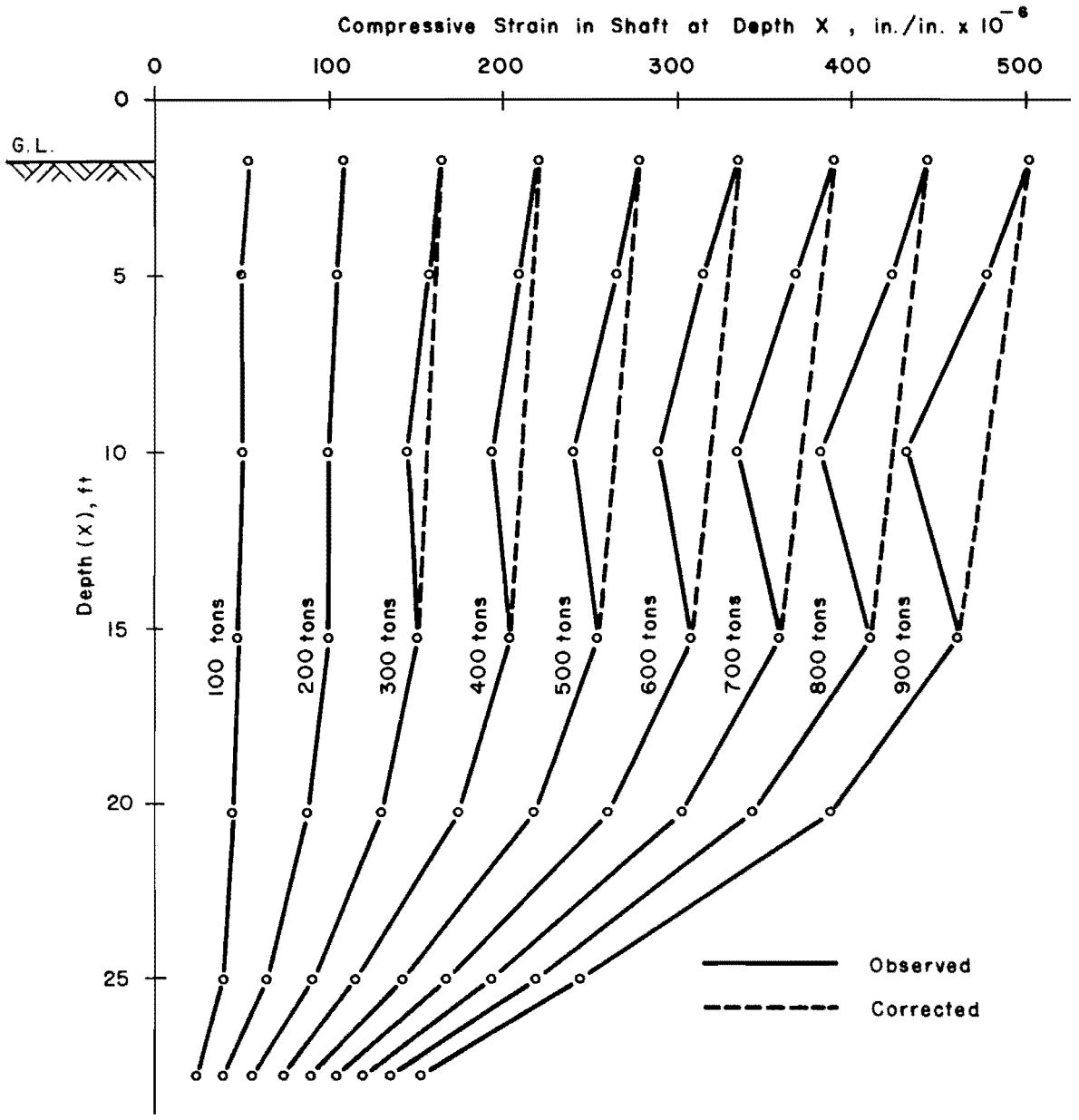

Fig 42. Strain variation along the shaft for various loadings during Test No. 5 (quick test).

release part of its precompression. In those sections of the shaft where the release of precompressive strain was greater than the strain caused by the compressive load at the top, a negative strain was recorded. This contention is also supported by larger negative strains at the bottom in Test No. 4 and no negative strain in Test No. 5, which was conducted on the same day as Test No. 4. During Tests No. 4 and 5 strain gages at a depth of 10 feet seemed to give erroneous results, which may be due to temperature effects in addition to the poor stability of gages.

Load Calibration. The strain gages located at the ground level, i.e., 1.71 feet below the top of the shaft, were installed at this depth so as to obtain the strain in the shaft before any load transfer to soil takes place. The strain observed for each load on top of the shaft was plotted separately for each test, as pointed out earlier in this chapter. A comparison of this curve, called the load-calibration curve, for Tests No. 2, 3, 4, and 5 is shown in Fig 43. Under ideal conditions of Hooke's law the load-calibration curves for all the tests would have been concurrent. But the conditions at the site were far from ideal as the residual stress history of the shaft before commencement of each test was unknown and the temperature conditions varied for each load test. It will seem from Figs 39, 41, and 42 that the strain in the shaft observed at the ground level for Tests No. 2, 4, and 5 was consistent with the trend of strain distribution along the depth. Hence, the load-calibration curves as shown in Fig 43 were used to compute load from the strain in the shaft for Tests No. 2, 4, and 5. However, the observed strain at the ground level for Test No. 3, as shown in Fig 40, was much smaller than at depths. This does not seem possible because it would mean a higher load in the shaft at greater depth than at the top. Therefore, for Test No. 3 the strain at ground level was computed by using the load-calibration curve of Test No. 2. The computed strain is shown in Fig 40 by an additional set of points at the ground level. Thus, for the analysis of data from each test, a separate load-calibration curve, as shown in Fig 41, was used except for Test No. 3 as mentioned above.

Load Distribution in the Shaft. When the strain distribution along the length of the shaft is determined and the load-calibration curve is known, the load P at any depth corresponding to strain ϵ can be computed from Eq 6.2.

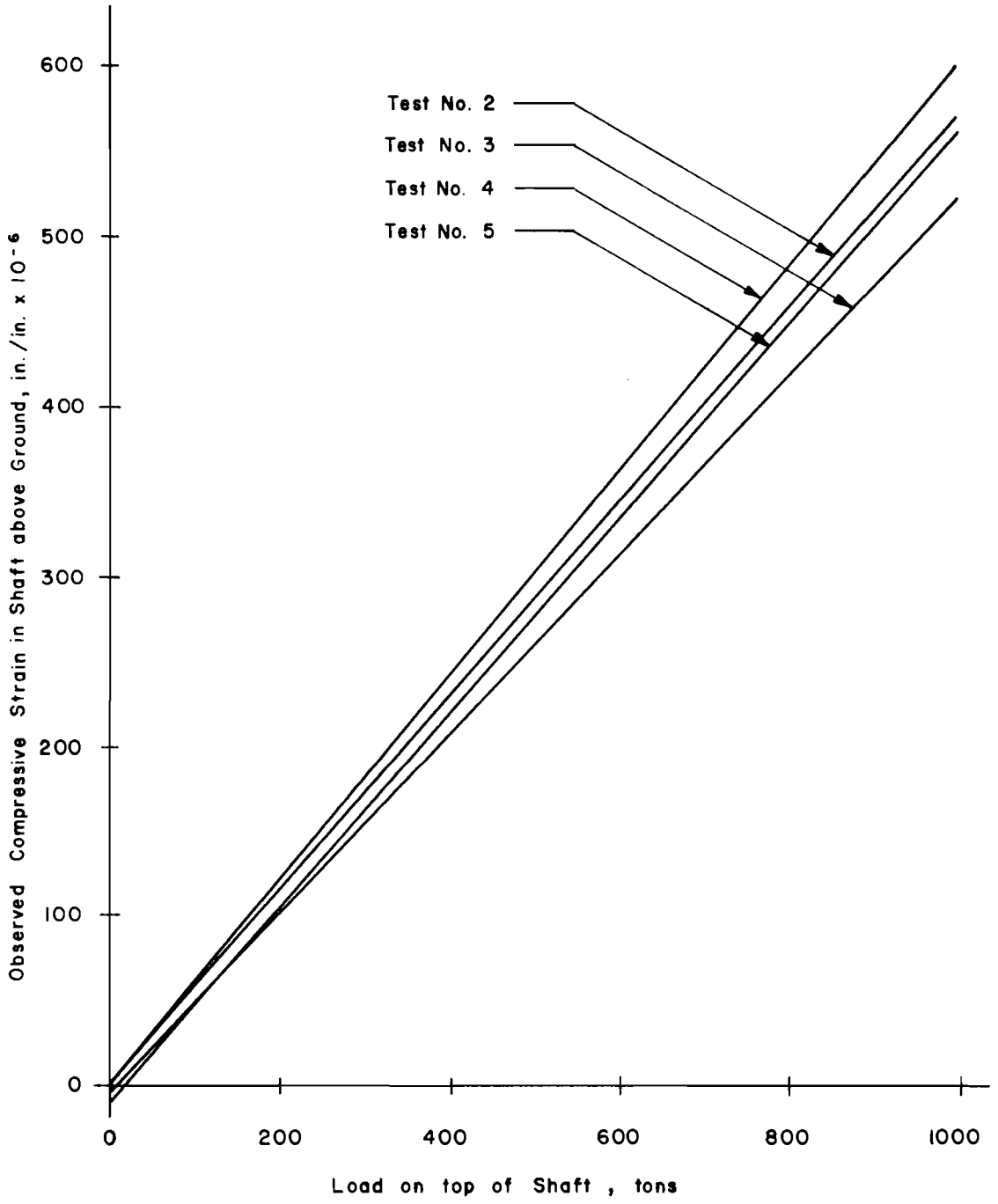

Fig 43. Load-calibration curves.

$$P = K\epsilon \tag{6.2}$$

where

K = calibration constant obtained from the slope of load-calibration curve in tons.

The plots for load distribution along the length of the shaft thus obtained for various load tests are shown in Figs 44 through 47. It can be seen from these figures that the load at the bottom, later referred to as tip load or tip resistance of the shaft, is only a small fraction of the load at the top of the shaft. The tip loads corresponding to various loads at the top for these tests are summarized in Table 3. Results of Test No. 5 show a significantly larger proportion of the load at the bottom than the other tests. This is probably due to the quick rate of loading, as the load transfer to soil increases with the increasing movement. In other words the shorter the time interval between loading increments the smaller will be the settlement and consequently the load transfer to soil which in turn would result in larger tip loads. It is interesting to note that the tip load expressed as a percentage of top load increases with the increase in load at the top of the shaft.

Load Transfer versus Settlement. It will be seen from load-distribution curves shown in Figs 44 through 47 that the rate of load transfer, i.e., load transferred to soil per unit surface area of the shaft, increases with depth. It will also be noticed that the load transfer at most depths increases with increasing load. In other words the load transfer at any depth is a function of depth and movement of shaft in addition to the shear strength of soil.

To obtain the relationship of load transfer and the downward movement of the shaft the following procedure was used:

(1) The shaft was divided into 8 sections, as shown in Fig 48(a), according to the strain gage locations.

(2) From the known strain at depths z_1 , z_2 , ... , z_8 and the load-calibration curve, the load in the shaft at these depths was computed.

(3) Elastic deformation of each section Δ_i corresponding to average load due to the load at the top and bottom of section was computed.

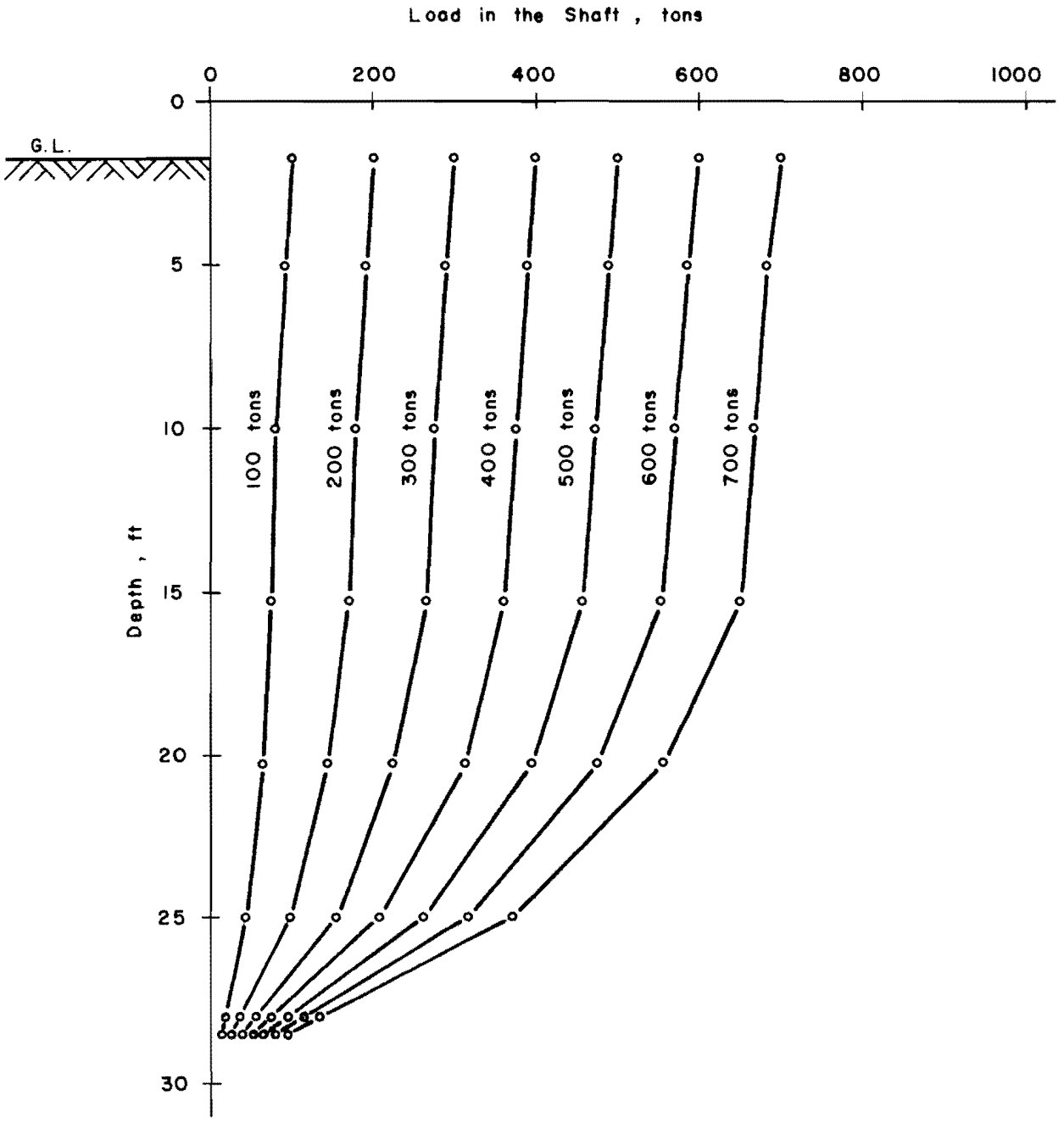

Fig 44. Load distribution along the shaft for various loadings during Test No. 2.

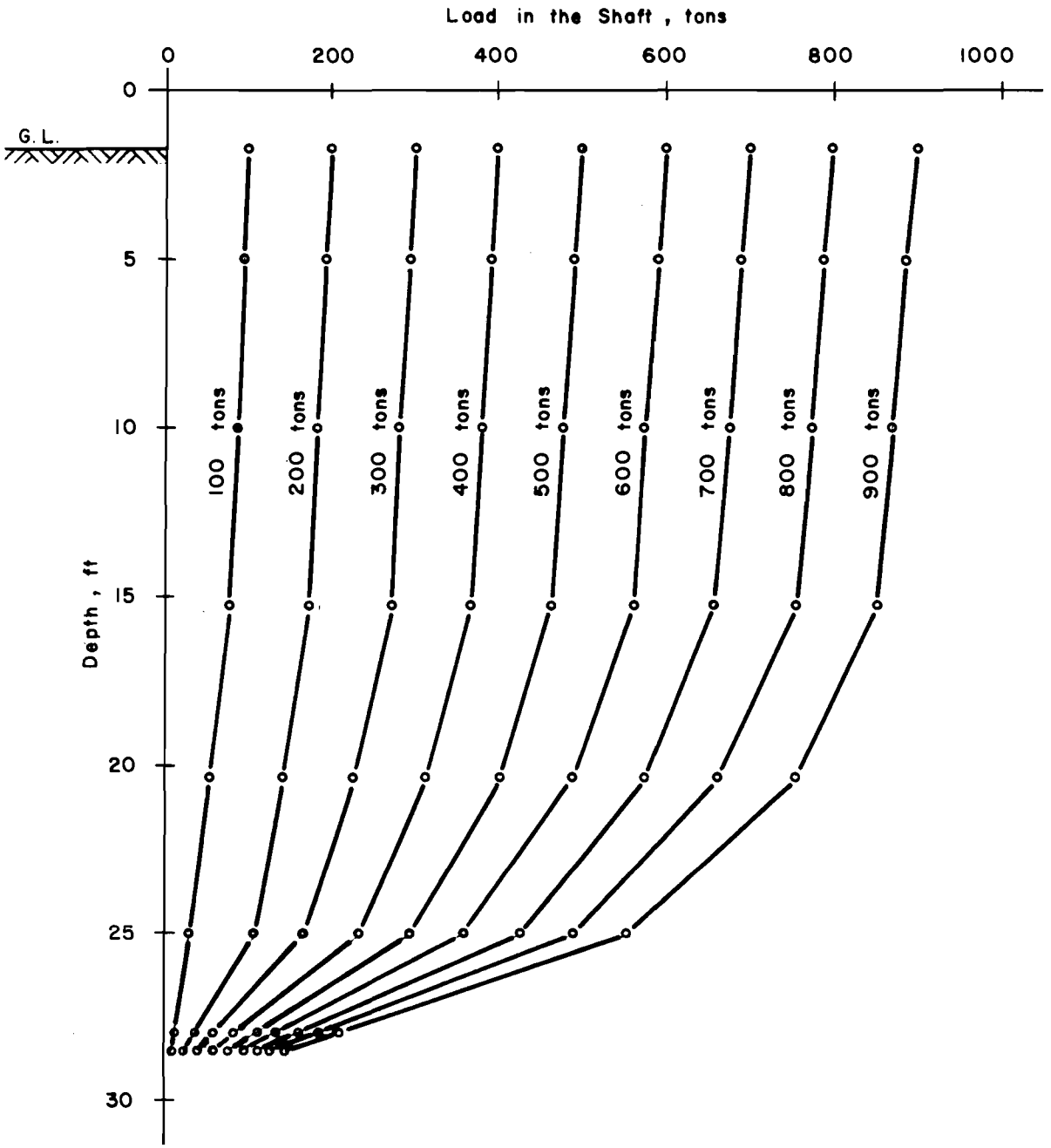

Fig 45. Load distribution along the shaft for various loadings during Test No. 3.

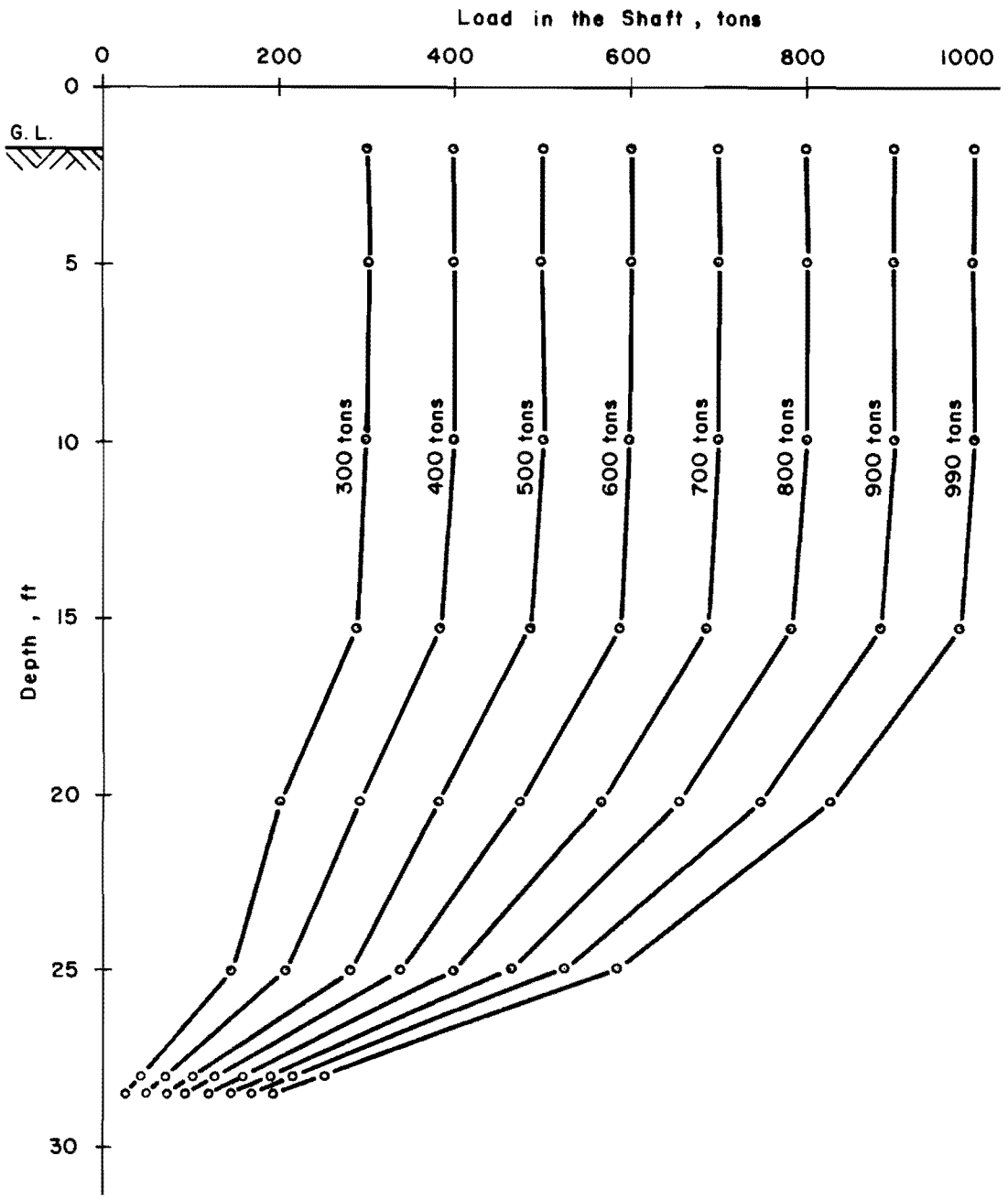

Fig 46. Load distribution along the shaft for various loadings during Test No. 4.

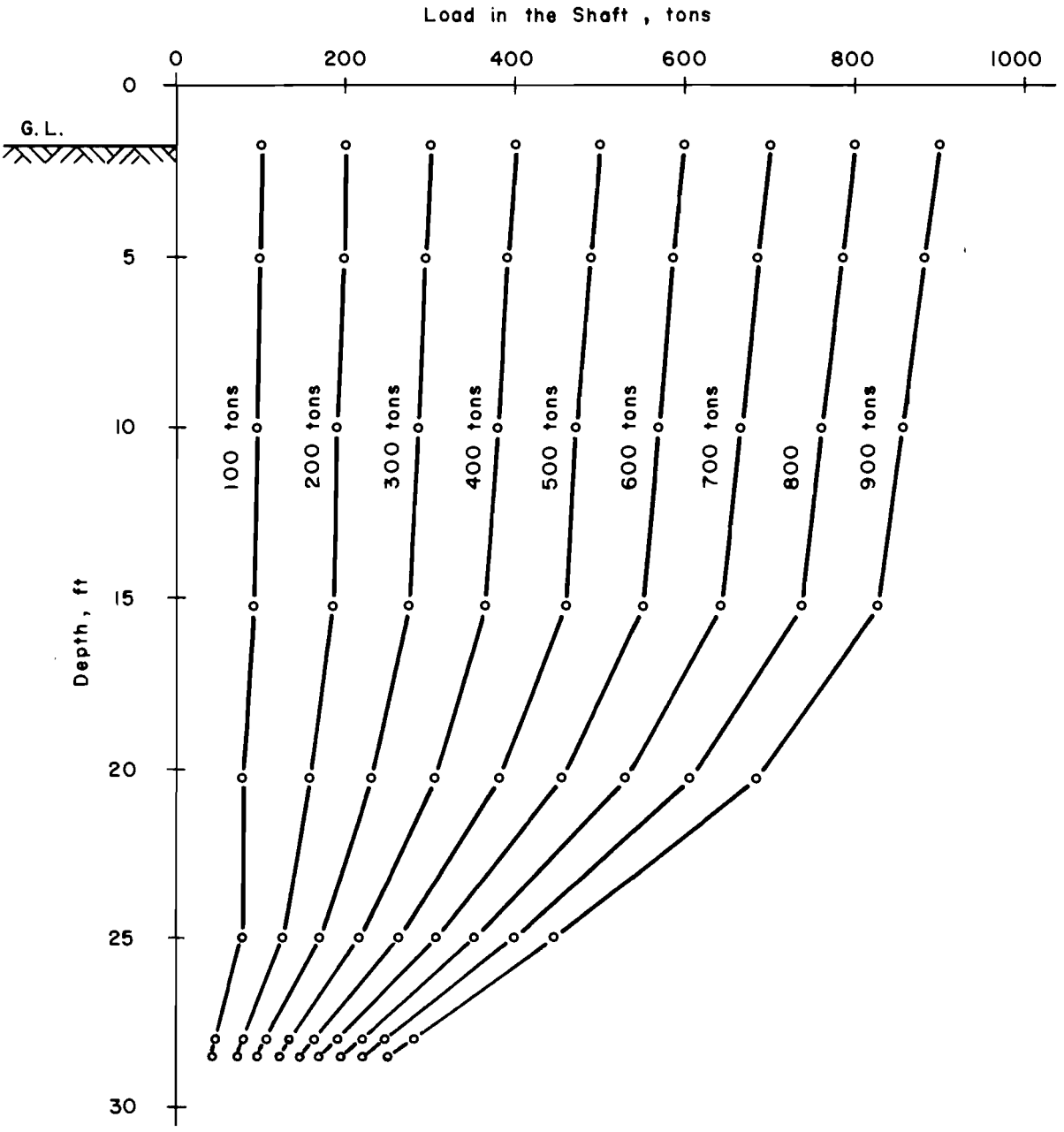

Fig 47. Load distribution along the shaft for various loadings during Test No. 5 (quick test).

TABLE 3. SUMMARY OF TIP RESISTANCE COMPUTED FROM STRAIN GAGES

Load on Top of Shaft, Tons	Tip Resistance of Shaft, Tons				Average Tip Resistance (For Nos. 2, 3, and 4) Tons	Tip Resistance as Percentage of Top Load
	Test No. 2	Test No. 3	Test No. 4	Test No. 5 (Quick)		
50	10.5	-1.7	--	33.0	4.4	8.8
100	16.8	6.9	--	45.9	11.8	11.8
150	23.2	15.6	--	58.7	19.4	12.9
200	29.6	24.3	--	71.6	27.0	13.5
250	35.9	33.0	12.9	84.4	27.3	10.9
300	42.3	41.6	24.5	97.3	36.1	12.0
350	48.7	50.0	36.1	110.2	44.9	12.8
400	55.0	59.0	47.7	123.0	53.9	13.5
450	61.4	67.7	59.3	135.9	62.8	13.9
500	67.8	76.4	70.9	148.7	71.7	14.3
550	74.1	85.0	82.5	161.6	80.5	14.6
600	80.0	93.7	94.2	174.4	89.3	14.8
650	86.9	102.4	105.8	187.3	98.4	15.1
700	93.3	111.1	117.4	200.1	107.3	15.3
750	--	120.0	129.0	213.0	124.5	16.6
800	--	128.4	140.6	225.8	134.5	16.8
850	--	137.1	152.2	238.7	144.6	17.0
900	--	145.8	163.8	251.6	154.8	17.2
950	--	--	175.5	--	175.5	18.5
990	--	--	184.7	--	184.7	18.6

(4) The downward movement due to elastic compression Δ_{xi} of midpoint of sections x_1, x_2, ..., x_i was computed from the relation

$$\Delta_{xi} = \sum_{n=1}^{i} \Delta_n - \frac{\Delta_i}{2}$$

(5) The net downward movement s_i of the midpoint x_i corresponding to the load Q_T at top was computed from

$$s_i = s - \Delta_{xi}$$

where

s = observed downward movement of shaft corresponding to the load Q_T.

(6) The load transfer T_i per unit area to soil for any midpoint x_i was computed from

$$T_i = \frac{(P_i - P_{i-1})}{\pi D(z_i - z_{i-1})}$$

where

P_i = load in shaft at depth z_i as shown in Fig 48(b),

D = diameter of the shaft.

(7) Steps 1 through 6 were repeated for different loads at the top.

A computer program "EMGAGE4" based on the procedure described above was written for the analysis. Details of the program are given in Appendix 3.

The results of such an analysis are presented in Figs 49 through 52 in the form of load transfer (tsf) versus movement at various depths. In these plots the average load transfer for each section is indicated at the center of the section and corresponds to the downward movement of the center of the section.

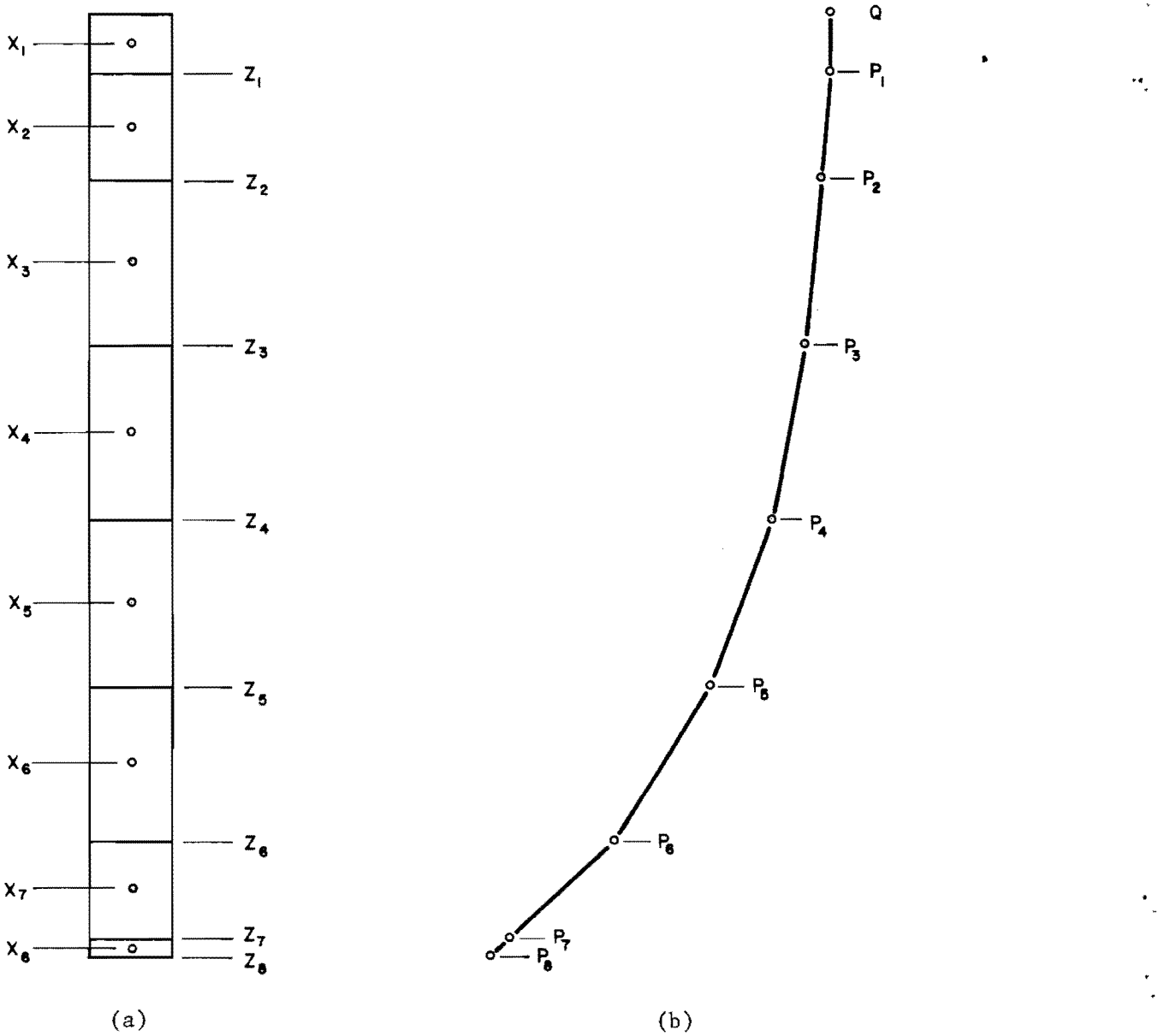

Fig 48. Division of the shaft in small sections according to the strain gage locations.

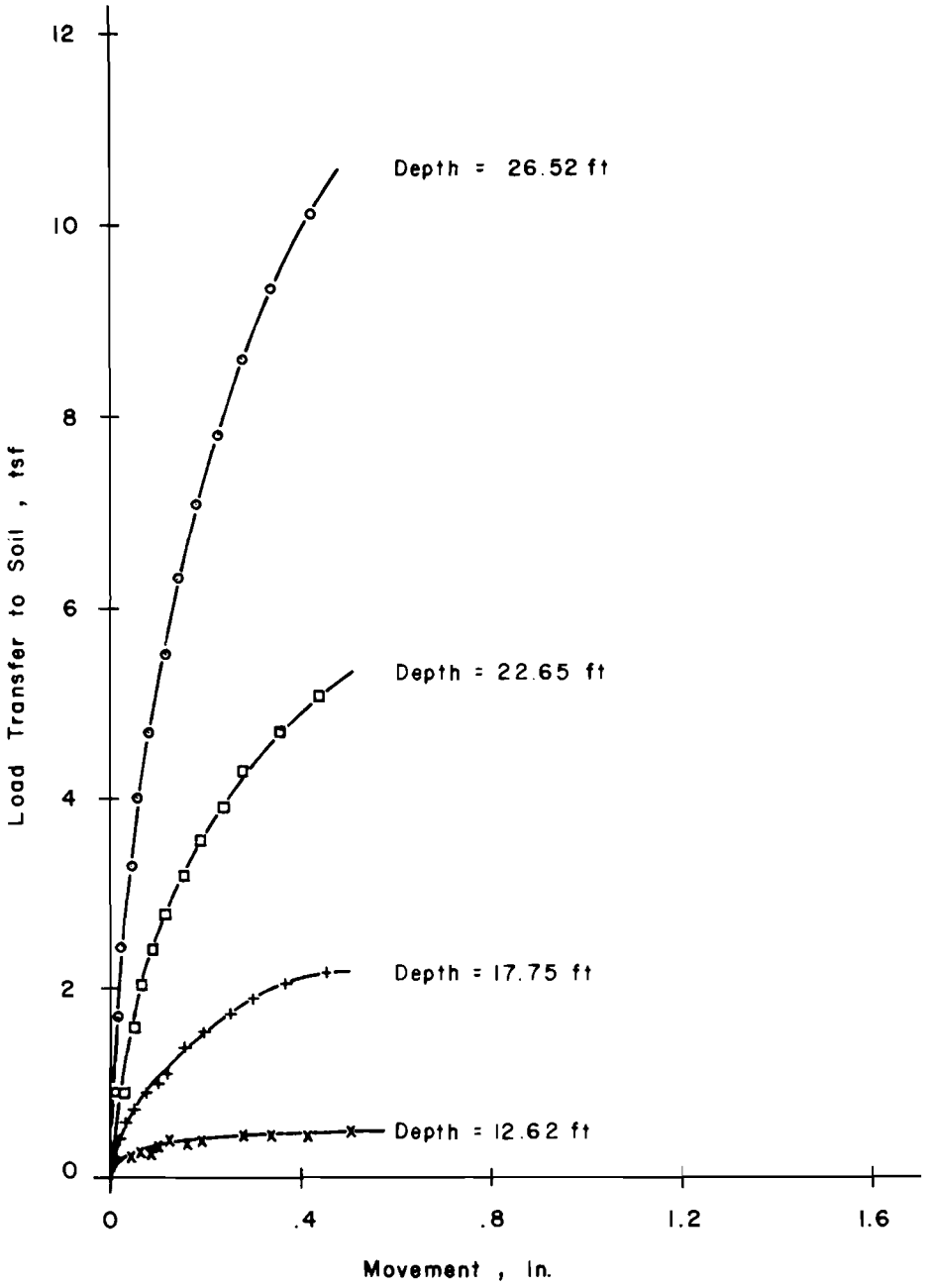

Fig 49. Relationship between load transfer and movement at various depths for Test No. 2.

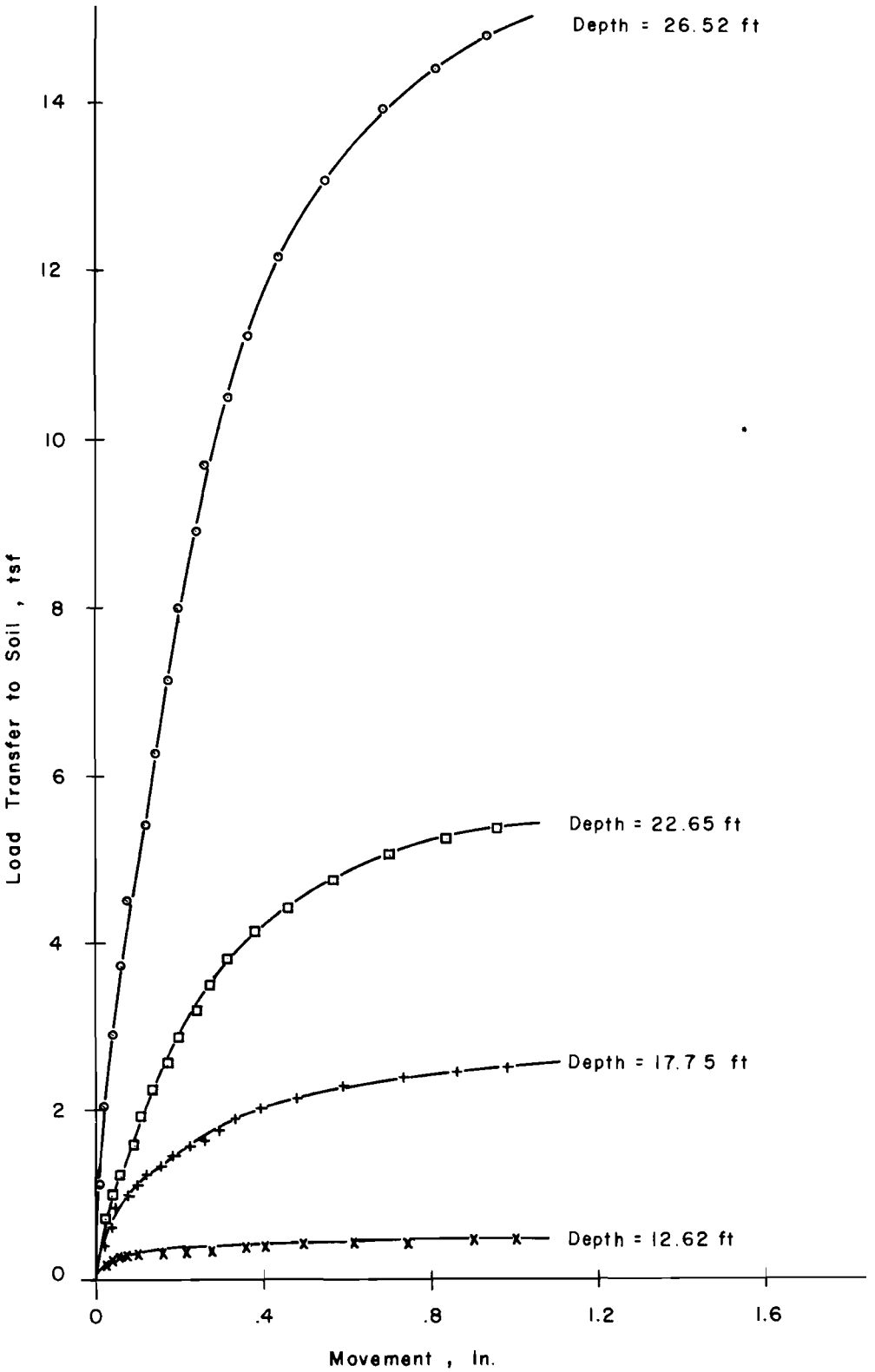

Fig 50. Relationship between load transfer and movement at various depths for Test No. 3.

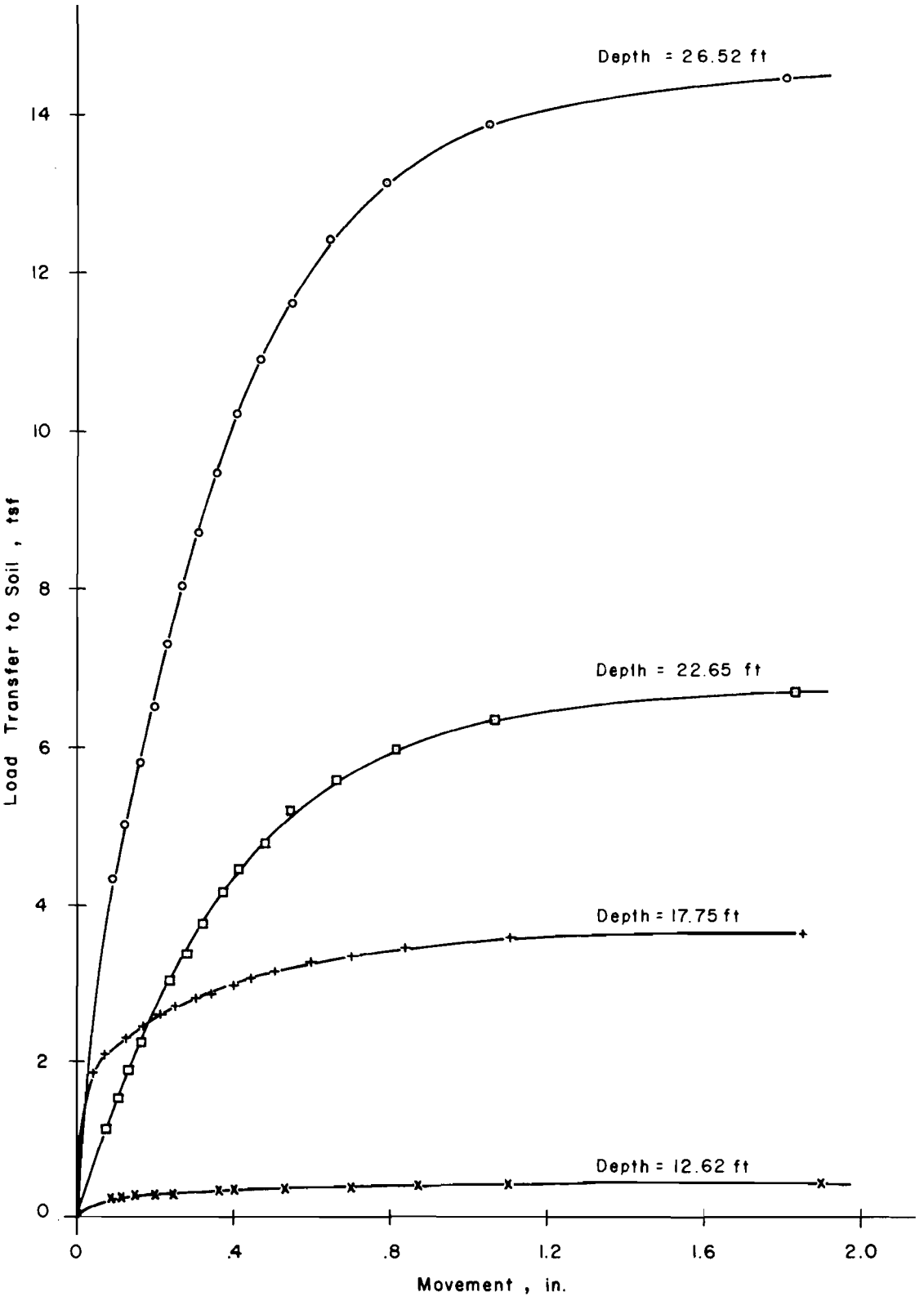

Fig 51. Relationship between load transfer and movement at various depths for Test No. 4.

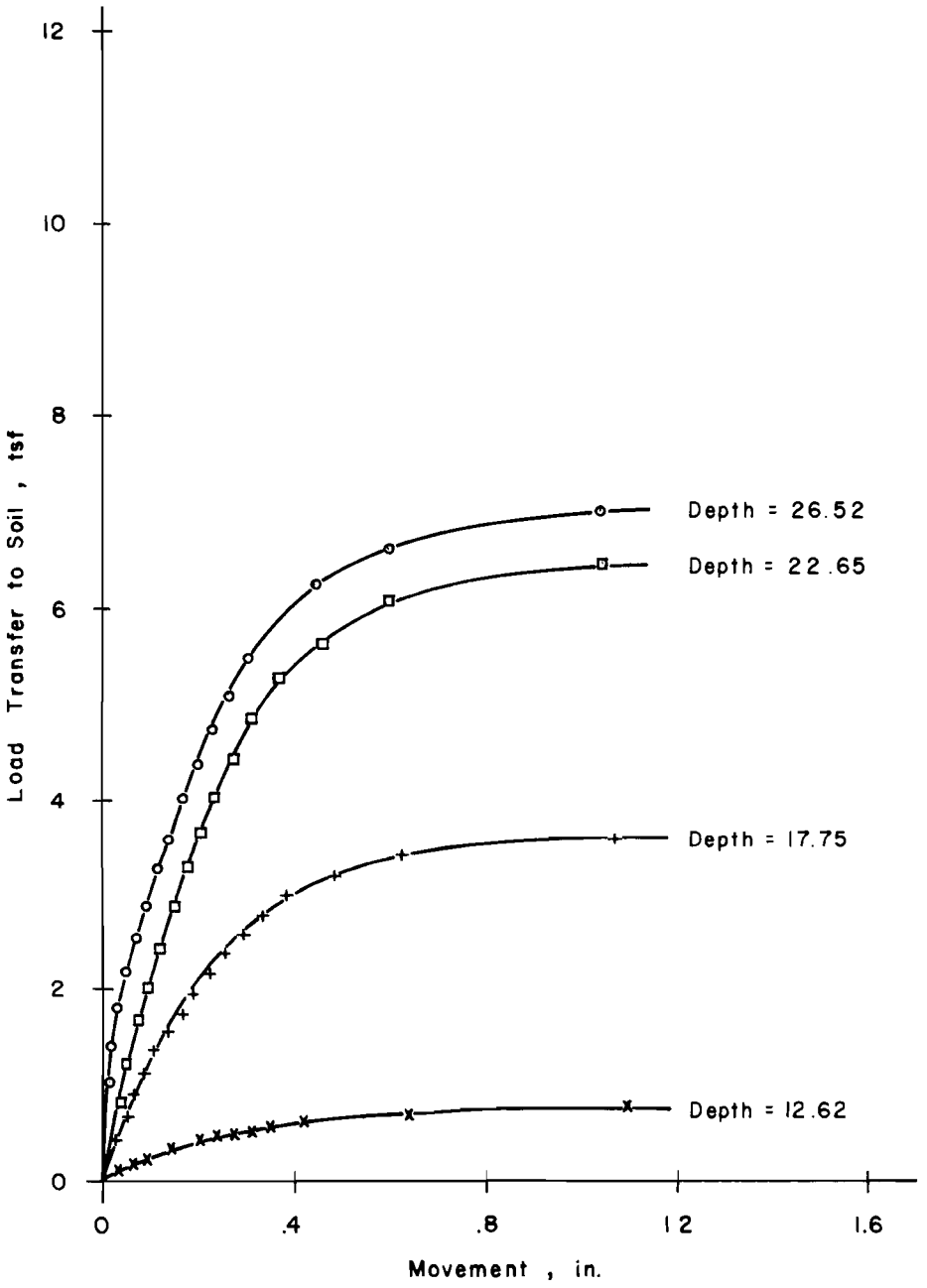

Fig 52. Relationship between load transfer and movement at various depths for Test No. 5 (quick test).

A typical relationship between the tip resistance and tip movement is shown in Fig 53, along with the load transfer. These curves are based on results of Test No. 3. It may be seen from this figure that more than 50 percent of total load transfer was developed for a tip movement of 0.2 inch. A very small increase in tip resistance and load transfer is indicated beyond 0.6 inch.

Analysis of Tell-Tale Data

Tell-tales of seven different lengths, as detailed in Chapter 3, were used to measure the deformation of the concrete shaft at seven different depths. The mechanism on which the measurement of deformation, corresponding to various lengths of concrete shaft, is based is as follows.

Consider two tell-tales of lengths L_1 and L_2, where $L_2 > L_1$, located in the concrete shaft as shown in Fig 54(a). When a load P is applied axially on top of the shaft, the elastic compression of the concrete shaft causes a reduction in the original length of the shaft. However, the tell-tales are so protected that they remain unstrained. A system of dial indicators (.0001 inch), supported on top of the shaft as shown in Fig 54(a), can be successfully used to measure the change in lengths L_1 and L_2 due to elastic compression in the shaft. The changes ΔL_1 and ΔL_2 measured by dial indicators would be

$$\Delta L_1 = L_1 - L_1'$$

$$\Delta L_2 = L_2 - L_2'$$

where

L_1' and L_2' are the deformed lengths as shown in Fig 54(b).

When the difference between the lengths L_1 and L_2 is relatively small compared to the original lengths, the average strain ε_i corresponding to a length of x_1 can be obtained from

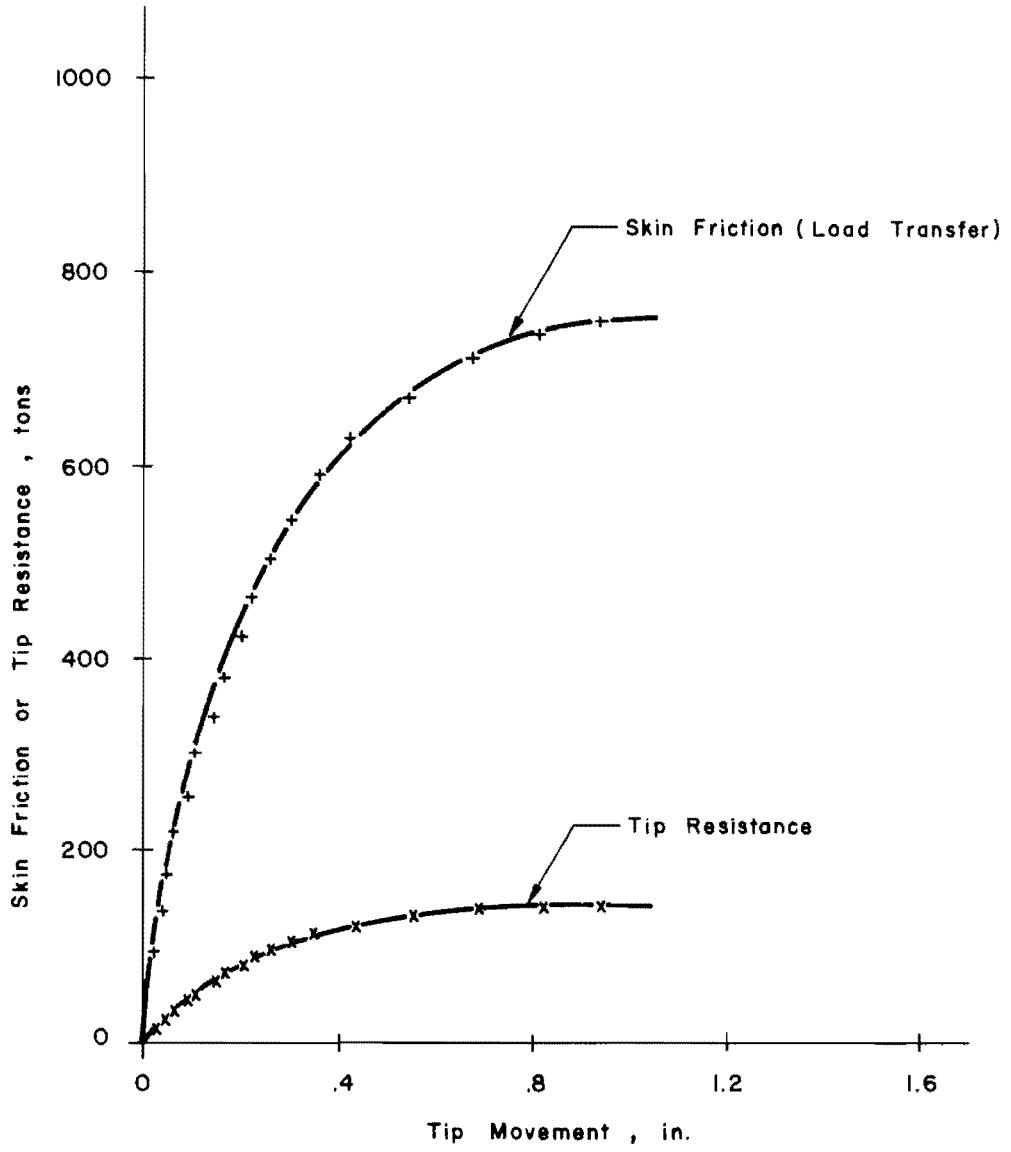

Fig 53. Typical relationship between tip resistance and skin friction and tip movement.

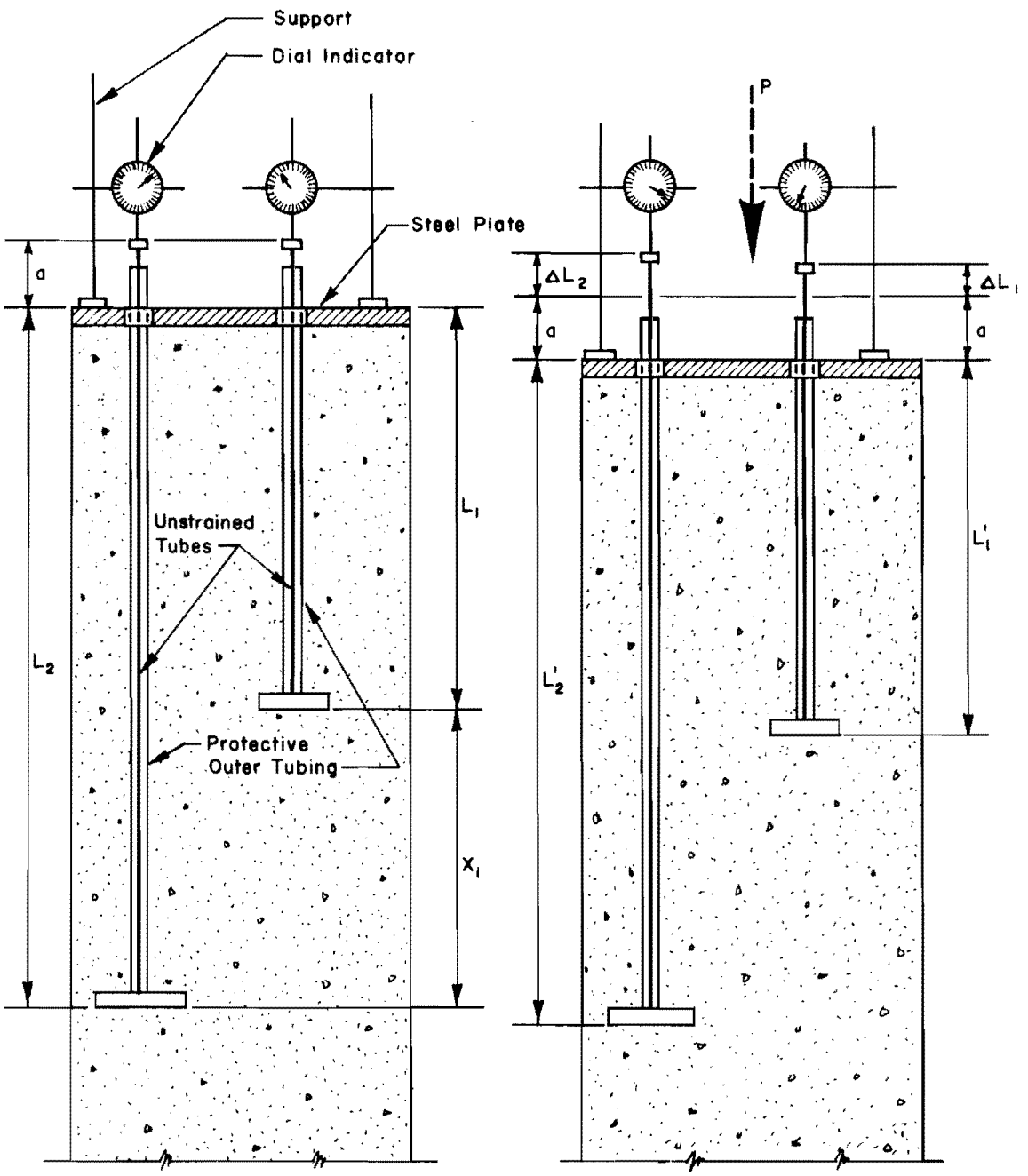

(a) Shaft with no load.

(b) Shaft after the application of load P .

Fig 54. Illustration of mechanism of tell-tales.

$$\epsilon_i = \frac{\Delta_1}{x_1} \tag{6.3}$$

where

$$\Delta_1 = \Delta L_2 - \Delta L_1$$

The average strain ϵ_1 is assumed to occur at the center of Section x_1. Thus, the load at the center of the Section x_1 can be computed from the known properties of the concrete shaft.

Test Results of Tell-Tales. The deformation ΔL corresponding to various lengths of the shaft, as observed in various load tests, is shown in Figs 55 through 58. The numbers along the curves indicate the axial load in tons on top of the shaft. It may be seen from these results that the data observed at shallow depths are irregular. This is probably due to the temperature variations near the ground surface and eccentric loading. The variation in air temperature causes the portion of the shaft which is above the ground surface to be affected more than that beneath the ground. Thus, the error introduced due to temperature variation in measurements of tell-tale readings would be more for tell-tales of smaller lengths. The magnitude of error can be seen from the illustration that follows.

Assume coefficient of thermal expansion of concrete = 5.5×10^{-6} in/in per degree F and coefficient of thermal expansion of tell-tale material steel = 6.5×10^{-6} in/in per degree F.

For a tell-tale with a 13.5-inch length below the top of the shaft and 4.5 inches in the air:

change in length in tell-tale per degree F = $18.0 \times 6.5 \times 10^{-6}$ inches

= 117×10^{-6} inches

change in length in concrete per degree F = $13.5 \times 5.5 \times 10^{-6}$ inches

= 74.3×10^{-6} inches

therefore error in measurement at this level = 0.427×10^{-4} inches per degree F. This would be an error of about 6 tons per degree F.

The air temperature during testing varies by about 8 to 10^{o} F in different tests. Thus, it can be seen that the tell-tales located near the ground

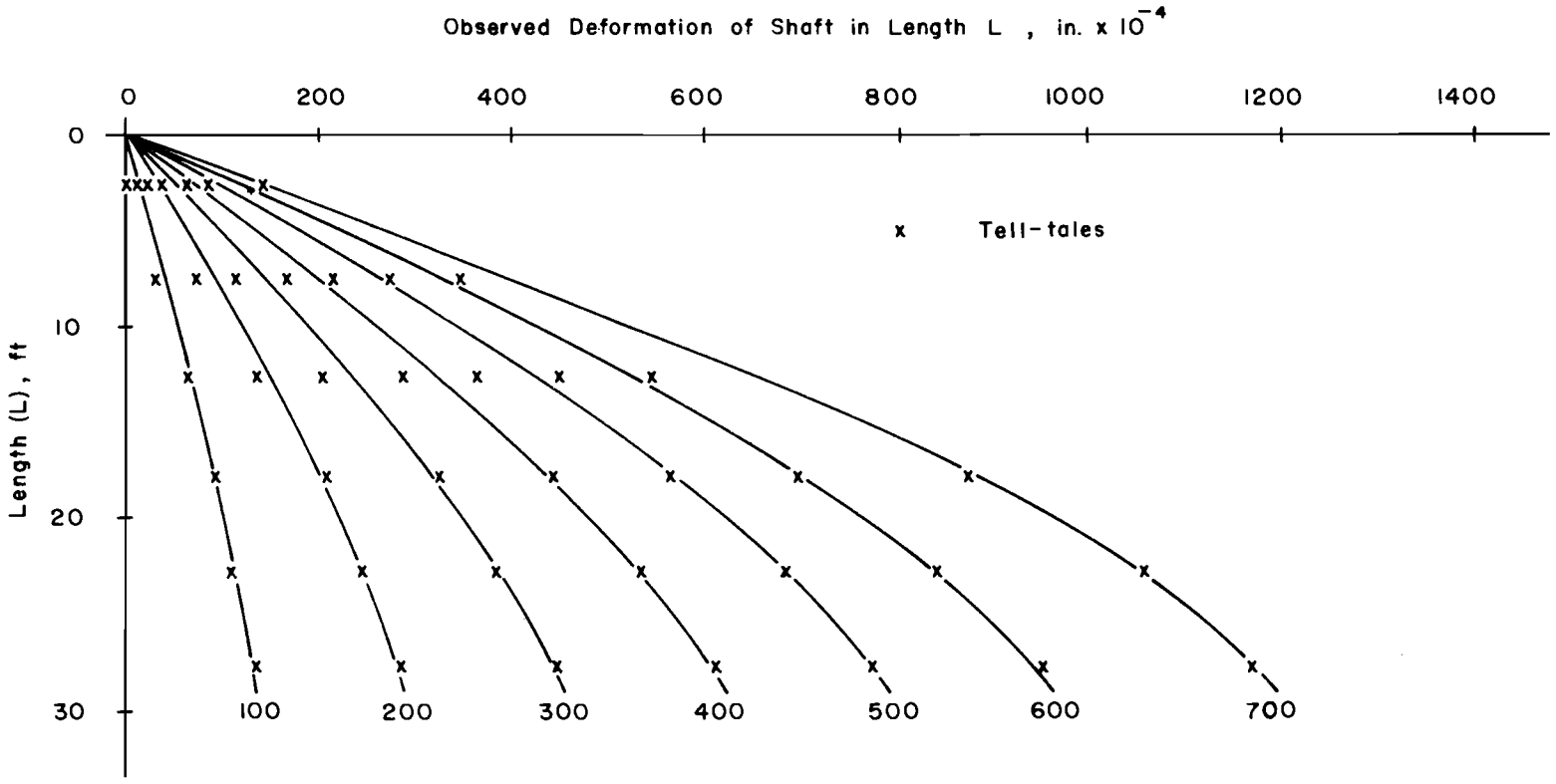

Fig 55. Observed deformation of shaft for various lengths for Test No. 2.

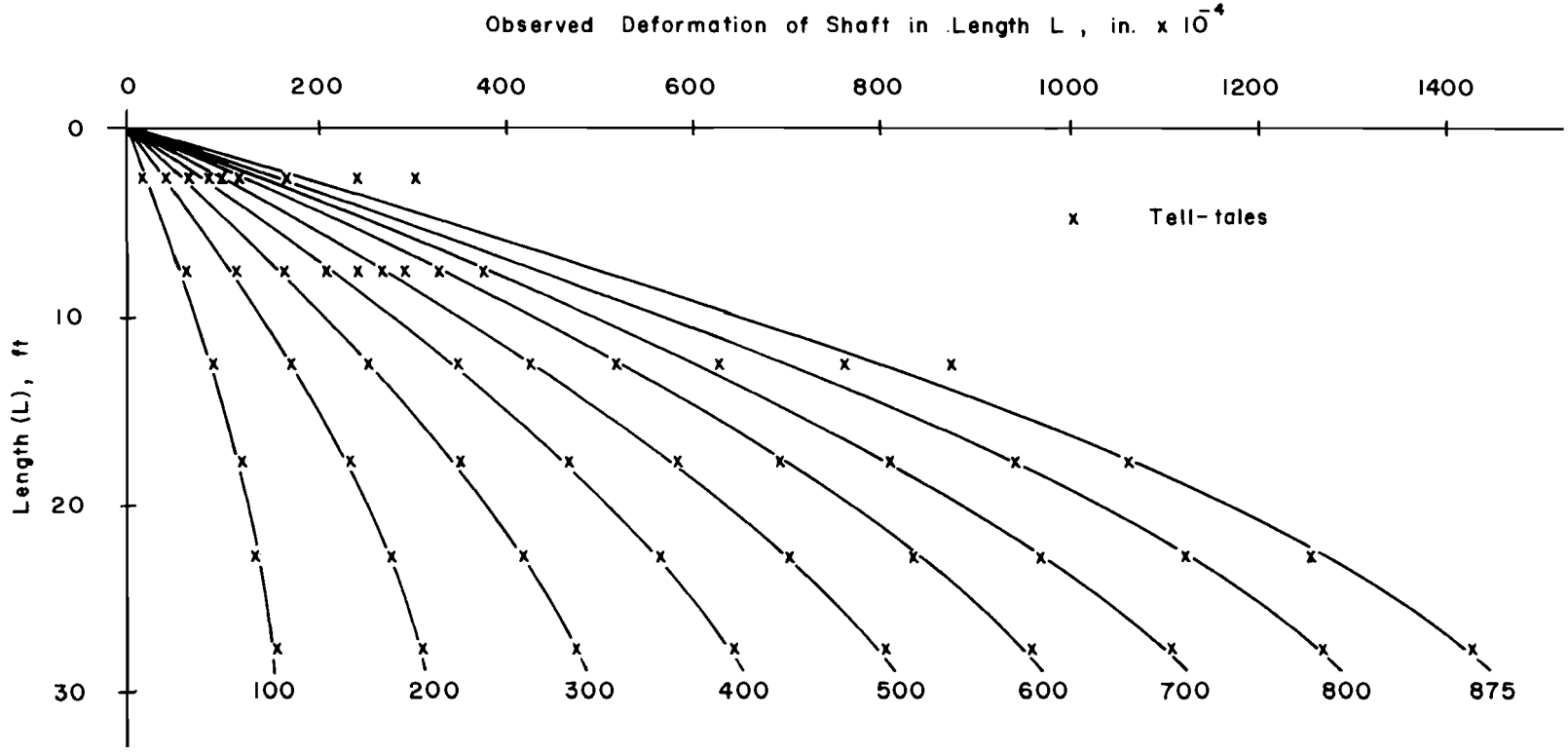

Fig 56. Observed deformation of shaft for various lengths for Test No. 3.

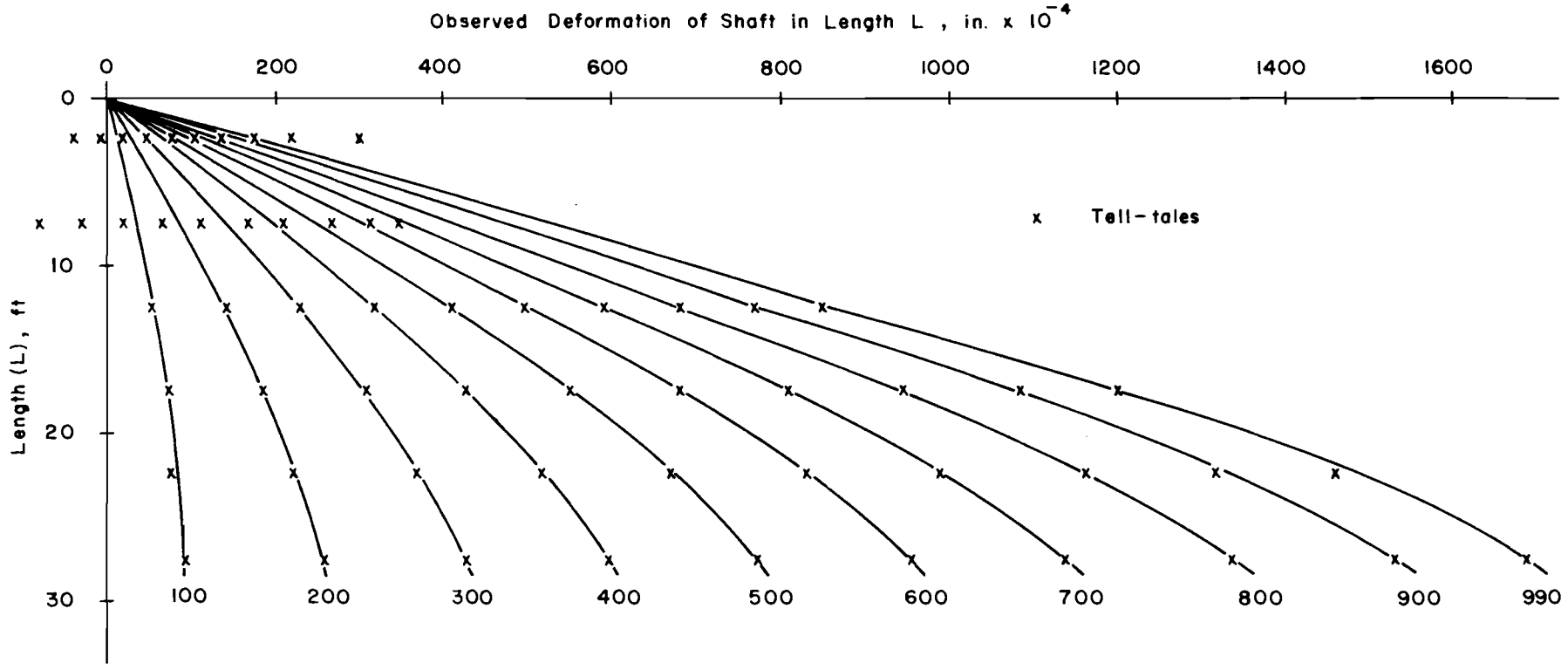

Fig 57. Observed deformation of shaft for various lengths for Test No. 4.

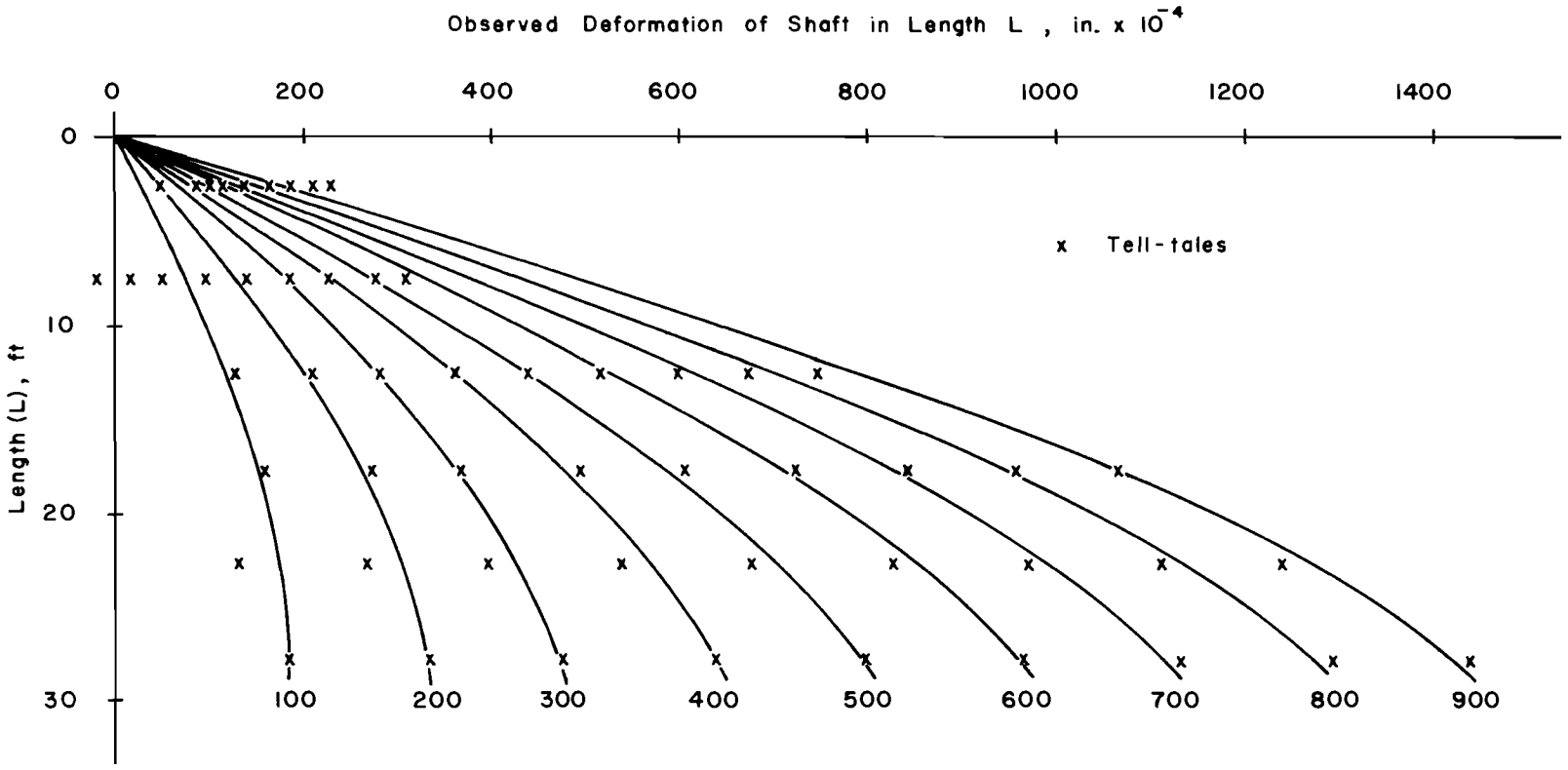

Fig 58. Observed deformation of shaft for various lengths for Test No. 5 (quick test).

surface were affected by temperature variations. However, very little temperature variation would be expected at relatively greater depths during the time of testing and hence no significant error would be introduced at greater depths.

Load-Distribution Computations. It may be recalled that the computation of load along the depth of the shaft involves the process of differentiation and hence any scatter in the observed data will increase the amount of scatter in the computed loads. To minimize this scatter the raw data were smoothed by drawing a smooth curve consistent with the original data, as shown by Figs 55 through 58. From these curves the deformation for various lengths was obtained and the strain computed by Eq 6.3. The initial portion of these curves is assumed to be a straight line so that the modulus of elasticity of the shaft can be determined. The load at various depths in the shaft can then be determined. The load-distribution curves thus obtained are shown in Figs 59 through 62. The change in tip load with the increase in load at the top of the shaft is summarized in Table 4. It may be seen from this table that the tell-tale computations indicate a tip load of about 40 percent of that at the top.

Comparison of Strain Gage and Tell-Tale Results

Load-distribution curves obtained from strain gages and from tell-tales are in fairly good agreement as can be seen from Figs 44 through 47 and Figs 59 through 62. However, the tip load indicated by strain gages is considerably lower than that indicated by tell-tales. This difference can be explained as follows.

In the case of strain gages the strain is measured almost at the tip of the shaft and hence the load computed corresponds to the actual load near the tip. But in the case of tell-tales the average strain is computed for the section of the shaft located between 24 and 28 feet deep. This strain, therefore, is representative of load in the shaft at a depth of 26 feet. A comparison of load in the shaft at a depth of 26 feet, both by strain gages and by tell-tales, is shown in Fig 63. It may be seen from this figure that the load in the shaft at a depth of 26 feet is in close agreement. Also, the poor stability of strain gages at the bottom may have resulted in smaller strain indications.

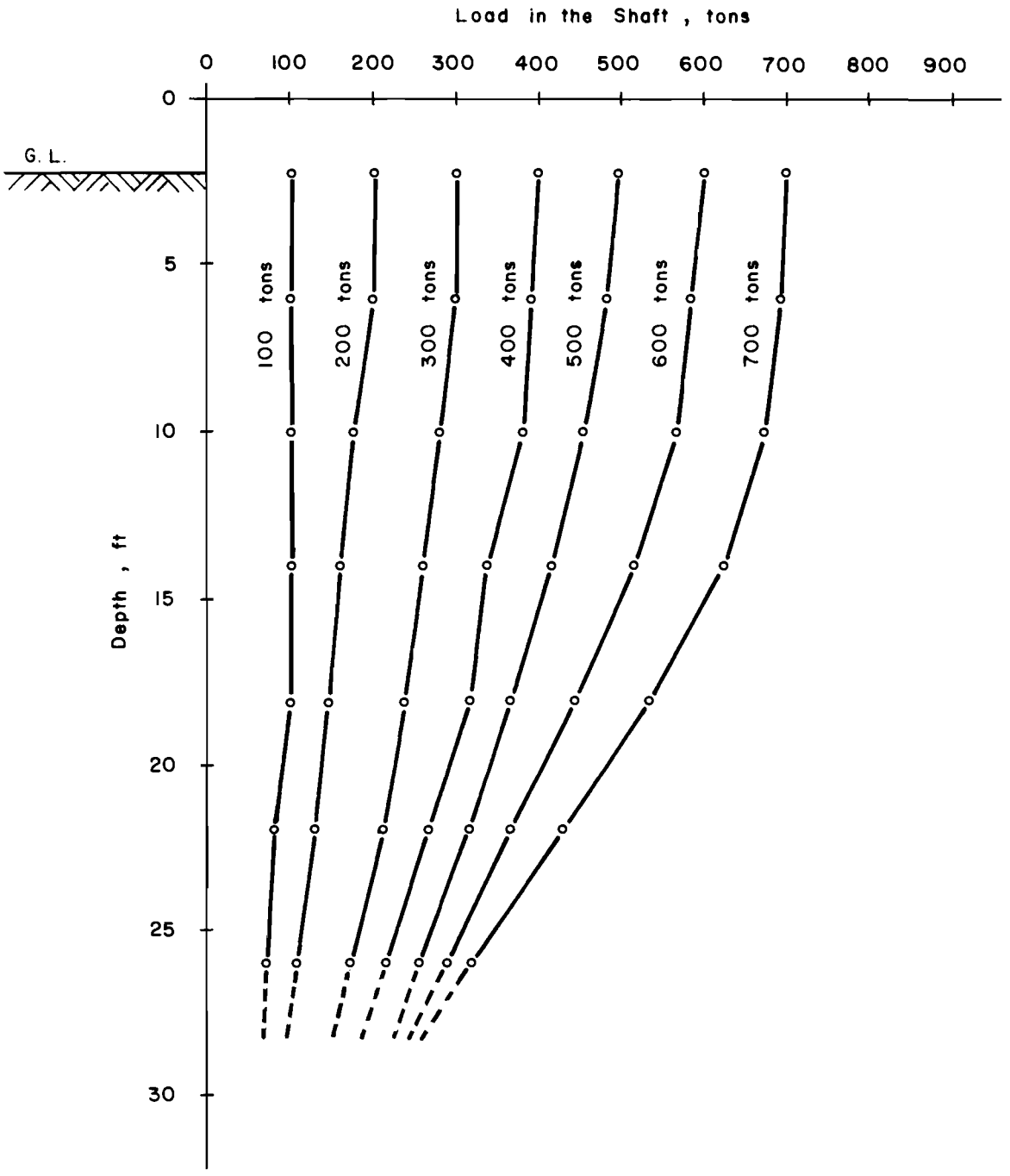

Fig 59. Load distribution along the shaft computed from tell-tale data (Test No. 2).

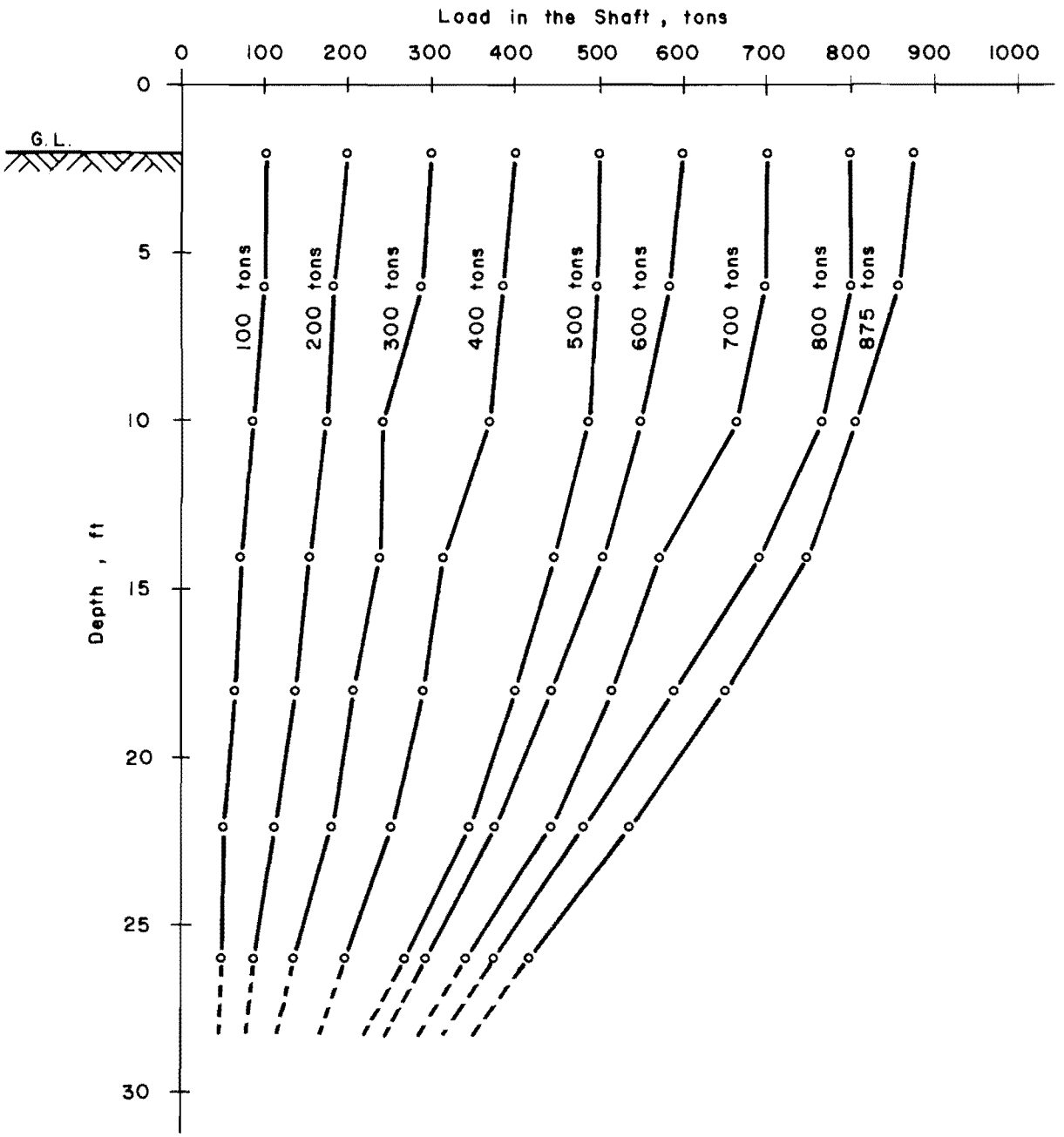

Fig 60. Load distribution along the shaft computed from tell-tale data (Test No. 3).

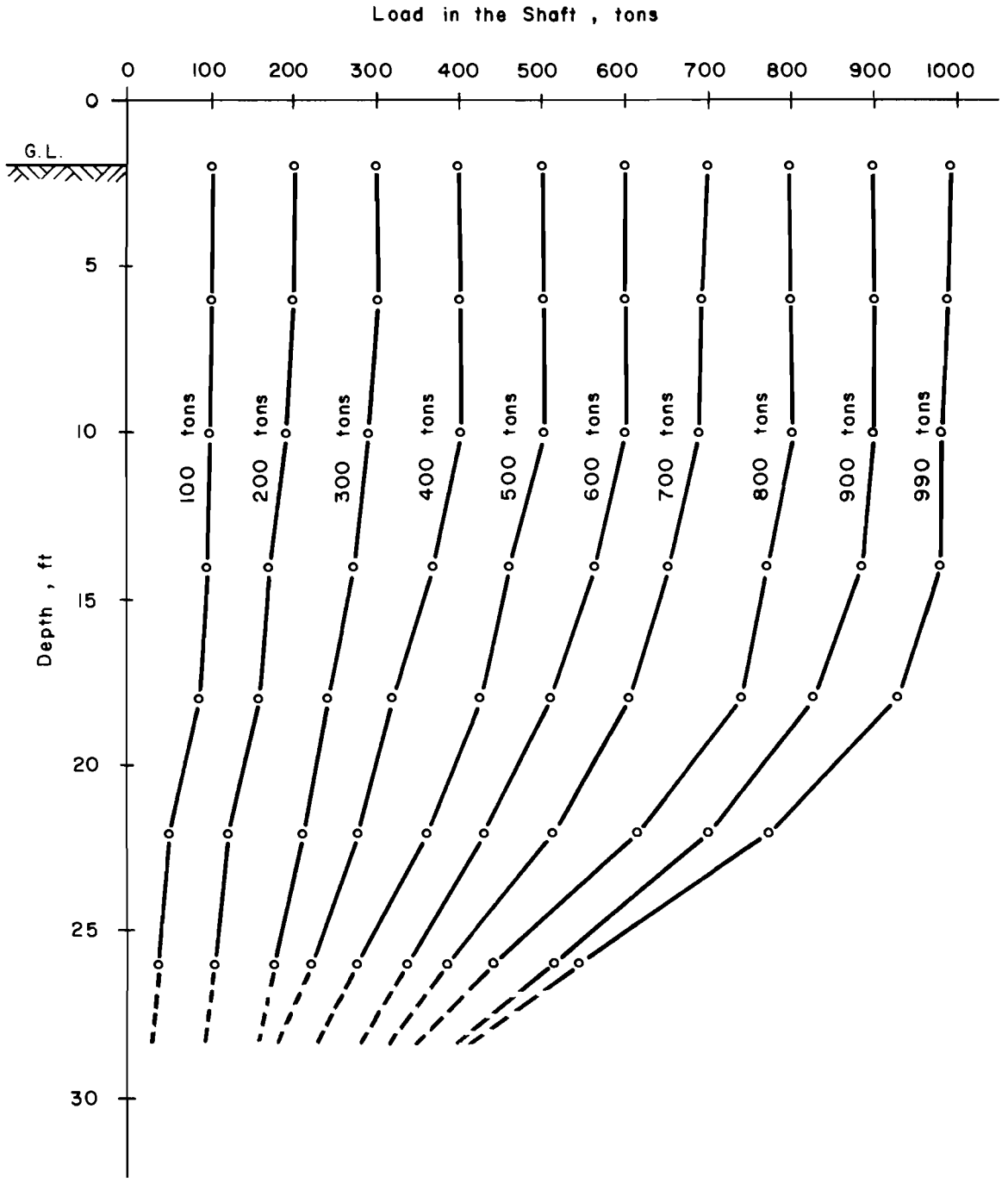

Fig 61. Load distribution along the shaft computed from tell-tale data (Test No. 4).

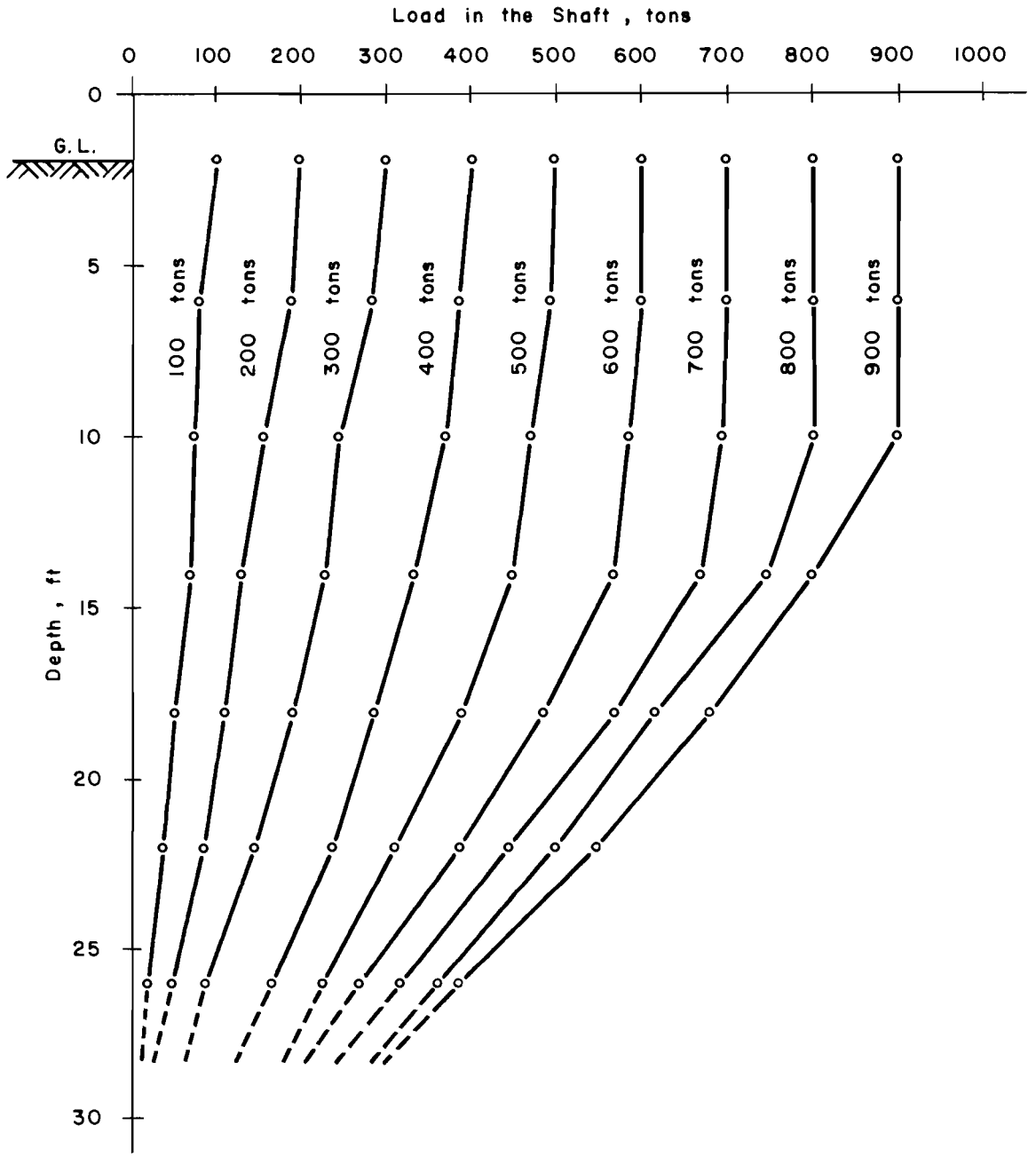

Fig 62. Load distribution along the shaft computed from tell-tale data (Test No. 5 - quick test).

TABLE 4. SUMMARY OF TIP RESISTANCE COMPUTED FROM TELL-TALES

Load on Top of Shaft, Tons	Tip Resistance of Shaft, Tons				Average Tip Resistance	Tip Resistance as Percentage of Top Load
	Test No. 2	Test No. 3	Test No. 4	Test No. 5 (Quick)		
100	63.7	44.6	27.9	7.1	45.4	45.4
200	89.0	71.2	91.1	20.1	83.8	41.9
300	153.5	109.6	152.1	54.9	138.4	46.1
400	180.0	162.1	174.3	116.1	172.1	43.0
500	221.4	218.1	221.9	171.4	220.5	44.1
600	236.6	236.5	278.9	196.4	250.7	41.8
700	233.9	278.2	308.6	232.6	273.6	39.1
800	--	306.7	336.4	279.5	321.5	40.2
875	--	343.6	--	--	343.6	39.2
900	--	--	391.7	286.2	391.7	43.5
990	--	--	398.9	--	398.9	40.3

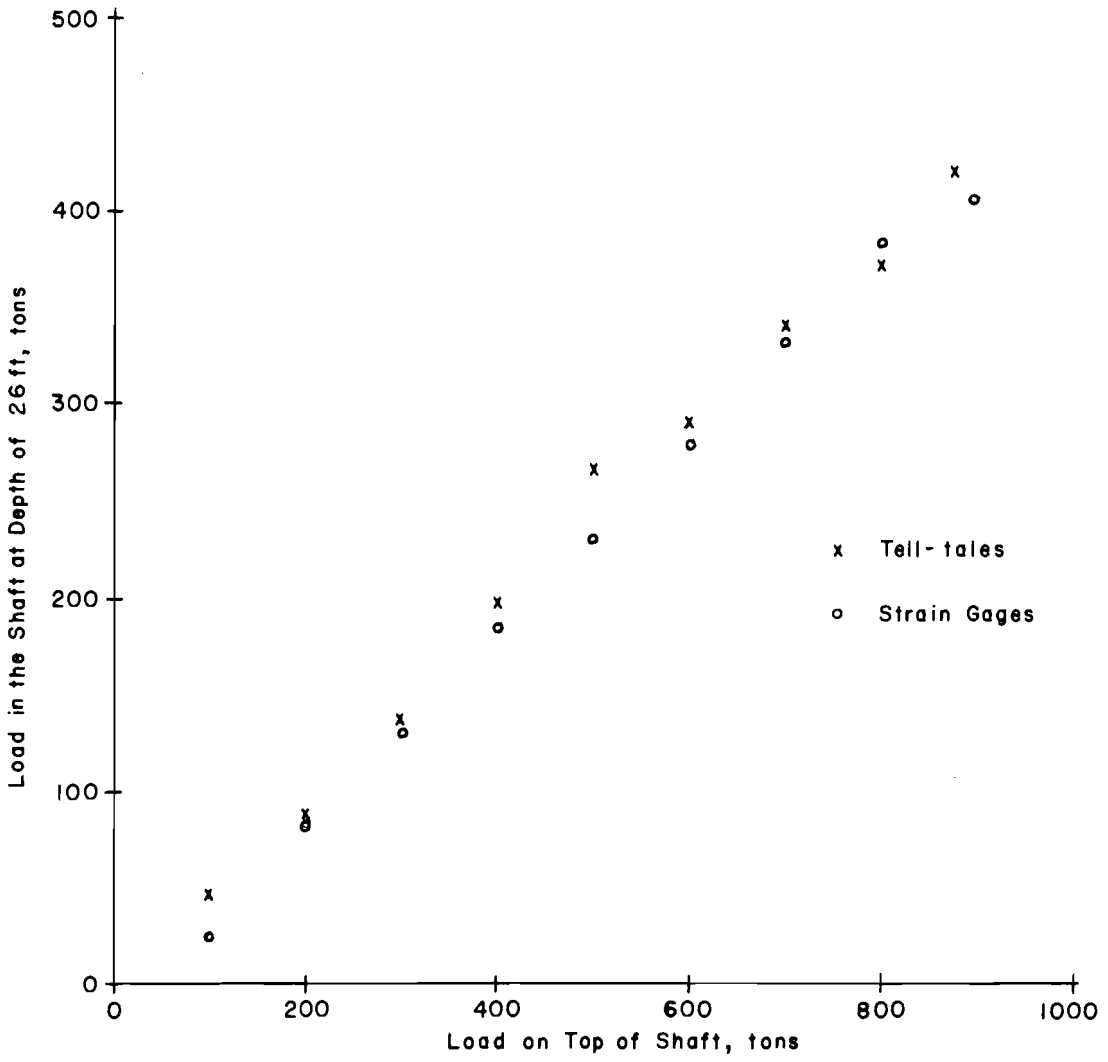

Fig 63. Comparison of load in the shaft at a depth of 26 feet computed from tell-tales and strain gages (Test No. 3).

CHAPTER 7. CORRELATION OF LOAD TRANSFER, SOIL PROPERTIES, AND SHAFT MOVEMENT

Variation of Penetration Resistance with Depth

In Chapter 4 it was pointed out that the conventional undisturbed shear strength of soil samples could not be determined below the depth of 18 feet. THD cone penetrometer tests were conducted at the test site to obtain variation of penetration resistance with depth. The results of these tests have been discussed and are presented in Figs 23(a) and 23(b). It may be noticed from these figures that the penetration resistance offered to the cone by the soil is expressed in terms of the number of blows N required to cause a cone penetration of 12 inches up to a depth of 18 feet. Below this depth, however, the penetration resistance is indicated in terms of the cone penetration in inches caused by 100 blows. For the purpose of correlation, however, it was considered desirable to express the variation in penetration resistance by one parameter throughout the entire depth. Therefore the cone penetration in inches obtained below the depth of 18 feet was converted into the equivalent value of N by the following relationship:

$$N = \frac{12}{s} \times 100 \tag{7.1}$$

where

s = penetration of cone in inches.

The variation of N values obtained or computed for various test bore holes is shown in Fig 64. It can be seen from this figure that there is a definite trend of N values down to a depth of about 18 feet. Below this depth the value of N increases considerably and a large scatter is indicated down to a depth of about 26 feet. For depths below 26 feet a constant value of N is indicated. To obtain the best estimate of N values a regression analysis of first order was performed for two zones separately. The equations for the lines of regression thus obtained for the two zones are

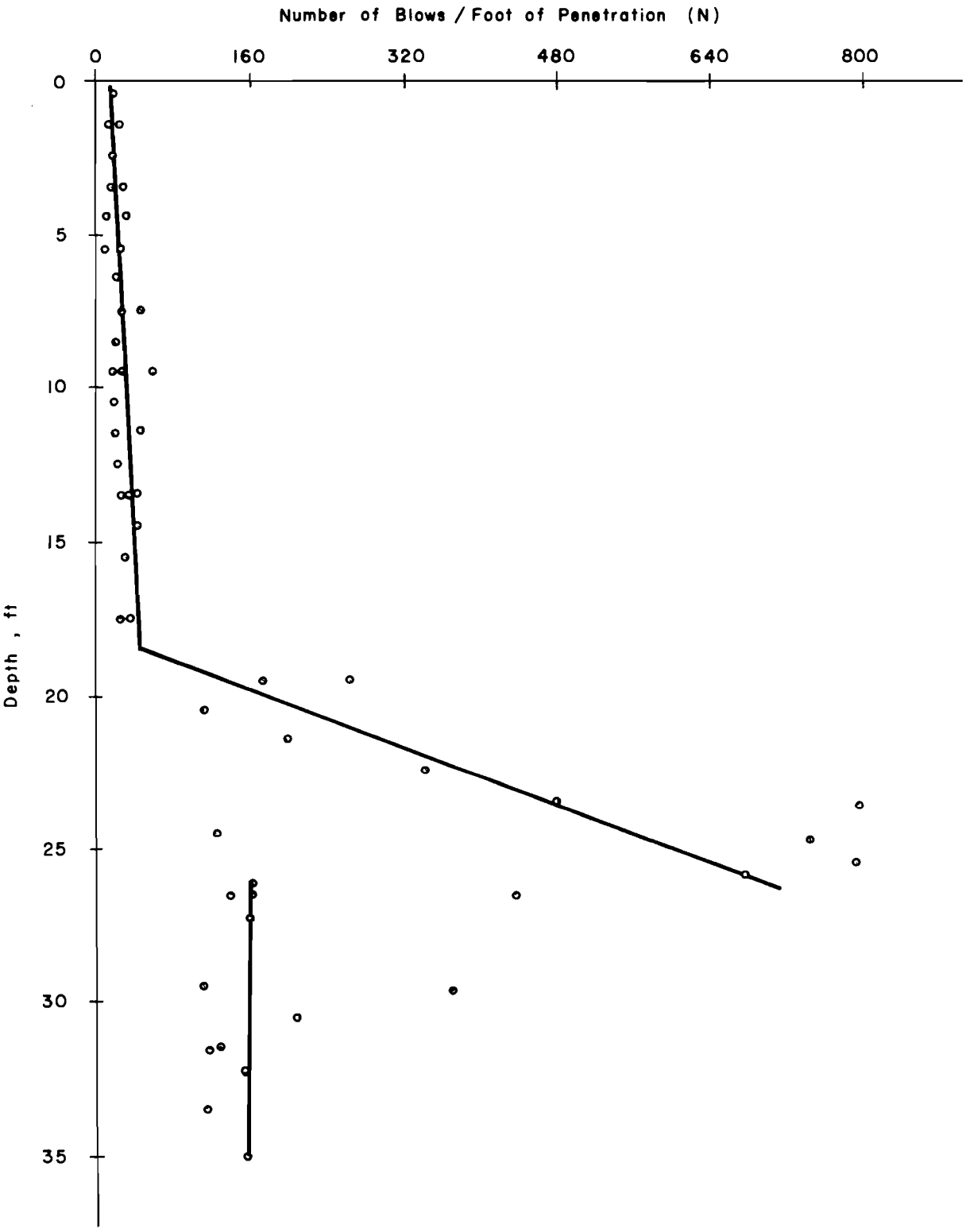

Fig 64. Variation of penetration resistance with depth.

ZONE I
(0 to 18 ft) $Y = 14 + 1.24\ X$ (7.2)

ZONE II
(18 to 26 ft) $Y = -1293 + 74.5\ X$ (7.3)

where

Y = best estimate of N value at a depth of X feet.

The standard error of estimate for Zone I was 8.5 and for Zone II was 199.

From these equations the values of N corresponding to the depth at which load transfer was computed were obtained.

A constant value of $N = 160$ was assumed for depths below 26 feet.

Relationship between Load Transfer and Shaft Movement

The variation of load transfer, in tons/ft^2, with shaft movement at certain depths, as obtained from the field load tests, was shown in Figs 49 through 52. It may be seen that the load transfer at any depth increases rapidly at smaller movements and then gradually tends to become constant after some movement. This nonlinear relationship of load transfer T, in tons/ft^2, at any depth with the shaft movement s, in inches, at that depth is found to be of the form

$$T = K \left[A_0 \sqrt{\frac{s}{s_0}} - B_0 \left(\frac{s}{s_0} \right) \right] \quad (7.4)$$

where

K = load transfer factor, and varies with depth,

A_0 = constant,

B_0 = constant,

s_0 = maximum settlement of shaft in inches, .05 to .06 × shaft diameter.

Now, assuming different values of K as 0.5, 2.5, 6.5, and 16, curves for T versus s/s_0 were obtained and are shown in Fig 65. The arbitrarily chosen values of K have some significance, as will be seen later. A comparison of this family of curves with those of load transfer versus movement curves shown in Figs 49 through 52 would indicate a remarkable similarity. This suggests that a certain value of K , called "load-transfer factor" in this study, is really representative of maximum load transfer under a set of conditions. Table 5 shows the values of maximum load transfer T_{max} obtained for the three load tests. Test No. 5, which was a quick test, is not shown. The values of K that were chosen arbitrarily earlier are also shown. This table indicates that the values of K equal to 0.5, 2.5, 6.5, and 16 are very close to the maximum load transfer T_{max} at depths of 10.91 feet, 16.05 feet, 20.94 feet, and 24.81 feet, respectively. Therefore, K can be expressed as

$$K = C_1 T_{max} \tag{7.5}$$

Substituting the value of K in Eq 7.4 we get

$$T = C_1 T_{max} \left[A_0 \sqrt{\frac{s}{s_0}} - B_0 \left(\frac{s}{s_0} \right) \right] \tag{7.6}$$

The load transfer T obtained from Eq 7.6 increases rapidly with increasing shaft movement up to $s/s_0 = 1$. Beyond this movement the value of T increases rather slowly.

The constants A_0 and B_0 also determine the value of constant C_1 . For maximum movement the ratio s/s_0 would be unity. It can be reasonably assumed that the load transfer would be maximum for the maximum movement. Therefore, for $s/s_0 = 1$, the Eq 7.6 would result in

$$T_{max} = T_{max} C_1 (A_0 - B_0) \tag{7.7}$$

If A_0 and B_0 are chosen such that $A_0 - B_0 = 1$, then the value of constant C_1 would be unity. The Eq 7.6 would then reduce to

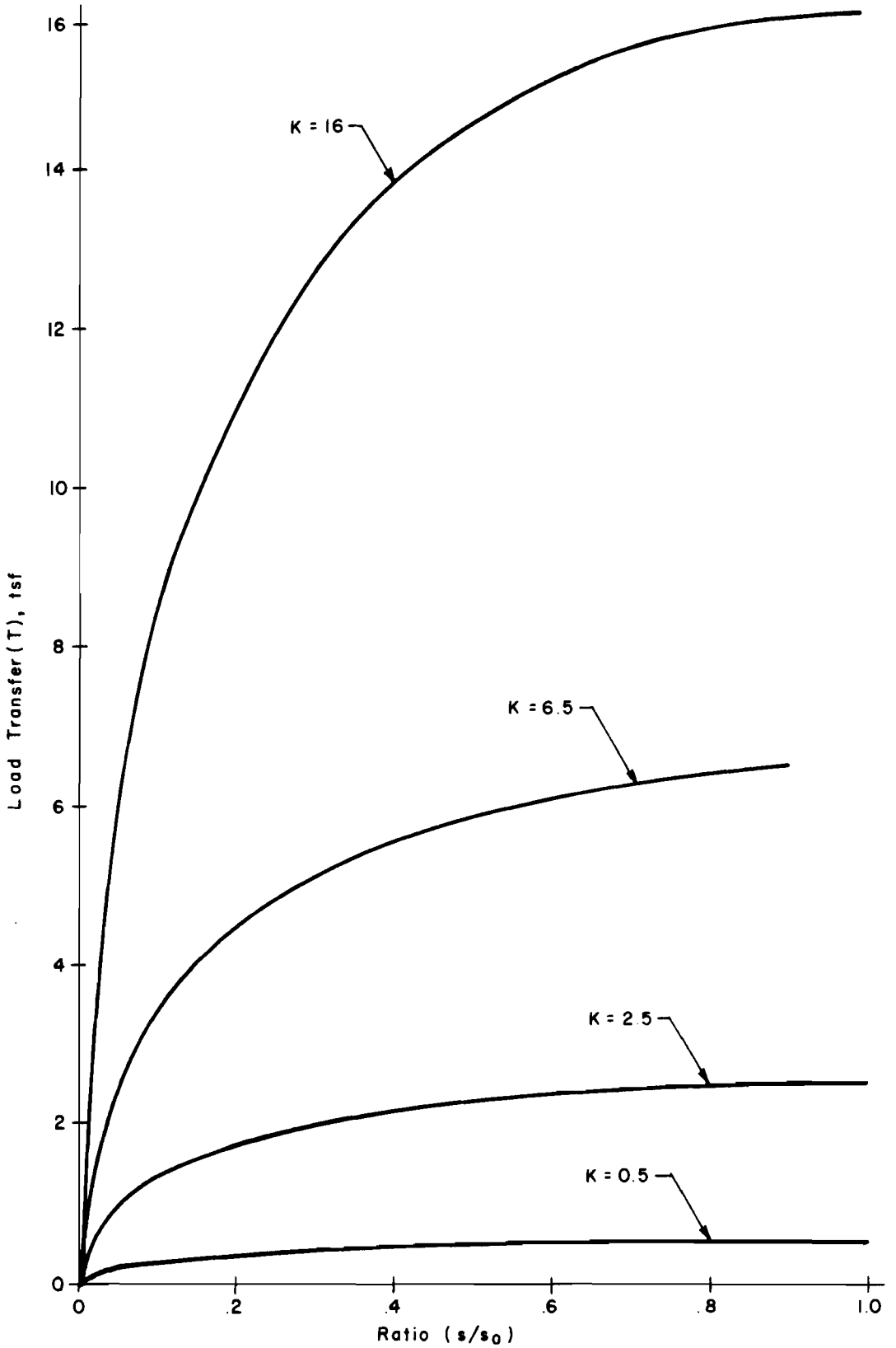

Fig 65. Theoretical load-transfer curves generated by Eq 7.4 for $A_o = 2$ and $B_o = 1$.

To obtain the appropriate values of constants C_2, A_0, and B_0 regression analysis was carried out on the data presented in Figs 49 through 52.

TABLE 5. MAXIMUM LOAD TRANSFER, T_{max} OBTAINED FROM LOAD TESTS

Depth Below Ground Surface, Feet	Maximum Load Transfer to Soil Tons/ft^2			Average T_{max} Tons/ft^2	K
	Test No. 2	Test No. 3	Test No. 4		
1.62	0.49	0.45	--	0.47	--
5.79	0.49	0.46	--	0.48	--
10.91	0.51	0.45	0.42	0.46	0.5
16.05	2.50	2.50	3.65	2.88	2.5
20.94	--	--	6.63	6.63	6.5
24.81	--	--	14.45	14.45	16.0

$$T = T_{max} \left[A_0 \sqrt{\frac{s}{s_0}} - B_0 \left(\frac{s}{s_0} \right) \right] \tag{7.8}$$

Relationship between T_{max} and N

If T_{max} at any depth can be obtained from the known value of N at that depth, Eq 7.6 can be further modified to predict T from the N values directly. To obtain such a relationship various parameters such as N , and Z , the depth at which T_{max} is considered, L the total embedded length of shaft, the ratio Z/L , and their various combinations were studied. A gradual development of such a relationship is shown in Table 6. It may be seen from this table that ratio N/T_{max} is approximately constant except at depths of 10.91 feet and 16.05 feet. At a depth of 10.91 feet the value of N may be actually slightly lower than 27. At a depth of 16.05 feet the value of N is difficult to estimate as this depth is close to the boundary of two zones which have widely different N values. It appears that the harder zone begins at a depth slightly shallower than indicated by the soil profile. From these considerations it appears that the maximum load transfer is proportional to the value of N and can be given by

$$T_{max} = \frac{N}{C_2} \tag{7.9}$$

where

C_2 = constant.

It may be observed that C_2 also can be evaluated in terms of the number of blows per foot of a standard penetrometer, but such an evaluation is beyond the scope of this report.

Thus the value of maximum load transfer T_{max} at any depth can be obtained from Eq 7.9, if the constant C_2 and N are known. Since the value of N at various depths is known, the value of constant C_2 remains to be determined. Assume that C_2 can be determined. Now substituting the value of T from Eq 7.9 into Eq 7.8 the following relationship is obtained.

$$T = \frac{N}{C_2} \left[A_0 \sqrt{\frac{s}{s_0}} - B_0 \left(\frac{s}{s_0} \right) \right] \tag{7.10}$$

TABLE 6. COMPARISON OF N AND T_{max} AT VARIOUS DEPTHS

Depth Below Ground Surface, Feet	T_{max} Tons/ft^2	N	Ratio $\frac{N}{T_{max}}$
1.62	0.47	16	34
5.79	0.48	21	44
10.91	0.46	27	59
16.05	2.88	60	21
20.94	6.63	267	40
24.81	14.45	594	41

The value of s_0 was assumed to be 6 percent of the shaft diameter. Program "STEP01" was used for the regression analysis. This program is a modified version of program "BMD02R" (Ref 8). The modification was carried out by the Center for Highway Research.

Two sets of constants A_0 and B_0, fulfilling the condition $A_0 - B_0 = 1$, were used for regression analysis. The results of this analysis are shown in Table 7. The value of constant C_2 varied approximately from 35 to 42, without considerably affecting the regression coefficient.

These sets of constants were used to compute load-settlement curves based on Eq 7.10 and were compared with the observed load-settlement curve. The procedure of computation will be given later in this chapter. The following equation gave the best results:

$$T = \frac{N}{35}\left(2\sqrt{\frac{s}{s_0}} - \frac{s}{s_0}\right) \qquad (7.11)$$

The load-settlement curve computed from Eq 7.11 is shown in Fig 66 along with the observed curve. It may be seen that these curves are in good agreement.

Examination of Eq 7.11 would indicate that the value of load transfer will be zero if either the movements or the value of N is zero. This is true as no skin friction can be mobilized without movement. Since N value is determined in the field the effect of degree of confinement is also included in it. For example if the cone penetration tests were to be carried out in a homogeneous clay with a practically constant value of cohesion, the value of N at large depths will be greater than at the surface. This implies a greater load transfer at larger depths for the same material due to the increasing confining pressure. Studies of Seed and Reese (Ref 18) with vane shear tests in clay also indicate an increasing load transfer with the increase in depth.

Correlation of Tip Resistance and N

The value of tip resistance observed during various load tests was shown in Table 3. It may be seen from that table that the value of tip resistance corresponding to failure load is approximately 185 tons. Test No. 5 was not

TABLE 7. SUMMARY OF REGRESSION ANALYSIS

Assumed Values of A_0 and B_0	Best Estimate of C_2	Regression Coefficient	Standard Error of Estimate
$A_0 = 2$ $B_0 = 1$	42	0.990	0.58
$A_0 = 1.5$ $B_0 = 0.5$	35.4	0.992	0.54

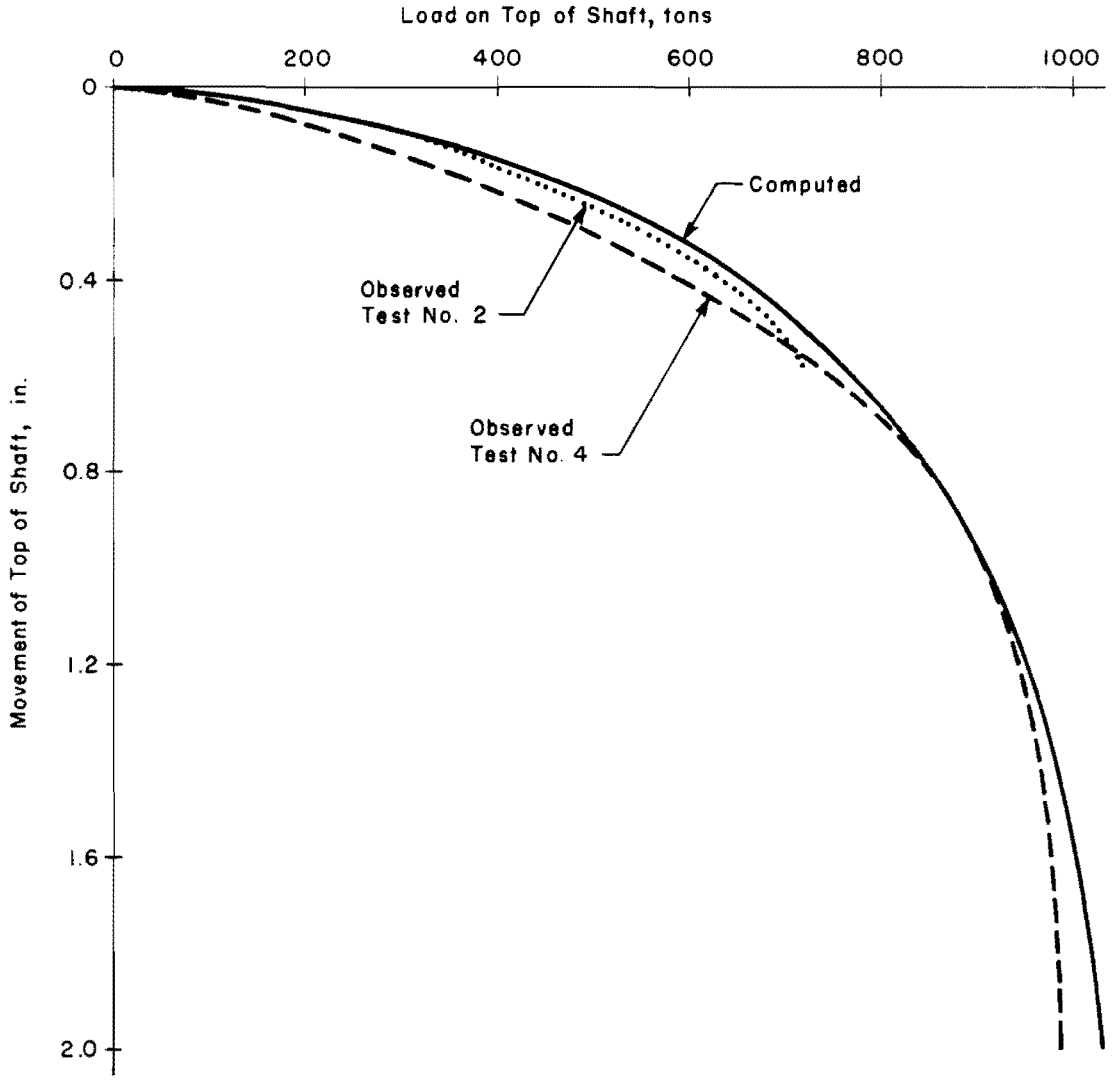

Fig 66. Comparison of observed and computed load-settlement curves.

considered as this was a quick test. The value of N at a depth corresponding to the tip of the shaft is 160 blows/ft. This suggests that the ultimate tip resistance Q_{bu}, in tons, may be expressed approximately as

$$Q_{bu} = 3\,A\,\sqrt{N} \tag{7.12}$$

where

A = cross-sectional area of shaft in square feet.

Alternatively the value of Q_{bu} can be computed from the relationship

$$Q_{bu} = N_c \cdot \frac{N}{C_2} \cdot A \tag{7.13}$$

where

N_c = bearing capacity factor.

For $N = 160$ and $A = 5\ ft^2$ and using Eq 7.12 the value of Q_{bu} is found to be 190 tons. Using Eq 7.13 and assuming $N_c = 9$ and $C_2 = 35$ the value of Q_{bu} is found to be 206 tons. Thus, it can be seen that the values of Q_{bu} obtained from Eqs 7.12 and 7.13 are in close agreement. However, for small values of N, Eq 7.12 would yield higher values of Q_{bu} as compared to those obtained by Eq 7.13. Further study in this direction seems necessary before any conclusive statement can be made.

The tip resistance at the bottom of the shaft as a function of tip movement is usually required to compute a load-settlement curve (Ref 11). Such a relationship can be approximately expressed as

$$Q_B = \left(\frac{s}{s_0}\right)\frac{1}{3}\,Q_{bu} \tag{7.14}$$

where

Q_B = tip resistance corresponding to the ratio s/s_0,

s = movement of tip,

s_0 = maximum settlement of shaft in inches.

Proposed Design Procedure for a Drilled Shaft

Based on the results of these tests the framework for a new method for designing a drilled shaft has been developed. This method is based on the relationship between load transfer and movement at various depths as indicated by Eq 7.11. In the method, load-settlement curves for various trial lengths of a shaft are generated. The load-settlement curve which fulfills the requirements of design load and/or the limiting settlement can be selected. If the shaft dimensions are already known, load-settlement curves can be obtained for the proposed shaft. The proposed method is as follows:

Case I. When Shaft Dimensions Are Known

(1) Obtain the variation of N , the number of blows per foot of penetration for the THD cone penetrometer, as a function of depth.

(2) Divide the embedded length of the shaft into a specific number of sections, say m .

(3) Compute the depth and the value of N corresponding to the center of these m sections.

(4) Assume an approximate value of load P_{m+1} and settlement s_{m+1} at the bottom of the shaft for the m^{th} section. Eq 7.10 can be used.

(5) Assume the tip settlement to be the movement of the midpoint of the m^{th} section of shaft (bottom section).

(6) Compute load transfer T_m in tons/ft^2 for the m^{th} section for the movement s_{m+1} assumed in Step 5 according to Eq 7.11.

(7) Compute incremental load transfer to soil for the m^{th} section by multiplying T_m by the surface area of the m^{th} section.

(8) Compute load on top of the m^{th} section P_m by adding the incremental load to the load at the bottom of the m^{th} section, $P_m = P_{m+1} + T_m$.

(9) Compute elastic compression Δ_m for the m^{th} section corresponding to the average load.

(10) Compute the movement of the bottom of the $(m - 1)^{th}$ section by assuming $s_m = s_{m+1} + \Delta_m$.

(11) Repeat Steps 4 through 10 for all the sections and obtain P_1 and s_1 at the ground level.

(12) Compute elastic compression s_0 for the exposed length of the shaft, if any, under the load P_1.

(13) Obtain the movement s at the top of the shaft by $s = s_1 + s_0$.

(14) Repeat Steps 4 through 13 for different sets of tip load and tip settlement values.

Case II. When Shaft Length Is Not Known

(1) Obtain the variation of N with depth.

(2) Assume a trial length of shaft with a trial diameter.

(3) Carry out the operations indicated in Case I from Steps 2 through 14.

(4) Repeat Steps 1 through 3 of Case II for various trial lengths.

A computer program called "SHAFT" based on the procedure outlined above has been written. Sample input, output, and a copy of the program are given in Appendix 4.

Prediction of Load-Settlement Curves

The load-settlement curve for a shaft of given dimensions can be computed by using Program "SHAFT." The computed load-settlement curve shown in Fig 66 was obtained by using this program.

Load-settlement curves were also computed for cases where the time interval between the loading increment was different. Figure 67 shows the comparison of the observed load-settlement curve for Test No. 5 (quick test) and the computed curve. The computed curve was obtained by using $C_2 = 40$, $A_0 = 2.5$, and $B_0 = 1.5$ in Eq 7.10. The two curves appear to be in good agreement. Another case of the quick test is shown in Fig 68, in which the observed load-settlement curve for another site is compared with the computed curve. For the computed curve the constants used were $C_2 = 38$, $A_0 = 3.5$, and $B_0 = 2.5$. The two curves are in fairly good agreement. Figure 69 shows the comparison of load-settlement curves for the case where the time interval between the loading increment was 30 minutes. The computed curve was obtained by using $C_2 = 36$, $A_0 = 1.5$, and $B_0 = 0.5$. The two curves appear to be in good agreement.

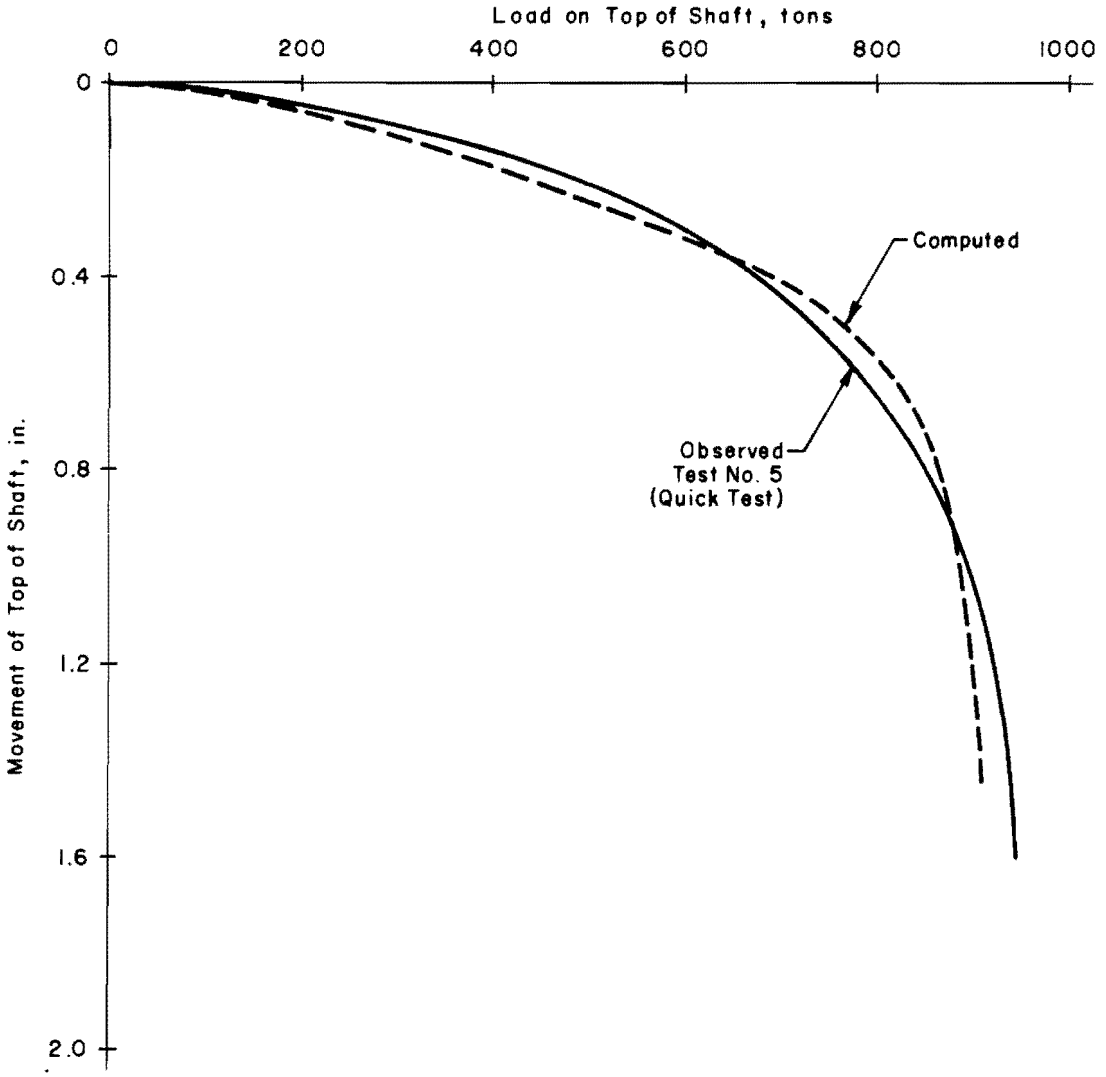

Fig 67. Comparison of observed and computed load-settlement curves for quick test.

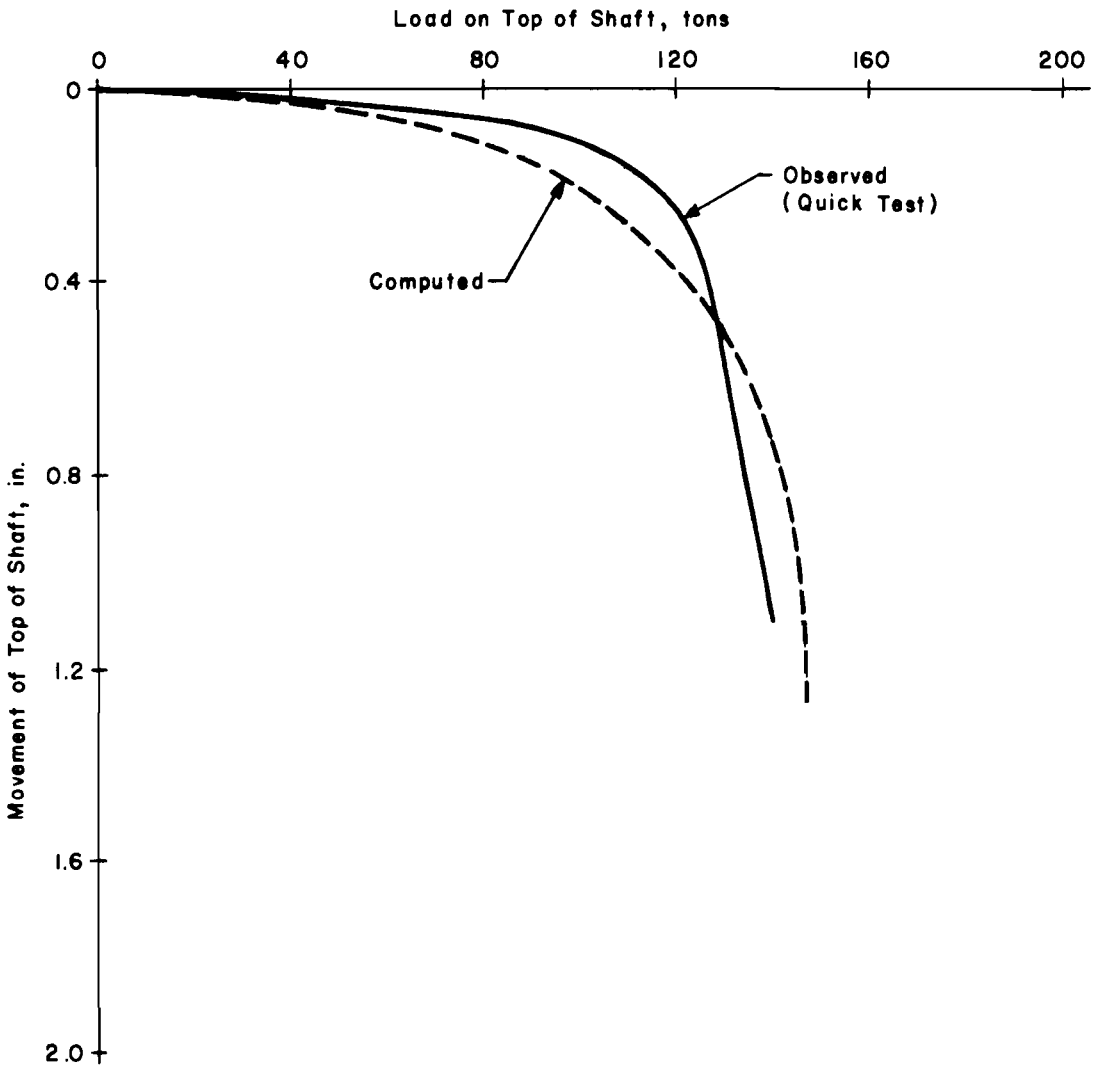

Fig 68. Comparison of observed and computed load-settlement curves for the Houston site.

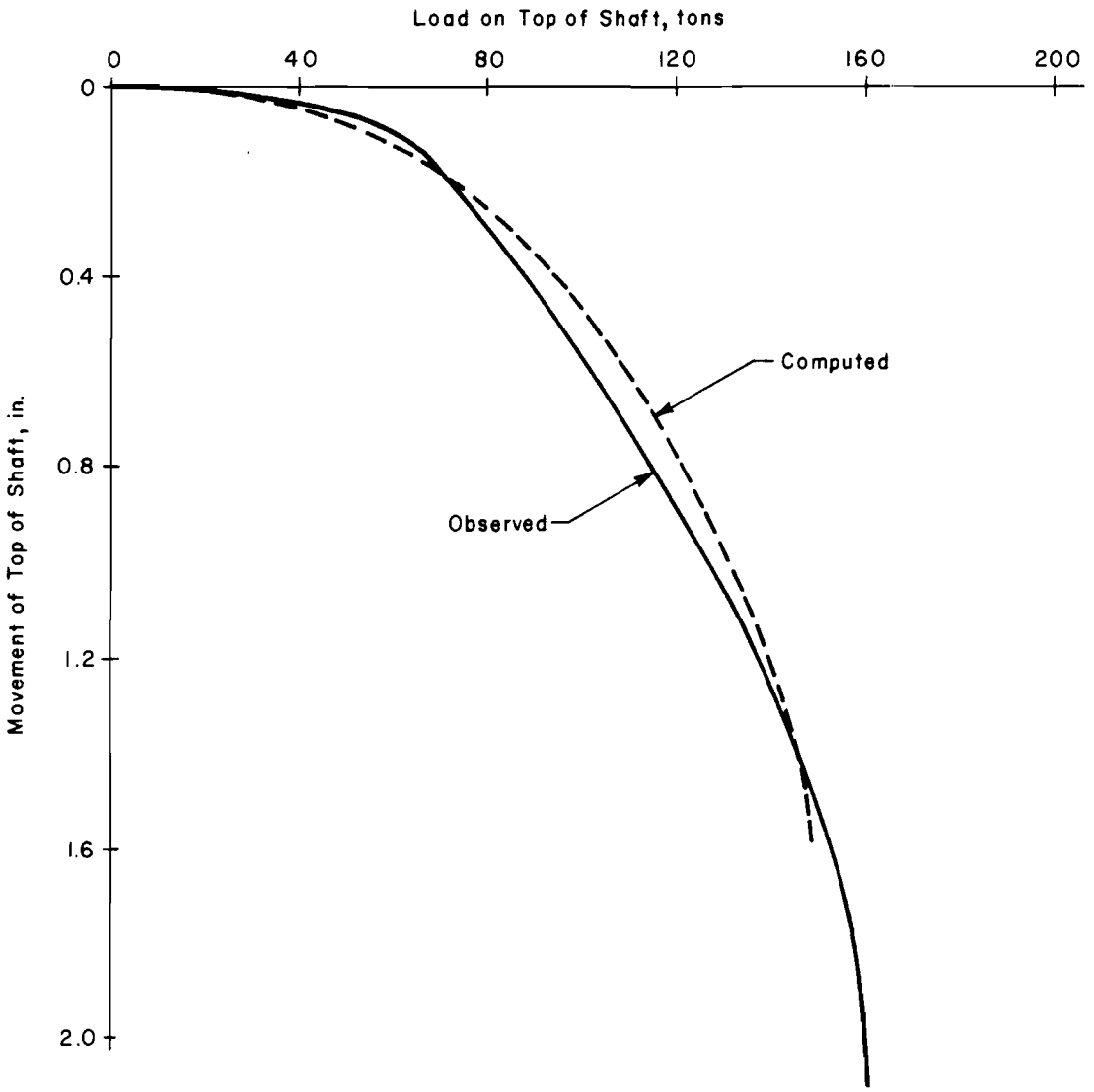

Fig 69. Comparison of observed and computed load-settlement curves for the Montopolis site.

It is interesting that the failure load computed by the proposed design method is in very good agreement with the observed one in every case studied. Further, it appears that the shape of the load-settlement curve can be changed by altering the constants. From the present study the following constants can be indicated for the various tests procedures:

(1) Quick test

$$C_2 = 38 \text{ to } 40$$

$$A_0 = 2.5 \text{ to } 3.5$$

$$B_0 = 1.5 \text{ to } 2.5$$

such that

$$A_0 - B_0 = 1 .$$

(2) Load tests where the time interval between loading increments is 12 to 15 minutes

$$C_2 = 35 \text{ to } 36$$

$$A_0 = 2.0$$

$$B_0 = 1.0$$

(3) Load tests where the time interval between loading increments is over 30 minutes

$$C_2 = 35 \text{ to } 36$$

$$A_0 = 1.5$$

$$B_0 = 0.5$$

Limitations

The relationship between T, N, and s given by Eq 7.11 has been developed for specific soil conditions that existed at the San Antonio site. The soil conditions at this site were far from homogeneous, as has been indicated in Fig 64. The value of N below the depth of 18 feet was found to vary considerably and the best estimate of N was obtained by using the statistical approach. The value of s_0 suggested in Eq 7.4 may not be valid for soft clays and extremely stiff clays or hard clay shale. For soft clays the value of s_0 may be much higher and for hard clay shale the value may be much smaller. The suggested values of constants A_0, B_0, and C_2 are based on the study of a limited number of cases. More case studies, under different conditions of soil and under different load test procedures are necessary before any firm recommendations can be made.

Under extreme conditions of weather, e.g., complete flooding or development of wide shrinkage cracks near the shaft due to shrinkage in the soil, the value of N should be adjusted while using the program shaft. A condition of no load transfer can be simulated by inputing $N = 0$ at any depth.

In the present form Eq 7.10 can be applied only to those cases where N, the number of blows per foot penetration, is known. However, it can be modified to make it more generalized by using the undrained, undisturbed shear strength, determined from conventional procedures, and evaluating an appropriate value of constant C_2. When the variation of shear strength with depth is known, Eq 7.10 can be used approximately by replacing N/C_2 with shear strength in tsf.

CHAPTER 8. CONCLUSIONS AND RECOMMENDATIONS

This study has provided information which will be valuable in the rational design procedure for drilled shafts. Specifically the following conclusions and recommendations can be made from this study.

Conclusions

(1) Embedment strain gages can be used reliably for short-term studies. However, with the passage of time the water from the soil migrates into the strain gages, thereby reducing the stability of the gages.

(2) Dummy strain gages used for the compensation of temperature effects did not prove very effective and need improvement.

(3) Tell-tales greater than 10 feet seem fairly satisfactory for measurements of axial deformations in the shaft. Tell-tales shorter than 10 feet seem to be affected considerably by temperature variations.

(4) The load-transfer T to soil at any depth is a function of penetration resistance as well as the movement at that depth and can be expressed as

$$T = \frac{N}{C_2}\left[A_0 \sqrt{\frac{s}{s_0}} - B_0 \left(\frac{s}{s_0} \right) \right]$$

(5) The maximum load transfer is directly proportional to the value of N at any depth.

(6) An estimate of ultimate tip resistance Q_{bu} can be obtained from

$$Q_{bu}\ (\text{tons}) = 3\ A\ \sqrt{N}$$

where

A = the area of the base in feet^2.

(7) For the soil conditions where the variation of N with depth is known the load-settlement curve for any given shaft dimensions can be satisfactorily predicted.

Recommendations

(1) The dummy strain gage should be improved by replacing the bare strain gage with a strain gage contained in the cement mortar block.

(2) To reduce the temperature effects on the tell-tale, it is suggested that the aluminum rods used for the support of dial indicators should be replaced by steel rods.

(3) More load tests should be carried out at the San Antonio site to evaluate the effects of periodic moisture variation and swelling and shrinkage on the load-carrying capacity of the shaft.

(4) The present study should be extended to determine the appropriate relationship between the number of blows N and the ultimate tip resistance.

(5) It appears that a relationship similar to that given by Eq 7.8 can also be developed in terms of conventional undisturbed shear strength, if such strength is precisely known as a function of depth.

(6) The present study should be extended to other sites and the value of constant C_2 in Eq 7.10 should be evaluated and modified if necessary.

REFERENCES

1. ASTM Standards 1968, Part XI, American Society for Testing and Materials, 1968, pp 377-380.

2. Broms, B. B., and L. Hellman, "End Bearing and Skin Friction Resistance of Piles," Journal of the Soil Mechanics and Foundations Division, American Society of Civil Engineers, March 1968, pp 421-429.

3. Chuang, J. W., and Lymon C. Reese, "Studies of Shearing Resistance between Cement Mortar and Soil," Research Report No. 89-3, Center for Highway Research, The University of Texas, Austin, January 1968.

4. Ehlers, Clarence J., Lymon C. Reese, and James N. Anagnos, "The Nuclear Method of Soil Moisture Determination at Depth," Research Report No. 89-4, Center for Highway Research, The University of Texas at Austin, June 1969.

5. Coyle, H. M., and Lymon C. Reese, "Load Transfer for Axially Loaded Piles in Clay," Journal of the Soil Mechanics and Foundations Division, American Society of Civil Engineers, March 1966, pp 2-26.

6. DuBose, L. A., "A Comprehensive Study of Factors Influencing the Load Carrying Capacity of Drilled and Cast-in-Place Concrete Piles," Part I and II, Texas Highway Department Project No. RP-4, Texas Transportation Institute, College Station, Texas, October 1956.

7. Dixon, W. J., Biomedical Computer Programs, University of California Press, Los Angelos, 1967, pp 234-247.

8. Hanna, T. H., "Distribution of Load in Long Piles," Ontario Hydro Research Quarterly, Vol 18, No. 4, 4th Quarter, 1966, pp 1-7.

9. Kerisel, J. L., "Vertical and Horizontal Bearing Capacity of Deep Foundations in Clay," Bearing Capacity and Settlement of Foundations, Proceedings of a Symposium held at Duke University, April 1965.

10. Koizumi, Y., and K. Ito, "Field Tests with Regard to Pile Driving and Bearing Capacity of Piled Foundations," Soil and Foundation, Vol VII, No. 3, 1967, pp 30-53.

11. Matich, M. A. J., and P. Kozicki, "Some Load Tests on Drilled Cast-in-Place Concrete Caissons," Canadian Geotechnique Journal, Vol IV, No. 4, November 1967.

12. McCracken, D. D., and W. S. Dorn, Numerical Methods and Fortran Programming, John Wiley and Sons, Inc., New York, 1964, pp 262-275.

13. Meyerhof, G. G., and L. J. Murdock, "An Investigation of the Bearing Capacity of Some Bored and Driven Piles in London Clay," Geotechnique, Vol III, No. 7, September 1953, pp 267-282.

14. Perry, C. C., and H. R. Lissner, The Strain Gage Primer, 2nd Edition, McGraw-Hill, New York, pp 6-7.

15. Reese, Lymon C., J. Crozier Brown, and H. H. Dalrymple, "Measurements of Lateral Earth Pressure in Drilled Shafts," Research Report No. 89-2, Center for Highway Research, The University of Texas, Austin, September 1968.

16. Reese, Lymon C., and H. B. Seed, "Pressure Distribution Along Friction Piles," Proceedings of the American Society for Testing and Materials, Vol 55, 1955, pp 1156-1182.

17. Reese, Lymon C., and W. Ronald Hudson, "Field Testing of Drilled Shafts to Develop Design Methods," Research Report No. 89-1, Center for Highway Research, The University of Texas, Austin, April 1968.

18. Seed, H. B., and Lymon C. Reese, "The Action of Soft Clay Along Friction Piles," Transactions, American Society of Civil Engineers, Vol 122, 1957.

19. Skempton, A. W., "The Bearing Capacity of Clays," Building Research Congress, 1951, pp 180-189.

20. Terzaghi, K., Theoretical Soil Mechanics, 12th Printing, John Wiley and Sons, Inc., New York, 1965, pp 134-137.

21. Texas Highway Department, Foundation Exploration and Design Manual, January 1964.

22. Texas Highway Department, Standard Specifications for Road and Bridge Construction, 1962, Special provision to Item 405 of 1965.

23. Whitaker, T., and R. W. Cooke, "An Investigation of the Shaft and Base Resistance of Large Bored Piles in London Clay," Symposium on Large Bored Piles, Institution of Civil Engineers, London, February 1966.

APPENDICES

APPENDIX 1

DETAILS OF REACTION FRAME

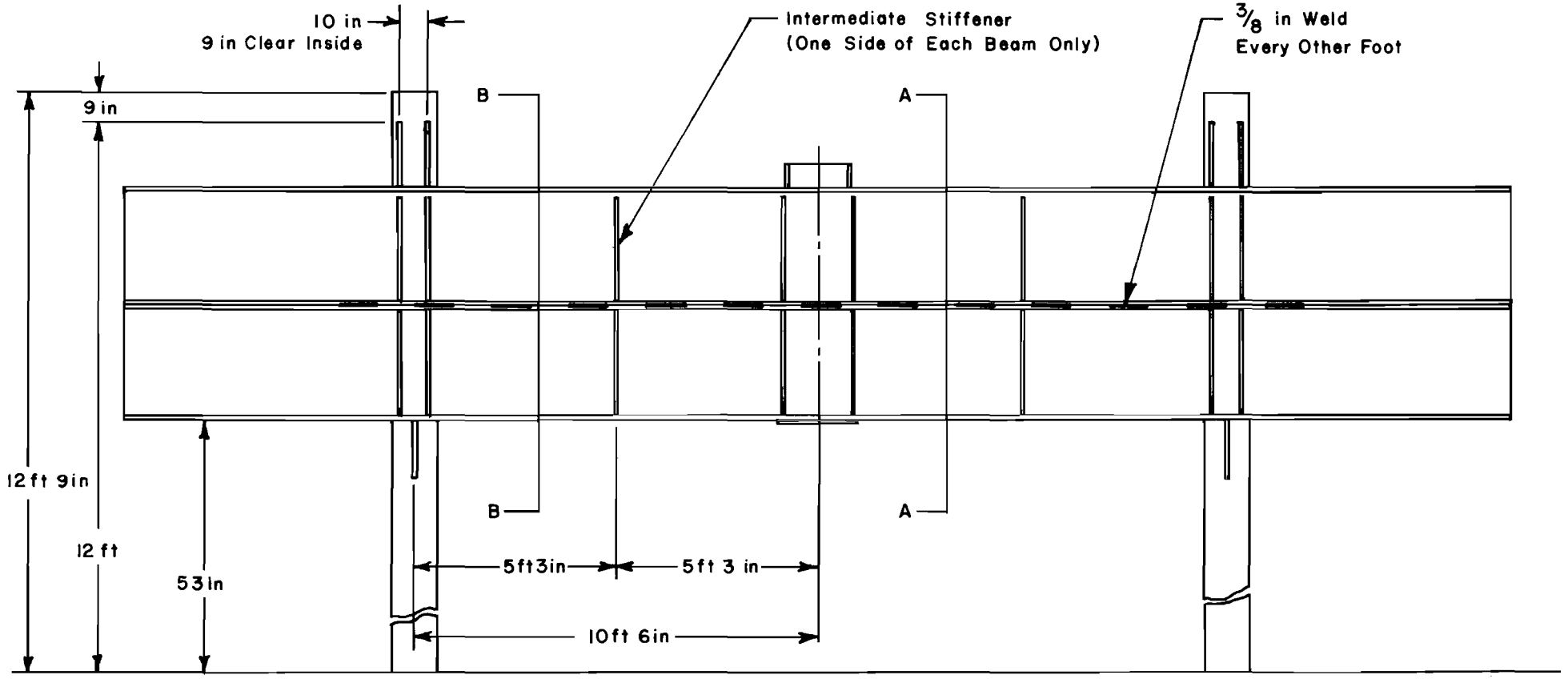

All Stiffeners Are 1/2 in Plate and
Are Connected by 3/8 in Fillet Weld

Fig A1.1. Side view of reaction frame.

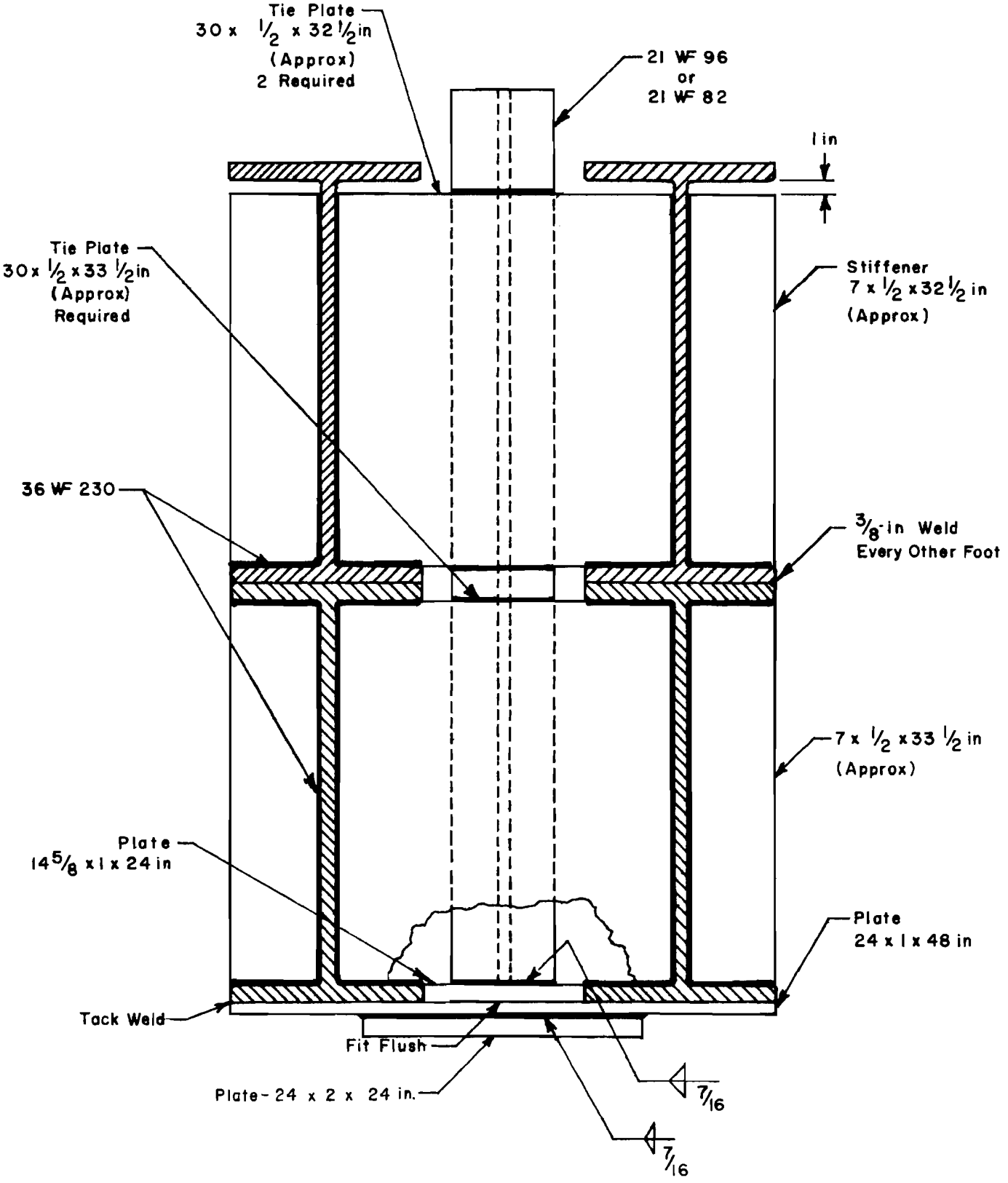

Fig A1.2. Section A-A.

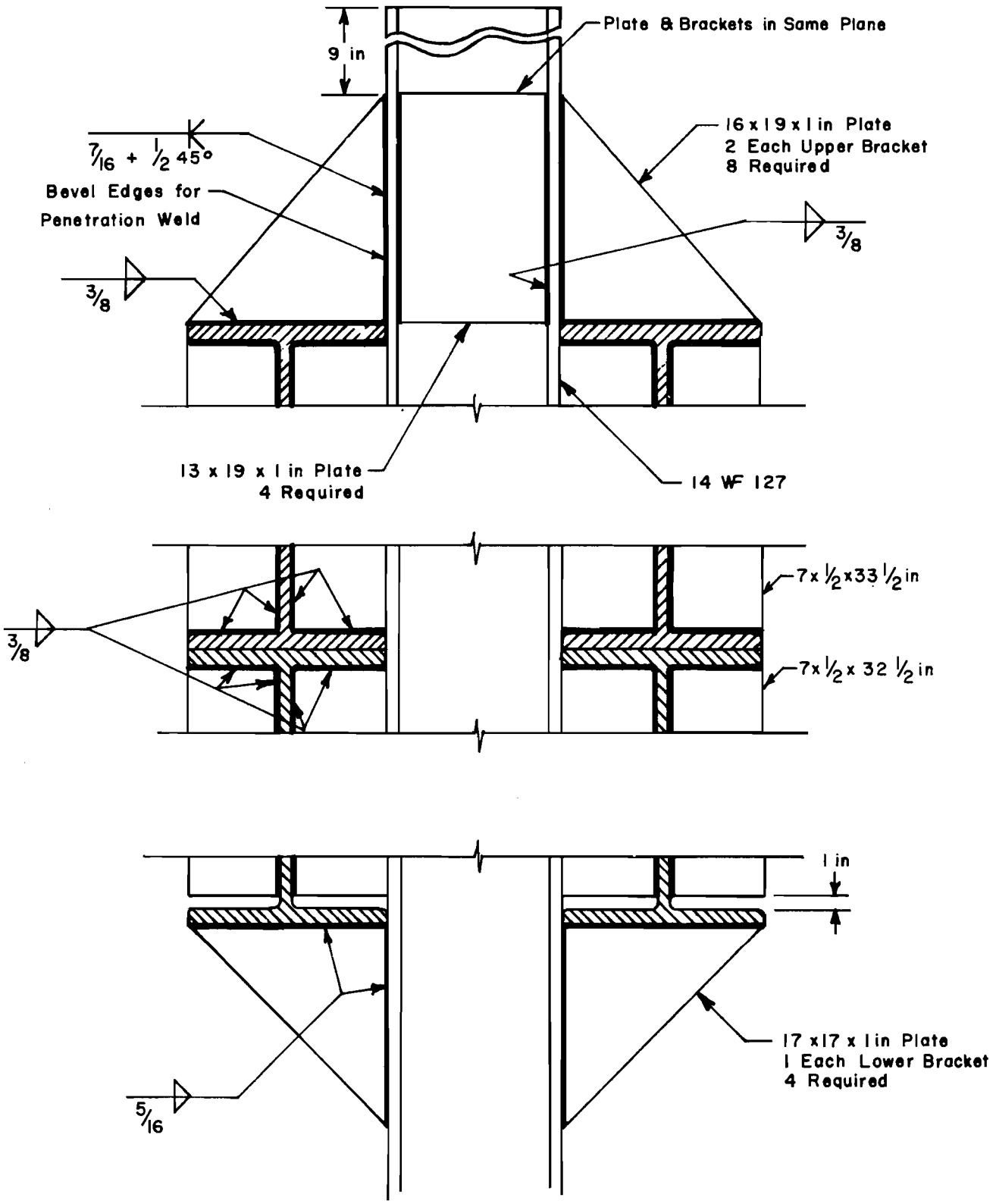

Fig A1.3. Section B-B.

APPENDIX 2

EMBEDMENT STRAIN GAGE DATA FOR TESTS NO. 3, 4, AND 5

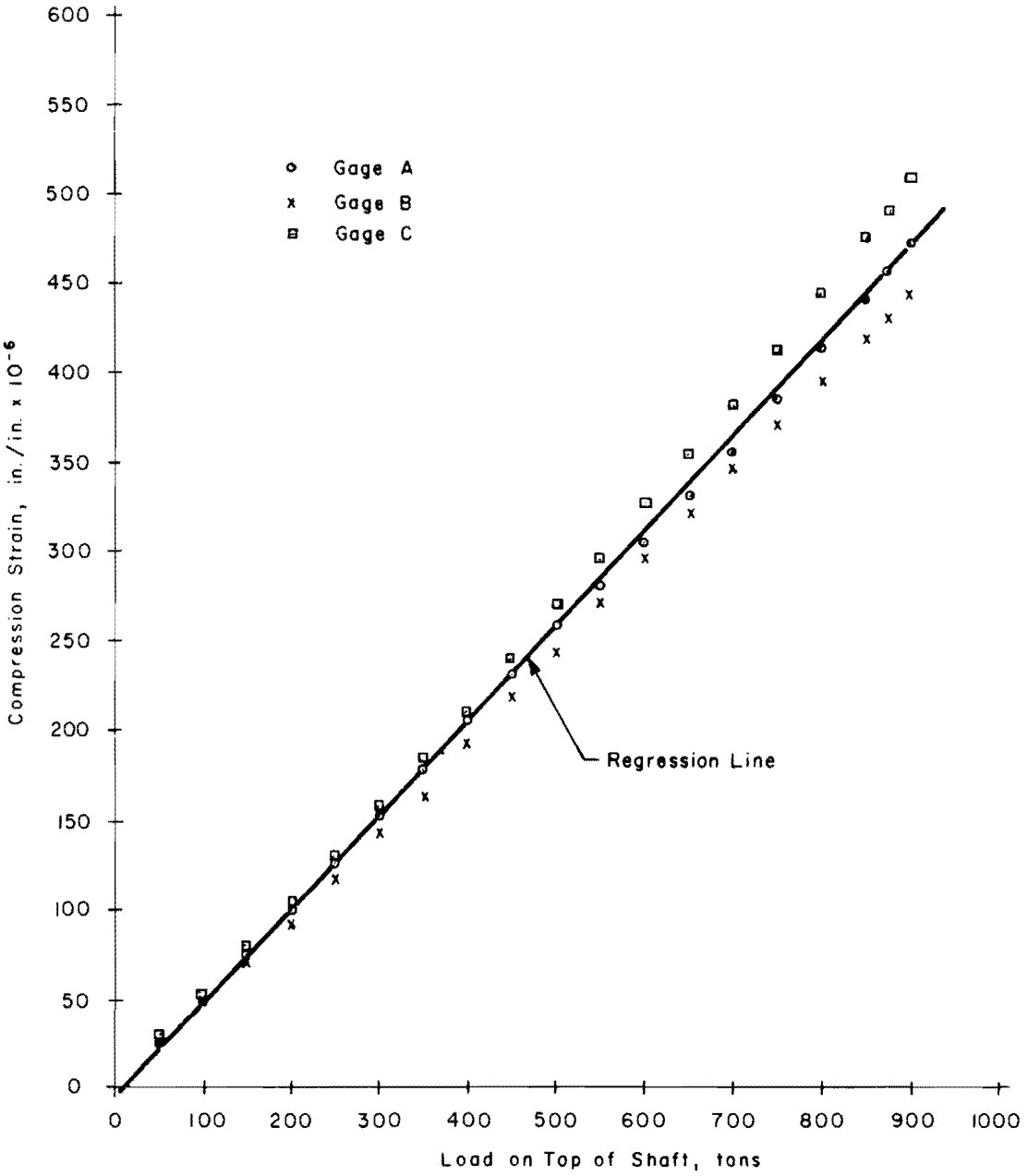

Fig A2.1. Observed strain at a depth of 1.71 feet below the top of the shaft (Test No. 3).

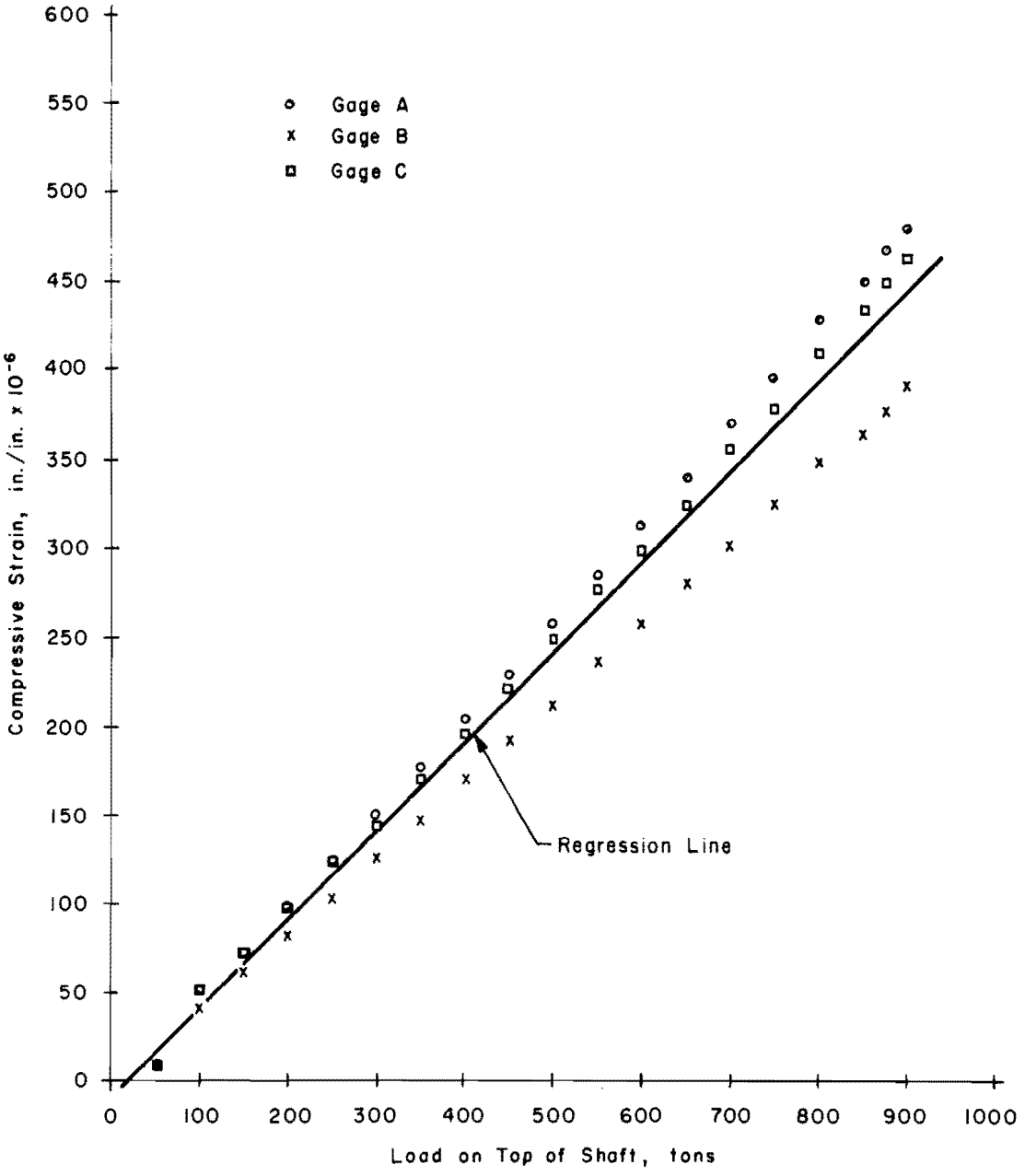

Fig A2.2. Observed strain at a depth of 4.96 feet below the top of the shaft (Test No. 3).

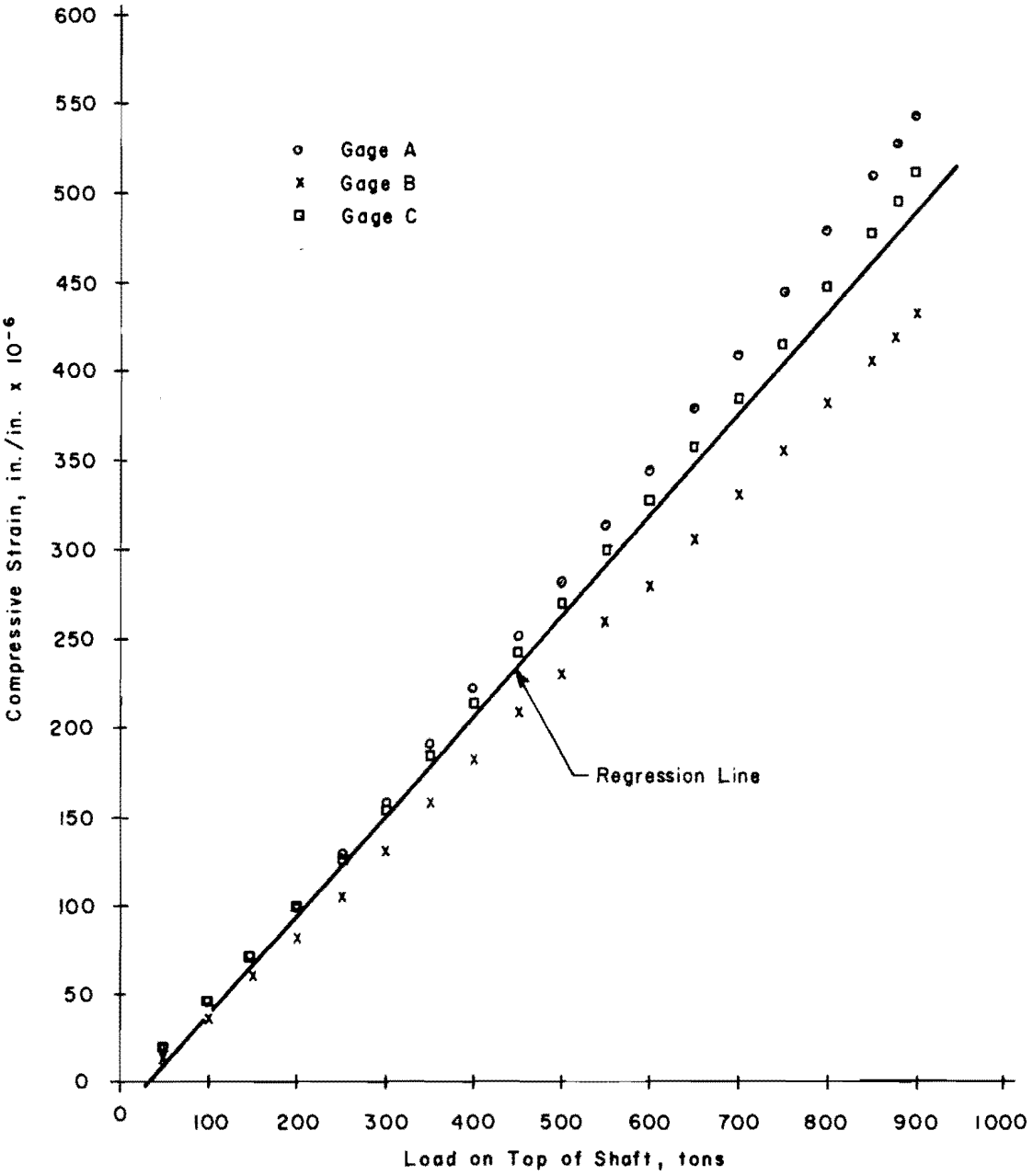

Fig A2.3. Observed strain at a depth of 10.05 feet below the top of the shaft (Test No. 3).

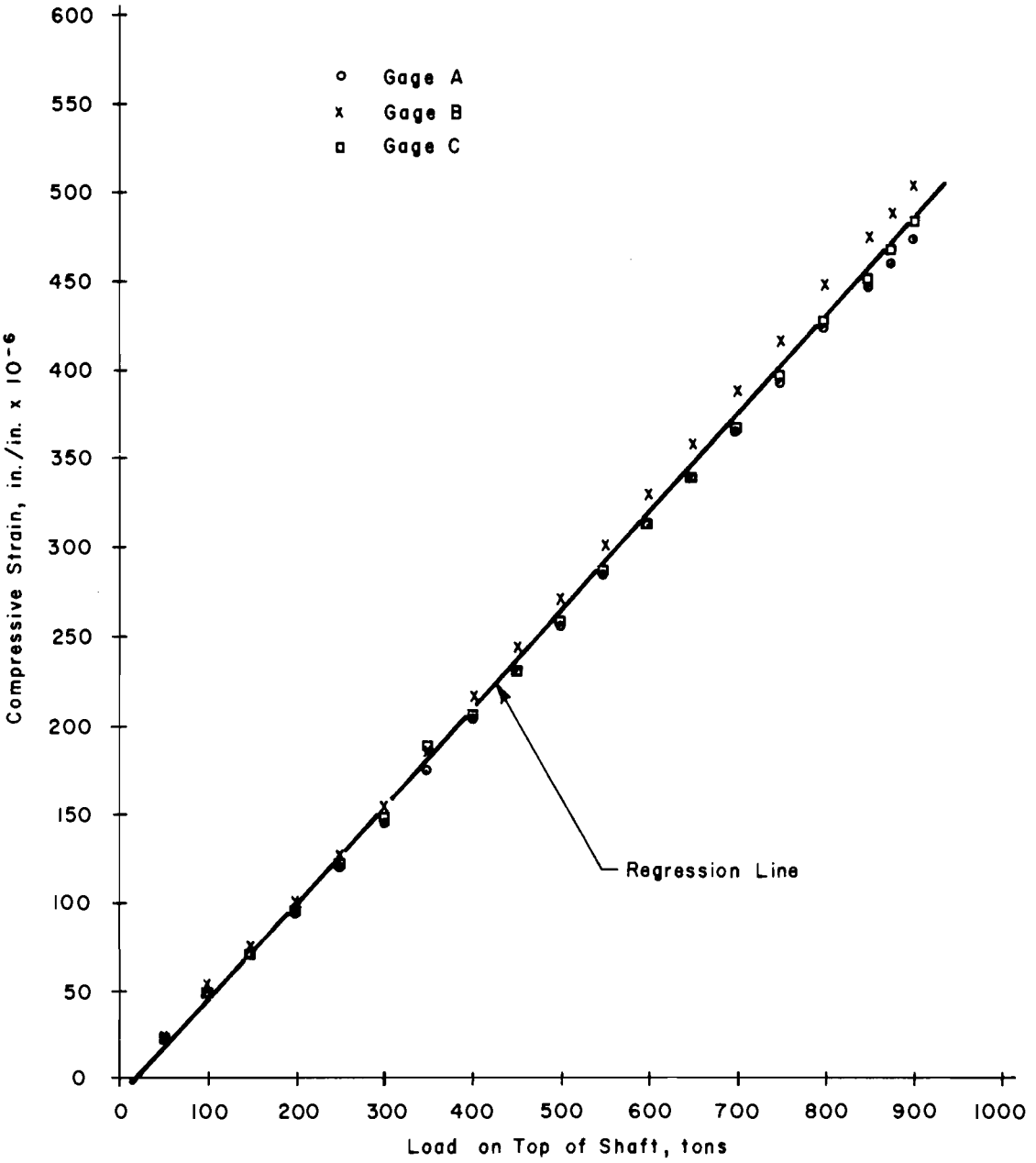

Fig A2.4. Observed strain at a depth of 15.20 feet below the top of the shaft (Test No. 3).

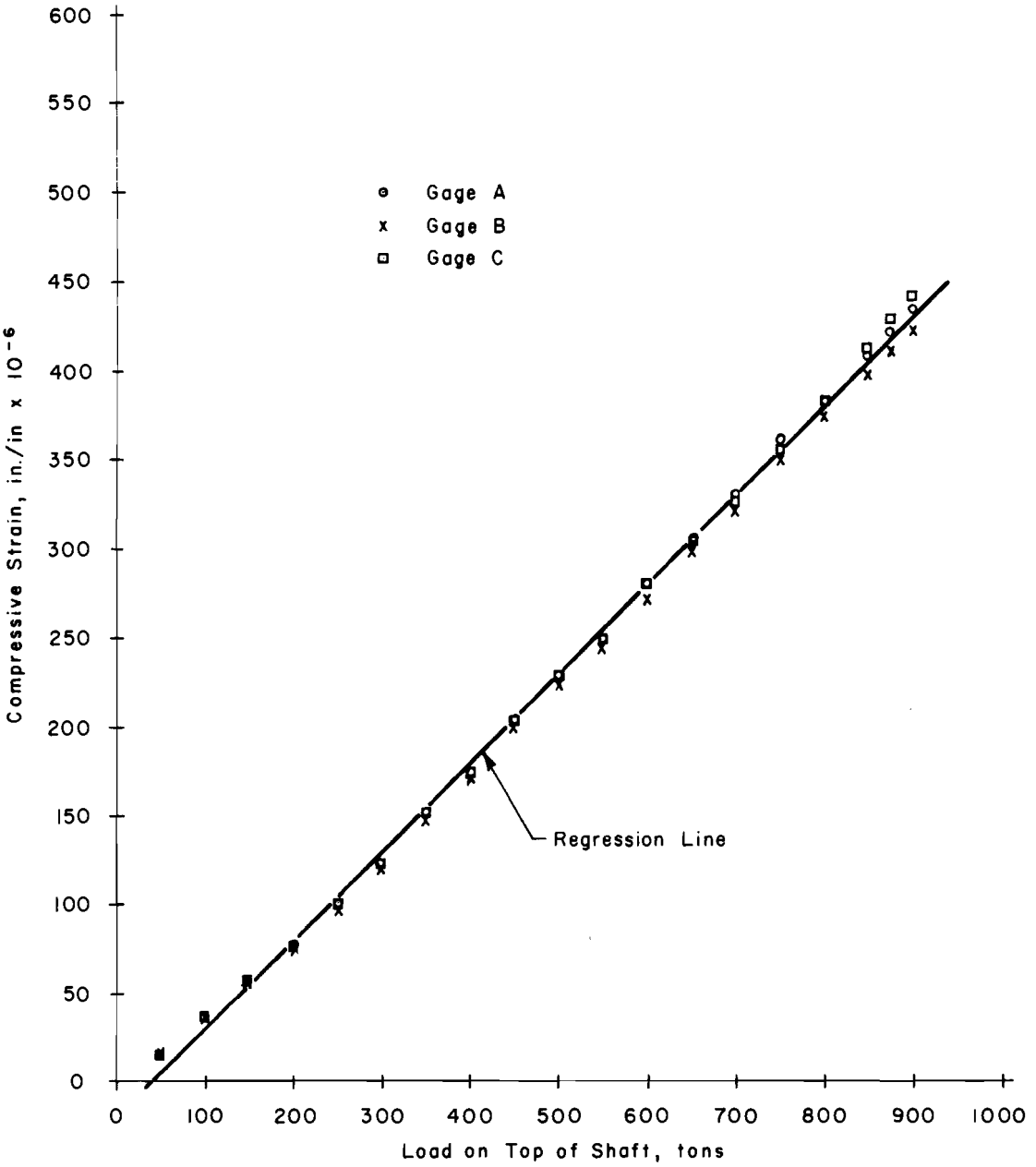

Fig A2.5. Observed strain at a depth of 20.30 feet below the top of the shaft (Test No. 3).

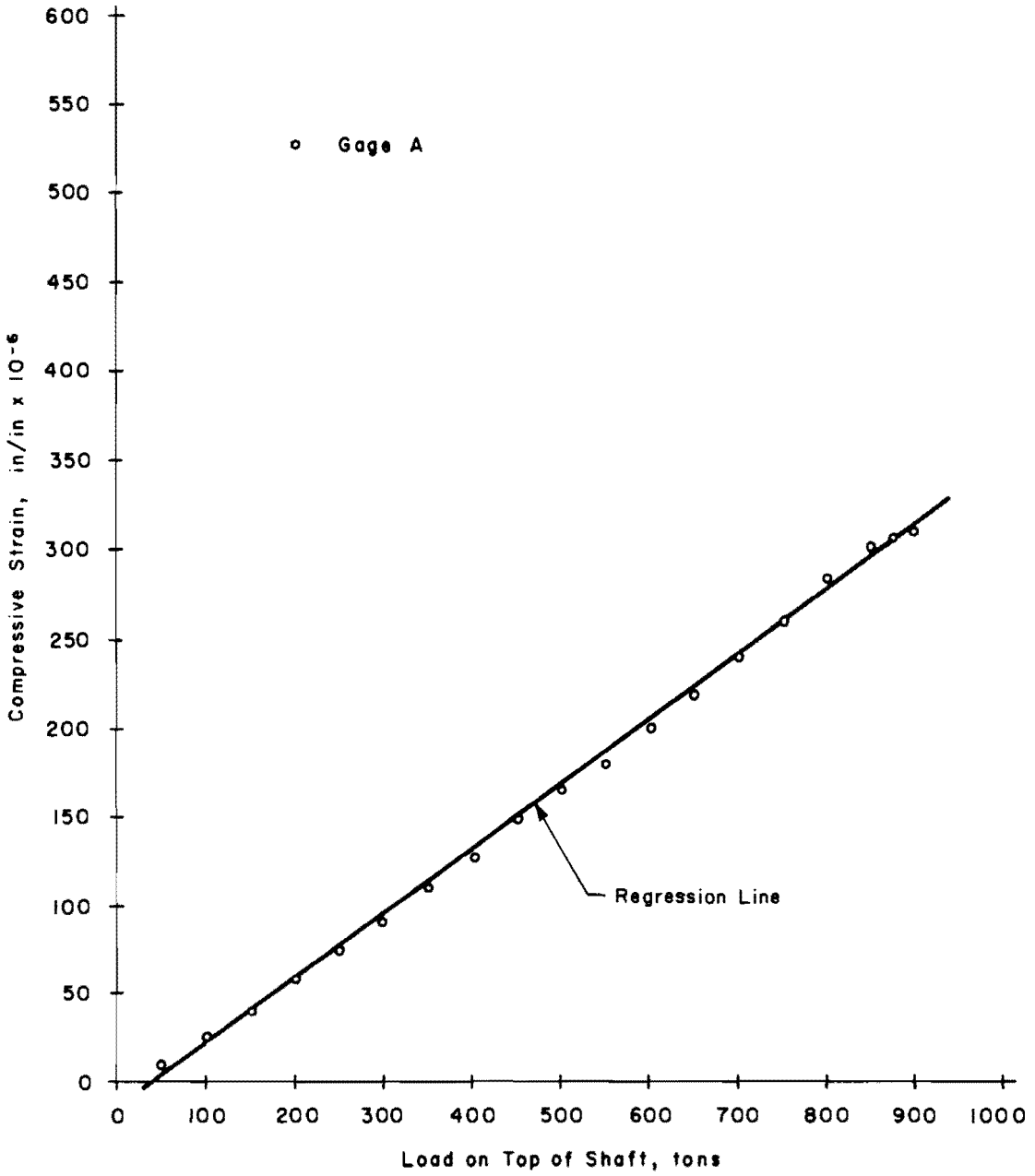

Fig A2.6. Observed strain at a depth of 25.00 feet below the top of the shaft (Test No. 3).

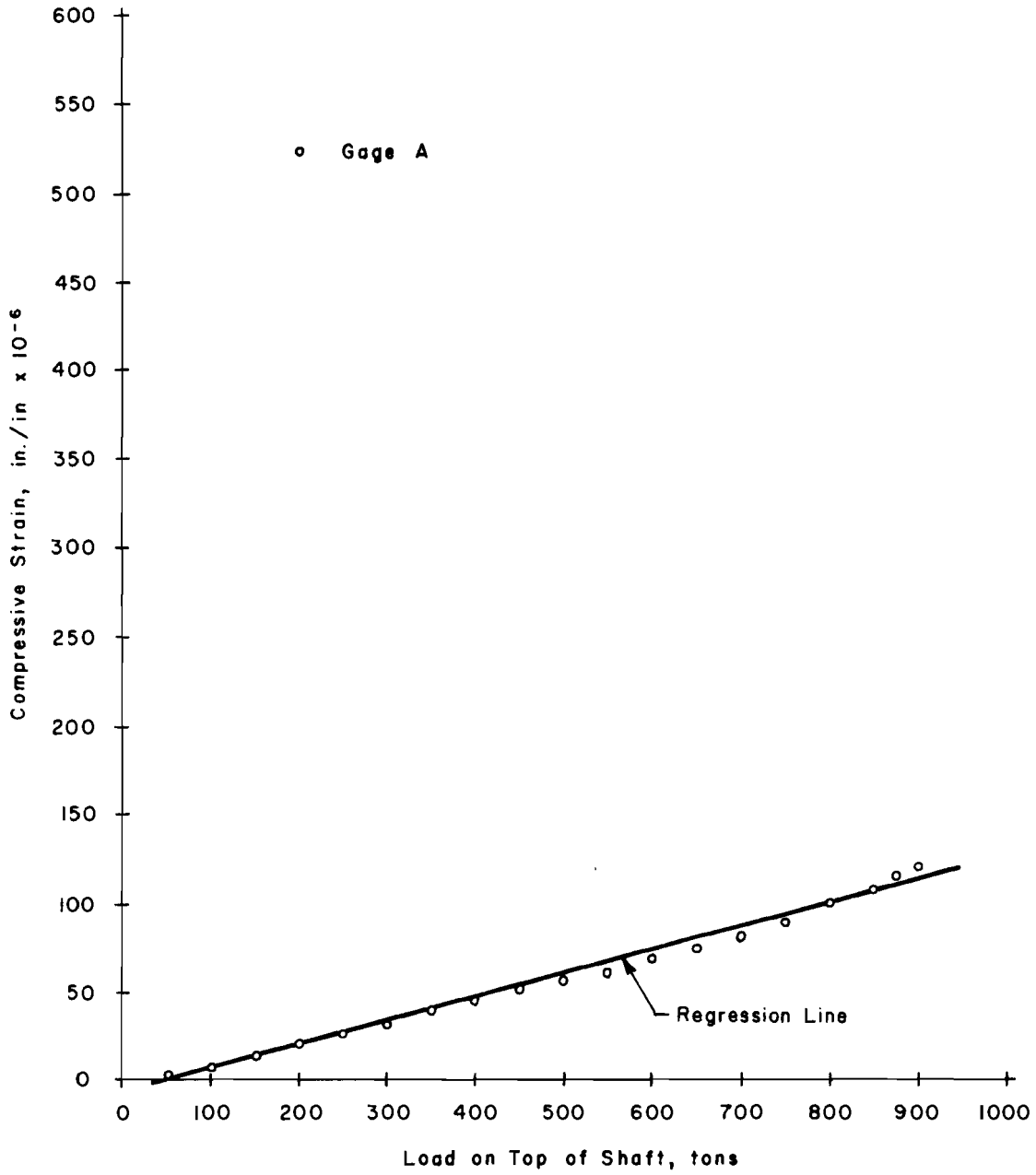

Fig A2.7. Observed strain at a depth of 28.05 feet below the top of the shaft (Test No. 3).

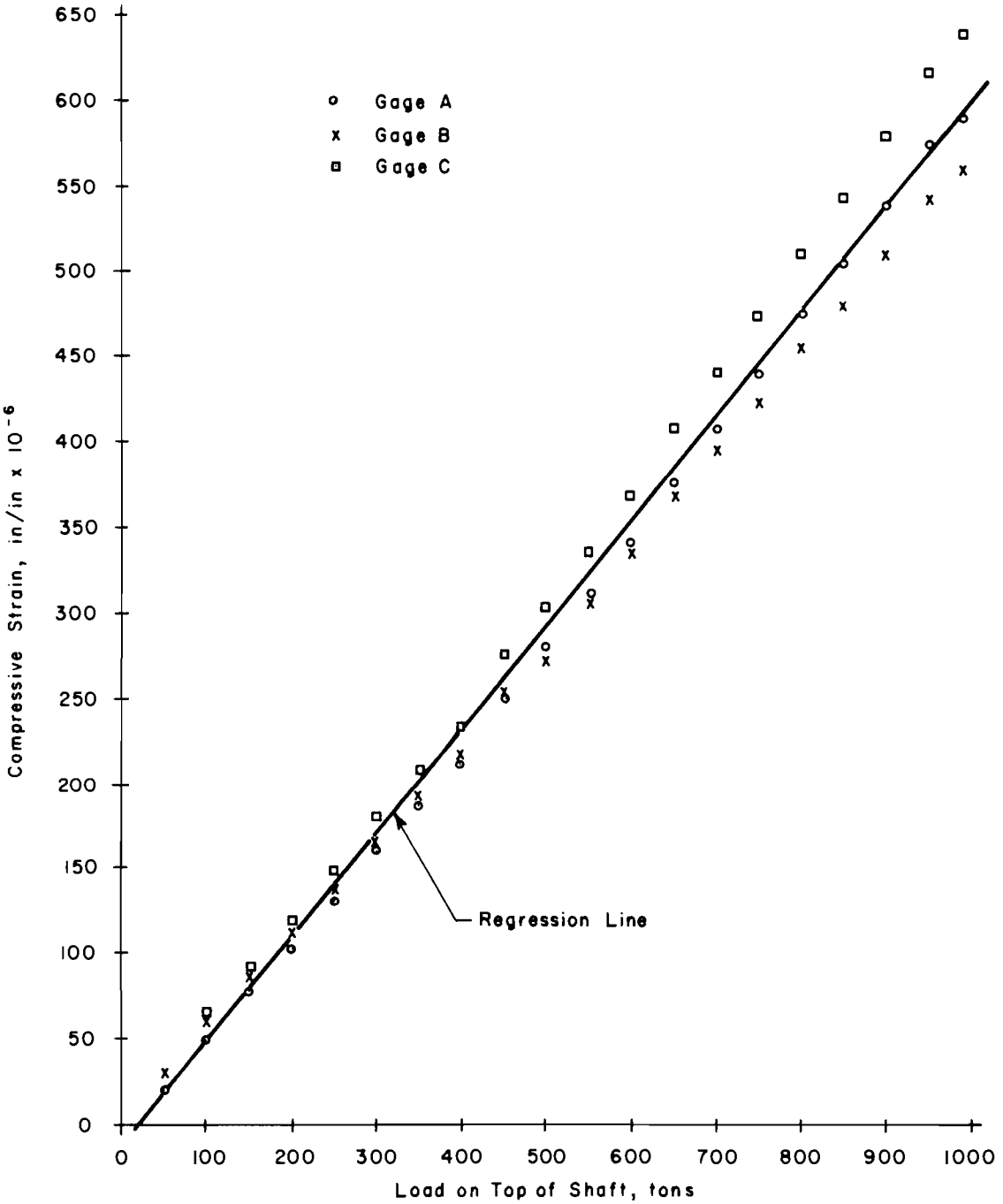

Fig A2.8. Observed strain at a depth of 1.7 feet below the top of the shaft (Test No. 4).

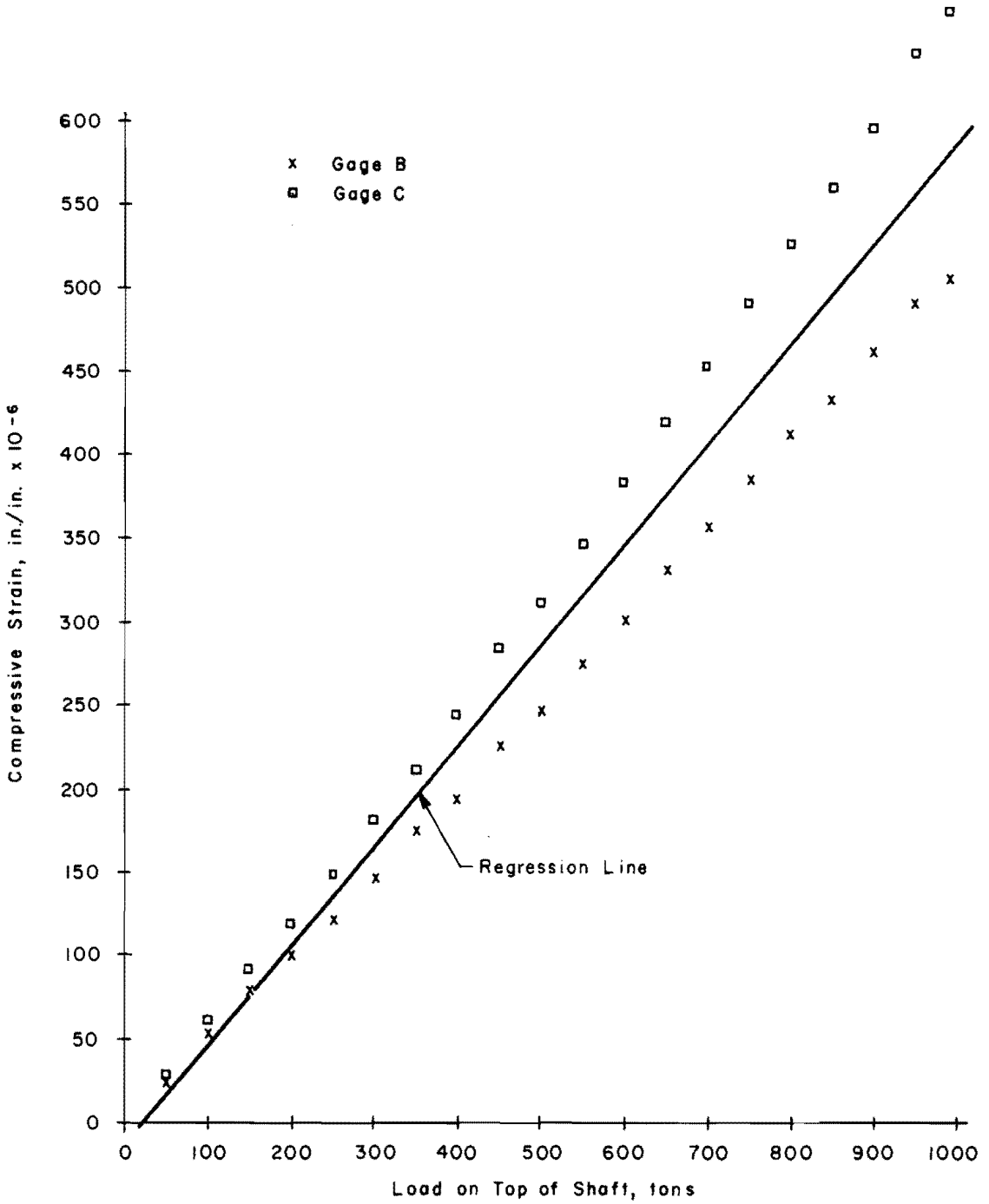

Fig A2.9. Observed strain at a depth of 4.96 feet below the top of the shaft (Test No. 4).

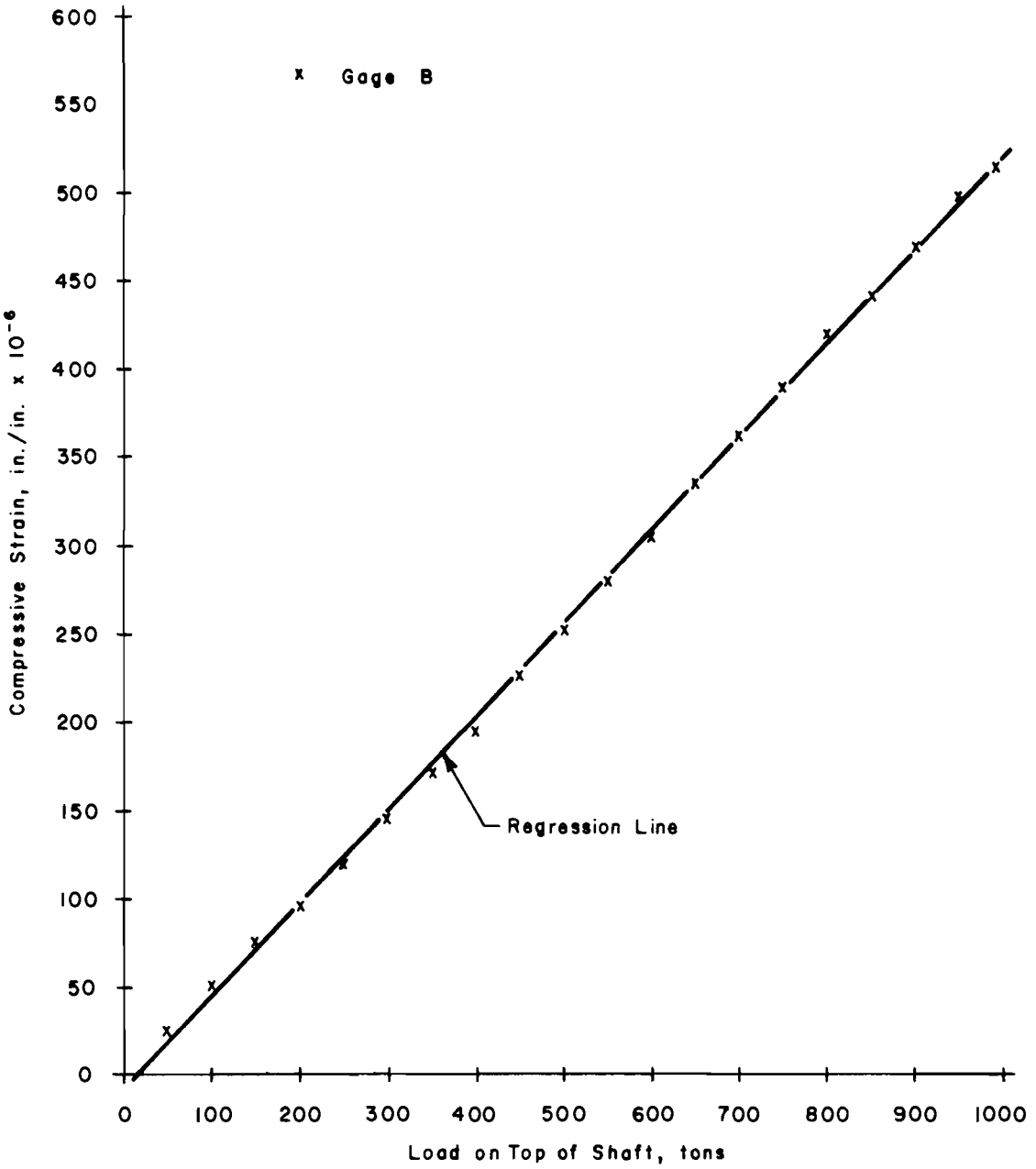

Fig A2.10. Observed strain at a depth of 10.05 feet below the top of the shaft (Test No. 4).

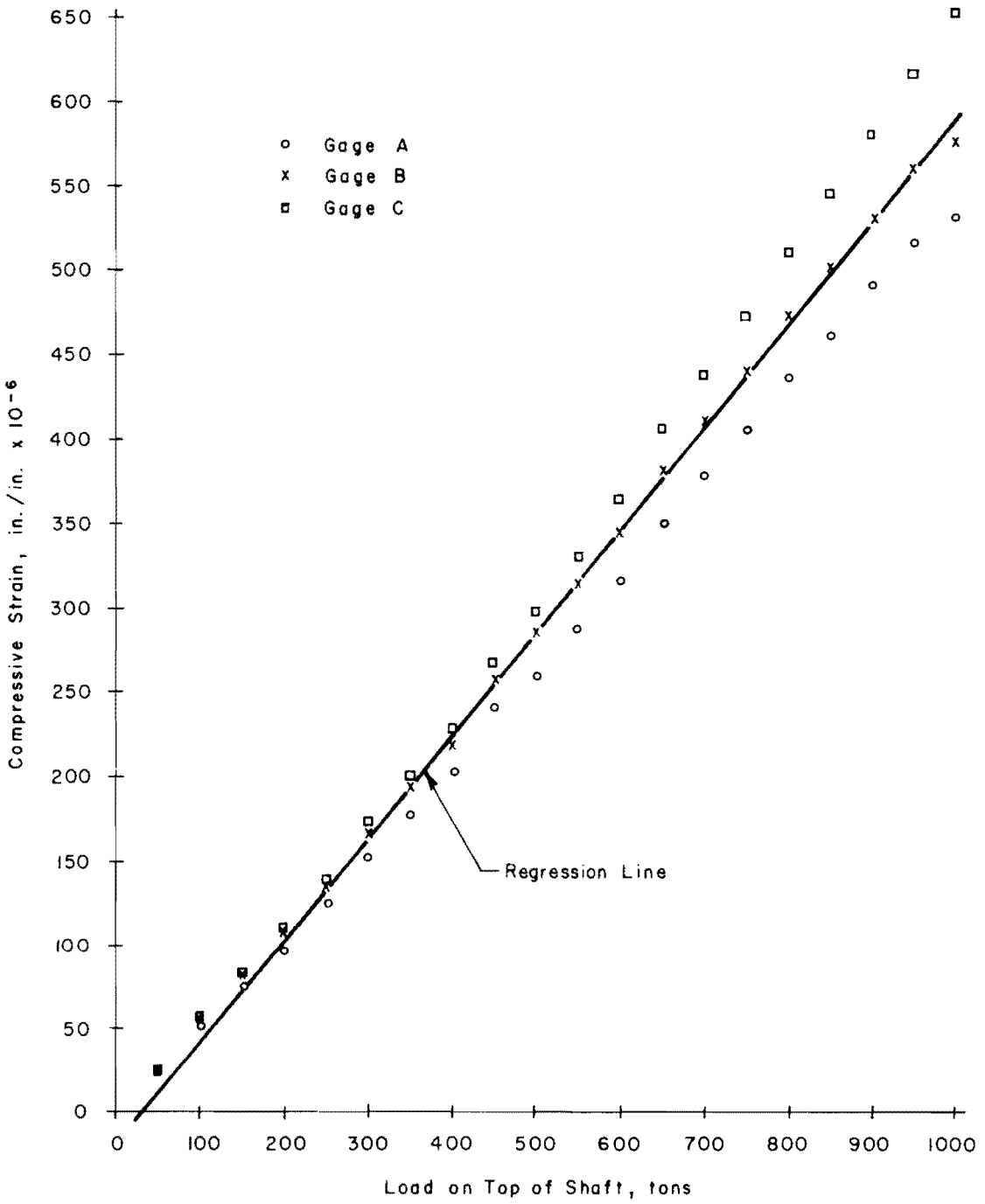

Fig A2.11. Observed strain at a depth of 15.20 feet below the top of the shaft (Test No. 4).

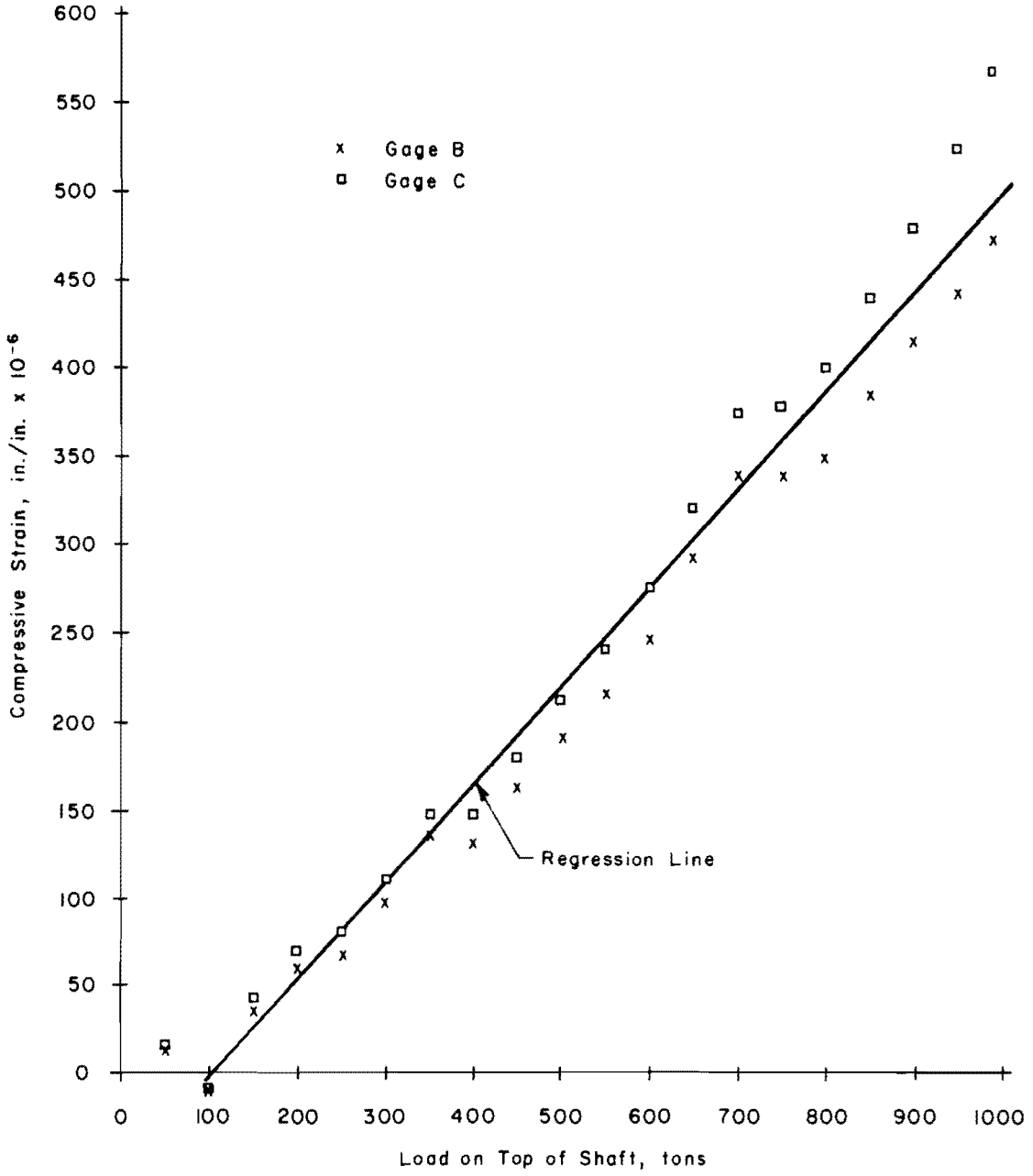

Fig A2.12. Observed strain at a depth of 20.30 feet below the top of the shaft (Test No. 4).

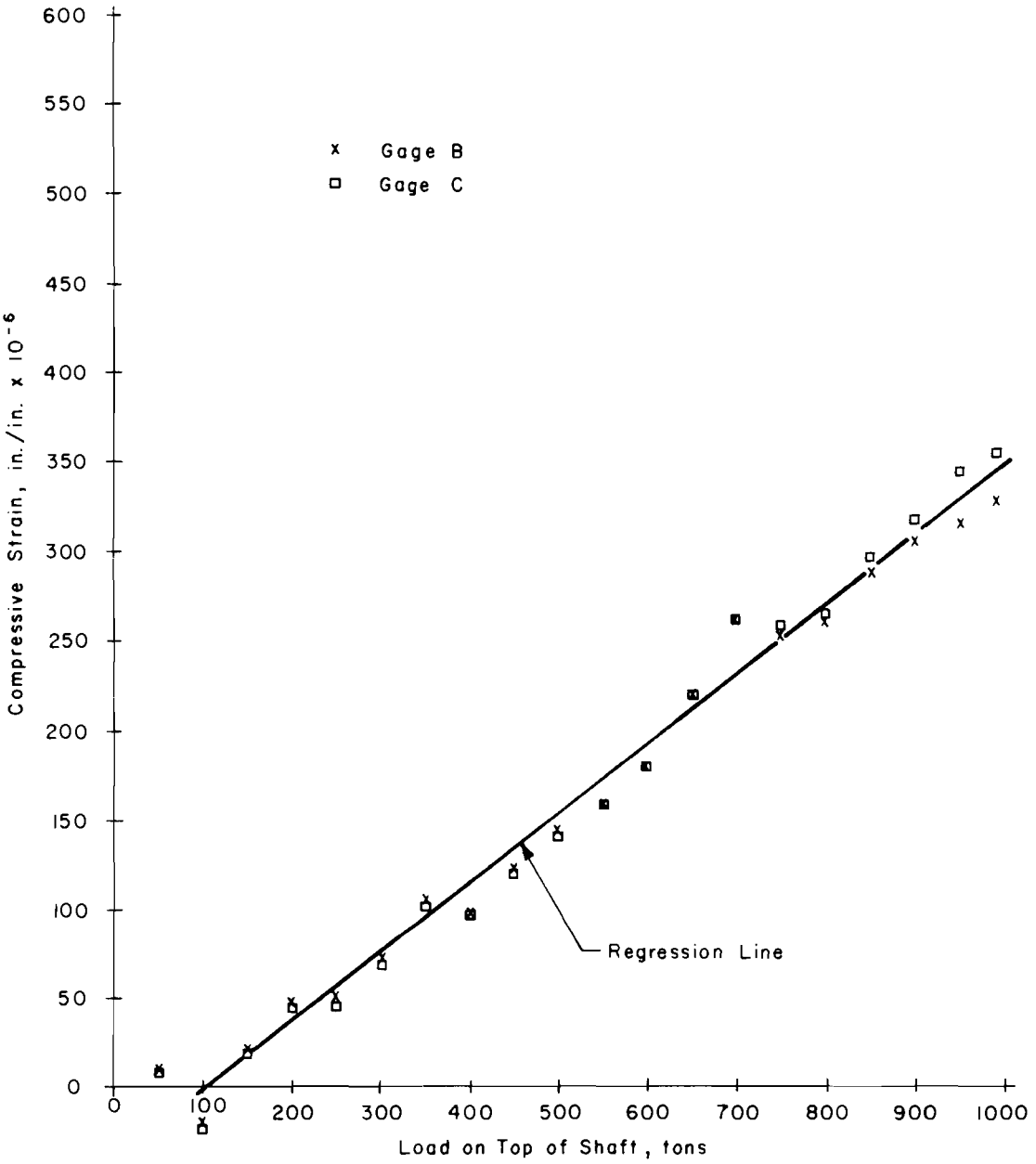

Fig A2.13. Observed strain at a depth of 25.00 feet below the top of the shaft (Test No. 4).

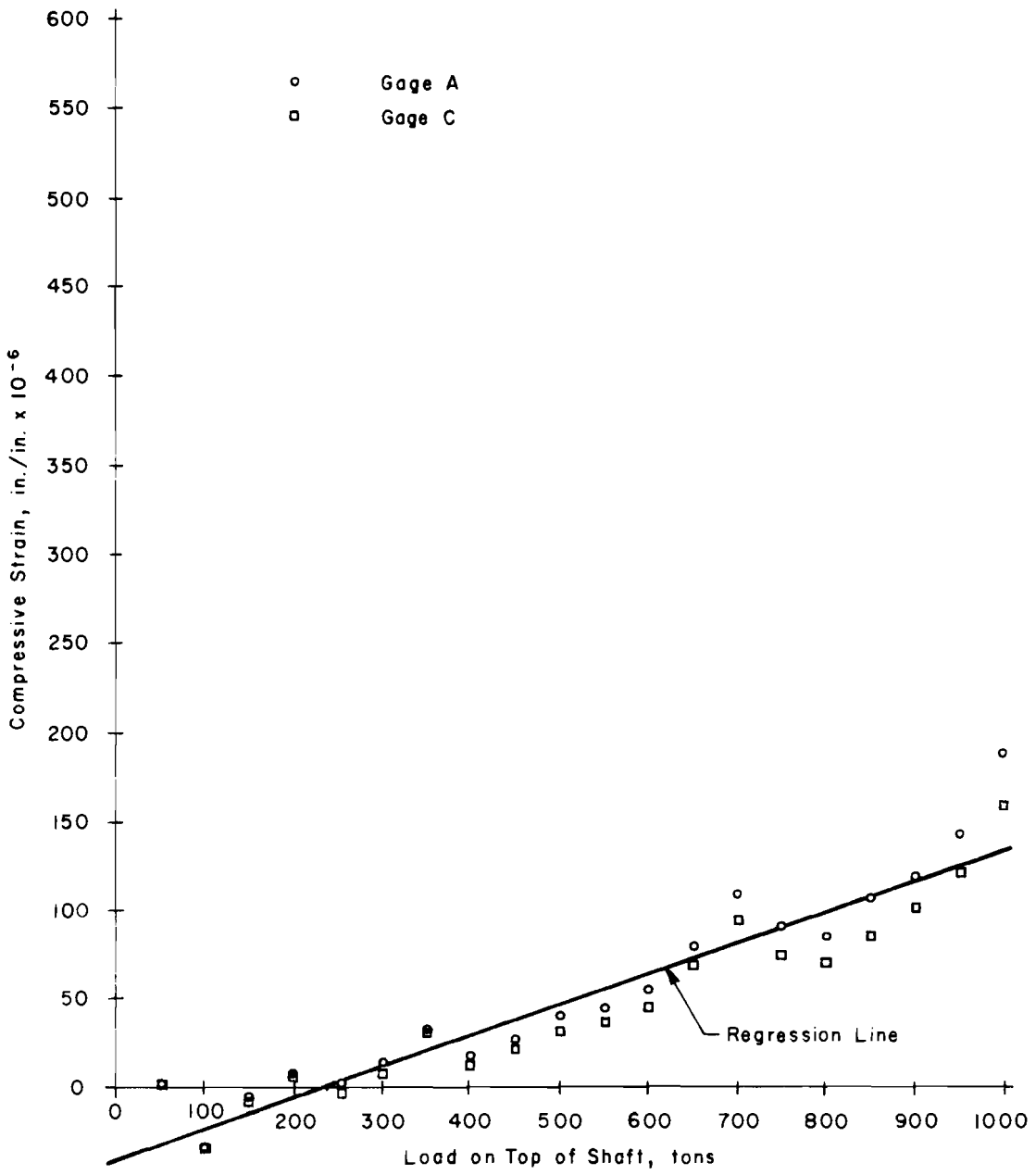

Fig A2.14. Observed strain at a depth of 28.05 feet below the top of the shaft (Test No. 4).

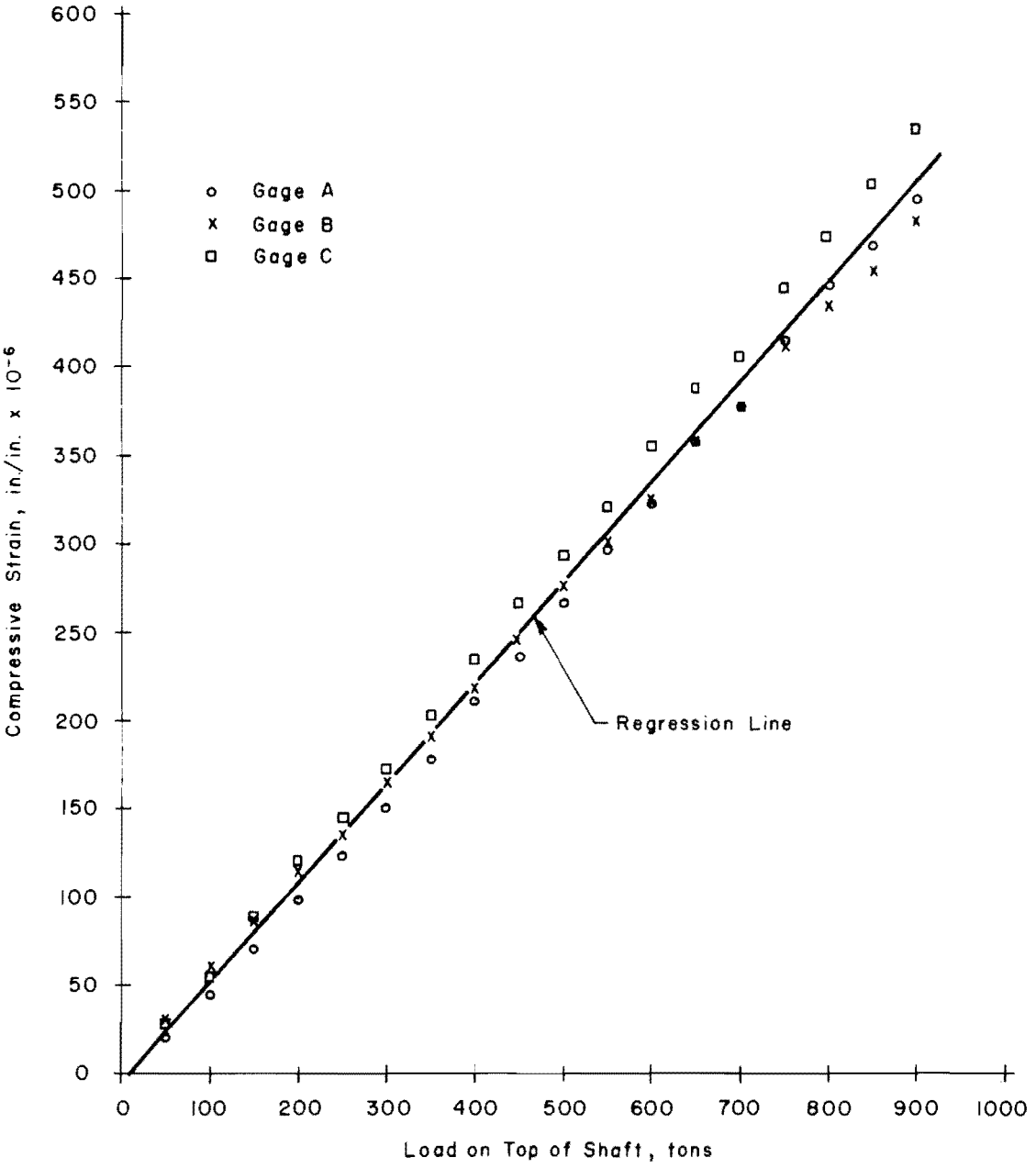

Fig A2.15. Observed strain at a depth of 1.71 feet below the top of the shaft (Test No. 5 - quick test).

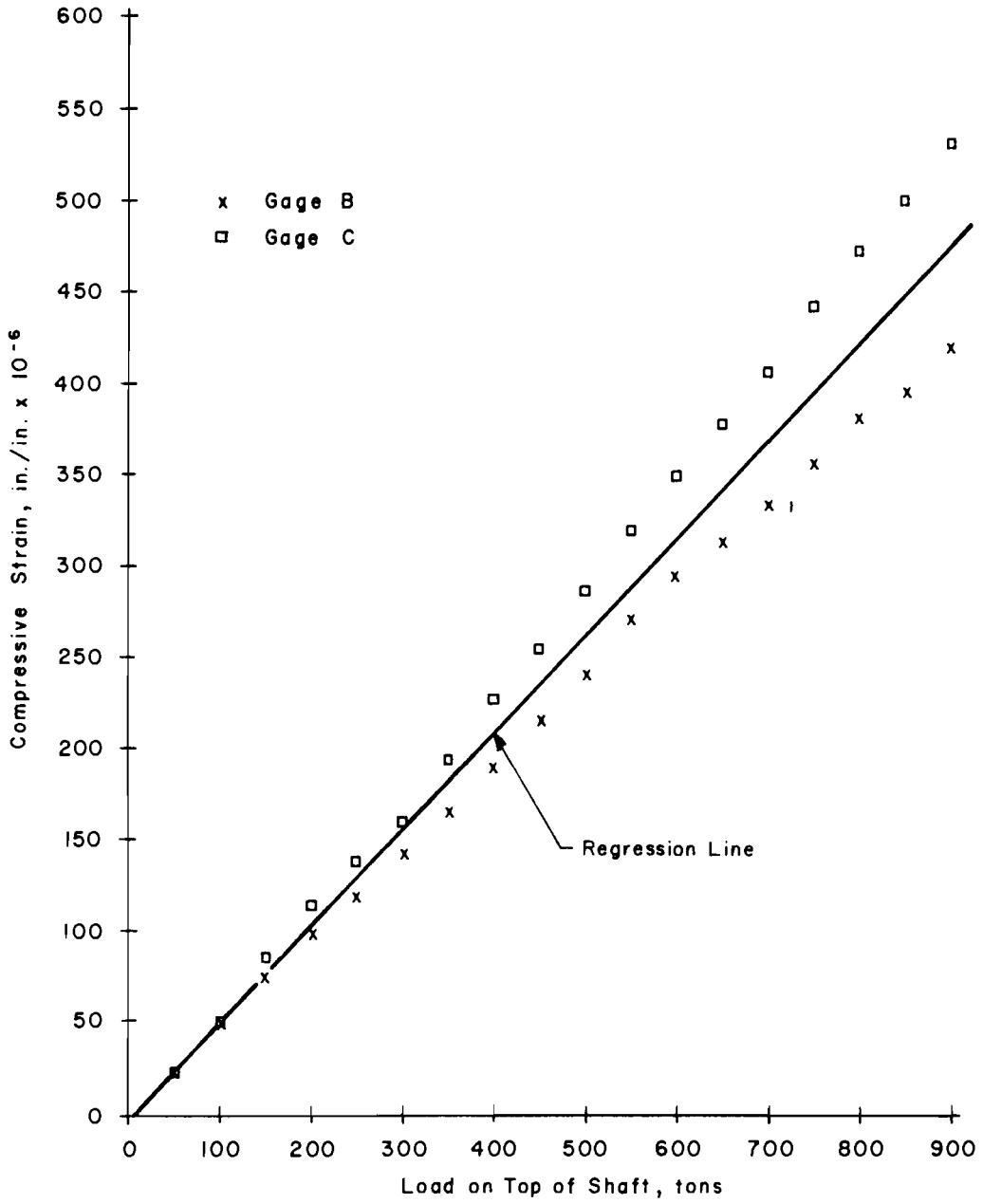

Fig A2.16. Observed strain at a depth of 4.96 feet below the top of the shaft (Test No. 5 - quick test).

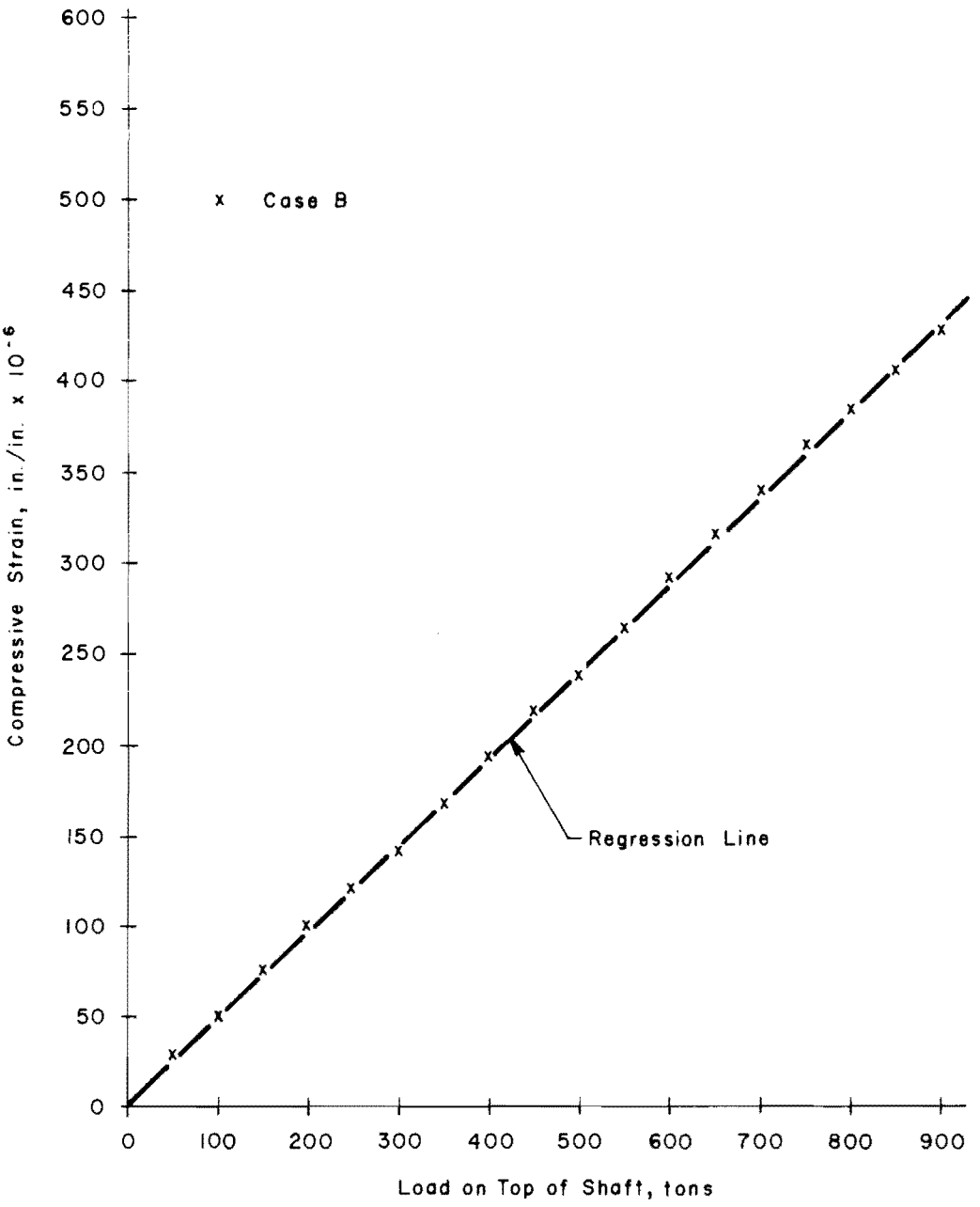

Fig A2.17. Observed strain at a depth of 10.05 feet below the top of the shaft (Test No. 5 - quick test).

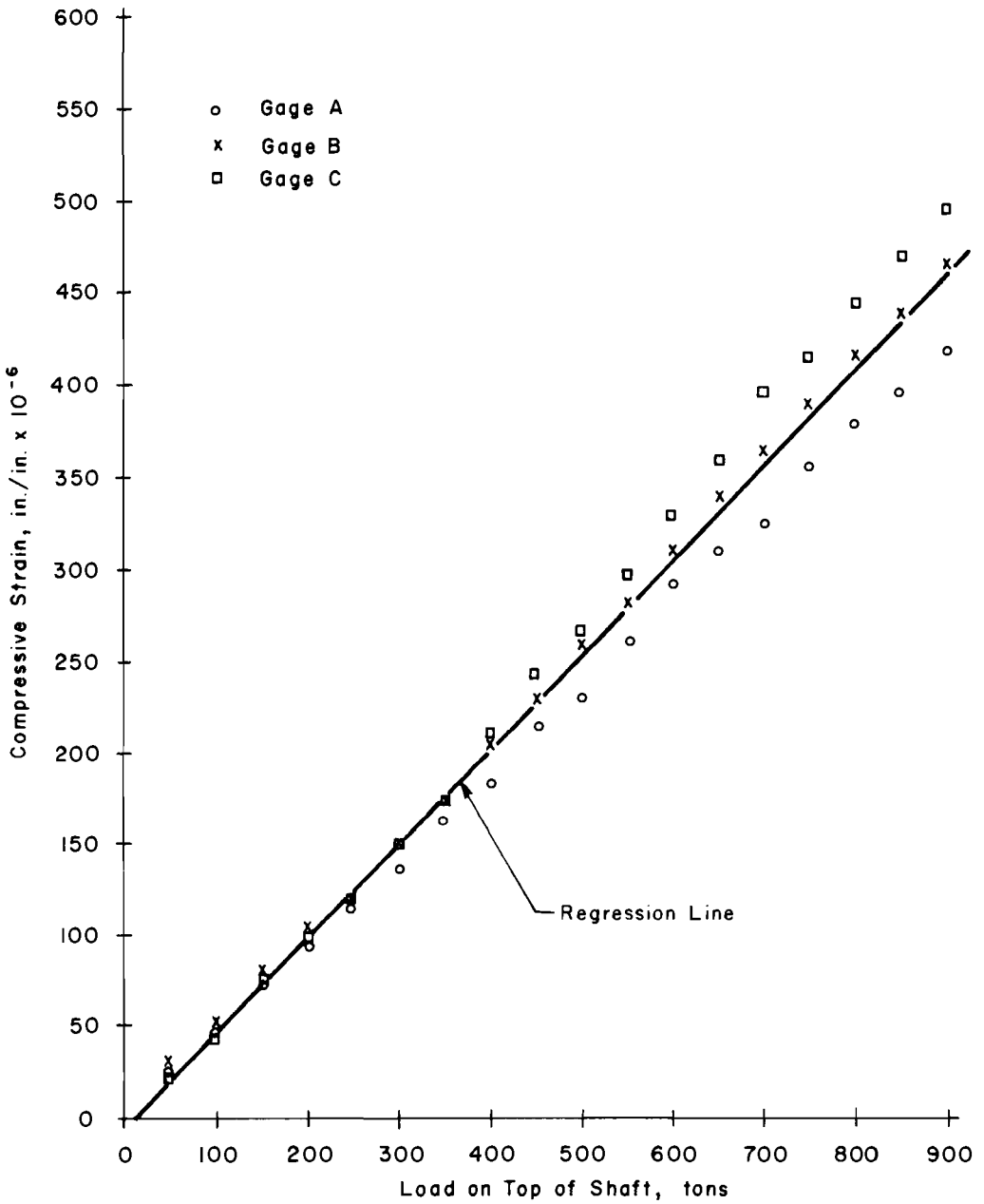

Fig A2.18. Observed strain at a depth of 15.20 feet below the top of the shaft (Test No. 5 - quick test).

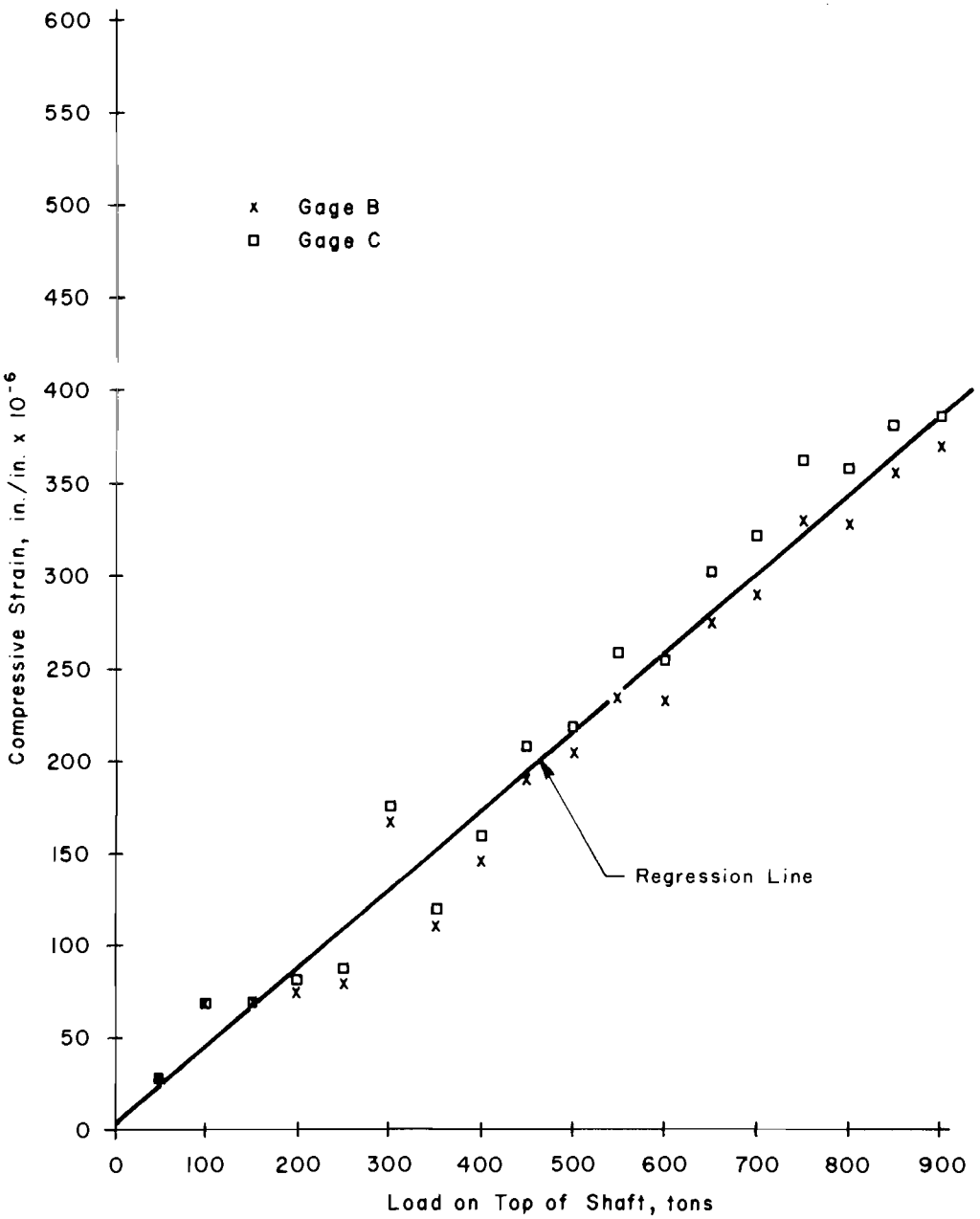

Fig A2.19. Observed strain at a depth of 20.30 feet below the top of the shaft (Test No. 5 - quick test).

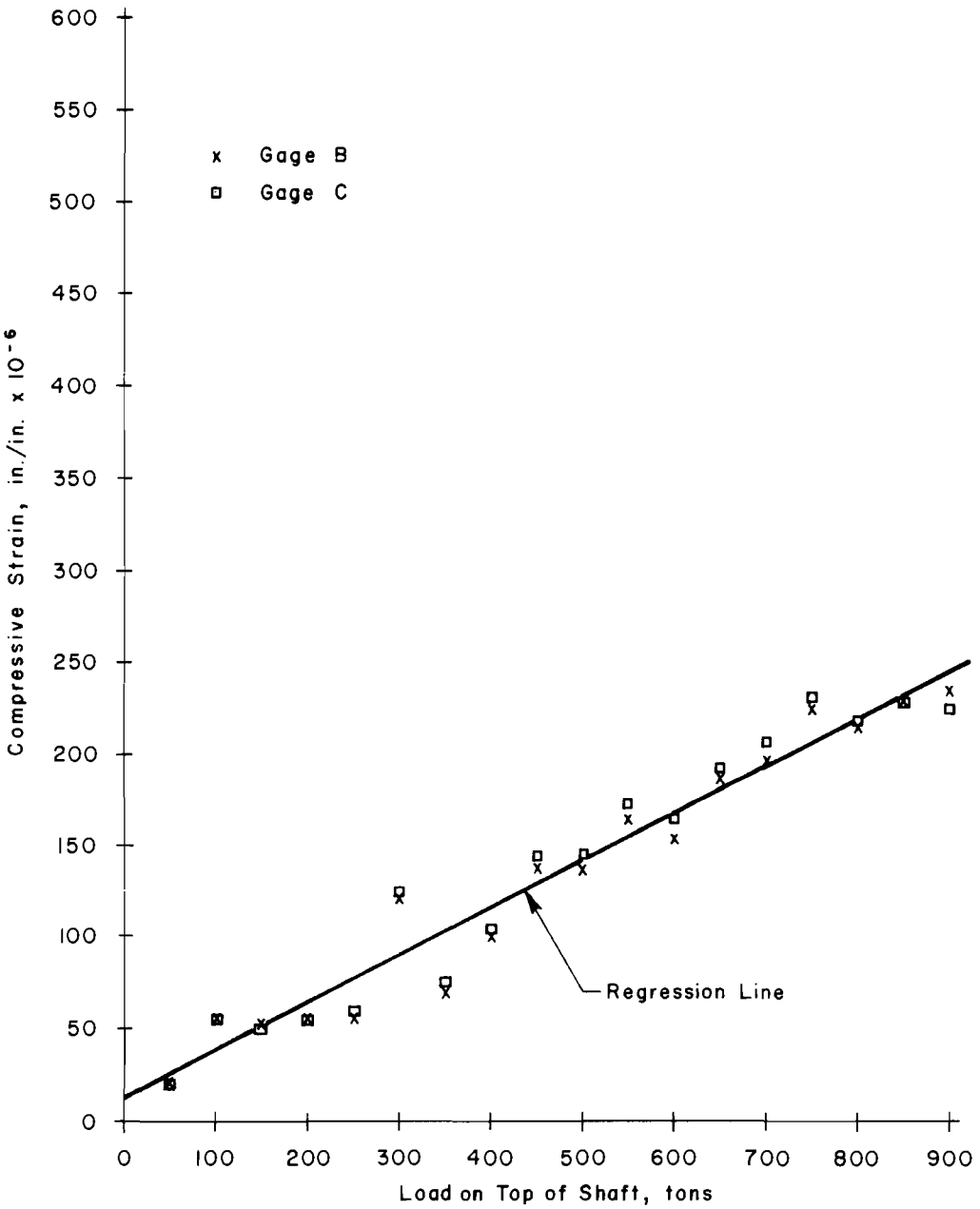

Fig A2.20. Observed strain at a depth of 25.00 feet below the top of the shaft (Test No. 5 - quick test).

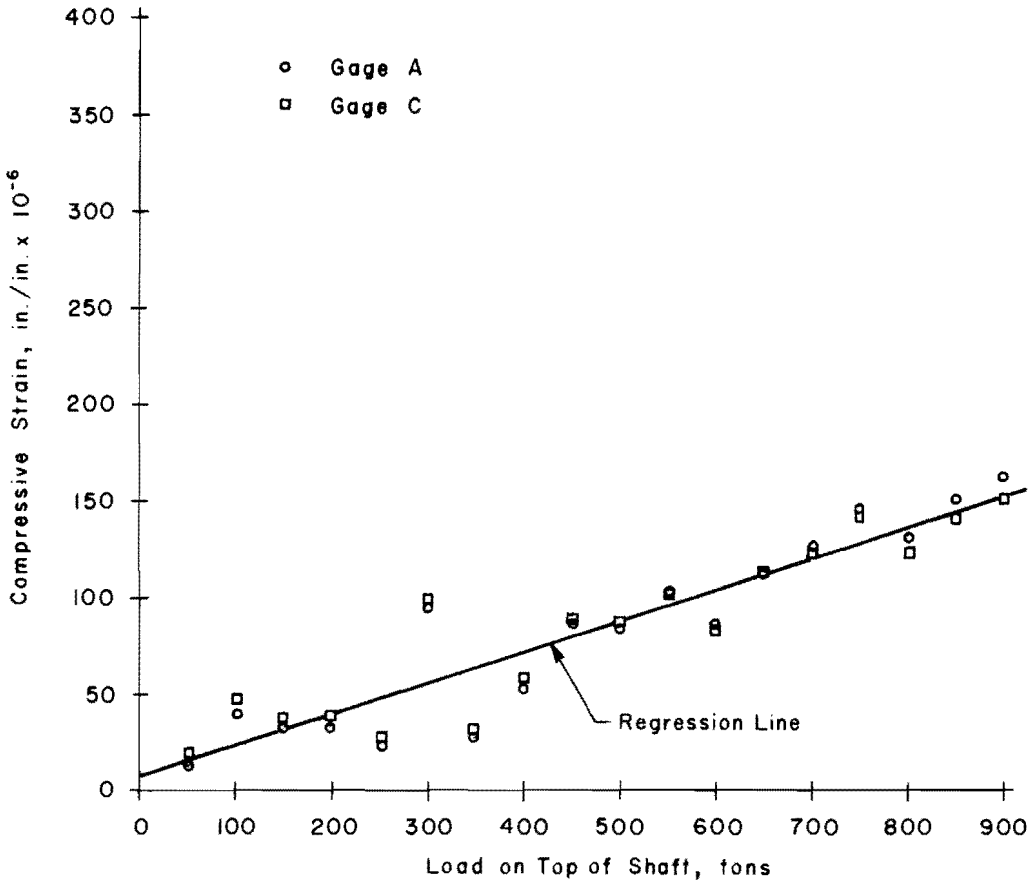

Fig A2.21. Observed strain at a depth of 28.05 feet below the top of the shaft (Test No. 5 - quick test).

APPENDIX 3

PROGRAM EMGAGE4

```
      PROGRAM EMGAGE4 ( INPUT , OUTPUT )
C          NOTATION FOR EMGAGE4
C          A          CONSTANT TERM IN FIRST ORDER CURVE FIT
C          AREA       AREA UNDER LOAD DISTRIBUTION CURVE UP TO DEPTH X
C          AVRD       AVERAGE OF UP AND DOWN EMBEDMENT GAGE READING
C          AVSTR(J)   BEST ESTIMATE OF STRAIN AT DEPTH FD(J)
C          B          COEFFICIENT OF FIRST POWER OF ABSCISSA IN CURVE FIT
C          COR        STRAIN FOR ANY LOAD FROM LOAD-CALIBRATION CURVE
C          DELTA      ELASTIC COMPRESSION OF PILE FOR LENGTH X
C          DIA        DIAMETER OF SHAFT IN FEET
C          DISNET     NET MOVEMENT OF ANY POINT X IN THE SHAFT FOR A LOAD P
C          DOWN       EMBEDMENT STRAIN GAGE READING GOING DOWNWARDS
C          ERROR      STANDARD ERROR OR ROOT MEAN SQUARE VALUE
C          FC         CORRECTION FACTOR FOR DUMMY DRIFT
C          FD         DEPTH OF EMBEDMENT GAGE BELOW PILE TOP IN FEET
C          FDM        FINAL DUMMY READING
C          FMULT      CALIBRATION CONSTANT FROM LOAD-STRAIN CALIBRATION CURVE
C          FSTR       OBSERVED STRAIN AFTER DRIFT CORRECTION
C          GROSS      DOWNWARD MOVEMENT OF TOP OF SHAFT CORRESPONDING TO
C                     THE LOAD Q, INCHES
C          ITEST      PARAMETER TO STOP PROGRAM
C          KASE   =   1 IF GAGE READINGS ARE INPUT BOTH UP AND DOWN
C          KASE   =   2 IF GAGE READINGS ARE INPUT AS DOWN ONLY
C          KOR        = -1 OR 1 IF CORRECTION IS NECESSARY AT ANY DEPTH.
C                     KOR = 0 FOR THE FIRST RUN
C          M          NUMBER OF LEVELS AT WHICH GAGES ARE LOCATED
C          N          NUMBER OF LOADINGS * NUMBER OF GAGES AT ANY DEPTH
C                     AND MAY VARY FROM DEPTH TO DEPTH
C          NPROB      PROBLEM NUMBER
C          NQ         TOTAL NUMBER OF LOADINGS IN THE LOAD TEST
C          ODM        INITIAL DUMMY READING
C          P          LOAD IN SHAFT AT DEPTH FD
C          PLEN       LENGTH OF SHAFT IN FEET
C          PM         LOAD IN SHAFT AT DEPTH X
C          Q          LOAD ON TOP OF SHAFT IN TONS
C          R          CORRELATION COEFFICIENT
C          STR        OBSERVED STRAIN BEFORE DUMMY CORRECTION
C          T          LOAD TRANSFER AT DEPTH X IN TONS / SQ.FT.
C          TOP        LOAD ON TOP OF SHAFT IN TONS
C          TRANS      LOAD TRANSFERED TO SOIL TONS
C          UP         EMB. GAGE READING WHILE READING UPWARDS-MICRO IN/IN
C          X          DEPTH OF POINT IN SHAFT WHERE LOAD TRANSFER AND
C                     NET MOVEMENT IS COMPUTED
C          ZERO       INITIAL EMBEDMENT GAGE READING-MICRO IN/IN
    1 FORMAT ( 1H1 )
    2 FORMAT (   52H   PROGRAM EMGAGE4 FOR ANALYSIS OF LOAD DISTRIBUTION
     1          / 57H   IN A DRILLED SHAFT BY V.N.VIJAYVERGIYA  FEB. 14,
     21968  // )
    3 FORMAT ( A5, 5X, 4( 3X, I2 ), 2E10.3 )
    4 FORMAT ( 16A5 )
    5 FORMAT ( / 18H   PROBLEM NUMBER , 5X, A5  // )
    6 FORMAT (   23H   GENERAL INFORMATION   // )
    7 FORMAT (// 42H          NUMBER OF GAGE STATIONS       = , I2 ,
     1          / 42H          KASE                          = , I2 ,
     3          / 42H          DIAMETER OF SHAFT             = , E10.3 ,
```

```
     4          / 42H           LENGTH OF SHAFTFT              = , E10.3 ,
     5          / 42H           TOTAL NUMBER OF LOADINGS       = , I2,
     6      /     42H           KOR                           =  , I2,
     7     ///    42H  NOTE - ADJUSTMENT IS MADE AT SOME
     8     /      42H           STATION IF KOR = 1 OR -1
     9      /     42H           NO ADJUSTMENT WHEN KOR = 0        , // )
    8 FORMAT ( F5.2 , 3X, I2 )
    9 FORMAT ( F10.2, 3( 5X, F5.0 ), 2F5.0 )
   10 FORMAT (   21H   DEPTH OF GAGES  = ,E10.3 ,  8H  FEET      )
   11 FORMAT (  /75H   LOAD ON TOP    ZERO GAGE    DOWN GAGE    UP GAGE
     1      STRAIN IN         ,/
     2            75H   OF SHAFT-TONS  READING      READING      READING
     3      COMPRESSION       ,       )
   12 FORMAT ( 4X, F10.2, 3( 8X, F5.0 ), 3X, E10.3 )
   13 FORMAT (// 40H           CURVE FITTING INFORMATION      //
     1            76H   DEPTH       A              B          ERROR
     2    R            SBO        / )
   14 FORMAT ( 3X, F5.2, 5( 3X, E10.3 ) )
   15 FORMAT ( 2E10.3 )
   16 FORMAT ( //37H   LOAD ON TOP OF SHAFT             = , E10.3 , /
     1            37H   GROSS MOVEMENT OF TOP PF SHAFT   = , E10.3  /  )
   17 FORMAT (   74H   DEPTH     STRAIN    LOAD IN      LOAD TRANS    MI
     1D DEPTH   ELAS. COMP. ,  /
     2            74H   X-FEET              SHAFT-TONS   TO SOIL-TONS
     3X-FEET    UP TO X- IN ,  /  )
   18 FORMAT ( 50X, E10.3, 3X, E10.3 )
   19 FORMAT ( 3X, F5.2, 3( 3X, E10.3 ) )
   20 FORMAT (// 57H   DEPTH OF    LOAD ON TOP    LOAD TRANS    NET MOVE
     1MENT  ,  /
     2            57H   X  FEET     OF SHAFT-TONS  TO SOIL-TSF   OF X-INC
     3H     ,  / )
   21 FORMAT ( 5X, F5.2 )
   22 FORMAT ( 15X, E10.3, 5X, E10.3, 5X, E10.3 )
   23 FORMAT (5X,  F5.2, 2E10.3 )
   24 FORMAT (// 50H   LOAD TRANSFER ANALYSIS IS ABONDONED, BECAUSE
     1      /     40H   CORRECTION IS NECESSARY AT STATION =  , I2,
     2      /     20H   DEPTH - FT    =  , F5.2  // )
   25 FORMAT ( //51H   CURVE FITTING INFORMATION  AFTER ADJUSTMENT
     1         // 40H   DEPTH FT   CONSTANT A   CONSTANT B   / )
   26 FORMAT ( 5X, F5.2, 4X, E10.3, 4X, E10.3 )
   27 FORMAT ( //52H   THERE IS AN ERROR IN THEINPUT OF LENGTH OF SHAFT
     1       /    30H   OR DEPTH OF LAST STATION     // )
      DIMENSION  FD(20), A(20), B(20), ERROR(20), AVSTR(20), COR(20),
     1           P(20), PM(20), TRANS(20), X(20), BLOCK(20), AREA(20),
     2           DELTA(20), DISNET(20,30), Q(30), GROSS(30), T(20,30),
     3           AN1(80), TOP(90), ZERO(90), DOWN(90), UP(90), ODM(90),
     4           FDM(90), AVRD(90), FC(90), STR(90), FSTR(90), Y(90),
     5       YE(90), SBO(20), R(20)
C
C          START EXECUTION OF PROGRAM EMGAGE4
C
       PRINT 1
           ITEST  =  5H
C
C          PROGRAM AND PROBLEM IDENTIFICATION
```

```
C
      PRINT 2
  110 READ 3, NPROB, KOR, M, NQ, KASE, DIA, PLEN
        IF ( NPROB - ITEST ) 120, 1010, 120
  120 READ 4, ( AN1(N), N = 1, 80 )
      PRINT 5, NPROB
      PRINT 6
      PRINT 4, ( AN1(N),  N = 1, 80 )
      PRINT 7, M, KASE, DIA, PLEN, NQ, KOR
  125   DO 400  J  = 1, M
      READ 8, FD(J), N
      READ 9, ( TOP(I), ZERO(I), DOWN(I), UP(I), ODM(I), FDM(I), I =1,N)
      PRINT 1
      PRINT 10, FD(J)
      PRINT 11
           SUMX       =  0.0
           SUMY       =  0.0
           SUMXX      =  0.0
           SUMXY      =  0.0
C
C          COMPUTE BEST ESTIMATE OF STRAIN
C
         DO  200  I = 1, N
        GO TO   ( 130, 140 ) KASE
  130     AVRD(I)    =  ( DOWN(I) + UP(I) ) / 2.0
        GO TO 150
  140     AVRD(I)    =  DOWN(I)
  150     FC(I)      =  ODM(I) - FDM(I)
          STR(I)     =  AVRD(I) - ZERO(I)
          FSTR(I)    =  STR(I) + FC(I)
          FSTR(I)    =  - FSTR(I)
          SUMX       =  SUMX + TOP(I)
          SUMY       =  SUMY + FSTR(I)
          SUMXX      =  SUMXX + TOP(I) * TOP(I)
          SUMXY      =  SUMXY + TOP(I) * FSTR(I)
      PRINT 12, TOP(I), ZERO(I), DOWN(I), UP(I), FSTR(I)
  200 CONTINUE
          XBAR       =  SUMX / N
          YBAR       =  SUMY / N
          F1         =  SUMXY
          F2         =  N * XBAR * YBAR
          F3         =  SUMXX
          F4         =  N * XBAR *  XBAR
          B(J)       =  ( F1 - F2 ) / ( F3 -F4 )
          A(J)       =  YBAR - B(J) * XBAR
          SS         =  0.0
          SSE        =  0.0
          CXX        =  0.0
         DO  300  I = 1, N
          Y(I)       =  FSTR(I)
          YE(I)      =  A(J) + B(J) * TOP(I)
          SSE        =  SSE + ( Y(I) - YE(I) ) * ( Y(I) - YE(I) )
          SS         =  SS + ( Y(I) - YBAR ) * ( Y(I) - YBAR)
          CXX        =  CXX + ( TOP(I) - XBAR ) * ( TOP(I) - XBAR )
  300 CONTINUE
```

```
          ERROR(J)   =  SQRT ( SSE / N )
          RR         =  1.0 - SSE / SS
          R(J)       =  SQRT( RR)
          F5         =  F3 / ( N * CXX )
          F6         =  SQRT( F5 )
          SBO(J)     =  F6 * ERROR(J)
C
C         ASSIGNING PROPER UNITS TO  A(J)  B(J)
C
          A(J)       =  A(J) / 10**6
          B(J)       =  B(J) / 10**6
  400 CONTINUE
      PRINT 13
      PRINT 14, ( FD(J), A(J), B(J),ERROR(J),R(J), SBO(J), J = 1, M  )
          MM         =  M - 1
        DO  410  J = 1, MM
          BJ         =  B(J)
          BJ1        =  B( J+1 )
        IF ( BJ - BJ1 ) 1001, 410, 410
  410 CONTINUE
        GO TO 450
  411   DO  420  J  = 1, M
          B(J)       =  0.0
          A(J)        =  0.0
  420 CONTINUE
  440 READ 23 , ( FD(J), A(J), B(J), J = 1, M )
      PRINT 25
      PRINT 26, ( FD(J), A(J), B(J),  J = 1, M )
      PRINT 1
C
C         REMOVE THESE COMMENT CARDS IF NECESSARY
C                          AND
C              INTRODUCE  THE REQUIRED
C                     CORRECTION
C
C
C
  450     FMULT      =  1.0 / B(1)
        DO  800  L = 1, NQ
      READ 15, Q(L), GROSS(L)
      PRINT 16, Q(L), GROSS(L)
         DO  500  J = 1, M
          AVSTR(J)  =  B(J) * Q(L) + A(J)
          COR(J)    =  AVSTR(J) - A(1)
  500 CONTINUE
          FDM       =  FD(M)
        IF ( FDM - PLEN ) 540, 550, 1003
  540     FD(M+1)   =  PLEN
          AVSTR(M+1)= -( AVSTR(M-1) - AVSTR(M) ) * ( FD(M+1) - FD(M) )
     1                / ( FD(M) - FD(M-1) )  + AVSTR(M)
          COR(M+1)  =  AVSTR(M+1) - A(1)
C
C         COMPUTATION OF LOAD TRANSFER IN THE DRILLED SHAFT
C
  550 PRINT 17
```

```
        P(1)       =  FMULT * COR(1)
        PM(1)      =  P(1)
        TRANS(1)   =  0.0
        X(1)       =  FD(1)
        BLOCK(1)   =  P(1) * FD(1)
        AREA(1)    =  BLOCK(1)
        DELTA(1)   =  AREA(1) / FMULT
       DISNET(1,L)=  GROSS(L) / 12.0 - DELTA(1)
        T(1,L)     =  0.0
        M1         =  M+1
       DO   600  J = 2, M1
        P(J)       =  FMULT * COR(J)
        PM(J)      =  ( P(J) + P(J-1) ) / 2.0
        TRANS(J)   =  Q(L) - P(J)
        TRANSJ     =  TRANS(J)
      IF ( TRANSJ ) 560, 570, 570
560     TRANS(J)   =  0.0
570     X(J)       =  ( FD(J) + FD(J-1) ) / 2.0
        BLOCK(J)   =  BLOCK(J-1) + ( FD(J) - FD(J-1) ) * PM(J)
        AREA(J)    =  BLOCK(J-1) + (PM(J) + P(J-1)) * (X(J)-FD(J-1))/2.
        DELTA(J)   =  AREA(J) / FMULT
      DISNET(J,L) =  GROSS(L) / 12.0 - DELTA(J)
        FP1        =  P(J-1)
        FP2        =  P(J)
      IF ( FP1 - FP2 ) 580,590,590
580     T(J,L)     =  0.0
      GO TO 600
590     T(J,L)     =  (P(J-1) - P(J) ) / (3.1416*DIA*(FD(J)-FD(J-1)))
600 CONTINUE
       DO  700  J = 1, M1
        DELTA(J)   =  DELTA(J) * 12.0
    PRINT 18, X(J), DELTA(J)
    PRINT 19,  FD(J), AVSTR(J), P(J), TRANS(J)
700 CONTINUE
800 CONTINUE
    PRINT 1
    PRINT 20
       DO  1000  J = 1,M1
    PRINT 21, X(J)
       DO  900  L = 1, NQ
        DISNET(J,L) =  DISNET(J,L) * 12.0
    PRINT 22, Q(L), T(J,L) , DISNET(J,L)
900 CONTINUE
1000 CONTINUE
      GO TO 110
1001 CONTINUE
      IF ( KOR ) 411, 1002, 411
1002 PRINT 24, J, FD(J)
      GO TO 110
1003 CONTINUE
    PRINT 27
      GO TO 110
1010 CONTINUE
    END
```

PROBLEM NUMBER AND CONSTANTS (Program stops if column 1 through 5 are left blank)

NPROB	KOR	M	NQ	KASE	DIA	PLEN
A5	I2	I2	I2	I2	E10.3	E10.3
1 5	14 15	19 20	24 25	29 30	40	50

DESCRIPTION OF PROBLEM (5 alphanumeric cards)

TEST SITE	16A5
1	80
TEST NUMBER	16A5
1	80
DATE OF TEST	16A5
1	80
TYPE OF TEST	16A5
1	80
TIME INTERVAL	16A5
1	80

INPUT OF STRAIN GAGE READINGS AT VARIOUS DEPTHS (M sets)

DEPTH AND NUMBER OF STRAIN GAGE READINGS FOR THE ENTIRE TEST AT THAT DEPTH

FD	N
F5.2	I2
1 5	9 10

LOAD AND CORRESPONDING STRAIN GAGE READINGS (number of cards = N)

TOP	ZERO	DOWN	UP	ODM	FEM
F10.2	F5.0	F5.0	F5.0	F5.0	F5.0
1 10	16 20	26 30	36 40	45	50

ADJUSTMENT OF STRAIN (number of cards = M if KOR = 1 or -1, otherwise these cards are not required)

FD	A	B
F5.2	E10.3	E10.3
6–10	20	30

INPUT OF OBSERVED LOAD SETTLEMENT CURVE (number of cards = NQ)

Q	GROSS
E10.3	E10.3
1–10	20

STOP CARD (one blank card to end run)
1–80

SAMPLE INPUT

```
   2          1    7   14     1 2.500E+00 2.850E+01
         TEST SITE                          SAN ANTONIO
         TEST NUMBER                        2
         DATE OF TEST                       JUNE 30, 1967
         TYPE OF TEST                       SLOW
         TIME INTERVAL                      12 MINUTES
1.71   42
    50.         -2472       -2510       -2510    00  -03
    50.         -3000       -3034       -3030    00  -03
    50.         -2905       -2940       -2937    00  -03
   100.         -2472       -2537       -2538    00  -03
   100.         -3000       -3058       -3054    00  -03
   100.         -2905       -2958       -2964    00  -03
```

```
4.96   42
    50.         -1921       -1948       -1952    00  -03
    50.         -1708       -1730       -1732    00  -03
    50.         -2398       -2422       -2424    00  -03
   100.         -1921       -1972       -1983    00  -03
   100.         -1708       -1746       -1754    00  -03
   100.         -2398       -2444       -2448    00  -03
   150.         -1921       -2008       -2010    00  -03
   150.         -1708       -1776       -1777    00  -03
   150.         -2398       -2475       -2475    00  -03
```

```
     0171-4.231E-07 5.702E-07
     0496-4.535E-06 5.659E-07
     1005-1.097E-05 5.592E-07
     1520-1.279E-05 5.449E-07
     2030-1.166E-05 4.710E-07
     2500-7.147E-06 3.119E-07
     2805 7.445E-07 1.034E-07
    50.   1.000E-02
   100.   2.350E-02
   150.   3.800E-02
```

SAMPLE OUTPUT*

```
ROGRAM EMGAGE4 FOR ANALYSIS OF LOAD DISTRIBUTION
N A DRILLED SHAFT BY M. W.VIJAYVERGIYA  FEB. 14, 1968


ROBLEM NUMBER


ENERAL INFORMATION

        TEST SITE                          SAN ANTONIO
        TEST NUMBER                        2
        DATE OF TEST                       JUNE 30, 1967
        TYPE OF TEST                       SLOW
        TIME INTERVAL                      12 MINUTES


        NUMBER OF GAGE STATIONS          =  7
        KASE                             =  1
        DIAMETER OF SHAFT                =  2.500E+00
        LENGTH OF SHAFT(FT               =  2.850E+01
        TOTAL NUMBER OF LOADINGS         =  14
        KOR                              =  1

TE = ADJUSTMENT IS MADE AT SOME
        STATION IF KOR = 1 OR -1
        NO ADJUSTMENT MADE KOR = 0


EPTH OF GAGES  =  1.710E+00  FEET

OAD ON TOP      ZERO GAGE      DOWN GAGE      UP GAGE        STRAIN I
F SHAFT-TONS    READING        READING        READING        COMPRESSION
      50.00        -2472          -2510          -2510      3.500E+01
      50.00        -3033          -3034          -3030      2.900E+01
      50.00        -2935          -2940          -2937      3.050E+01
     100.00        -2472          -2537          -2538      6.250E+01
     100.00        -3033          -3058          -3054      5.300E+01
```

*Total output is 30 pages.

DEPTH OF GAGES = 4.960E+00 FEET

LOAD ON TOP OF SHAFT-TONS	ZERO GAGE READING	DOWN GAGE READING	UP GAGE READING	STRAIN IN COMPRESSION
50.00	-1921	-1948	-1952	2.600E+01
50.00	-1718	-1730	-1732	2.000E+01
50.00	-2398	-2422	-2424	2.200E+01
100.00	-1921	-1972	-1983	5.350E+01
100.00	-1718	-1746	-1754	3.900E+01
100.00	-2398	-2444	-2448	4.500E+01
150.00	-1921	-2008	-2010	8.500E+01

CURVE FITTING INFORMATION

DEPTH	A	B	ERROR	R	SBO
1.71	-4.231E-07	5.702E-07	1.521E+01	9.914E-01	4.956E+00
4.96	-7.973E-06	5.454E-07	2.398E+01	9.770E-01	7.814E+00
10.05	-1.097E-05	5.592E-07	2.456E+01	9.771E-01	8.004E+00
15.20	-1.279E-05	5.449E-07	4.177E+00	9.993E-01	1.361E+00
20.30	-1.166E-05	4.710E-07	6.060E+00	9.980E-01	1.975E+00
25.00	-7.147E-06	3.119E-07	1.590E+01	9.695E-01	5.182E+00
28.05	7.445E-07	1.034E-07	3.566E+00	9.857E-01	1.424E+00

CURVE FITTING INFORMATION AFTER ADJUSTMENT

DEPTH FT	CONSTANT A	CONSTANT B
1.71	-4.231E-07	5.702E-07
4.96	-4.535E-06	5.659E-07
10.05	-1.097E-05	5.592E-07
15.20	-1.279E-05	5.449E-07
20.30	-1.166E-05	4.710E-07
25.00	-7.147E-06	3.119E-07
28.05	7.445E-07	1.034E-07

LOAD ON TOP OF SHAFT = 5.000E+01
GROSS MOVEMENT OF TOP OF SHAFT = 1.000E-02

DEPTH X-FEET	STRAIN	LOAD IN SHAFT-TONS	LOAD TRANS TO SOIL-TONS	MID DEPTH X-FEET	ELAS. COMP. UP TO X- IN
				1.710E+00	5.850E-04
1.71	2.809E-05	5.000E+01	0.		
				3.335E+00	1.120E-03
4.96	2.376E-05	4.241E+01	7.588E+00		
				7.505E+00	2.299E-03
10.05	1.699E-05	3.054E+01	1.946E+01		

15.20	1.445E-05	2.609E+01	2.391E+01	1.262E+01	3.401E-03
20.30	1.189E-05	2.159E+01	2.841E+01	1.775E+01	4.316E-03
25.00	8.448E-06	1.556E+01	3.444E+01	2.265E+01	5.036E-03
28.05	5.914E-06	1.111E+01	3.889E+01	2.652E+01	5.461E-03
28.50	5.541E-06	1.046E+01	3.954E+01	2.827E+01	5.605E-03

LOAD ON TOP OF SHAFT = 1.000E+02
GROSS MOVEMENT OF TOP OF SHAFT = 2.350E-02

DEPTH X-FEET	STRAIN	LOAD IN SHAFT-TONS	LOAD TRANS TO SOIL-TONS	MID DEPTH X-FEET	ELAS. COMP. UP TO X- IN
1.71	5.66[illegible]E-05	1.000E+02	0.	1.710E+00	1.170E-03
4.96	5.205E-05	9.203E+01	7.965E+00	3.335E+00	2.260E-03
10.05	4.495E-05	7.957E+01	2.043E+01	7.505E+00	4.854E-03
15.20	4.170E-05	7.387E+01	2.613E+01	1.262E+01	7.671E-03
20.30	3.544E-05	6.290E+01	3.710E+01	1.775E+01	1.024E-02
25.00	2.404E-05	4.291E+01	5.709E+01	2.265E+01	1.231E-02
28.05	1.108E-05	2.018E+01	7.982E+01	2.652E+01	1.347E-02
28.50	9.173E-06	1.683E+01	8.317E+01	2.827E+01	1.377E-02

LOAD ON TOP OF SHAFT = 1.500E+02
GROSS MOVEMENT OF TOP OF SHAFT = 3.800E-02

DEPTH X-FEET	STRAIN	LOAD IN SHAFT-TONS	LOAD TRANS TO SOIL-TONS	MID DEPTH X-FEET	ELAS. COMP. UP TO X- IN

DEPTH OF X FEET	LOAD ON TOP OF SHAFT-TONS	LOAD TRANS TO SOIL-TSF	NET MOVEMENT OF X-INCH
1.71			
	5.000E+01	0.	9.415E-03
	1.000E+02	0.	2.233E-02
	1.500E+02	0.	3.624E-02
	2.000E+02	0.	5.216E-02
	2.500E+02	0.	7.657E-02
	3.000E+02	0.	1.020E-01
	3.500E+02	0.	1.314E-01
	4.000E+02	0.	1.668E-01
	4.500E+02	0.	2.077E-01
	5.000E+02	0.	2.521E-01
	5.500E+02	0.	3.081E-01

	6.000E+02	0.	3.625E-01
	6.500E+02	0.	4.389E-01
	7.000E+02	0.	5.268E-01
3.33			
	5.000E+01	2.973E-01	8.880E-03
	1.000E+02	3.121E-01	2.124E-02
	1.500E+02	3.268E-01	3.460E-02
	2.000E+02	3.416E-01	4.996E-02
	2.500E+02	3.564E-01	7.382E-02
	3.000E+02	3.711E-01	9.848E-02
	3.500E+02	3.859E-01	1.275E-01
	4.000E+02	4.007E-01	1.624E-01
	4.500E+02	4.155E-01	2.028E-01
	5.000E+02	4.302E-01	2.466E-01
	5.500E+02	4.450E-01	3.020E-01
	6.000E+02	4.598E-01	3.558E-01
	6.500E+02	4.745E-01	4.317E-01
	7.000E+02	4.893E-01	5.141E-01
7.50			
	5.000E+01	2.970E-01	7.701E-03
	1.000E+02	3.117E-01	1.865E-02
	1.500E+02	3.264E-01	3.054E-02
	2.000E+02	3.411E-01	4.454E-02
	2.500E+02	3.559E-01	6.099E-02
	3.000E+02	3.705E-01	9.043E-02
	3.500E+02	3.852E-01	1.179E-01
	4.000E+02	3.999E-01	1.513E-01
	4.500E+02	4.146E-01	1.903E-01
	5.000E+02	4.293E-01	2.327E-01
	5.500E+02	4.440E-01	2.867E-01
	6.000E+02	4.587E-01	3.391E-01
	6.500E+02	4.734E-01	4.135E-01
	7.000E+02	4.880E-01	4.995E-01
12.62			
	5.000E+01	1.099E-01	6.599E-03
	1.000E+02	1.409E-01	1.583E-02
	1.500E+02	1.719E-01	2.606E-02
	2.000E+02	2.024E-01	3.824E-02
	2.500E+02	2.334E-01	5.902E-02
	3.000E+02	2.644E-01	8.075E-02

APPENDIX 4

PROGRAM SHAFT

```
      PROGRAM SHAFT ( INPUT, OUTPUT )
C     PROGRAM SHAFT FOR AXIALLY LOADED PILES
C         AA AND BB   CONSTANTS = 2.0 AND 1.0 RESPECTIVELY  IF NOT KNOWN
C         AE          AREA TIMES MODULUS OF ELASTICITY FOR PILE , TONS
C         AN1         DESCRIPTION AND IDENTIFICATION OF PROBLEM
C         BLOS        N VALUE
C         BLX(I)      COMPUTED VALUE OF N AT DEPTH X(I)
C         DIA         DIAMETER OF PILE , FEET
C         EXL         THE EXPOSED LENGTH OF SHAFT , FEET
C         FD          THE DEPTH BELOW GROUND SUR. AT WHICH N IS SPECIFIED
C         FK          CONSTANT C2 = 35 IF NOT KNOWN
C         ITEST       A PARAMETER TO STOP PROGRAM
C         KK          = 0 IF ONLY LOAD SETTLEMENT CURVE IS REQUIRED
C                     = 1 IF LOAD TRANSFER DATA IS REQUIRED
C         M           NUMBER OF PILE SECTIONS DESIRED
C         NBD         NUMBER OF DEPTHS AT WHICH N VALUES ARE SPECIFIED
C         NL          NUMBER OF TRIAL LENGTHS OF PILE
C         NPROB       PROBLEM NUMBER
C         NQS         NUMBER OF POINTS ON TIP LOAD SETTLEMENT CURVE
C         P(I)        LOAD ON TOP OF I TH SECTION , TONS
C         PLEN        PILE LENGTH , FEET
C         Q           TIP LOAD , TONS
C         S           TIP SETTLEMENT , INCH
C         SS          MAXIMUM SETTLEMENT OF SHAFT , INCH
C                     = 5 TO 6 PERCENT OF SHAFT DIAMETER
C         SE(I)       ELASTIC COMPRESS OF SECTION I
C         SM(I)       SETTLEMENT AT THE MIDDLE OF SECTION I
C         ST(I)       SETTLEMENT AT THE BOTTOM OF SECTION I
C         T(I)        LOAD TRANSFER AT DEPTH X(I)
C         X(I)        THE DEPTH TO THE CENTER OF ITH SECTION , FEET
C         BEGIN EXECUTION OF PROGRAM
      DIMENSION  AN1(32), FD(60), BLOS(60), XX(200), X(200), BLX(200),
     1            SM(200), ST(200), P(200), T(200), TLD(200), SE(200)
    1 FORMAT ( 1H1 )
    2 FORMAT (   51H   PROGRAM SHAFT FOR DESIGN OF AXIALLY LOADED PILES
     1         / 35H   BY VIJAY VERGIYA OCTOBER 1968    //  )
      PRINT 1
      PRINT 2
          ITEST = 5H
  101 READ 11, NPROB, KK
   11 FORMAT ( A5 , 4X, I1 )
        IF ( ITEST - NPROB ) 102, 5001, 102
  102 READ 12, ( AN1(I), I = 1, 32  )
   12 FORMAT ( 16A5 )
      PRINT 13, NPROB
   13 FORMAT ( // 22H  PROBLEM NUMBER    =  ,A5 // )
      PRINT 12,( AN1(I), I = 1, 32 )
      READ 14, NBD
   14 FORMAT ( 5X, I5 )
      READ 15, ( FD(J), BLOS(J), J = 1, NBD  )
   15 FORMAT ( 8F10.2 )
      PRINT 16
   16 FORMAT (// 40H   INPUT OF N VALUES AT VARIOUS DEPTHS  ,  )
      PRINT 17
   17 FORMAT (// 33H   DEPTH-FT.  NUMBER OF BLOWS- N  ,  // )
```

```
      DO 200 J = 1, NBD
200 PRINT 18, FD(J), BLOS(J)
 18 FORMAT ( 3X, F10.2, 5X, F10.2  )
    READ 19, M, DIA, NL, AE, EXL , FK, SS, AA, BB
 19 FORMAT ( 5X, I5, E10.3, 5X, I5, 2E10.3 , 5X, F5.2, F10.3, 2F5.2 )
      DO 3000 J = 1, NL
    READ 20, PLEN , NQS
 20 FORMAT ( E10.3, I5 )
    PRINT 21, PLEN, EXL, DIA, AE, SS, FK , AA, BB
 21 FORMAT ( //30H   LENGTH OF THE SHAFT EMBEDED, F10.3, 5H FEET , /
   1            30H   LENGTH OF THE SHAFT EXPOSED, F10.3, 5H FEET, /
   2            30H   DIAMETER OF THE SHAFT      , F10.3, 5H FEET, /
   3            30H   STIFFNESS OF THE SHAFT     , E10.3, 5H TONS, /
   4            30H   ASSUMED MAX SETTLEMENT     , F10.3, 5H INCH, /
   5            30H   CONSTANT FK                , 5X, F5.2,  /
   6            30H   CONSTANT AA                       , 5X, F5.2, /
   7            30H   CONSTANT BB                       , 5X, F5.2 // )
      IF(KK) 150,50,150
 50 PRINT 23
 23 FORMAT (   50H           ASSUMED FOR TIP         COMPUTED FOR TOP
   1   /       50H       LOAD         MOVEMENT     LOAD       MOVEMENT
   2  /        48H       TON          INCH         TON        INCH   //)
150   DO 2000 K = 1, NQS
    READ 24, Q, S
 24 FORMAT ( 2E10.3 )
      IF (KK) 201, 202 , 201
201 PRINT 26
 26 FORMAT ( / 52H   ELEMENT  DEPTH X, FT  LOAD TRANS. MOVEMENT
   1       /   45H   NUMBER   BELOW G.L.      TSF      AT X, IN   // )
202 SECL = PLEN / M
    ST(M+1) = S
    P(M+1)  = Q
      DO  550  I = 1, M
    FF     = I
    XX(I) = FF * SECL
    X(I)  = XX(I) - SECL / 2.0
    NB     = 1
300   IF ( X(I) - FD(NB) ) 500, 500, 400
400 NB     = NB+1
      GO TO 300
500 BLX(I)= ( BLOS(NB) - BLOS(NB-1) )*( X(I) - FD(NB-1) ) /
   1         ( FD(NB)- FD(NB-1) ) + BLOS(NB-1)
550 CONTINUE
      DO 800 I = 1, M
    NN    = M - I + 1
    T(NN) = BLX(NN) * (  AA * SQRT( ST(NN+1) / SS ) -  BB * ST(NN+1) /
   1          SS ) / FK
    TNN   = T(NN)
      IF ( TNN ) 600, 700, 700
600 T(NN) = 0.0
700 TLD(NN)  = T(NN) * 3.14 * DIA * SECL
    P(NN)   = P(NN+1) + TLD(NN)
    SE(NN) = ( P(NN) + P(NN+1) ) * SECL * 12.0 /  ( 2.0 * AE  )
    SM(NN) = SE(NN) / 2.0 + ST(NN+1)
    ST(NN) = SE(NN) + ST(NN+1)
```

```
      IF (KK) 701, 800, 701
  701 PRINT 27, NN, X(NN), T(NN), SM(NN)
   27 FORMAT ( 4X, I5, 3X, F8.3, 5X, F8.3, 3X, F8.4 )
  800 CONTINUE
      IF(KK) 801, 802, 801
  801 PRINT 22
   22 FORMAT (   50H           ASSUMED FOR TIP         COMPUTED FOR TOP
     1   /       50H       LOAD         MOVEMENT     LOAD       MOVEMENT
     2  /        48H       TON          INCH         TON        INCH    //)
  802   IF( EXL ) 1000, 900, 1000
  900 PRINT 25, Q, S, P(1), ST(1)
 1000 ST(1) = ST(1) + P(1)*EXL * 12.0 / AE
      PRINT 25, Q, S, P(1), ST(1)
 2000 CONTINUE
   25 FORMAT ( 8X, F8.1, 3X, F8.3,  5X, F8.1, 3X, F8.3 )
 3000 CONTINUE
      PRINT 1
      GO TO 101
 5001 CONTINUE
      END
```

SHAFT GUIDE FOR DATA INPUT -- Card forms

IDENTIFICATION OF PROBLEM (one card for each problem; program stops if Col. 1 through 5 are left blank)

NPROB	KK
A5	I1
1 5	9 10

DESCRIPTION OF PROBLEM (two alphanumeric cards for each problem)

1	80
1	80

INPUT OF N VALUES AT VARIOUS DEPTHS

NUMBER OF DEPTHS

NBD
I5
6 10

DEPTH AND CORRESPONDING N VALUE (number of pairs = NBD, as many cards as required by NBD pairs)

FD(1)	BLOS(1)	FD(2)	BLOS(2)				
F10.2	F10.2	F10.2	F10.2				
1 10	20	30	40	50	60	70	80

CONSTANTS AND SHAFT PROPERTIES

M	DIA	NL	AE	EXL	FK	SS	AA	BB
I5	E10.3	I5	E10.3	E10.3	F5.2	F10.3	F5.2	F5.2
6–10	20	26–30	40	50	56–60	70	75	80

INPUT OF TRIAL LENGTHS, TIP LOAD, AND TIP SETTLEMENT CURVES (NL sets per problem)

TRIAL LENGTH AND NUMBER OF POINTS ON TIP LOAD AND TIP SETTLEMENT CURVE (one card)

PLEN	NQS
E10.3	I5
1–10	15

TIP LOAD AND TIP SETTLEMENT (number of cards = NQS)

Q	S
E10.3	E10.3
1–10	20

STOP CARD (one blank card to end run)

1–80

SAMPLE INPUT - PROBLEM NO. 1

```
   1
         COMPUTED LOAD SETTLEMENT CURVE FOR
         SAN ANTONIO SITE
           5
     0.00       14.00      10.00       26.40       18.00       36.00       20.94       267.0
    27.00       718.0
        53 2.500E+00           1 1.790E+06 1.710E+00        34.0         1.8   2.5   1.5
2.680E+01    14
5.200E+01 3.600E-02
7.000E+01 9.000E-02
8.800E+01 1.800E-01
1.110E+02 3.600E-01
1.270E+02 5.400E-01
1.400E+02 7.200E-01
1.510E+02 9.000E-01
1.600E+02 1.080E+00
1.690E+02 1.260E+00
1.760E+02 1.440E+00
1.840E+02 1.620E+00
1.870E+02 1.710E+00
1.900E+02 1.800E+00
1.900E+02 1.980E+00
```

SAMPLE OUTPUTS

PROGRAM SHAFT FOR DESIGN OF AXIALLY LOADED PILES
BY VIJAYVERGIYA OCTOBER 1968

PROBLEM NUMBER = 1

COMPUTED LOAD SETTLEMENT CURVE FOR
SAN ANTONIO SITE

INPUT OF N VALUES AT VARIOUS DEPTHS

DEPTH-FT.	NUMBER OF BLOWS- N
0.0	14.00
10.00	26.40
18.00	36.00
20.94	267.00
27.00	718.00

LENGTH OF THE SHAFT EMBEDED	26.800 FEET
LENGTH OF THE SHAFT EXPOSED	1.710 FEET
DIAMETER OF THE SHAFT	2.500 FEET
STIFFNESS OF THE SHAFT	1.790E+06 TONS
ASSUMED MAX SETTLEMENT	1.800 INCH
CONSTANT FK	35.00
CONSTANT AA	2.00
CONSTANT BB	1.00

ASSUMED FOR TIP		COMPUTED FOR TOP	
LOAD TON	MOVEMENT INCH	LOAD TON	MOVEMENT INCH
52.0	.036	285.0	.082
70.0	.090	413.9	.158
88.0	.180	543.4	.269
111.0	.360	699.9	.475
127.0	.540	799.0	.671
140.0	.720	869.1	.863
151.0	.900	920.4	1.051
160.0	1.080	957.9	1.238
169.0	1.260	986.5	1.423
176.0	1.440	1005.9	1.606
184.0	1.620	1020.5	1.789
190.0	1.800	1028.3	1.970
190.0	1.980	1025.9	2.150

PROGRAM SHAFT FOR DESIGN OF AXIALLY LOADED PILES
BY VIJAYVERGIYA OCTOBER 1968

PROBLEM NUMBER = 2

COMPUTED LOAD SETTLEMENT CURVE FOR
HOUSTON SITE

INPUT OF N VALUES AT VARIOUS DEPTHS

DEPTH-FT.	NUMBER OF BLOWS- N
0.0	9.00
18.00	25.00
18.10	16.00
24.00	16.00

LENGTH OF THE SHAFT EMBEDED	23.000 FEET
LENGTH OF THE SHAFT EXPOSED	2.500 FEET
DIAMETER OF THE SHAFT	2.500 FEET
STIFFNESS OF THE SHAFT	1.790E+06 TONS
ASSUMED MAX SETTLEMENT	1.800 INCH
CONSTANT FK	38.00
CONSTANT AA	3.50
CONSTANT BB	2.50

ASSUMED FOR TIP		COMPUTED FOR TOP	
LOAD TON	MOVEMENT INCH	LOAD TON	MOVEMENT INCH
16.0	.036	52.3	.042
20.0	.072	68.5	.080
23.0	.108	80.0	.118
27.5	.180	96.3	.192
34.0	.360	119.2	.374
39.5	.540	132.7	.556
43.5	.720	140.3	.737
46.0	.900	143.7	.918
50.0	1.080	146.5	1.098
52.5	1.260	146.4	1.278
55.0	1.440	145.0	1.458
57.0	1.620	142.2	1.638
58.0	1.710	140.5	1.728
59.0	1.800	138.5	1.818
59.0	1.960	133.0	1.978

PROGRAM SHAFT FOR DESIGN OF AXIALLY LOADED PILES
BY VIJAYVERGIYA OCTOBER 1968

PROBLEM NUMBER = 3

COMPUTED LOAD SETTLEMENT CURVE FOR
MONTOPOLIS SITE

INPUT OF N VALUES AT VARIOUS DEPTHS

DEPTH-FT.	NUMBER OF BLOWS- N
0.0	30.0
3.00	30.0
3.10	44.0
15.00	44.0

LENGTH OF THE SHAFT EMBEDED	12.000 FEET
LENGTH OF THE SHAFT EXPOSED	1.300 FEET
DIAMETER OF THE SHAFT	2.000 FEET
STIFFNESS OF THE SHAFT	1.150E+06 TONS
ASSUMED MAX SETTLEMENT	1.440 INCH
CONSTANT FK	36.00
CONSTANT AA	1.50
CONSTANT BB	0.50

ASSUMED FOR TIP		COMPUTED FOR TOP	
LOAD TON	MOVEMENT INCH	LOAD TON	MOVEMENT INCH
17.0	.029	34.5	.033
23.0	.072	49.6	.077
24.5	.086	53.2	.091
29.0	.144	65.2	.151
36.5	.288	85.1	.297
42.0	.432	99.1	.442
46.0	.576	109.6	.587
49.5	.720	118.4	.732
52.5	.865	125.7	.878
55.5	1.010	132.4	1.024
58.0	1.150	137.9	1.164
60.5	1.300	143.1	1.315
61.5	1.370	145.3	1.385
62.5	1.440	147.4	1.455
62.5	1.580	149.3	1.596

APPENDIX 5

DRILLING REPORTS

Texas Highway Department
Form 554

DRILLING REPORT

(For use with Undisturbed Sampling & Testing)

Sheet 1 of 2

County Bexar | Structure San Antonio | District No. 15
Highway No. US 90 | Hole No. SA-1 | Date 7-5-66
Control 24-8 | Station 254+80 | Grd. Elev.
Project No. Research Project 3-5-65-89 | Loc. from Centerline Rt. 130' Lt. | Grd. Water Elev.

Elev. (Ft.)	Depth (Ft.)	† Samples	LOG	THD PEN. TEST No. of Blows 1st 6"	2nd 6"	Sample Number	Lat. Press. (PSI)	Ult. Stress (PSI)	Wet Density (pcf)	Moisture Content (%)	Liquid Limit (%)	Plasticity Index (%)	DESCRIPTION OF MATERIAL	Remarks
													Dark Gray Clay with Gravel	
	5					SA-1-1								
													Light Gray Clay with Gravel	
	10					SA-1-2A							Yellow Stiff Clay	
						SA-1-2B								
						SA-1-3								
						SA-1-4								
						SA-1-5								
	15					SA-1-6							Silt Pockets at 15'	
						SA-1-7								
						SA-1-8							Seashells at 17'	
						SA-1-9								
													Yellow and Gray Clay Shale with Sandstone Layers	
	20												Pockets of Red Clay and Gravel at 21'	
	25													

Driller _____ Logger _____ Title _____

†Indicate each foot by shading for core recovery, leaving blank for no core recovery, and crossing (X) for undisturbed laboratory samples taken.

Texas Highway Department
Form 554

DRILLING REPORT

(For use with Undisturbed Sampling & Testing)

County Bexar | Structure San Antonio | District No. 15
Highway No. US 90 | Hole No. SA-1 | Date 7-7-66
Control 24-8 | Station 254+80 | Grd. Elev.
Project No. Research Project 3-5-65-89 | Loc. from Centerline Rt. 130' Lt. | Grd. Water Elev.

Elev. (Ft.)	Depth (Ft.)	† Samples	LOG	THD PEN. TEST No. of Blows 1st 6"	2nd 6"	Sample Number	Lat. Press. (PSI)	Ult. Stress (PSI)	Wet Density (pcf)	Moisture Content (%)	Liquid Limit (%)	Plasticity Index (%)	DESCRIPTION OF MATERIAL	Remarks
	35													
		X				SA-1-10							Blue Clay, Shale, with Tan Streaks	
	40	X				SA-1-11							at 38' and at 48'	
		X				SA-1-12								
		X				SA-1-13A								
		X				SA-1-13B								
		X				SA-1-14								
		X				SA-1-15								
	45	X				SA-1-16								
		X				SA-1-17								
		X				SA-1-18								
		X				SA-1-19								
		X				SA-1-20								
	50													1
1 Boring Completion Depth at 50' on July 7, 1966.														

Driller _____ Logger _____ Title _____

†Indicate each foot by shading for core recovery, leaving blank for no core recovery, and crossing (X) for undisturbed laboratory samples taken.

Texas Highway Department
Form 554

DRILLING REPORT

(For use with Undisturbed Sampling & Testing)

Sheet 1 of 2

County Bexar | Structure San Antonio | District No. 15
Highway No. US 90 | Hole No. SA-3 | Date 7-8-66
Control 24-8 | Station 254+25 | Grd. Elev.
Project No. Research Project 3-5-65-89 | Loc. from Centerline Rt. 132' Lt. | Grd. Water Elev.

Elev. (Ft.)	Depth (Ft.)	† Samples	LOG	THD PEN. TEST No. of Blows 1st 6"	THD PEN. TEST No. of Blows 2nd 6"	Sample Number	Lat. Press. (PSI)	Ult. Stress (PSI)	Wet Density (pcf)	Moisture Content (%)	Liquid Limit (%)	Plasticity Index (%)	DESCRIPTION OF MATERIAL	Remarks
						SA-3-1A							Dark Gray and Tan Clay	
						-1B								
						SA-3-2A								
						-2B								
						SA-3-3								
	5												Gray Below 5'	
						SA-3-4								
						SA-3-5								
						SA-3-6A							Yellow and Gray Clay with Small Gravel	
	10					-6B								
						SA-3-7A								
						-7B								
	15													
						-7C								
						SA-3-8A								
						-8B								
						-8C							Yellow, Red and Gray Clay Shale with Sandstone	
	20					-8D							Layers and Seashells	
						SA-3-9A								
						-9B								
						-9C							Yellow and Gray Below 24.5'	
	25					-9D								
						SA-3-10A								
						-10B								
						-10C								
						-10D								
	30													

Driller _____ Logger _____ Title _____

†Indicate each foot by shading for core recovery, leaving blank for no core recovery, and crossing (X) for undisturbed laboratory samples taken.

Texas Highway Department
Form 554

DRILLING REPORT

(For use with Undisturbed Sampling & Testing)

Sheet 2 of 2

County Bexar | Structure San Antonio | District No. 15
Highway No. US 90 | Hole No. SA-3 | Date 7-8-66
Control 24-8 | Station 254+25 | Grd. Elev.
Project No. Research Project 3-5-65-89 | Loc. from Centerline Rt. 132' Lt. | Grd. Water Elev.

Elev. (Ft.)	Depth (Ft.)	† Samples	LOG	THD PEN. TEST No. of Blows 1st 6"	THD PEN. TEST No. of Blows 2nd 6"	Sample Number	Lat. Press. (PSI)	Ult. Stress (PSI)	Wet Density (pcf)	Moisture Content (%)	Liquid Limit (%)	Plasticity Index (%)	DESCRIPTION OF MATERIAL	Remarks
	35					SA-3-12A							Yellow, Gray and Blue Clay Shale with Gypsum	
						-12B								
						-12C								
	40					-12D								1

1 Boring Completion Depth at 40' on July 8, 1966.

Driller _____ Logger _____ Title _____

†Indicate each foot by shading for core recovery, leaving blank for no core recovery, and crossing (X) for undisturbed laboratory samples taken.

Texas Highway Department
Form 554

DRILLING REPORT

(For use with Undisturbed Sampling & Testing)

Sheet 1 of 2

County Bexar | Structure San Antonio | District No. 15
Highway No. US 90 | Hole No. SA-4 | Date 1-16-68
Control 24-8 | Station 254+90 | Grd. Elev.
Project No. Research Project 3-5-65-89 | Loc. from Centerline Rt. 137' Lt. | Grd. Water Elev.

Elev. (Ft.)	Depth (Ft.)	† Samples	LOG	THD PEN. TEST No. of Blows 1st 6"	2nd 6"	Sample Number	Lat. Press. (PSI)	Ult. Stress (PSI)	Wet Density (pcf)	Moisture Content (%)	Liquid Limit (%)	Plasticity Index (%)	DESCRIPTION OF MATERIAL	Remarks
				6	11								Gray Clay with Gravel	
						SA-4-1								
				5	11	SA-4-2								
						SA-4-3								
	5			5	5									
						SA-4-4								
				12	12	SA-4-5								
													Yellow Clay with Some Gravel	
				9	9	SA-4-6								
	10													
				8	9	SA-4-7								
				8	13									
						SA-4-8								
	15			22	13									
						SA-4-9								
				17	18									
						SA-4-10								
	20			35	65/4"									
						SA-4-11							Yellow and Gray Clay Shale with Sandstone Layers	
				50/2½"	50/1"								and Sea Shells	
				50	50/3½"	SA-4-12								
	25					SA-4-13								
				50/2"	50/3¼"									
						SA-4-14								
						SA-4-15								
				50/1¼"	50/2"									
	30													

Driller _____ Logger _____ Title _____

†Indicate each foot by shading for core recovery, leaving blank for no core recovery, and crossing (X) for undisturbed laboratory samples taken.

Texas Highway Department
Form 554

DRILLING REPORT

(For use with Undisturbed Sampling & Testing)

Sheet 2 of 2

190

County Bexar — Structure San Antonio — District No. 15
Highway No. US 90 — Hole No. SA-4 — Date 1-17-68
Control 24-8 — Station 254+90 — Grd. Elev.
Project No. Research Project 3-5-65-89 — Loc. from Centerline — Rt. 137' — Lt. — Grd. Water Elev.

Elev. (Ft.)	Depth (Ft.)	† Samples	LOG	THD PEN. TEST No. of Blows 1st 6"	THD PEN. TEST No. of Blows 2nd 6"	Sample Number	Lat. Press. (PSI)	Ult. Stress (PSI)	Wet Density (pcf)	Moisture Content (%)	Liquid Limit (%)	Plasticity Index (%)	DESCRIPTION OF MATERIAL	Remarks
						SA-4-16								
				46	54/3½"									
						SA-4-17								
				50/2¼"	50/¾"									
	35													1

[1] Boring Completion Depth at 34' on January 17, 1968.

Driller — Logger — Title

†Indicate each foot by shading for core recovery, leaving blank for no core recovery, and crossing (X) for undisturbed laboratory samples taken.

Texas Highway Department
Form 554

DRILLING REPORT

(For use with Undisturbed Sampling & Testing)

Sheet 1 of 2

County Bexar | Structure San Antonio | District No. 15
Highway No. US 90 | Hole No. SA-5 | Date 1-15-68
Control 24-8 | Station 254+95 | Grd. Elev.
Project No. Research Project 3-5-65-89 | Loc. from Centerline Rt. 164' Lt. | Grd. Water Elev.

Elev. (Ft.)	Depth (Ft.)	Samples †	Log	THD PEN. TEST No. of Blows 1st 6"	THD PEN. TEST No. of Blows 2nd 6"	Sample Number	Lat. Press. (PSI)	Ult. Stress (PSI)	Wet Density (pcf)	Moisture Content (%)	Liquid Limit (%)	Plasticity Index (%)	DESCRIPTION OF MATERIAL	Remarks
													Gray Clay with Gravel	
				13	7									
				12	7									
	5													
				4	6									
				20	25								Pocket of Large Gravel from 7' to 9'	
	10			7	11								Yellow Clay	
				7	8									
				14	16									
	15													
				16	16									
				11	15									
				50/3½"	50/1"								Yellow and Gray Clay Shale with Some Gravel,	
	20												Sandstone, and Seashells	
				50/3½"	50/2½"									
				50/1½"	50/1"									
	25			50/1"	50/½"									
				50/3½"	50/4"									
	30			46	54/4½"									

Driller _____ Logger _____ Title _____

†Indicate each foot by shading for core recovery, leaving blank for no core recovery, and crossing (X) for undisturbed laboratory samples taken.

Texas Highway Department
Form 554

DRILLING REPORT

(For use with Undisturbed Sampling & Testing)

County Bexar — Structure San Antonio — District No. 15
Highway No. US 90 — Hole No. SA-5 — Date 1-16-68
Control Research Project 3-5-65-89 — Station 254+95 — Grd. Elev.
Project No. — Loc. from Centerline — Rt. 164' — Lt. — Grd. Water Elev.

Elev. (Ft.)	Depth (Ft.)	Samples	LOG	THD PEN. TEST No. of Blows 1st 6"	THD PEN. TEST No. of Blows 2nd 6"	Sample Number	Lat. Press. (PSI)	Ult. Stress (PSI)	Wet Density (pcf)	Moisture Content (%)	Liquid Limit (%)	Plasticity Index (%)	DESCRIPTION OF MATERIAL	Remarks
				50/3"	50/7"									
				50/3¾"	50/6¾"									
	35													1

[1]Boring Completion Depth at 34' on January 16, 1968.

Driller — Logger — Title

†Indicate each foot by shading for core recovery, leaving blank for no core recovery, and crossing (X) for undisturbed laboratory samples taken.

Texas Highway Department
Form 554

DRILLING REPORT

(For use with Undisturbed Sampling & Testing)

County Bexar | Structure San Antonio | District No. 15
Highway No. US 90 | Hole No. SA-6 | Date 1-16-68
Control 24-8 | Station 254+89 | Grd. Elev.
Project No. Research Project 3-5-65-89 | Loc. from Centerline Rt. 164' Lt. | Grd. Water Elev.

Elev. (Ft.)	Depth (Ft.)	Samples†	Log	THD PEN. TEST No. of Blows 1st 6"	2nd 6"	Sample Number	Lat. Press. (PSI)	Ult. Stress (PSI)	Wet Density (pcf)	Moisture Content (%)	Liquid Limit (%)	Plasticity Index (%)	DESCRIPTION OF MATERIAL	Remarks
													Gray Clay with Gravel	
				6	5									
				9	9									
	5													
				7	12									
				12	13									
				12	15									
	10												Yellow Clay	
				21	25									
				18	19									1
	15													

[1] Boring Completion Depth at 14' on January 16, 1968.

Driller ______ Logger ______ Title ______

†Indicate each foot by shading for core recovery, leaving blank for no core recovery, and crossing (X) for undisturbed laboratory samples taken.